C J BROUCKAERT
S WADLEY
Q E HURT

RESEARCH ON THE MODELLING OF TUBULAR REVERSE OSMOSIS SYSTEMS

Report to the
WATER RESEARCH COMMISSION
by the
POLLUTION RESEARCH GROUP
DEPARTMENT OF CHEMICAL ENGINEERING
UNIVERSITY OF NATAL

WRC Report No 325/1/95

WATER RESEARCH COMMISSION PROJECT NO. 325

RESEARCH ON THE MODELLING OF TUBULAR REVERSE OSMOSIS SYSTEMS

FINAL REPORT TO THE WATER RESEARCH COMMISSION

Compiled by
C J Brouckaert, S Wadley and Q E Hurt

Pollution Research Group
Department of Chemical Engineering
University of Natal
Durban

February 1995

Head of Pollution Research Group : Professor C A Buckley

Project Leader : C J Brouckaert

WRC REPORT NO 325/1/95
ISBN 1 86845 193 3

EXECUTIVE SUMMARY

1 BACKGROUND TO THE PROJECT

A significant research and development effort has been undertaken in South Africa to produce membrane separation equipment and processes for the purification of water. Much of this work has been funded through the Water Research Commission, whose priorities have led to a greater emphasis on waste-water treatment and reclamation than is typical of the membrane separation field as a whole, which has tended to focus on more financially rewarding applications. Tubular membrane systems are often the most suitable configuration for waste-water applications because of their greater tolerance of particulate matter and fouling.

The experience of the tubular reverse osmosis plant installed at the Lethabo Power Station had revealed a lack of knowledge in the operation of a plant consisting of a large array of tubular reverse osmosis modules. It was thought that the design of large-scale plants could be undertaken more knowledgeably if there was a better understanding of currently installed plants, which could be achieved through modelling.

2 PROJECT OBJECTIVES

The broad aim of this project was to assemble computer software and modelling methodology which would support the implementation of membrane separation technology for waste-water treatment using tubular systems. Data taken from existing installations, such as the tubular reverse osmosis plant at the Lethabo Power Station was to be used to verify the modelling procedures, and to identify aspects which it was important to represent.

In more detail, the aims of the project were :

1. To devise techniques for understanding the causes of operational problems in large tubular reverse osmosis plants ;
2. To develop these techniques to allow the improvement of the operation of currently installed tubular reverse osmosis plants ;
3. To develop techniques for the optimum design of new plants ;
4. To undertake case studies concerning industrial applications.

It became clear early in the project that there were three major areas where computer modelling could make a contribution to improving the application of membrane separation processes to waste-water treatment:

Interpretation of pilot-plant data

The variability of waste-water streams, both from site to site and with time at a particular site, usually makes it necessary to undertake a pilot-plant investigation before embarking on a full-scale design. This same variability often makes the measured data difficult to interpret.

A computer model which is able to account for measurable variations in feed-stream characteristics and operating conditions would make it easier to identify and quantify site specific phenomena which might affect the design and operation of the eventual process.

Design of a full-scale process

During pilot-plant trials it is often difficult to foresee the entire range of conditions which will be encountered in the process in its final configuration, once technical and economic factors have been fully evaluated and optimised. The design process would be assisted by a model which is capable of extrapolating results obtained from small-scale equipment to conditions which might be met on a large plant.

Process monitoring

Running a simulation in parallel with an operating plant and comparing measured and simulated performance can provide a sensitive means of monitoring the state of the plant, and help to guide the management of the process, for example when determining optimum times for membrane cleaning or replacement.

The project was originally planned to run from 1990 to the end of 1992. During 1991 and 1992 personnel from the project became involved in assisting WRC project 239 entitled *Transfer of Waste Water Management Technology to the Meat Processing Industry* with the ultrafiltration and reverse osmosis pilot-plant trials at the Cato Ridge Abattoir. This project (WRC project 325) was extended in 1993 for one year to concentrate on technology transfer of the reverse osmosis modelling, which included carrying out further pilot plant and modelling work at the abattoir. During this extension of the project, the objective was to promote membrane separation modelling by applying it to industrial problems, in particular at Cato Ridge, and by conducting courses in the principles and use of the model.

3 PROJECT RESULTS

3.1 Computer Programs

Two versions of the membrane transport computer model have been produced, both of which run on IBM-compatible personal computers.

The single solute model

The initial version provided for only a single solute to be separated from water. It was tested using data supplied by Eskom, taken from the pilot-plant study which preceded the design and construction of the tubular reverse osmosis plant at the Lethabo Power Station.

The program is based largely on the theory developed by Sourirajan and Matsuura. It features the ability to determine membrane transport parameters from laboratory, pilot-plant or full-scale process measurements, and, using these parameters, to predict the performance of plants with different physical configurations, or different feed streams and operating conditions.

A modified version of the program was produced which models membrane modules with *spiral wound* construction. This version was tested using measurements made in the University of Natal's laboratories.

The provision for only a single solute is not quite as restrictive as it appears, in that a mixed solute can sometimes be satisfactorily represented as a single entity with average properties. This approximation is most often acceptable when modelling the treatment of ionic solutions with highly rejecting reverse osmosis membranes, when differences in the rates of transport of the ionic species are of relatively minor importance. Instrumentation on such plants usually involves measurements of summarizing parameters such as conductivity or total dissolved solids, which gives insufficient information on which to base a more detailed model.

The multi-solute model

The approximations involved in treating a variety of solutes together as though they were a single entity become less and less tenable as one moves from considering reverse osmosis to nanofiltration and ultrafiltration. For example, in nanofiltration the retention of divalent ions is very much higher than that of monovalent ions, while in ultrafiltration dissolved inorganic salts are hardly retained at all while colloidal and macromolecular components are retained. Thus a model that can handle a number of solutes with different retention characteristics becomes essential when dealing with these processes.

The modelling program that has been developed runs in a Microsoft-Windows environment. It is based on theory developed by Spiegler and Kedem. Although this approaches the membrane transport mechanism from a different viewpoint to that of Sourirajan, in the reverse osmosis case it leads to equations which are virtually identical. It is able to account for effects observed on nanofiltration and ultrafiltration separations in a simpler way than that in Sourirajan's treatment, which requires physico-chemical data on the membrane-water-solute interactions which cannot be obtained directly from membrane filtration experiments alone, but requires separate laboratory measurements.

This program has been tested on nanofiltration and ultrafiltration data obtained from pilot-plants, operating at the Huletts Sugar Refinery and the Cato Ridge Abattoir, respectively (the experimental data was generated partly by this project, and partly by other WRC projects). At the sugar refinery, the stream being treated was an ion-exchange regenerant effluent containing about 10 % sodium chloride by mass and coloured organic material adsorbed from the impure sugar solution by the ion-exchange resin in the refining process. In this case the key modelling issue was the separation of strongly retained organic material from the salt, which was only slightly retained. The resulting brine could then be reused in the ion-exchange regeneration process, thereby reducing the salt consumed and effluent produced.

At the abattoir, the pilot-plant was treating a mixed final effluent stream, with the objective of recycling the permeate for limited use in non-critical areas of the abattoir such as floor washing, and reducing the volume of concentrated effluent to render it more readily and economically treatable. In this case the most significant feature requiring modelling was the rapid fouling of the membranes by proteins and lipids in the effluent, which caused the membranes' operating characteristics to alter significantly during operation.

The program was intended to eventually provide a whole package of facilities with which to perform the computational tasks associated with all aspects of a modelling exercise. Apart from the central calculation of transport through the membranes, and determination of transport parameters from experimental data, these tasks include charge-balancing of chemical analyses, speciation of solutions, prediction of solution properties such as osmotic pressure and conductivity, and predicting saturation limits of potential precipitants. To support these diverse functions, the structure of the program was designed to be modular and flexible, so that such features could be added to the package or modified without requiring extensive modification of existing features. Unfortunately, establishing a suitably comprehensive and sophisticated infrastructure has taken longer than anticipated, and the ancillary functions still have to be carried out separately, using techniques which were established during the various investigations which were parts of the project.

3.2 Technology Transfer

3.2.1 Case Studies

The development of the computer models has provided the thematic focus for the project. A considerable part of the effort has, however, been devoted to investigations of real processes to ensure the relevance of the computational techniques.

3.2.1.1 The Lethabo Power Station Tubular Reverse Osmosis Plant

The Lethabo tubular reverse osmosis plant and its problems formed a large part of the original motivation of the project, and data from the Lethabo pilot-plant study was used extensively in verifying the model. This work has been reported in two published papers (**Appendices 1 and 2** of the final report) and in two conference papers. The operation of the full-scale plant has been very troubled, with much down time, poor membrane life and many module failures. It was thought that modelling might help to uncover the underlying causes of these problems.

Once the model had been verified, an investigation was undertaken at Lethabo to apply the model to the full-scale plant operation. During the setting up of the model - that is, gathering the required data from the plant and operating records - it became clear that the plant's problems were not due to hidden internal factors which might be revealed and remedied through modelling, but due to quite straightforward mechanical design faults. The operating personnel were largely aware of these faults, and have been gradually eliminating them. These included inadequate filtration of the feed which led to damage to the high pressure pumps, poor hydraulic design of the sponge-ball traps which made it possible for them to be plugged by the sponge balls, and a very abrupt flow reversal system which caused sharp pressure changes. These pressure shocks, in particular, were almost certainly responsible for the frequent tube ruptures that were being experienced at the time, as the other problems had been largely eliminated by then. A detailed report on the situation was submitted to the Lethabo Power station; which is included as **Appendix 3** of the final report.

3.2.1.2 The Secunda Pilot Plant

Data from a pilot plant treating mine water at Secunda was provided by Sastech for analysis using the model. This modelling exercise followed closely along the lines of that for the Lethabo pilot plant, and served to confirm the conclusions reached previously. At that time Sastech appeared to decide against using reverse osmosis, and the modelling work was discontinued. Recently Sastech's interest in reverse osmosis has revived, and the Pollution Research Group has been involved in advising on design and operational aspects of a proposed new tubular reverse osmosis plant.

3.2.1.3 The Cato Ridge Abattoir

Experimental work

A two stage ultrafiltration/reverse-osmosis pilot-plant supplied by Membratek was operated on the effluent stream at the Cato Ridge Abattoir as part of WRC project 239 entitled *Transfer of waste-water management technology to the red meat industry*. In 1991 and 1992 the current project, together with Dr. E. Jacobs from the Institute of Polymer Science at the University of Stellenbosch, became involved in assisting the abattoir with the running of the pilot plant and the interpretation of the results. This work was successful in establishing a very effective membrane cleaning strategy to overcome a severe fouling problem which threatened the viability of the process.

When project no 239 came to an end, it had reached a point where the process looked very promising because the fouling problem had been solved. However, because attention had been focussed on this aspect, the plant had been operated at only one set of conditions which involved, in particular, very low water recovery. It was also evident that the performance of the system was limited chiefly by *gel polarisation*, which phenomenon is known to be strongly dependent on the hydraulic conditions prevailing at the membrane surfaces. Since the conceptual design for a membrane plant handling an abattoir's effluent called for a water recovery of 90 % or more, the data did not provide a good basis for an accurate optimal design.

In 1993 the Steering Committee decided to continue the work at the abattoir as part of the current project, with the objective of generating data which covered the range of conditions which might be encountered in a full-scale plant. At the same time this would provide a comprehensive data set with which to verify ultrafiltration models. The prospect of developing a model allowed a further idea to be tried. The Institute for Polymer Science had developed a very low cost design of ultrafiltration module, which involved unsupported 9 mm diameter tubes in a poly(vinyl chloride) housing. The chief limitation of the design was a maximum pressure of about 500 kPa, which was thought not to be of concern since *gel polarisation* prevented any improvement in flux as the pressure increased above about 300 to 400 kPa. The new trials could be carried out using the experimental modules, and even if these proved unsuitable, the effort would not be wasted since results obtained could be translated to the conventional module configuration using the model.

A pilot plant was constructed using the experimental Institute for Polymer Science modules. These were equipped with two types of poly(ether sulphone) membranes: the standard medium molecular mass cut-off 719 membranes (which were the same as those used in the previous work), and a new low molecular mass cut-off formulation known as 442 membranes (according to the Institute for Polymer Science and Membratek designations). The two types of membrane modules were set up in parallel, and operated simultaneously, so that both were subjected to exactly the same sequence of conditions, and a precise comparison of their performance could be made.

Experiments were conducted which covered a range of pressures and flow rates, and water recoveries between 0 and 90 %. The results were very encouraging for the viability of the process, as reasonable fluxes were still obtained at high water recoveries. The comparison between the 719 and 442 membranes was very interesting. The tighter 442 membranes would be expected to give lower permeate fluxes than the 719, and at low pressures and high cross-flow velocities this was indeed the case. However, they appeared to be less subject to gel polarisation, and at higher pressures and lower flow rates they actually produced the higher fluxes. Under most conditions the quality of the permeate produced from the two membranes was much the same, indicating that the separation occurred largely as a result of self-filtration in a dynamic layer at the membrane surface produced by the organic material in the effluent. This conclusion was supported by the observation that at the lowest pressures and immediately after cleaning the quality of the permeate from the 719 membranes deteriorated markedly.

The experimental modules performed well, with one possible reservation. They were constructed with the membrane tubes connected in parallel, which precluded the use of sponge-balls when cleaning. The cleaning regime that had been established in the previous study with the standard module design had used sponge-balls in conjunction with a sequence of enzymatic detergents, a chlorine based sanitizer and fresh water. Without the sponge balls, the chemical cleaning did not prove to be as effective in restoring pure water fluxes as had been the case previously. During the course of the experiments this did not appear to affect the fluxes measured while treating effluent. An attempt was made to use air-purging as a substitute for sponge balls in the cleaning procedure, but this proved to have little effect. In the previous study restoration of the pure water flux was seen to be the key to maintaining the long-term productivity of the membranes, so this issue casts some doubt on whether they would be completely suitable. The Institute for Polymer Science have indicated that they will be looking further into this aspect.

A feasibility study concerning a proposed ultrafiltration effluent treatment plant for the Port Elizabeth abattoir has been prepared by Steffen Robertson and Kirsten (SRK Report 197133/10, April 1994), in which it was found that the replacement cost of membranes, which is determined by the ratio of module cost and its lifetime, was a major factor in determining the economic viability of the process. The use of this inexpensive module design may make a crucial difference in this regard, so it is important that these remaining questions be resolved.

Modelling

The construction of the experimental rig was such that it proved difficult to set operating pressures and flow rates to precise pre-determined values, although, once set, these could be measured accurately. A further difficulty in obtaining reproducible operating conditions was due to the rapid fouling of the membranes which caused their characteristics to change continuously while the measurements were taking place. The fact that almost all the process variables changed between different data sets made it difficult to interpret the results in terms of trends. As far as the design of the equipment was concerned, sophisticated controls were not provided because it was anticipated that a model would be developed, and would be able to compensate for variations in conditions; however nothing could have been done to avoid membrane fouling in any case.

The most significant new characteristics of the process, when compared to those that had been modelled previously, were gel polarisation and membrane fouling. Although fouling was a factor in the Lethabo pilot-plant study, it occurred so gradually that it could be accounted for as a slow drift in the membrane transport parameters over a period of days. In the case of the abattoir effluent, its effect was noticeable in the time that it took to make a single measurement, and so needed to be accounted for explicitly in the model.

A model was constructed which combined the Spiegler-Kedem model for the transport through the membrane, and a model proposed by Sourirajan and Matsuura for the fouling.* This was very successful in correlating the data, and formed the basis of a paper presented at the *Engineering of Membrane Processes. Environmental Applications* Conference, held in Il Ciocco, Italy, 26-28 April, 1994.

In summary, the major results of this experimental and modelling study are:

i) The ultrafiltration of abattoir effluent is a technically viable process.

ii) With some reservations concerning membrane cleaning noted above, the low pressure PVC module design seems to be a suitable candidate for the application.

iii) The low molecular mass cut-off 442 membranes have an advantage over the medium molecular mass cut-off 719 membranes under gel-polarised conditions.

iv) The model is able to represent the performance of membranes over a range of conditions, and should be useful in producing an efficient plant design.

3.2.1.4 The Huletts Sugar Refinery

A nanofiltration pilot plant was built and operated at the Huletts Sugar Refinery in Durban as part of WRC Project 308 entitled *Research into recovery of water and chemicals from ion-exchange regeneration effluents.* The plant was operated on the brine effluent from the regeneration of the ion-exchange columns used to decolorise the sugar, and produced a brine permeate from which the organic colour components had been removed, and a concentrated organic stream for disposal. The permeate can be recycled to the regeneration process, thereby reducing the refinery's consumption of both water and salt (sodium chloride). Project 308 was suspended for a year in

---

1993, and its project leader, Ms. S. Wadley, transferred to project 325. Work on the nanofiltration was continued as it was appropriate to the goals of this project with the addition of a modelling component. The experimental work formed the basis of Ms Wadley's MScEng thesis.

As mentioned earlier, consideration of nanofiltration required the use of a multi-solute model, and a departure from the Sourirajan theory to account for a solute (in this case the sodium chloride) which is only slightly retained by the membrane. The data provided by the pilot plant was therefore ideal for testing and verifying the model.

The model was able to correlate the experimental data successfully, and was used in a conceptual design study for a plant to treat the entire regeneration effluent stream. A preliminary costing of the plant by Tongaat-Huletts has indicated that the process would have a pay-back period of about two years, based on the reduced sodium chloride consumption and effluent disposal cost. This work was presented at the *Engineering of Membrane Processes. Environmental Applications* Conference, held in Il Ciocco, Italy, 26-28 April, 1994.

3.2.1.5 Mass Transfer Enhancement for Reverse Osmosis

Concentration polarisation is one of the limiting factors in membrane separation processes. The standard way of reducing its impact is to increase the diffusion of solute away from the membrane surface by increasing the cross-flow velocity, and hence the film mass transfer coefficient which governs diffusion of solute away from the membrane surface. This has the effect of improving permeate flux and quality, but at the expense of water recovery and pumping power.

The direct measurement of concentration polarization would be an extremely difficult experimental task, as it is difficult to conceive of a measuring device which would not interfere with the phenomenon. As concentration polarisation is a key element in the membrane transport model, the model was used to infer its extent from conventional measurements of permeate flux and concentration.

The use of oscillatory flow and baffle inserts, separately and in combination, to enhance mass transfer in tubular reverse osmosis systems was the MScEng thesis topic of Mr Q.E. Hurt. Both methods increase shear stresses in the flow, and therefore the frictional pressure drop. However, in an reverse osmosis system, the pressure drop due to flow through the modules is usually small compared to that across the back-pressure valve, so these methods improve the membrane productivity with a much smaller energy consumption penalty than would be incurred by simply increasing the cross flow velocity.

Measurements were made in the laboratory on the reverse osmosis of sodium nitrate solutions with various combinations of oscillatory and baffled flow, and the reverse osmosis modelling program was used to infer the mass transfer coefficient, which could then be expressed as functions of average cross-flow velocity and the amplitude and frequency of the oscillatory flow. Expressed in this way, the results should be independent of the particular membrane and solution that was studied, and can be applied to any tubular system with the same baffle arrangement.

The investigation demonstrated significant increases in mass transfer coefficients in all cases; however, for reverse osmosis, these do not give rise to dramatic improvements in filtration performance. This is because the intrinsic resistance of the membrane to permeation is very high, and rapidly becomes limiting as that due to concentration polarisation is reduced. From a practical point of view the techniques are more likely to be useful in ultrafiltration where concentration polarisation or gel polarisation resistance is usually more dominant.

3.2.2 Instruction

Three courses were conducted on the principles and use of the tubular reverse osmosis modelling programs. The first was a presentation to Eskom at Megawatt Park in 1992, which was attended by personnel from the Lethabo Power Station, the Technical Research and Investigation division, and Eskom head office. The second took place during the 1993 Water Institute of Southern Africa conference in Durban, and was attended by ten conference delegates. The second took place at the 1994 Afriwater conference, and was attended by eight conference delegates. Copies of the modelling software were supplied to those attending. A further course is planned for the Water Institute of Southern Africa-Membrane Technology Division meeting at Van Staden's River Mouth in October 1994.

The use of the membrane separation model is also introduced to final year chemical engineering students as part of a course in Advanced Mass Transfer in 1992, 1993 and 1994.

3.2.3 Publications

Six journal papers, seven conference presentations, and five poster presentations have been based on the work carried out as part of this project. Additionally, a chapter on 'RO applications in brackish water desalination and in the treatment of industrial effluents' was contributed to the textbook *Reverse Osmosis: Membrane Technology, Water Chemistry and Industrial Applications*, edited by Z. Amjad and published by Van Nostrand Reinhold (1993).

3.2.4 Patent

A South African patent was lodged for the idea of using the single-solute model as an on-line *observer* of a reverse osmosis plant. As shown by the Lethabo pilot-plant study, these parameters are sensitive indicators of the state of the membranes, and would be useful in the management of the plant. This would involve operating data being obtained directly from the plant's instrumentation by an algorithm running on a supervisory control computer, and using the model's regression capability to infer membrane transport parameters. The use of the model as part of an automatic controller of the plant is also described in the patent.

3.2.5 Internet

The computer model has been made available to the world-wide Internet community through the *Electronic Membrane Information LibrarY* (EMILY) which is hosted by the Computing Centre for Water Research at Pietermaritzburg. The intention is to use the model as a thematic focus for membrane research, and to encourage users to add to it, both in terms of a library of experimental data and corresponding model parameters, and new facilities and algorithms. In this way it is hoped that it will develop much further and faster than could be effected by the Pollution Research Group alone. EMILY was launched at the *Engineering of Membrane Processes* conference in Italy at the end of April 1994, where it aroused considerable interest. A number of requests related to the model have already been received, however it is too early to judge how successful the concept will prove to be.

4 CONCLUSIONS

Membrane separation is a mature technology in terms of materials and equipment, but still needs a great deal of development in terms of processes, particularly in the field of industrial waste-water treatment. Computer modelling has a role to play in process development through its ability to interpret, correlate and extrapolate experimental data. The modelling techniques applied during this project have not been developed to the point where they can replace experimental data, but they can be used to reduce experimental effort.

To do this most effectively, modelling should be carried out at the same time as the experimental programme, so that the implications of any results can be assessed immediately, and areas where data are lacking can be identified.

Modelling can also be used in the finding the optimal design for a new plant, in optimising the operation of an existing plant, or in monitoring its performance and investigating operational problems. The Lethabo experience has shown that even when the modelling does not help directly to identify a problem, the discipline of gathering the data required to describe the process in a fundamental way will probably lead to identifying the cause of the problem.

With regard to the generalised multi-solute computer program developed during this project: as it now exists, it does not yet incorporate all the techniques which were found useful in the application case studies, although its framework has been designed to incorporate them. Thus there is still a need to improve its capability and ease of use.

The promotion of the use of membrane separation modelling has only been partially successful so far, in that, although a variety of people have been introduced to the programs developed during this project, we are not aware that anyone else has made use of them independently. This may relate to the points made in the previous paragraph.

5 RECOMMENDATIONS

i) Membrane researchers, consultants and users should be encouraged to use modelling in data interpretation, plant design and process monitoring. The Electronic Membrane Information LibrarY (EMILY) on the Computing Centre for Water Research computer is the natural way to support this. Data obtained from experimental investigations could be reduced to model parameters and stored on EMILY where it would easily available to others. There is a possibility that, if the model continues to develop along these lines, it could form the basis of an International Association for Water Quality recognized model.

ii) Courses on membrane separation modelling should continue to be given occasionally, as demand justifies.

iii) The computer programs which constitute the model need further refinement to make them accessible to a wider range of users. These improvements involve the coding of well-defined procedures, and could be effected by short, targetted exercises - for instance involving post-graduate students. Such mini-projects would only be undertaken in response to needs identified by users or potential users.

iv) The programming framework which has been developed has potential as the basis for modelling other water related unit operations. For instance, the *IMPULSE* computer program for residence time distribution modelling was developed using the same basis. The concerns of modelling are usually similar in most fields of application, and, in a family of related models, developments made to a particular model would be of benefit to the others. Thus consideration should be given to applying the same modelling framework to other water treatment unit operations.

ACKNOWLEGEMENTS

The work in this report was funded by the Water Research Commission, for a project entitled : *Research on the Modelling of Tubular Reverse Osmosis Systems.*

The investigations were guided by a Steering Committee which, over the period of the project, consisted of :

Dr H.M. Saayman : Water Research Commission (Chairman)
Mr P.W. Weidemann : Water Research Commission (Secretary)
Dr O.O. Hart : Water Research Commission
Mr. G. Offringa : Water Research Commission
Mr J.D. Aspden : Eskom
Dr. R.D. Sanderson : University of Stellenbosch
Dr. E.P. Jacobs : University of Stellensbosch
Mr R.W. Busby : Chamber of Mines Research Organisation
Mr W. Pulles : Chamber of Mines Research Organisation
Mr D.J. De Lange : Chamber of Mines Research Organisation
Professor C.A. Buckley : University of Natal
Dr C.A. Kerr : University of Natal
Mr R.J.J. Egenes : University of Natal
Professor D.I.Exall : University of Natal

The financing of the project by the Water Research Commission and the contributions by the members of the Steering Committee are gratefully acknowledged.

During the course of the project a number of organisations and persons made very significant contributions to the work. Thanks are extended to :

Eskom, in particular Mr D. Hanekom of the Lethabo Power Station.
Abakor, in particular Mr J. Muller and Mrs. F. MacTavish.
Huletts Sugar Refinery, in particular Mr D. Meadows.
Dr. E.P. Jacobs of the Institute for Polymer Science at the University of Stellenbosch.
Dr O.O. Hart of the Water Research Commission.
Miss B.M. Brouckaert, a student at the University of Natal.

Table of Contents

List of Figures

List of Appendices

Appendix 1	Modelling of Lethabo Power Station TRO Pilot Plant - *Simulation of Tubular Reverse Osmosis* Published in WaterSA, Vol 18, No 3, 1992
Appendix 2	Modelling of Lethabo Power Station TRO Pilot Plant - *The use of Computer Simulation of Tubular Reverse Osmosis in conjunction with Pilot-Plant Studies.* Published in Water Science and Technology, Vol 25, No 10, 1992
Appendix 3	Report on a visit to the Lethabo Power Station TRO Plant.
Appendix 4	Experimental Data from Cato Ridge Abattoir Effluent Investigation.
Appendix 5	Modelling of Ultrafiltration of Effluent at the Cato Ridge Abattoir. Presented at Engineering of Membrane Processes II : Environmental Applications Il Ciocco, Italy, 26-28 April 1994.
Appendix 6	Modelling of Nanofiltration of Brine Effluent at Hulett Refineries Ltd. Presented at Engineering of Membrane Processes II : Environmental Applications Il Ciocco, Italy, 26-28 April 1994.
Appendix 7	Mass Transfer Enhancement in TRO Systems.
Appendix 8	Roughing Demineralisation in Ultrapure Water Production at Power Stations.
Appendix 9	User Manual for the Single-Solute TRO Modelling Program.
Appendix 10	User Manual for the Multi-Solute Membrane Separation Modelling Program.

List of Symbols

A : Sourirajan membrane parameter, kg.m^{-2}.kPa^{-1}.h^{-1}
$\bar{A}$: local solute permeability, m^2.s^{-1}
A : overall solute permeability, m.s^{-1}
A : (in Debye-Huckel Eqn 25), a function of the dielectric constant and temperature
$\bar{A}_h$: specific hydraulic permeability, m^3.s.kg^{-1}
a_i : activity of component i in solution
B : function of dielectric constant and temperature (kg^{0,5}.cm^{-1}mol$^{-0,5}$)
b : ion specific parameter, kg.mol^{-1}
C : discharge or loss coefficient dependent on flow geometry
c : concentration of solute in solution, mol.m^{-3}
$\bar{c}$: concentration of solute in membrane, mol.m^{-3} of membrane
c_s : concentration of salt in solution, mol.m^{-3}
c_x : concentration of multifunctional organic anion ($X^{\nu-}$), mol.m^{-3}
D : diffusion coefficient, m^2.s^{-1}
$\mathcal{D}$: the solute transport parameter, $\left(\frac{D_{AM}}{K\delta}\right)$
d : tube diameter, m
E : local electrical potential gradient
e : charge of an electron
F : a flow parameter, defined in Eqn (21)
F : fraction of the membrane area gel polarised, in Eqn 84.
$\bar{G}$: partial molar Gibbs Free Energy
h : flow channel width in spiral wound modules, m
I : ionc strength (defined in Eqn 25)
i : a number in a series
J_s : molar salt flux through membrane, mol.m^{-2}.s^{-1}
J_v : volume flux through membrane, m.s^{-1}
j : a number in a series
$\mathcal{K}$: mass transfer coefficient
K : constant specific to the use
k : constant specific to the use
L : effective length of flow path, m
l : thickness of concentrated boundary layer solution, m
l_{sp} : mesh spacing of spiral wound module spacer net, m

m : molality, mol.kg^{-1}
N : Avagadro's number
N_i : molar flux of component i, mol.m^{-2}.s^{-1}
n : a number (usually of moles)
P : pressure, Pa (or kg.m^{-1}.s^{-2})
p_k : ion size parameter, cm
Q : volumetric flowrate, m^3.s^{-1}
$\mathcal{R}$: the universal gas constant in Eqn 22, 8,314 m^3.Pa.mol^{-1}.K^{-1}
R : retention coefficient
R : mean pore radius in Eqn 63, m
R_m : intrinsic membrane resistance, kg.m^{-2}.s^{-1}
R_{obs} : observed retention coefficient
R_p : resistances due to gel polarised layer and boundary layer
$\mathcal{R}e$: Reynolds number
Sc : Schmidt number
Sh : Sherwood number
T : temperature, K
T_c : temperature, °C
u : linear flow velocity, m.s^{-1}
V : volume, m^3
v : diffusion velocity of an ion, m.s^{-1}
x : mole fraction
x : vertical distance from the membrane surface, m
Z_k : charge number of the kth species
z : ionic charge on an ion

Greek letters

α : coefficient for salt permeability, defined in Equation (96), m/s
α : constant in the Davies Eqn 27
β : coefficient for concentration dependence of salt permeability, defined in Equation (96)
γ_i : activity coefficient of the ith ion
Δx : membrane thickness, m
ϵ : surface porosity

μ : viscosity, Pa.s
μ_{sp} : mixing efficiency factor
μ_i : ionic mobility
K : specific conductivity
Λ : equivalent conductivity
λ : limiting conductivity
ν : number of (negatively) charged groups carried by the organic ion
π : osmotic pressure, kPa
ρ : density of solution, kg.m^{-3}
σ : reflection coefficient
Φ : a constant defined in Eqn 72

Subscripts

$2g$: concentration at the gel polarised layer, kg.m^{-3}
$2w$: concentration at the membrane wall, kg.m^{-3}
a : anion
c : cation
f : feed
h : hydraulic
m : membrane
obs : observed (retention coefficient)
p : permeate
s : solute or salt (NaCl)
T : transmembrane
v : volume
x : organic anion (X^{ν})

Abbreviations

CCWR	Computing Centre for Water Research
COMRO	Chamber of Mines Research Organisation
EMILY	Electronic Membrane Information Library (hosted by the CCWR)
IAWPRC	International Association for Water Pollution Research and Control (Now renamed International Association for Water Quality - IAWQ)
IPS	Institute for Polymer Science
MINTEQA2	Aqueous speciation computer model
MTD	Membrane Technology Division
NF	Nanofiltration
PRG	Pollution Research Group, University of Natal
PSCF	Preferential Sorption Capilliary Flow (membrane transport model)
RO	Reverse Osmosis
SF-PF	Surface Force- Pore Flow (membrane transport model)
SPARRO	Slurry Precipitation and Recycle Reverse Osmosis
SDI	Silt Density Index
TRO	Tubular reverse osmosis
UF	Ultrafiltration
WISA	Water Institute of Southern Africa

1 INTRODUCTION

A significant research and development effort has been undertaken in the Republic of South Africa in producing tubular reverse osmosis (TRO) modules for the desalination of water. Plants have been installed at Eskom's Lethabo Power Station and at a Port Elizabeth sewage works. A number of smaller brack water and effluent treatment plants have also been installed. At the time of the project motivation, the Chamber of Mines Research Organisation (COMRO) was evaluating the slurry precipitation and recycle reverse osmosis (SPARRO) process for the desalination of mine service water.

The necessity of desalination techniques for effluent treatment, the preservation of the quality of water resources and the provision of potable water from brack water sources has been well documented. The use of commercially viable desalination techniques is becoming increasingly important.

The experience of the Lethabo TRO plant had revealed a lack of knowledge in the operation of a large plant consisting of a large array of tubular reverse osmosis modules. This was thought to be due to the complex interaction between factors such as pipe geometry, module array configuration, flow rates, pressure distribution, solute concentration and the physico-chemical processes which take place at the fluid-membrane interface.

It was thought that the following particular problems could be experienced :

- reverse osmosis flows leading to precipitation and fluid blockages
- difficulty in assessing the state of the membranes if the quality of the feed solution varies significantly

Similar problems could occur and similar information would be required in order for other reverse osmosis process researchers to fully evaluate their research programmes.

The design of large-scale plants could be undertaken more knowledgeably if there was a better understanding of the currently installed plants. Once it had been demonstrated that existing plants could be modelled satisfactorily, the techniques which were developed as part of this project could be used in the design of new plants or in increasing the capacity of existing plants.

The aims of this project were :

1. The development of techniques for understanding the causes of operational problems in large tubular reverse osmosis plants;
2. To develop these techniques to allow the improvement of the operation of currently installed TRO plants, and
3. To develop techniques for the optimum design of new plants.
4. To undertake case studies concerning industrial applications.

During the course of project, as a result of opportunities to become involved in industrial case study projects, the scope of the modelling was widened to include tubular nanofiltration (NF) and ultrafiltration (UF) systems, as well as spiral-wrapped systems. Investigations into ultrafiltration of effluent from the Cato Ridge Abattoir, and nanofiltration of brine effluent from the Huletts Sugar Refinery in Durban, developed to the point where the project was able to make significant contributions to the development of the technologies involved.

2 THEORY

2.1 Reverse Osmosis Transport Fundamentals

There are two major theories for transport through RO membranes reported in the literature : the solution-diffusion model and the preferential sorption-capillary flow model (Rautenbach and Albrecht, 1989). The latter model is largely due to the work since 1960 of Sourirajan and co-workers (Sourirajan and Matsuura, 1985). It has been shown (Muldowney and Punzi, 1988) that the predictions of the two models are virtually identical in practice. The modelling in this work is based primarily on Sourirajan's theory, although, where his theory becomes unwieldy for computer modelling, the Spiegler-Kedem theory is used. It is not the aim of this report to reproduce all of his theory, but rather to highlight some of it.

The first section deals with the case of single solute reverse osmosis. The second section deals with the case of multi-solute reverse osmosis. The theory for coping with the multi-solute case is extrapolated from the single-solute instance.

2.1.1 Single solute

The following treatment is taken from Sourirajan and Matsuura (1985). The equations deal with a binary solution consisting of a solute, A , and a solvent, B , (usually water). They concern the fluxes N_A and N_B through the membrane, at steady state, under the influence of an applied pressure, P, across the membrane. The permeate side pressure is considered to be negligible. The equations are set up for a *point* in a RO system, which implies that there are negligible changes in conditions of pressure, flow or concentration, in the region of interest, as a result of the permeate withdrawal. Three zones are considered (see Fig. 1) :

1. The bulk solution on the high-pressure side of the membrane.
2. A thin, concentrated boundary layer zone adjacent to the membrane surface on the high pressure side.
3. The low pressure permeate solution on the opposite side of the membrane.

Concentrations of the components are represented as the product of the overall molar concentration (i.e., solute plus solvent) in zone i , C_i and the mole fraction of the component at that point, i.e. $C_i x_{ij}$

2.1.1.1 Water flux through the membrane

$$N_A = A[P - \pi(x_{A2}) + \pi(x_{A3})] \qquad (1)$$

Here $\pi(x)$ is the osmotic pressure as a result of the mole fraction of solute, x .

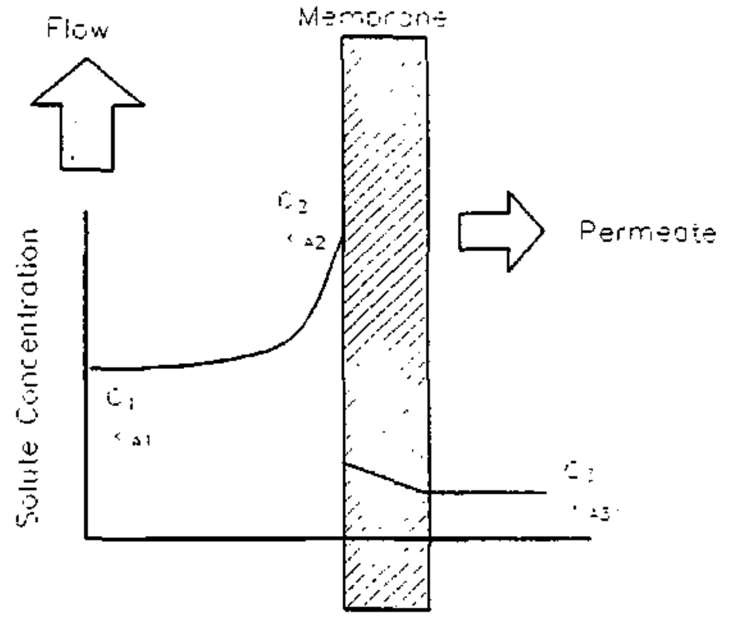

Figure 1 : A schematic diagram of the reverse osmosis model

2.1.1.2 Solute flux through the membrane

$$N_A = \left(\frac{D_{AM}}{K\delta}\right) (c_2 x_{A2} - c_3 x_{A3}) \tag{2}$$

The solute transport parameter $\left(\frac{D_{AM}}{K\delta}\right)$ is characteristic of a solute/membrane combination.

Since the three parameters which make it up are never used separately, it will be represented by the symbol $\mathcal{D}$ for brevity.

2.1.1.3 *Mass transfer on the high pressure side of the membrane*

The solute which is rejected by the membrane concentrates in a layer adjacent to the membrane surface, and at steady-state it must be removed by diffusion back into the bulk solution flow. Applying standard film mass-transfer theory yields the relationship :

$$\ln\left[\frac{x_{A2} - x_{A3}}{x_{A1} - x_{A3}}\right] = \frac{N_A + N_B}{C_1 \mathcal{K}} \tag{3}$$

where $\mathcal{K}$ is a film mass-transfer coefficient.

2.1.1.4 Transformation of the equations for solution

The simultaneous solution of Eqns (1), (2) and (3) forms the basis for the description of the RO process at a single point within a RO tube. In the basic modelling situation, the variables, P , x_{A1} and C_1 are known, as are the parameters $\mathcal{A}$, $\mathcal{K}$ and $\mathcal{D}$, whereas the variables N_A, N_B, x_{A2} and x_{A3} are unknown. Because of the non-linear nature of the equations, a numerical method must be employed for solution, and it is advantageous to reduce the number of equations involved in the core solution procedure as much as possible. It is in fact possible to reduce the set to only two equations. Sourirajan and Matsuura chose to do this in the following way :

Consideration of the material balance on the solute in the permeate yields :

$$x_{A3} = \frac{N_A}{N_A + N_B} \tag{4}$$

which can be rearranged to :

$$N_A + N_B = \frac{N_B}{1 - x_{A3}} \tag{5}$$

Combining this with Eqn (3) gives :

$$N_B = C_1\mathcal{K}(1 - x_{A3})\ln\left[\frac{x_{A2} - x_{A3}}{x_{A1} - x_{A3}}\right] \tag{6}$$

Another rearrangement of Eqn (4) gives :

$$N_B = \frac{(1 - x_{A3})}{x_{A3}} N_A \tag{7}$$

Combining Eqn (7) with Eqn (2) :

$$N_B = \mathcal{D}\frac{(1 - x_{A3})}{x_{A3}}(c_2x_{A2} - c_3x_{A3}) \tag{8}$$

Equating Eqns (6) and (8) :

$$\mathcal{D}\frac{(1 - x_{A3})}{x_{A3}}(c_2x_{A2} - c_3x_{A3}) = c_1\mathcal{K}(1 - x_{A3})\ln\left[\frac{x_{A2} - x_{A3}}{x_{A1} - x_{A3}}\right] \tag{9}$$

Now in most practical situations the variation of the overall molar concentration is negligible, so that $c_1 = c_2 = c_3$, so Eqn (9) can be reduced to :

$$\mathcal{D}\frac{(x_{A2} - x_{A3})}{x_{A3}} - \mathcal{K}\ln\left[\frac{x_{A2} - x_{A3}}{x_{A1} - x_{A3}}\right] = 0 \tag{10}$$

The other equation was obtained by combining Eqn (1) with Eqn (8) :

$$A[P - \pi(x_{A2}) + \pi(x_{A3})] - c_1\mathcal{D}\frac{(1 - x_{A3})}{x_{A3}}(x_{A2} - x_{A3}) = 0 \tag{11}$$

The core modelling problem is thus the simultaneous solution of Eqns (10) and (11) for the unknown x_{A2} and x_{A3}, after which the remaining unknown variables can be calculated directly from the other equations.

2.1.2 Multiple solutes

While the single-solute version of the model has been reasonably successful in representing multi-solute solutions, considering total dissolved solids to be a single solute, it is unable to predict effects which depend on the differential permeability of RO membranes for different solutes.

This section deals with the mathematical basis of an algorithm which is able to solve the core of the TRO modelling problem, namely solving the Sourirajan formulation of the solute and solvent transport equations through the membrane.

2.1.2.1 Initial assumptions

The following assumptions are made regarding the system :

(i) An aqueous solution is being driven through a reverse osmosis membrane by a pressure P . The pressure on the permeate side of the membrane is effectively zero. Three positions in the system are considered: the bulk solution on the high-pressure side of the membrane, which is designated by the subscript 1; a layer very close to the separating membrane surface on the high-pressure side in which the solutes become relatively highly concentrated, which is designated by the subscript 2; the permeate solution on the low- pressure side of the membrane which is depleted in solute, and which is designated by the subscript 3.

(ii) An aqueous solution is considered, containing n solutes. The mole fraction of the *ith* solute at position p is x_{ip}.

(iii) The transport of each solute is independent of any other, except in that its concentration contributes to the osmotic pressure of the solution. Hence each solute has its own membrane transport coefficient $\mathcal{D}_i$ (in Sourirajan's notation this would be $\left(\frac{D_{AB}}{K\delta}\right)_i$)

(iv) The molar flux of the *ith* solute through the membrane is given by the equation

$$N_i = \mathcal{D}_i c(x_{i2} - x_{i3}) \qquad i = 1,n \tag{12}$$

Here c is the total molar concentration of the solution (mol.m^{-3}). In most practical cases this is very close to the molar concentration of water.

(v) The molar flux of water through the membrane is given by

$$N_w = A(P - \pi_2 + \pi_3) \tag{13}$$

π_2 and π_3 *are the osmotic pressures at the respective positions in the solution.*

(vi) The flux of each solute from the bulk solution to the membrane surface is opposed by a back diffusion down the concentration gradient. The equations describing the interaction between the fluxes and the concentration profiles are

$$\ln\left(\frac{x_{i2} - x_{i3}}{x_{i1} - x_{i3}}\right) = \frac{N_w + \sum_{j=1}^{n} N_j}{\mathcal{K} c} \tag{14}$$

Here $\mathcal{K}$ is the film-diffusion mass-transfer coefficient under the hydrodynamic conditions prevailing in the tube.

2.1.2.2 Re-formulation of the equations

A material balance on the *ith* component in the permeate stream gives

$$x_{3i} = \frac{N_i}{N_w + \sum_j N_j}$$

Hence

$$N_w + \sum_j N_j = \frac{N_i}{x_{i3}} \tag{15}$$

Combining this result with Eqns (12) and (14) and rearranging yields

$$\frac{x_{i2} - x_{i3}}{x_{i1} - x_{i3}} = \exp\left(\frac{\mathcal{D}_i (x_{i2} - x_{i3})}{\mathcal{K} x_{i3}}\right) \tag{16}$$

Combining Eqn (15) with Eqns (12) and (13) and rearranging yields

$$\mathcal{D}_i c(x_{i2} - x_{i3}) = \left(\sum_j \mathcal{D}_j c(x_{j2} - x_{j3}) + A(P - \pi_2 + \pi_3)\right) x_{i3} \tag{17}$$

There is one pair of equations of the forms (16) and (17) for each component i. Thus they constitute a set of $2n$ equations in $2n$ unknown variables (x_{i2} and x_{i3}). It is assumed that the bulk concentrations x_{i1} are known. Thus the set of equations can be solved by a suitable non-linear simultaneous equation solving technique. Once the values of the solute mole-fractions have been obtained, the relevant fluxes can be obtained directly from Eqns (12) to (15). The core modelling problem is therefore the solution of the Eqns (16) and (17).

2.1.3 The Spiegler-Kedem theory

The Spiegler-Kedem theory is a theory of reverse osmosis based on non-equilibrium thermodynamics and the assumptions of the friction model of membrane transport processes. It describes a mechanism for retention of salts, but does not explicitly take equilibrium membrane-solute interactions into account, although these may be indirectly represented via by the reflection coefficient (Spiegler and Kedem, 1966).

For a system involving a single electrolyte in aqueous solution, the salt retention can be described by three transport coefficients :

(i) specific hydraulic permeability, $\bar{A}_h$,

(ii) local solute permeability, $\bar{A}$, and

(iii) the reflection coefficient, σ.

To obtain the relationship between salt retention and flow rate, the following assumptions are made concerning the system (Perry and Linder, 1989) :

(i) the salt can be treated as a single electroneutral species, and

(ii) the differential equations for volume flow (J_V) and salt flow (N_A) are linear.

The local flux equations are given by

$$J_V = -\bar{A}_h\left(\frac{dP}{dx} - \sigma\frac{d\pi}{dx}\right) \tag{18}$$

and

$$N_A = -\bar{A}\left(\frac{dc_A}{dx}\right) + (1-\sigma)c_A J_V \tag{19}$$

where J_V = volume flux, m.s^{-1}

N_A = solute flux, mol.m^{-2}.s^{-1}

P = pressure, Pa

π = osmotic pressure, Pa

x = vertical distance from membrane surface, m

c_A = local solute concentration, mol.m^{-3}

The salt retention coefficient (R) is defined by the salt concentrations in the feed (c_{A1}) and the permeate (c_{A3}), i.e.

$$R = 1 - \frac{c_{A3}}{c_{A1}} \tag{20}$$

Integration of Eqns (18) and (19) yields the expression for salt retention as a function of volume flow,

$$R = \frac{(1-F)\sigma}{1-\sigma F} \tag{21}$$

where $F = \exp\left(-J_V\frac{1-\sigma}{A}\right)$

A is the overall salt permeability, $\left(\frac{\bar{A}}{\delta x}\right)$

The Spiegler-Kedem theory has the advantage that it is able to account for the coupling of solute and solvent fluxes which is an important feature of nanofiltration and ultrafiltration separations, although it is usually negligible for reverse osmosis. The simple Sourirajan PSCF model does not account for flux coupling. While the more complex Sourirajan SF-PF model does so, it involves many more parameters, some of which require detailed laboratory investigation to determine. This makes the practical use of the Sourirajan SF-PF model unlikely in the context of industrial and pilot-scale equipment.

2.2 Prediction of Osmotic Pressure

The osmotic pressure of a solution is a key variable in the consideration of its treatment using a membrane separation process such as reverse osmosis or nanofiltration. Measurements of osmotic pressure are not commonly made as a part of water analysis, and it is advantageous to designers of membrane separation plants to be able to predict osmotic pressures from the conventional chemical analysis of solutions.

Osmotic pressure may be defined in terms of the activity of water (Robinson and Stokes, 1959) as:

$$\pi = -\frac{\mathcal{R}T}{V_w}\ln a_w \tag{22}$$

where π = osmotic pressure, kPa
a_w = activity of water
$\mathcal{R}$ = universal gas constant = 8,314 ℓ.kPa.mol^{-1}.K^{-1}
T = absolute temperature, K
V_w = molar volume of water = 0,018067 ℓ.mol^{-1} at 25 °C

2.2.1 Theory

The activity of water may be calculated by integrating the Gibbs-Duhem equation which for constant temperature and pressure is

$$n_w d\ln a_w = -\sum_j n_j d\ln a_j \tag{23}$$

where n = number of moles
a = activity
j = the jth solute species

The boundary condition for the integration is pure water (a_w).

To perform the integration, the activity coefficients of all solute species must be known functions of concentration. The extended Debye-Huckel equation (Robinson and Stokes, 1959) gives the activity coefficients of charged species as functions of ionic strength:

$$\log\gamma_k = -Az_k^2\left[\frac{\sqrt{I}}{(1+B\rho_k\sqrt{I})}\right]+b_k I \tag{25}$$

where
γ_k = activity coefficient of kth charged species
I = ionic strength $\frac{1}{2}\sum_k z_k^2 m_k$, mol.kg^{-1}

z_k = charge number of *kth* species
m_k = molality of *kth* species, mol.kg^{-1}
A = function of dielectric constant and temperature
= 0,509 kg^{½}.mol$^{-½}$ at 25 °C
B = function of dielectric constant and temperature (kg^{½}.cm^{-1}mol$^{-½}$)
p_k = ion size parameter, cm
b_k = ion specific parameter, kg.mol^{-1}

The first term in the expression for $\log \gamma_k$ is derived from theoretical consideration of the electrostatic interactions between ions in the solution, and the second term is empirical, arising from the observation that at higher solution concentrations $\log \gamma_k$ varies linearly with I.

The Davies equation (Davies, 1962) is a simplified version of the Debye-Huckel equation which avoids the use of individual ion parameters other than charge:

$$\log \gamma_k = -A z_k^2 \left[\frac{\sqrt{I}}{(1+\sqrt{I})} - bI \right] \tag{26}$$

Here b is an average value of all the relevant b_k values.

Figure 2 shows the activity coefficients for each charge number as calculated by the Davies equation. The higher the charge, the smaller the activity coefficient of the species and hence the smaller its effect on the activity of water.

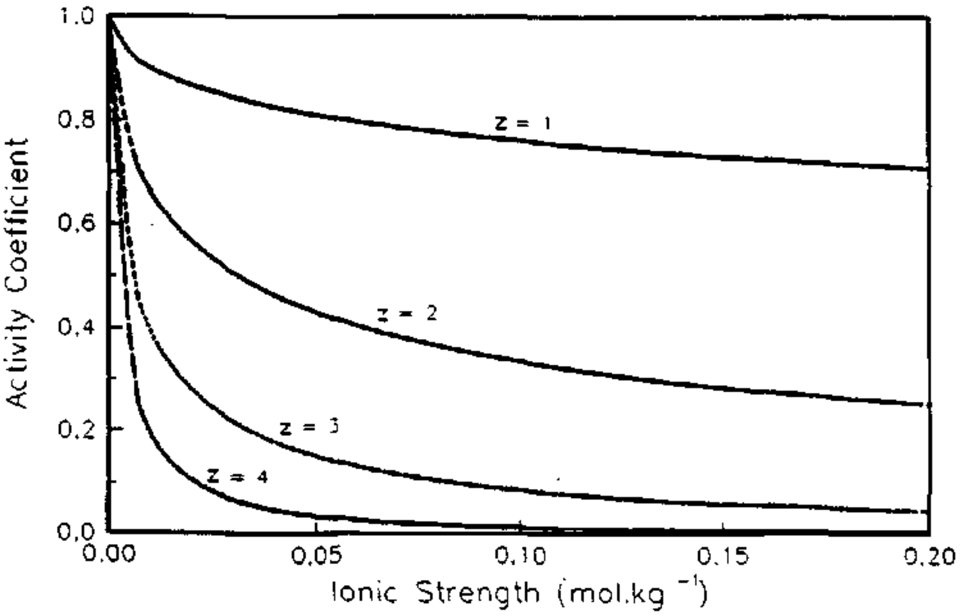

Figure 2 : Activity coefficients of charged species predicted by the Davies equation

The activity coefficients of neutral species may be modelled (Helgeson, 1969),

$$\ln \gamma_i = \alpha I \qquad (27)$$

where α is a constant.

2.2.2 Method of investigation

1. An expression for the activity of water was derived from Eqns (23), (24) and (25).
2. Speciation data from a previous investigation (Brouckaert, 1992) was substituted into the equation and the results used in Eqn (22). Optimum values for the parameter b were found by minimising the sum of square errors of the osmotic pressure estimates.
3. The osmotic pressures calculated from the new activity of water estimate were compared to those obtained using the linear correlation.
4. The effect of pH on speciation and osmotic pressure for sodium triphosphate acidified with phosphoric acid was investigated using MINTEQA2 (Allison, Brown and Novo-Gradac, 1990). A 0,08 mol.kg^{-1} solution of Na_3PO_4 was acidified to various pH values from 2 to 12 by replacing Na^+ by H^+ and the resulting speciation and osmotic pressures plotted against pH.

2.2.3 Results

(i) Theoretically based estimate of the activity of water:

The final result of the integration was:

$$55.52 \ln a_w = -\sum_i m_i - \sum_k m_k - 4.606A\left[1 + \sqrt{I} - 2\ln(1 + \sqrt{I}) - \frac{1}{(1 + \sqrt{I})}\right] - 2.303AbI^2 \qquad (27)$$

The first two terms give the total concentration of solute species, the third gives the electrostatic contribution and the fourth is empirical.

(ii) Optimisation of the parameter b:

Davies originally suggested a value of 0,1 ℓ.mol^{-1} for the product Ab, ie. b = 0,197 kg$^{\frac{1}{2}}$.mol$^{-\frac{1}{2}}$ at 25 °C. For the set of solutes in this investigation, however, the smallest average square error was given by b = 0,067 kg$^{\frac{1}{2}}$.mol$^{-\frac{1}{2}}$. It was noted that the five data points with literature osmotic pressures greater than 2 000 kPa had a disproportionate effect on the error function and hence on the value of b obtained. Excluding these data points from the error function gave an optimum b = 0,079 kg$^{\frac{1}{2}}$.mol$^{-\frac{1}{2}}$. The second value was used in the comparison with literature values shown in Fig. 3.

The osmotic pressure estimates showed good agreement with literature values up to 2 000 kPa but were increasingly inaccurate at high concentrations.

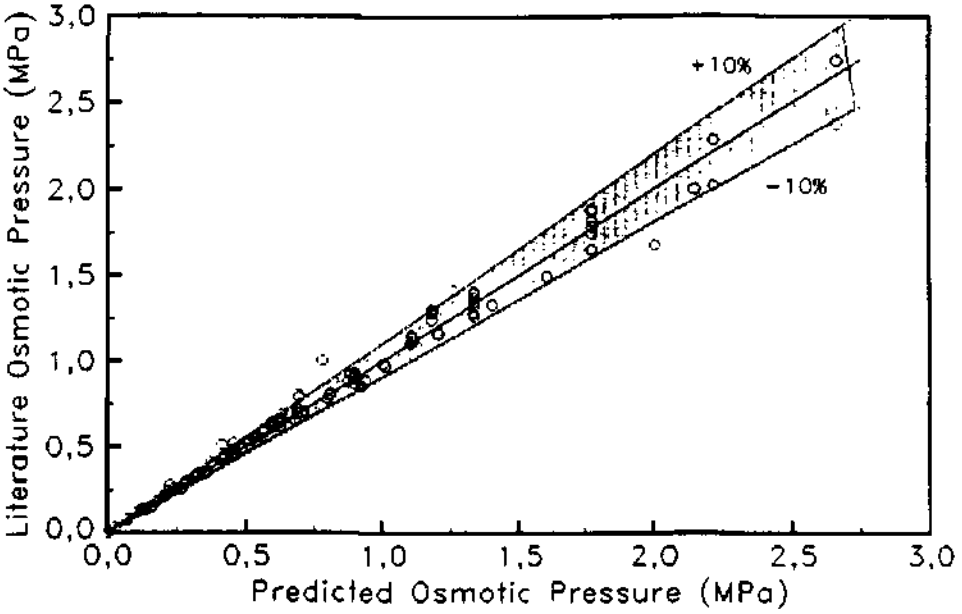

Figure 3 : Literature vs predicted osmotic pressure

Optimising b for solutions representing typical feeds, permeates and concentrates from a reverse osmosis plant treating cooling water at the Lethabo power station (Brouckaert, 1991) gave a value of 0,254 $kg^{\frac{1}{2}}.mol^{-1}$. The apparently large discrepancy between this and the average value for b shows that the optimum value depends on the set of data considered. However, the difference in the osmotic pressure estimates for these dilute solutions using the two different values was negligible: the correlation is only sensitive to the value of b at high concentrations.

(iii) Relationship between osmotic pressure and speciation for trisodium phosphate

The osmotic pressure curve in Fig. 4 closely follows the concentration of Na^+, the most prevalent species. The net contribution of the other species decreases with increasing pH as the charge of the second most prevalent species increases.

A similar investigation was carried out on the Lethabo data involving carbonates. Although the speciation of the carbonates changed significantly with pH, it was in such a way that the osmotic pressure remained practically constant.

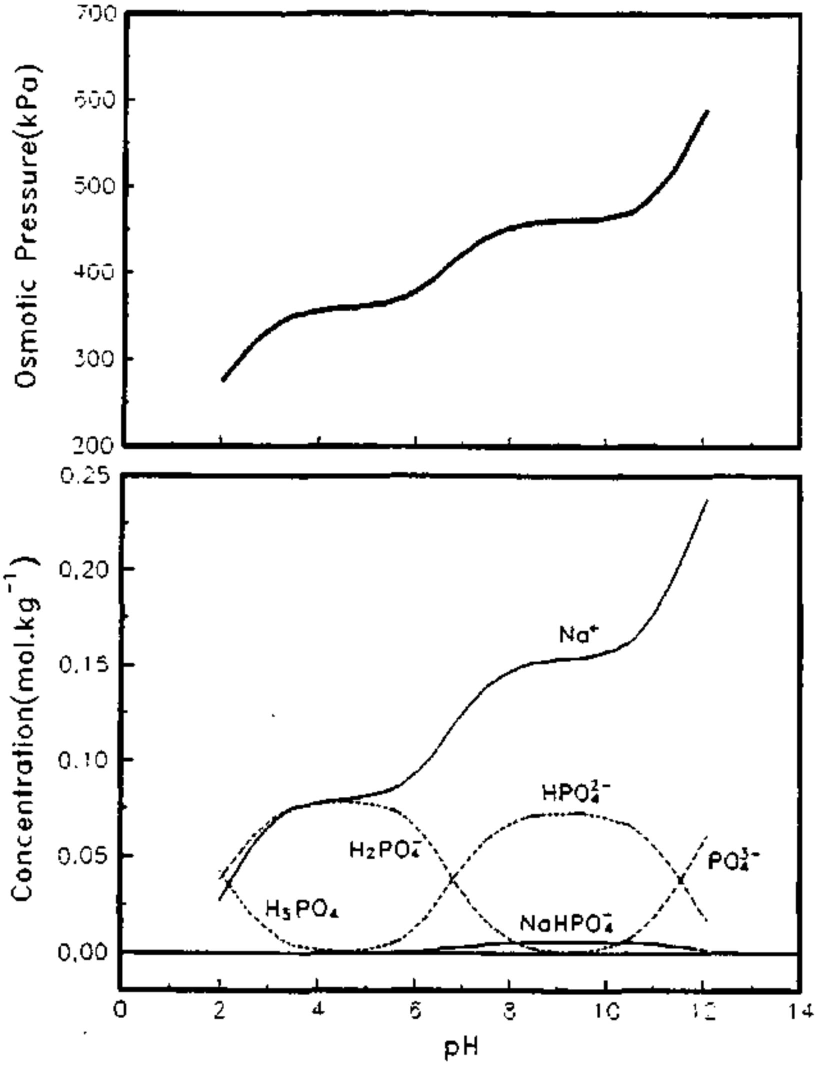

Figure 4 : Speciation and osmotic pressure as functions of pH for tri-sodium phosphate

2.2.4 Discussion

Eqn (27) is a convenient estimate of the activity of water involving only two variables: the total concentration of species and the ionic strength and one fitted parameter.

Its disadvantage is that the Debye-Huckel theory only holds up to $I \approx 0.1$ mol.kg^{-1} and although the empirical term greatly increases its useful concentration range, it probably will not give reliable results at higher concentrations than have been used here.

Theoretically, a better correlation could be obtained by using the more rigourous Debye-Huckel equation instead of Davies. However, this would involve a much more complicated integration and would also require values of b_k and ρ_k for each species, which might not be available.

Since the osmotic pressure correlation is not usually sensitive to b except at high concentrations, using the average optimum value should be quite adequate in most cases. However, in some cases it may be advantageous to optimise b for the solutes and concentration range relevant to a particular application.

Graphs presenting osmotic pressure as a function of pH for a particular process stream could be a useful means of estimating osmotic pressure on site.

All the data required in Eqn (27) is already part of the MINTEQA2 output and therefore it could easily replace the unsatisfactory activity of water estimate used at present.

2.2.5 Conclusion

Osmotic pressures of aqueous ionic solutions may be estimated within ±10% up to 2 MPa for a wide range of inorganic salts using Eqns (22) and (27). The optimum value for the parameter b depends on the solutes and concentrations involved, however, since the correlation is only sensitive to b at high concentrations, using the average value of $b = 0{,}079\ \mathrm{kg}^{\frac{1}{2}}.\mathrm{mol}^{-\frac{1}{2}}$ should be adequate in most cases. Eqn (27) is an improvement on both the linear correlation developed previously and the one used in MINTEQA2.

2.3 Prediction of Conductivity

Conductivity is often used as an overall indicator of concentration of ionic solutes in the streams associated with reverse osmosis plants. Frequently it is the only such indicator available for a particular stream. While it is not possible to deduce the underlying solution composition from the conductivity alone, it may be possible to estimate composition from the conductivity together with information on other streams through modelling of the RO process. This requires the relationship between composition and conductivity to be known. An investigation was undertaken to establish a means of predicting conductivity from solution composition, using published data on the conductivities of various solutions. Since conductivity is some product of ionic mobility in solution and the ionic charge, it was apparent that the speciation of ions in a solution should be taken into account.

2.3.1 Theoretical background

The theory of ionic conductivity has been reviewed by Erdey-Grúz (1974). Equivalent conductivity Λ is the conductivity of the solution divided by the number of molar equivalents of ions dissolved in it. For a dissociated electrolyte, the limiting value of equivalent conductivity, Λ°, for an extremely dilute solution is

$$\Lambda^{\circ} = \lambda_c^{\circ} + \lambda_a^{\circ} \tag{28}$$

where λ_c° = limiting conductivity of the cation

λ_a° = limiting conductivity of the anion

In the limit, the conductivity of each ion is independent of that of other ions present in the solution. Because of interactions between ions, the mobility of a given ion depends on the nature and concentrations of other ions present and, in a solution of finite dilution, the law of independent migration is not valid.

For very dilute solutions the empirical *square root law of Kolrausch* is valid:

$$\Lambda = \Lambda^{\circ} - K\sqrt{c} \tag{29}$$

where Λ = the equivalent conductivity of a known solution
c = the concentration of the known solution
K = a constant dependent on the valence of the ion

The higher the ion valence, the higher the value of K. At higher concentrations, the square root dependence on composition no longer holds.

For solutions containing more than two ions, Eqns (28) and (29) are generalized as :

$$\kappa = \sum c_i \; |z_i| \; \lambda_i \tag{30}$$

where κ = the specific conductivity of the solution
c_i = the concentration of i th ion
z_i = the ionic charge on the i th ion

For mixed electrolytes at higher concentrations the theory does not predict conductivity accurately.

2.3.2 Basis of the present correlation

The correlation developed here makes use of four basic ideas :

a) equilibrium speciation to obtain the distribution of ions actually present in the solution.

b) a limiting specific solution conductivity at 20 °C calculated from the distribution of ions and the limiting equivalent conductivities of the original ions.

c) a correction for concentration of similar form to the Kolrausch law.

d) a correction for temperature of the form (Talbot, House and Pethybridge, 1990)

$$\kappa(T) = \kappa(20^{\circ}C)\left[\frac{\mu(20^{\circ}C)}{\mu(T)}\right]^{0.896} \tag{31}$$

The MINTEQA2 program (Allison, Brown and Novo-Gradac, 1990) was used for the speciation step, and the following equations were used for steps *b* and *c* :

$$\kappa^{\circ} = \sum c_i \; |z_i| \; \lambda_i^{\circ} \tag{32}$$

$$\kappa = \kappa^{\circ} - K_1 I^{K_2} \tag{33}$$

$$I = \frac{1}{2}\sum z_i^2 c_i \tag{34}$$

where I = the ionic strength of the solution

K_i = are constants that are fitted to the experimental data

The constants were fitted to data obtained from Weast (1983) for solutions of $CaCl_2$, KNO_3, $MgCl_2$, $MgSO_4$, Na_2SO_4 and K_2SO_4 (which contain the major ions found in power station cooling water and mine effluents). Solute concentrations up to 0,7M ionic strength were considered. The values of K_1 and K_2 which gave the best results were $K_1 = 27.606$ and $K_2 = 1.28$.

A graphical comparison of measured and fitted values for these solutions at 20 °C is presented in Fig. 5.

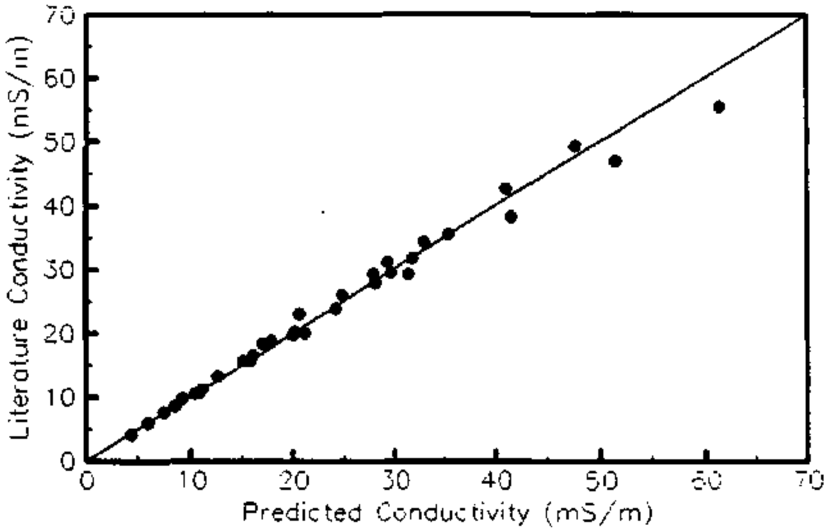

Figure 5 : Comparison of conductivity predictions with literature data at 20 °C

2.3.3 Discussion

Although the correlation shows excellent agreement with the data, it is not clear how well it will perform with solutions of other electrolytes. Because of the data available, the solutions considered contained only one electrolyte per run. Its predictive power for mixed electrolytes is therefore also unproven. Problems also arise with solutes which form complex ions for which the limiting equivalent conductivities are not known. Thus there is room for further work to improve and verify the method. Nevertheless it provides a reasonable basis for estimating conductivity in the absence of more specific information.

2.4 The Turbulent Film Mass Transfer Coefficient, $\mathcal{K}$

The film mass transfer coefficient on the high pressure side of the membrane is an important parameter for determining the extent of concentration polarisation that occurs (refer to section 2.1.1). Various correlations appear in the literature which refer to specific geometric and hydrodynamic situations.

2.4.1 Tubular modules

The following correlation (Belfort, 1984) may be used to determine the mass transfer coefficient in tubular membranes for turbulent flow conditions:

$$Sh = 0.0096\, Re^{0.913}\, Sc^{0.346} \tag{35}$$

where

$$Sh = \frac{\mathcal{K}\, d}{D_{AB}} \tag{36}$$

$$Re = \frac{\rho\, d\, u}{\eta} \tag{37}$$

$$Sc = \frac{\eta}{\rho\, D_{AB}} \tag{38}$$

D_{AB} is the diffusion coefficient of the solute in water
d is the diameter of the tube
ρ is the density of the feed solution
η is the viscosity of the feed solution
v is the linear flow velocity of the feed

The equations used in the current model were not modified. It was found that the expression of the model flux and rejections are not very sensitive to the form of the correlation. This justified the use of equations that gave the right magnitude.

2.4.2 Spiral wound modules

A number of correlations were found in the literature for mass transfer coefficients in spiral wound modules. However, in most cases, these were specific to a particular make and model of module. An equation quoted by Rautenbach and Albrecht (1989) from Chiolle et al. (1987) contains terms which account for the module design.

$$Sh = 1{,}065 \left[\frac{h}{l_{sp}} \times \frac{\mu_{sp}}{2-\mu_{sp}} \right]^{0.5} Re^{0.5}\; Sc^{0.333} \tag{39}$$

where h = the flow channel width
l_{sp} = mesh spacing of spacer net
μ_{sp} = mixing efficiency factor

The correlation was evaluated against experimental results on a FilmTec NF40-2514 module consisting of four leaves of flat sheet membranes, separated by polypropylene mesh spacers, and wound into typical spiral configuration. The correlation was shown to give reasonable approximation to the experimental conditions.

2.5 Miscellaneous Correlations

The correlations require values of viscosity, solute diffusivity and pressure drop through the modules. The evaluation of these variables is fundamental to the accurate calculation of the membrane performance variables but the evaluation procedure is not necessarily part of the portfolio of membrane theory. The equations from which these values can be determined are presented in the sections below for completeness.

2.5.1 Viscosity and density of water

The following formulae for the viscosity of water are given by the CRC Handbook of Chemistry and Physics (Weast, 1975).

For the temperature range 0 to 20 °C :

$$\log_{10}\mu = \frac{1301.0}{998.333 + 8.1855(T_c - 20) + 0.00585(T_c - 20)^2} - 3.3023 \qquad (40)$$

where μ = the viscosity of water in centipoise

T_c = the temperature in °C

For the temperature range 20 °C to 100 °C :

$$\log_{10}\left(\frac{\mu}{1.002}\right) = \frac{1.3272(20 - T_c) - 0.001053(T_c - 20)^2}{T_c - 105} \qquad (41)$$

2.5.2 Diffusivities of solutes in water

Electrolyte diffusivities in dilute solutions are commonly available at 25 °C (298 K) (e.g. the CRC Handbook of Chemistry and Physics). To convert to different temperatures, Reid, Prausnitz and Polling (1987) recommend the correlation for electrolytes :

$$D(T) = \frac{D(298)T}{334\mu} \qquad (42)$$

where D = the diffusivity of the solute in water

μ = the viscosity of water in centipoise at T

T = the absolute temperature in K

2.5.3 Calculation of the average diffusivity of a mixed ionic solute

When modelling a mixed ionic solute as a single entity, a problem arises in determining a representative value from the individual ionic mobilities. The diffusion of ionic mixtures is a complex phenomenon because the motion of the ions is subject to the electroneutrality constraint, which prevents their motions being independent. In the case of a single cation and a single anion the analysis is relatively simple, since the two ions are constrained to move at the same velocity, and the effective diffusivity of the neutral salt is the combination of the individual ionic diffusivities according to the Nernst-Hartley equation (Robinson and Stokes, 1959). In the case of a mixture of ionic salts, electroneutrality can be satisfied in a number of ways, and the interaction between ionic mobilities becomes complex (Reid, Prausnitz and Poling, 1989).

If the mixed solute is to be treated as a single entity, with a single average value of diffusivity, it becomes appropriate to approximate the situation as being represented by a single diffusion velocity applied to all the ions present. The average diffusivity should therefore be calculated by a multi-component extension to the Nernst-Hartley equation. The following derivation is modelled on the treatment of the Nernst-Hartley equation in Robinson and Stokes.

As ions diffuse through the solution under the influence of a concentration gradient, their unequal mobilities give rise to a charge separation, which in turn causes an electrical potential gradient, which limits the extent of the charge separation to the extent that it can be neglected for all purposes except calculating the potential gradient. A force balance on the ith ion gives:

$$v = \mu_i\left(-\frac{1}{N}\frac{\partial \bar{G}_i}{\partial x} + z_i e E\right) \tag{43}$$

where:

v	is the diffusion velocity of the ion, which is here taken as the same for all the ions in the solution
μ_i	is the ionic mobility.
$\frac{\partial \bar{G}_i}{\partial x}$	is the gradient of partial molal Gibbs Free Energy of the ion as a result of its concentration gradient.
N	is Avogadro's number.
z_i	is the ionic charge number.
e	is the charge of an electron.
E	is the local electrical potential gradient.

This equation applies to every ion in the solution, and may be re-arranged to:

$$z_i = \frac{1}{eE}\left(\frac{v}{\mu_i} + \frac{1}{N}\frac{\partial \bar{G}_i}{\partial x}\right) \tag{44}$$

The electroneutrality condition is expressed as

$$\sum_i n_i z_i = 0 \tag{45}$$

where:

n_i is the number of i - ions in the solution.

Substituting for z_i from Eqn (44) and re-arranging gives

$$v = -\sum_i \frac{n_i}{N}\frac{\partial \bar{G}_i}{\partial x} \;/\; \sum_i \frac{n_i}{\mu_i} \tag{46}$$

The partial molal Gibbs Free Energy is expressed as

$$\bar{G}_i = G_i^\circ + \mathcal{R}T\ln(\gamma_i m_i) \tag{47}$$

where:

G_i° is the molar Gibbs Free Energy of the ion in its standard state.
m_i is the ion's concentration (mol/kg)
γ_i is the ion's activity coefficient.

Thus

$$\frac{\partial \bar{G}_i}{\partial x} = \mathcal{R}T\left(\frac{\partial \ln m_i}{\partial x} + \frac{\partial \ln \gamma_i}{\partial x}\right) \tag{48}$$

If the variation of activity coefficient is neglected, substituting this into Eqn (46) gives

$$v = -\mathcal{R}T\sum_i \frac{\partial m_i}{\partial x} \;/\; \sum_i \frac{n_i}{\mu_i} \tag{49}$$

The overall solute flux is given by

$$J = \sum_i m_i v = -\mathcal{R}T\sum_i m_i \sum_i \frac{\partial m_i}{\partial x} \;/\; \sum_i \frac{n_i}{\mu_i} \tag{50}$$

This expression is compared with the defining expression for diffusivity

$$J = -\mathcal{D}\frac{\partial m}{\partial x} \tag{51}$$

Since the solutes are all being treated as one substance

$$\frac{\partial m}{\partial x} = \sum_i \frac{\partial m_i}{\partial x} \tag{52}$$

so

$$\mathcal{D} = \mathcal{R}T\sum_i m_i \;/\; \sum_i \frac{n_i}{\mu_i} \tag{53}$$

Finally, the ionic mobilities are related to the limiting ionic equivalent conductivities λ_i by

$$\mu_i = \frac{N\lambda_i}{|z_i|F^2} \tag{54}$$

so the average diffusivity is given by

$$D = \frac{\mathcal{R}T}{F^2}\sum_i m_i \;/\; \sum_i \frac{m_i}{|z_i|\lambda_i} \tag{55}$$

Limiting equivalent ionic conductivities are tabulated in a number of texts, for instance Weast (1984) and Reid, Prausnitz and Poling (1988).

2.5.4 Pressure drop in membrane modules

There is usually a significant pressure reduction between the inlet and retentate outlet of a membrane separation plant which needs to be accounted for in calculating the overall permeate and solute flux rates through the membranes. The pressure drop can be considered as originating in three ways:

a) due to cross flow tangential to the membrane surface.

b) due to flow distribution fittings within the modules.

c) due to piping, manifolds and fittings external to the modules.

In practice, empirical equations are often supplied by manufacturers for their modules which incorporate the affects of both *a* and *b* above. In the relatively simple case of a tubular membrane module, reasonably accurate predictions of the pressure drop can be made by considering the geometry of the tubes and internal fittings, however for other designs, such as spiral wound modules, the pressure drop is dependent on details of the spacer mesh which is placed between the membrane surfaces, and is not reliably predictable from first principles.

2.5.4.1 Tubular modules

According to Rautenbach and Albrecht (1989) the following equations may be used for the pressure drop in the tubes:

$$\frac{dP}{dL} = -\frac{\xi \rho v^2}{2d} \tag{56}$$

$$\xi = 0.316\,Re^{-0.25} \qquad 2\ 000 < Re < 100\ 000 \tag{57}$$

$$\xi = \frac{64}{Re} \qquad Re < 2\ 000 \tag{58}$$

where P = the pressure at a point in the tube
L = the length of tube through which the fluid passes
ρ = the solution density
v = the flow velocity at the point
d = the tube diameter
μ = the solution viscosity
Re = the Reynolds number $\frac{\rho v d}{\mu}$.

The tubes in a series flow tubular module are connected by 180° bends. Pressure drop is such bends is frequently described in terms of a *loss coefficient* C thus:

$$\Delta P = C\frac{\rho v^2}{2} \tag{59}$$

Perry, Green and Maloney (1984) suggest a value for C for smooth 180° bends of 1,5.

One example of a manufacturer supplied empirical equation for the pressure drop across a module (in kPa), ΔP, for a tubular module is that for a Membratek RO module:

$$\Delta P = (19{,}13 + 9{,}56 \cdot L)v^2 \tag{60}$$

The relationship of the equation to the individual pressure drop contributions discussed above is evident.

Wherever possible, one would use the manufacturer's data for modelling. Where these correlations are not available, one must use equations such as (59) and obtain the necessary constants by regression on the performance data.

2.5.4.2 Spiral wound modules

According to Rautenbach and Albrecht (1989) the equation for pressure drop in a spiral wound module is similar to that for a tubular module:

$$\frac{dP}{dL} = -\frac{\xi \rho v^2}{2d} \tag{61}$$

where $\xi = C\,Re^{-K}$

The coefficients C and K depend on the detailed geometry of the spacer mesh which holds the sheets of membrane apart; examples of values C in the range 1 000 to 2 000 and K in the range 0,78 to 1,0 are quoted for various modules.

Spiral wound modules do not usually have any internal fittings which contribute significantly to the overall pressure drop.

Rautenbach and Albrecht (1989) quote an empirical equation for an 8 inch diameter Toray 1200 spiral wound module :

$$\Delta P = 1{,}342 \times 10^{-5} v^2 \tag{62}$$

where ΔP is expressed in bar and v is in m.s^{-1}. This is equivalent to treating the friction factor ξ as a constant.

2.6 Ultrafiltration Theory

2.6.1 Introduction

Ultrafiltration membranes are typically used to concentrate the colloidal or macromolecule components of feed liquors. The membranes have larger average pore sizes than reverse osmosis membranes and operate at lower pressures. Ultrafiltration is a suitable pretreatment for many reverse osmosis applications. This study is restricted to the modelling of tubular ultrafiltration.

The tubular membrane element has relatively large flow channels compared with other designs, hence they are less prone to blocking and higher flow velocities can be attained with lower pressure drops. This is important in the ultrafiltration of industrial effluents which contain suspended matter, are highly concentrated or viscous, or contain components with gel forming properties.

Since ultrafiltration systems operate at relatively low pressures, the pressure drop across the modules can be substantial compared to the inlet pressure. Determination of the relationship between the linear flow velocity in the tubes and the pressure drop across the modules in any configuration is required to compare various module configurations and to optimise the flow velocity.

2.6.2 Models for predicting flux

Assuming an ideal situation (all the pores in the membrane are of the same size and uniformly distributed, no fouling and negligible concentration polarisation), the fluid flow through an ultrafiltration membrane can be described using the Hagen-Poiseuille law for stream-line flow through channels (Cheryan, 1986) :

$$J = \frac{\epsilon R^2 P_T}{8 \eta \Delta x} \qquad (63)$$

where J = permeate volume flux, $m^3.m^{-2}.s^{-1}$
R = mean pore radius, m
P_T = applied transmembrane pressure, Pa
η = viscosity of the fluid permeating the membrane, $kg.m^{-1}.s^{-1}$
Δx = membrane thickness, m
ϵ = surface porosity, dimensionless

The driving force (P_T) should be replaced by the difference between the transmembrane hydrostatic pressure and the transmembrane osmotic pressure ($P_T - \Delta\pi_T$), when real feed solutions are considered. This is not usually done since the osmotic pressures of retained solutes is usually negligible due to their high molecular masses.

According to this model, the flux is directly proportional to the applied transmembrane pressure and inversely proportional to the viscosity. The viscosity can be decreased by decreasing the solute concentration or increasing the temperature. Increases in the pressure or temperature only lead to increases in flux when the pressure and feed concentration are sufficiently low and the feed flow rate is sufficiently high. Under conditions of strong concentration polarisation the Hagen-Poiseuille model no longer applies and mass transfer limited models must be used.

2.6.3 Models for predicting limiting flux

Limiting flux behaviour is generally attributed to the hydrodynamic resistance of the gel and boundary layers. Convective transport of solute towards the membrane leads to the development of a steep concentration gradient in the boundary layer between the bulk feed and the membrane surface (see Fig. 6). Back transport of the solute into the bulk feed occurs by diffusion. A steady state is eventually reached in which these two effects are balanced and the solute concentration in this gel-layer it at its maximum, denoted c_{2g}. The higher this concentration, the greater the chance of precipitation of solute on the membrane, i.e. membrane fouling.

This dense gel-layer causes flux to be independent of pressure at sufficiently high pressure. Increases in pressure cause the gel layer to become thicker or more dense. When the pressure is increased, the flux increases initially and then decreases again. The flux can be increased by enhancing the rate of back transport of the solutes from the gel-layer into the bulk feed. If the pressure or the feed concentration can be decreased or the feed flow rate increased, then it may be possible to return to the pressure-controlled region (see Fig. 7). If membrane fouling has occurred, then cleaning will be required to increase the flux (Cheryan, 1986).

Four models for predicting the limiting flux are discussed here :

(i) the mass transfer model (film theory)

(ii) the resistances in series model

(iii) the osmotic pressure model

(iv) Flemmer's model

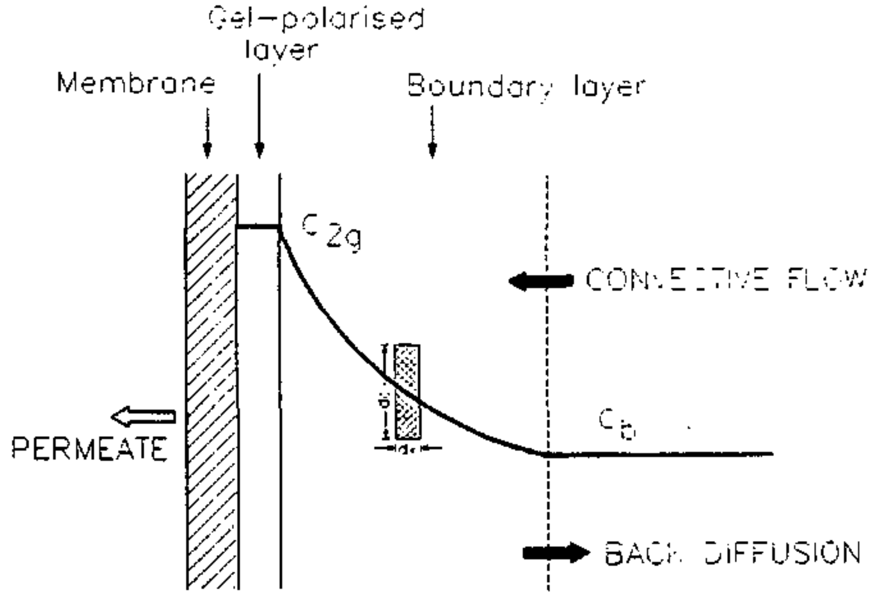

Figure 6 : Schematic diagram showing mechanism of formation of gel-polarised layer and boundary layer

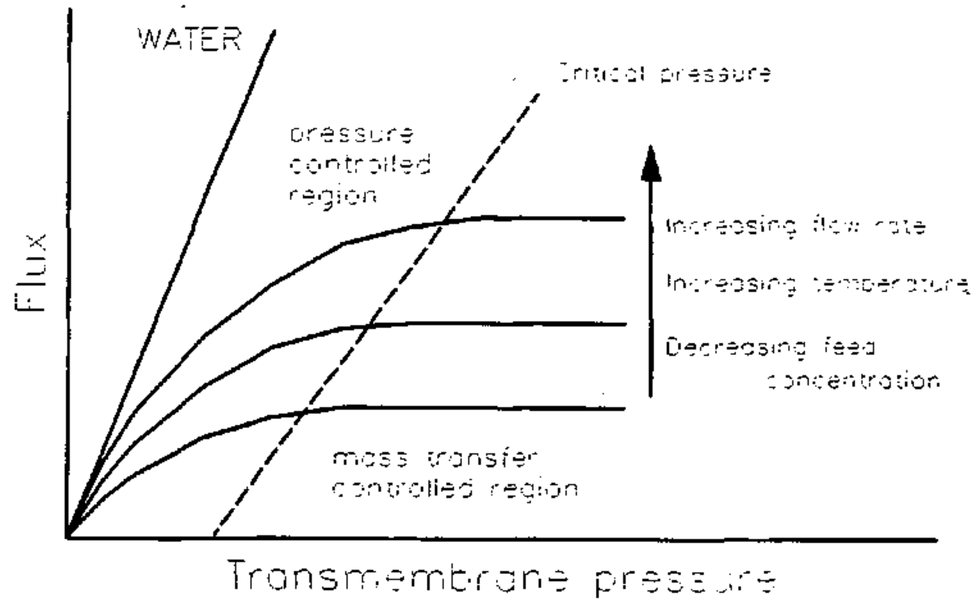

Figure 7 : Generalised correlation between operating parameters and flux, indicating the areas of pressure control and mass transfer control and the critical pressure at which gel polarisation occurs

2.6.3.1 Mass transfer model (film theory)

The mass transfer model is valid only in the pressure-independent region. There are two solute transport mechanisms operating on the high pressure side of the membrane. The first is the transport of solute to the membrane surface by convective transport at rate,

$$J_s = J c_l \tag{64}$$

where J_s = permeate solute flux (kg.m^{-2}.s^{-1})
J = permeate volume flux (m^3.m^{-2}.s^{-1})
c_1 = bulk concentration of the retained solute (kg.m^{-3})

This leads to the development of a concentration gradient in the boundary layer adjacent to the membrane surface. The second transport mechanism is hence the back-transport of solute into the bulk solution by diffusion, at rate (assuming there are no axial concentration gradients),

$$J_s = -D\frac{dc}{dx} \tag{65}$$

where D = diffusion coefficient (m^2.s^{-1})
$\frac{dc}{dx}$ = concentration gradient over a differential element in the boundary layer (kg.m^{-4})

At steady state, these two transport mechanisms occur at the same rate, and the resulting equation can be integrated over the boundary layer, i.e.,

$$J\int_0^l dx = -D\int_{c_1}^{c_{2g}} \frac{dc}{c} \tag{66}$$

where l = thickness of the boundary layer, m

c_{2g} = concentration of the solute in the gel-polarised layer kg.m^{-3}

Hence,

$$J = -\frac{D}{l}\ln\left(\frac{c_{2g}}{c_1}\right) = -\mathcal{K}\ln\left(\frac{c_{2g}}{c_1}\right) \tag{67}$$

where $\mathcal{K}$ = mass transfer coefficient m.s^{-1}

There is no pressure term involved this model, hence it is valid only in the pressure-independent region. The flux is controlled by the rate of back-transport of the solute into the bulk solution. Generally, c_{2g} and c_1 are fixed, so flux can only be improved by increasing $\mathcal{K}$, by increasing the flow rate or temperature, for example.

2.6.3.2 Resistance model

The resistance model can be used to describe the pressure-flux relationship for all pressures. For an ideal membrane and solution

$$J = \frac{AP}{\mu} \tag{68}$$

where A = membrane permeability coefficient, m

The relationship

$$\frac{A}{\mu} = \frac{1}{R_m} \tag{69}$$

where R_m = intrinsic membrane resistance using pure water as feed, kg.m^{-2}.s^{-1}

gives

$$J = \frac{P}{R_m} \tag{70}$$

The resistance of the membrane itself (R_m) is only part of the total resistance experienced during operation on an actual feed solution. The intrinsic resistance of the membrane is affected by membrane fouling due to physico-chemical interactions and the associated resistance is unaffected by the operating parameters. Hence, the resistance due to fouling is combined with the intrinsic membrane resistance to give R'_m. The resistance due to the polarised layer (R_p) is affected by the operating parameters. Hence the flux is given by

$$J = \frac{P}{R'_m + R_p} \tag{71}$$

R_p consists of resistances due to the gel-polarised layer and the boundary layer, and is a function of applied pressure, hence the resistance model becomes

$$J = \frac{P}{R'_m + \phi P} \tag{72}$$

where ϕ = a constant

2.6.3.3 Osmotic pressure model

In the osmotic pressure model, it is assumed that the deviations from the pure water flux are due only to the osmotic pressure at the membrane surface, i.e.

$$J = \frac{P_T - \Delta\pi_T}{R_m} = \frac{P_T - \pi_m}{R_m} \tag{73}$$

For most macromolecules, the osmotic pressure can be expressed by the virial expansion :

$$\pi = K_1 c + K_2 c^2 + K_3 c^3 + \ldots \tag{74}$$

or even

$$\pi = K c_2^n \tag{75}$$

where c_2 is the concentration at the membrane surface

K_i are constants

$n > 1$

In general,

$$\pi_2 = f(c_2) \tag{76}$$

c_2 can be determined using the film theory,

$$c_2 = c_1 \exp\left(\frac{J}{K}\right) \tag{77}$$

Hence,

$$J = \frac{P - f\left(c_1 \exp\left[\frac{J}{K}\right]\right)}{R_m} \tag{78}$$

2.6.3.4 Flemmer's model

In the case of complete gel-polarisation, this model is represented by an equation of similar form to the Mass Transfer Model (Eqn (61)). However, this model accounts for the more general case in which only some of the surface area of the membrane is under gel-polarisation. The model was originally developed for spiral-wound modules with turbulence-promoting nets, however the general form of the resulting equations should be the same as for tubular modules.

Case 1 : Complete Gel-Polarisation

The derivation of the model was described by Flemmer et al. (1982). The final expression for the case of complete gel polarisation is

$$J = \alpha c_1^{\beta} Q^{\gamma} \ln\left(\frac{c_{2g}}{c_1}\right) \tag{79}$$

where α, β and γ are constants (for a particular module, operated at a fixed temperature and solute)

c_1 = bulk concentration of the retentate, kg.m^{-3}

c_{2g} = concentration in the gel layer, kg.m^{-3}

Q = volumetric flow rate of the retentate, m^3.s^{-1}

Note that the since the membrane is gel-polarised, the model contains no term involving pressure.

Case 2 : Incomplete Gel-Polarisation

The following analysis is due to Flemmer (1983). In this case it is assumed that due to the variation of pressure in the system, some of the membrane area will be exposed to conditions under which gel-polarisation does not occur. The total transmembrane pressure has two components. The first is due to resistance to flow through the membrane itself, while the second is due to resistance to flow through the gel layer. When gel-polarisation occurs, the second component increases with the prevailing transmembrane pressure and the permeate flux is controlled by the mass transfer in the retentate. In addition, increasing osmotic pressure reduces the effective transmembrane pressure. It is assumed that at any point on the membrane surface, either gel-polarisation occurs or the turbulence in the retentate is such that gel-polarisation does not occur. Hence, the relationship determined in the case where complete gel-polarisation occurs is now interpreted as

$$J = \alpha c_1^{\beta} Q^{\gamma} \ln\left(\frac{c_{2w}}{c_1}\right) \tag{80}$$

where c_{2w} = concentration at the membrane wall, kg.m^{-3}

When gel-polarisation occurs, $c_{2w} = c_{2g}$. If c_{2g} is fixed for a particular gel, then for lower permeate fluxes, Eqn (80) cannot apply and the flux is not mass transfer controlled. Hence, if the system is such that Eqn (80) demands that $c_{2w} < c_{2g}$, then the gel layer will be stripped away (if it exists).

For a module with pressure P_{in} at the inlet and P_{out} at the outlet, there will be some critical pressure P_c above which gel-polarised conditions occur. (P_c may occur outside the range P_{out} to P_{in}.) Assuming that the permeate flow through the membrane is laminar, a constant δ can be defined to describe the permeability of the membrane, i.e.,

$$J = \delta P_T \tag{81}$$

where P_T = transmembrane pressure at point under consideration

δ depends on the membrane and its condition of fouling, but is not related to any gel layer on the membrane surface. At the critical pressure P_c, from Eqns (79) and (81),

$$J = \delta(P_c - \pi) = \alpha c_1^{\beta} Q^{\gamma} \ln\left(\frac{c_{2g}}{c_1}\right) \tag{82}$$

At the critical pressure, the permeate flux has increased to the point where the process is limited by mass transfer and

$$P_c = \alpha c_1^{\beta} Q^{\gamma} \ln \frac{(c_{2g}/c_1)}{\delta} + \pi \tag{83}$$

If it is assumed that the nature of the retentate does not change along the module, then the local pressure will vary linearly along the module. A fraction F of the total area of the membrane will be under conditions of gel-polarisation, where

$$F = \frac{P_{in} - P_c}{P_{in} - P_{out}} \tag{84}$$

If $P_c < P_{out}$, then $F = 1$ and if $P_c > P_{in}$, then $F = 0$. If it is assumed that the osmotic pressure is controlled by the colligative properties of the solution, say $\pi = \zeta c_1$, then

$$J = \alpha c_1^{\beta} Q^{\gamma} \ln\left(\frac{c_{2g}}{c_1}\right) F + \delta\left[\frac{(P_c + P_{out})}{2} - \zeta c_1\right](1 - F) \tag{85}$$

where $P_c = P_{in}$ for $F = 0$.

In Eqn (85), the first term represents the flux through the portion which is polarised, whereas the second term represents the flux through the portion that not polarised. ζ and c_{2g} can be found in the literature for some feed solutions. δ describes the condition of fouling of the membrane, while α, β and γ are constant for a particular module type and solute.

2.7 Nanofiltration Theory

Nanofiltration usually involves the use of modified thin-film composite membranes. The membranes are generally formed by chemically grafting a high density of negatively charged hydrophilic groups onto a hydrophobic ultrafiltration substrate. Since nanofiltration membranes have a negative surface charge, co-ions (negatively charged) will be repelled and, since electroneutrality must be maintained, the counter-ion (positively charged) is also prevented from passing through the membrane. The degree of ion exclusion increases with increasing valency of the co-ions, due to increased repulsion by the membrane. However, the degree of ion exclusion decreases with increasing valence of the counter-ions, since high valency counter-ions cause membrane charge shielding. In addition, high electrolyte concentrations cause the membrane charge to be more effectively shielded by the counter ions, thus reducing the selectivity of the membrane (Mickley, 1985).

The nominal *molar mass cut-off* for many commercially available nanofiltration membranes is in the range 200 to 500 g.mol^{-1}. Nanofiltration is often referred to as *intermediate reverse osmosis-ultrafiltration*, *charged membrane ultrafiltration* or *selective reverse osmosis*.

The application of the Spiegler-Kedem theory (refer to Section 2.1.3) to nanofiltration is described in this section. The analysis deals with the case where the solutes are sodium chloride and a highly retained multivalent organic anion. The theory accounts for the negative retention of sodium chloride that occurs under certain operating conditions. A further modification by Schirg and Widmer (1992), which takes concentration polarisation into account, is also described.

For a mixture of electrolytes, the differences in the permeabilities of the ions lead to an electric field. This affects the velocity of each ion, hence the transport coefficients pertaining to each single salt cannot be used in isolation. For a system involving a negatively charged membrane, sodium chloride and the sodium salt of a fully dissociated multifunctional organic anion ($X^{\nu -}$) with ν negatively charged groups per molecule, Perry and Linder (1989) obtained the following relationship for the salt concentration at the membrane/feed interface :

$$\bar{c}_A = c_{A1}\left(1 + \nu\frac{c_{x1}}{c_{A1}}\right)^{0,5} \qquad (86)$$

This provides a boundary condition in the integration of Eqn (19). Assuming that σ and A_1 are constant, the result of this integration is

$$\frac{J_V(1-\sigma)\Delta x}{\bar{A}} = \ln\frac{c_{A3}\sigma}{c_{A3}-\bar{c}_A(1-\sigma)} \qquad (87)$$

Using the definitions of F, B and A from Eqn (21) gives

$$F = \frac{c_{A3}-\bar{c}_A(1-\sigma)}{c_{A3}\sigma} \qquad (88)$$

Using Eqn (20), the expression for the salt retention in the presence of a retained organic ion becomes

$$R = 1 - (1-\sigma)\frac{\left(1+v\frac{c_{sl}}{c_{s1}}\right)^{0.5}}{1-\sigma F} \tag{89}$$

The retention of a membrane for a particular solute depends on its concentration at the membrane-feed interface rather than on its concentration in the bulk feed solution. The concentration at the interface cannot be determined by direct measurement, however it can be evaluated from experimental data by using the results of the following analysis which is due to Schirg and Widmer (1992).

A balance over a differential element in the membrane/feed interface and the membrane gives

$$J_v c - D\frac{dc}{dx} = J_v c_3 \tag{90}$$

Integration of Eqn (90) with boundary conditions :
$c = c_1$ at $x = 0$ and $c = c_2$ at $x = \ell$, gives

$$\frac{c_2 - c_3}{c_1 - c_3} = \exp\left[\frac{J_v}{D}\ell\right] \tag{91}$$

where ℓ is defined as :

$$\ell = \frac{d}{Sh}$$

The observed solute retention is defined by

$$R_{obs} = 1 - \frac{c_3}{c_1} \tag{92}$$

while the real retention coefficient is defined by

$$R = 1 - \frac{c_3}{c_2} \tag{93}$$

Hence,

$$R = \left[1 + \frac{(1 - R_{obs})}{R_{obs}}\exp\left(-\frac{J_v}{D}\ell\right)\right]^{-1} \tag{94}$$

The observed retention coefficient (R_{obs}) and the volume flux (J_v) can be measured, the diffusion coefficient (D) must be known for the solute involved. The boundary layer thickness (ℓ) is found using the membrane tube diameter d and correlations for the Sherwood number, Sh.

Eqn (21) can be written as :

$$R = 1 - \frac{1-\sigma}{1-\sigma\exp\left(\frac{(\sigma-1)J_v}{A}\right)} \tag{95}$$

Schirg and Widmer (1992) found that the concentration dependence of the solute permeability, A, could be described by

$$A = \alpha(c_2)^{\beta} \tag{96}$$

Hence, for a single electrolyte,

$$R = 1 - \frac{1-\sigma}{1-\sigma\exp\left(\frac{(\sigma-1)J_V}{\alpha(c_2)^{\beta}}\right)} \tag{97}$$

To evaluate the three unknown variables (σ, α and β), at least three sets of experimental measurements using the same feed solution and membrane are required and R must be determined using Eqn (94).

For mixtures of sodium chloride and organic anions, Eqn (97) becomes

$$R_s = 1 - \frac{(1-\sigma_s)\left(1+\frac{v(c_{x2})}{(c_{s2})}\right)^{0.5}}{1-\sigma_s\exp\left(\frac{(\sigma_s-1)J_V}{\alpha_s(c_{s2})^{\beta_s}}\right)} \tag{98}$$

and

$$R_x = 1 - \frac{(1-\sigma_x)\left(1+\frac{(c_{s2})}{v(c_{x2})}\right)^{0.5}}{1-\sigma_x\exp\left(\frac{(\sigma_x-1)J_V}{\alpha_x(c_{x2})^{\beta_x}}\right)} \tag{99}$$

for sodium chloride and the organic anion, respectively.

2.8 Numerical Methods

2.8.1 Solution of the membrane transport equations

2.8.1.1 Single solute reverse osmosis

In all Sourirajan's publications, the parameter A has been determined from tests using pure water, followed by determination of $\mathcal{D}$ and k from tests with feeds containing the solutes of interest. This procedure is unlikely to be convenient when working with a relatively large-scale pilot plant or full-scale operating plant. It would be desirable to determine all the parameters by regression from data using whatever feed solutions the plant was operating on. Because of the non-linear nature of the equations, such regression algorithms inevitably involve some form of procedure which evaluates the model for trial values of the parameters. During this process, two levels of trial-and-error occur, the outer level involving the choice of parameters, and the inner level involving the solution of the non-linear equations for x_{A2} and x_{A3}.

During the course of these trials, it frequently occurs that quite unrealistic combinations of parameters are tried - it is very difficult to ensure that automatic optimisation routines limit their choices to *realistic* regions or, indeed, to determine beforehand what the boundaries of such a region are. Eqns (10) and (11) proved to be sensitive to unfortunate combinations of trial values of the quantities involved. The symptoms of the problem were either values of x_{A2} and x_{A3} which diverged, so that no solution could be reached, or values which caused the argument of the logarithmic term in (10) to be negative.

The first approach adopted to overcome these problems involved detecting the conditions as they occurred, and attempting to *steer* the regression away from such points by adding a penalty term to the calculated objective function. This did not prove particularly successful, as it gave the objective function of a discontinuous character, which appeared to *confuse* the search algorithm, and sent it in the wrong direction as often as the right one.

The approach that has ultimately proved successful was to reformulate the set of equations into a form that is more robust with respect to unrealistic combinations of parameters.

The problem of negative arguments for the logarithmic function was easily eliminated by an exponential transformation. Equation (10) became :

$$\left[\frac{x_{A2} - x_{A3}}{x_{A1} - x_{A3}}\right] = \exp\left[\frac{\mathcal{D}(x_{A2} - x_{A3})}{k \; x_{A3}}\right] \qquad (100)$$

This did not eliminate the problem of diverging values for x_{A2} and x_{A3}, however. It also introduced a new problem, in that the argument of the exponential function could become large and cause floating point overflow errors. A closer examination of the equation formulations, and how they related to the regression situation was required.

The data that the model is fitted to consists primarily of values of permeate flux and concentration, with the operating pressure and temperature as auxiliary parameters. The most natural objective function to be minimized is the sum of squared errors between the model and measured fluxes and permeate concentrations. The model flux is most directly affected by the value of the permeability parameter, A, via Eqn (1). The solute flux is given by Eqn (2) which depends on the value of $\mathcal{D}$. The permeate concentration is thus determined by the ratio of solute flux to water flux, which is affected by the ratio $\mathcal{D}/A$. In Sourirajan's formulation, everything is related to the water flux N_B (Eqns (6), (8) and (9)). This is well suited to the case where A is accurately known from a separate experiment with pure water, and thus N_B is known to a good approximation, but not (in hindsight) to the case where both $\mathcal{D}$ and A are being sought by trial. It seemed that one of the equations should be based on the water flux, N_A, and therefore be sensitive to the value of A, and the other based on N_B, making it sensitive to $\mathcal{D}$.

Eqn (2) is one expression for N_B. A second one can be constructed from Eqn (4) :

$$N_A = N_B\left(\frac{x_{A3}}{1 - x_{A3}}\right) \tag{101}$$

Equating Eqns (2) and (101),

$$N_A\left(\frac{x_{A3}}{1 - x_{A3}}\right) = \mathcal{D}(c_2 x_{A2} - c_3 x_{A3})$$

Substituting for N_b from Eqn (1), and using the approximation $c_2 = c_3 = c_1$ gives

$$A[P - \pi(x_{A2}) + \pi(x_{A3})]\left(\frac{x_{A3}}{1 - x_{A3}}\right) = Dc_1(x_{A2} - x_{A3})$$

Rearranging gives

$$A[P - \pi(x_{A2}) + \pi(x_{A3})]x_{A3} - \mathcal{D}c_1(1 - x_{A3})(x_{A2} - x_{A3}) = 0 \tag{102}$$

This rearrangement eliminates the possibility of encountering a division by zero error in the (unlikely) event that the procedure should try a value of 1 for x_{A3}.

The other equation in the set is a similar rearrangement of Eqn (100) :

$$x_{A2} - x_{A3} - (x_{A1} - x_{A3})\exp\left[\frac{\mathcal{D}(x_{A2} - x_{A3})}{\mathcal{K}x_{A3}}\right] = 0 \tag{103}$$

The ratio in the exponential argument cannot be avoided.

The model based on Eqns (102) and (103) has, in fact, turned out to be much more robust with respect to poor choices of parameters. In regressing on experimental data, it has been able to converge using starting estimates of parameters that were (deliberately) set incorrect by two orders of magnitude.

This is not to say that it is infallible; as expected it sometimes fails because of floating point overflow in evaluating the exponential in Eqn (103), and occasionally the Newton-Raphson solution procedure for x_{A2} and x_{A3} fails to converge. However, it is relatively easy to estimate order-of-magnitude values for A and $\mathcal{D}$ from experimental data, so this has not constituted a serious draw-back in practice.

2.8.1.2 Multiple solute reverse osmosis

Derivation of a numerical algorithm

The Newton-Raphson algorithm is one of the most widely used methods for solving non-linear equations. A special adaptation of the Newton-Raphson method has been derived which takes advantage of the structure of Eqns (16) and (17), and which therefore involves significantly less computational effort than a standard implementation would.

The variables x_{i2} and x_{i3} can be considered as two vectors

$$\vec{x}_2 = (x_{12}, x_{22}, \ldots, x_{n2})^T$$

and

$$\vec{x}_3 = (x_{13}, x_{23}, \ldots x_{n3})^T$$

The vector functions $\vec{F}(\vec{x}_2, \vec{x}_3)$ and $\vec{G}(\vec{x}_2, \vec{x}_3)$ are defined such that there elements are given by

$$F_i = (x_{i2} - x_{i3}) - (x_{i1} - x_{i3})\exp\left(\frac{\mathcal{D}_i(x_{i2} - x_{i3})}{\mathcal{K}x_{i3}}\right) \tag{104}$$

and

$$G_i = \mathcal{D}_i c(x_{i2} - x_{i3}) - \left(\sum_j \mathcal{D}_j c(x_{j2} - x_{j3}) + A(P - \pi_2 + \pi_3)\right)x_{i3} \tag{105}$$

Then Eqns (16) and (17) may be written

$$\vec{F}(\vec{x}_2, \vec{x}_3) = \vec{0} \quad \text{and} \quad \vec{F}(\vec{x}_2, \vec{x}_3) = \vec{0}$$

At some point in the $(\vec{x}_2, \vec{x}_3)$ space, close to the point where Eqns (16) and (17) are satisfied, $\vec{F}$ and $\vec{G}$ are non-zero. If the functions are linearized about the point, then the vector difference between the point and the solution point $(\overline{\Delta x}_2, \overline{\Delta x}_3)^T$ is estimated by the solution to the vector equations

$$\frac{\partial \vec{F}}{\partial \vec{x}_2}\overline{\Delta x}_2 + \frac{\partial \vec{F}}{\partial \vec{x}_3}\overline{\Delta x}_3 = -\vec{F} \tag{106}$$

and

$$\frac{\partial \vec{G}}{\partial \vec{x}_2}\overline{\Delta x}_2 + \frac{\partial \vec{G}}{\partial \vec{x}_3}\overline{\Delta x}_3 = -\vec{G} \tag{107}$$

In the above equation, the terms with the form $\partial\vec{F} / \partial\vec{x}_2$ are matrices, the ij *th* element of which is of the form $\partial F_i / \partial x_{j2}$.

Differentiation of Eqn (104) gives:

$$\frac{\partial F_i}{\partial x_{j2}} = 1 - \frac{\mathcal{D}_i(x_{i1} - x_{i3})}{\mathcal{K}x_{i3}}\exp\left(\frac{(x_{i2} - x_{i3})}{\mathcal{K}x_{i3}}\right) \tag{108}$$

when $j = i$, and zero when $j \neq i$.

$$\frac{\partial F_i}{\partial x_{j3}} = \left(1 + \frac{\mathcal{D}_i x_{i2}(x_{i1} - x_{i3})}{\mathcal{K}x_{i3}^2}\right)\exp\left(\frac{(x_{i2} - x_{i3})}{\mathcal{K}x_{i3}}\right) \tag{109}$$

when $j = i$, and zero when $j \neq i$.

Hence $\partial \vec{F} / \partial \vec{x}_2$ and $\partial \vec{F} / \partial \vec{x}_3$ are diagonal matrices, a circumstance which can be used to advantage when solving the system of equations.

In the same way, $\vec{G}$ is differentiated, as in Eqn (105) to obtain the remaining coefficient matrices.

$$\frac{\partial G_i}{\partial x_{i2}} = \mathcal{D}_i c + x_{i3}\left(\mathcal{A}\frac{\partial \pi_2}{\partial x_{i2}} - \mathcal{D}_i c\right) \tag{110}$$

$$\frac{\partial G_i}{\partial x_{j2}} = x_{i3}\left(\mathcal{A}\frac{\partial \pi_2}{\partial x_{j2}} - \mathcal{D}_j c\right) \tag{111}$$

$$\frac{\partial G_i}{\partial x_{i3}} = x_{i3}\left(\mathcal{A}\frac{\partial \pi_3}{\partial x_{i3}} - \mathcal{D}_i c\right) - \left(\mathcal{D}_i c + \sum_j \mathcal{D}_j (x_{j2} - x_{j3}) + (\mathcal{A} - \pi_2 + \pi_3)\right) \tag{112}$$

$$\frac{\partial G_i}{\partial x_{j3}} = x_{i3}\left(\mathcal{A}\frac{\partial \pi_3}{\partial x_{j3}} - \mathcal{D}_j c\right) \tag{113}$$

Solution of the matrix equations

For convenience Eqns (106) and (107) are re-written in the following notation :

$$\Phi_2 \overline{\Delta \vec{x}}_2 + \Phi_3 \overline{\Delta \vec{x}}_3 = -\vec{F} \tag{114}$$

and

$$\Gamma_2 \overline{\Delta \vec{x}}_2 + \Gamma_3 \overline{\Delta \vec{x}}_3 = -\vec{G} \tag{115}$$

Eliminating $\overline{\Delta \vec{x}}_2$ from these two equation yields the following equation for $\overline{\Delta \vec{x}}_2$:

$$[\Gamma_3 - \Gamma_2 \Phi_2^{-1} \Phi_3) \overline{\Delta \vec{x}}_3 = [\Gamma_2 \Phi_2^{-1}] \vec{F} - \vec{G} \tag{116}$$

This equation may be solved for $\overline{\Delta \vec{x}}_3$ by any standard simultaneous linear equation solution algorithm. Since Φ_2 is a diagonal matrix, a matrix inversion routine is not required to evaluate Φ_2^{-1}.

Once $\overline{\Delta \vec{x}}_3$ has been obtained, one can solve Eqn. (114) for $\overline{\Delta \vec{x}}_2$:

$$\overline{\Delta \vec{x}}_2 = -(\Phi_2^{-1} \vec{F} + \Phi_2^{-1} \Phi_3 \overline{\Delta \vec{x}}_3) \tag{117}$$

Summary

In comparison with a straightforward Newton-Raphson algorithm which would solve simultaneously for all the unknowns together, this method solves two sets of equations for half the number of variables at a time. Since the number of arithmetic operations required for solving linear equations is proportional to the cube of the number of equations, this should result in a considerable improvement in the time required to perform a simulation.

2.8.2 Implementation of the model for nanofiltration and ultrafiltration

2.8.2.1 Volumetric flux

In Eqn (18) it was assumed that the active membrane thickness was sufficiently small to regard the derivative terms as constant. It was further assumed that the osmotic pressure, π, could be expressed as a linear function of solute concentrations, i.e.,

$$\pi = \sum_i \phi_i c_i \tag{118}$$

It was necessary to use different values of the osmotic factor, ϕ, for the organic component on the high and low pressure sides of the membrane. This was probably caused by the organic material not being a single substance and the difference between the molecular mass distribution of the fraction which penetrated the membrane and the mass distribution of the retained fraction.

Given these assumptions, Eqn (118) can be modified to :

$$J_V = A_n\left[P_T - \sum_i \sigma_i(\phi_{i2}c_{i2} - \phi_{i3}c_{i3})\right] \tag{119}$$

2.8.2.2 Solute fluxes

Integrating Eqn (19) over the membrane, between the concentrations c_{i2} and c_{i3} gives

$$c_{i3} = c_{i2}\left[\frac{1-\sigma_i}{1-\sigma_i F_i}\right], \quad \text{where } F_i = \exp\left[\frac{(1-\sigma_i)J_V}{A_i}\right] \tag{120}$$

Rearranging Eqn (91) as follows :

$$\frac{c_{i2}-c_{i3}}{c_{i1}-c_{i3}} = G_i = \exp\left[\frac{J_V}{D_i}l\right] \tag{121}$$

Combining these last two equations gives :

$$c_{i2} = c_{i1}\left[\frac{G_i(1-\sigma_i F_i)}{1-\sigma_i F_i-(1-\sigma_i)(1-G_i)}\right] \tag{122}$$

and

$$c_{i3} = c_{i1}\left[\frac{G_i}{1-G_i}\right]\left[\frac{(1-\sigma_i F_i)}{1-\sigma_i F_i-(1-\sigma_i)(1-G_i)}\right] \tag{123}$$

which may be substituted back into Eqn (119).

When $\sigma_i = 1$, the above expressions cause numerical difficulties. In this instance,

$$c_{i2} = \frac{c_{i1}(J_V + A_i)}{J_V + A_i G_i} \tag{124}$$

and

$$c_{i3} = \frac{c_{i3} P_i}{J_V + P_i G_i} \tag{125}$$

2.8.2.3 Modelling procedure

In the standard modelling procedure, the flow rate, concentration and pressure on the pressurised side of the membrane are known, as are the model parameters. The term l/D_i in Eqn (121) is the film mass transfer coefficient, which may be calculated from established correlations for flow inside tubes (see Eqn 35). Since the coefficients F_i and G_i *depend on the value of* J_V, Eqns *(124)* and *(125)* have to be solved by an iterative procedure. Once J_V has been found, all the remaining values may be calculated from Eqns (120) to (125).

2.8.3 Parameter estimation : $\mathcal{A}$, $\mathcal{D}$ and $\mathcal{K}$

These parameters are expected to be functions of operating conditions, and, their variability is partly predictable. Sourirajan has investigated these variations reasonably thoroughly and a summary of the modelling analysis is presented in the following section.

2.8.3.1 The membrane permeability parameter, $\mathcal{A}$

The main influence on $\mathcal{A}$ is the viscosity of water, which in turn depends on temperature. Since the water is relatively pure in the membrane pores, solute concentration effects are likely to be minimal. Sourirajan also found a dependence on operating pressure, due to compaction of the membrane. This has a reversible and an irreversible component, the latter leading to a gradual decline in fluxes over the lifetime of a membrane. Sourirajan found that the reversible component could be described by a term of the form :

$$A = A_o \exp(-\alpha P) \tag{126}$$

where α *is a small constant, characteristic of the membrane. Sourirajan quotes values* between 0,003 and 0,0055 atm^{-1}. At a representative pressure of 4 MPa, this range represents a variation in the exponential factor of 0,8 to 0,9. Since numerical experiments fitting the model to data measured on Membratek RO membranes gave no significant improvement in fit by including α as a regression parameter, it was decided to simply use a median value of 0,0043 as a fixed parameter.

At present, the irreversible component of membrane compaction is not explicitly catered for, Harries (1984) found that the flux of Membratek membranes declined gradually over a period of 1 000 hours, after which it remained more-or-less constant.

At this point no data has yet been analysed over such a long period of operation, so the issue has not arisen.

The sub-model for $\mathcal{A}$ is :

$$\mathcal{A} = \frac{k_1}{\mu}\exp(-0.0043\,P) \tag{127}$$

2.8.3.2 The solute transport parameter, $\mathcal{D}$

Although $\mathcal{D}$ is a single parameter from the macroscopic viewpoint, in Sourirajan's original theoretical analysis, it consist of 3 terms, $\left(\frac{D_{AM}}{K\delta}\right)$. D_{AM} is the diffusivity of the solute in the membrane phase, K is a partition coefficient of solute between the solution phase and the membrane phase, and δ is an effective pore length through the membrane. The individual terms are not separately observable in an RO experiment. However, certain correlations are possible, guided by the expected behaviour of the individual terms. Perhaps the most interesting is the correlation of $\frac{D_{AM}}{K\delta}$ with free energies of adsorption of ions onto the membrane, which allows predictions of the value for one ionic solute from a known value for another. Following the empirical correlations described by Sourirajan, the current sub-model for $\mathcal{D}$ is :

$$\mathcal{D} = k_2\exp(0.005\,T)\,P^{-\beta} \tag{128}$$

k_2 and β are regression parameters, T is the absolute temperature in K.

2.8.4 Integration of the equations for tubes

Transport equations can be solved at the entrance to a tube, to yield permeate flux and concentration. From a material balance and hydraulic pressure drop calculation, the change in the conditions of the solution flowing in the tubes may be calculated as it passes through a length of the tubes, ΔL Repeated application of this procedure constitutes a Euler method numerical integration of the whole process along the lengths of the tubes.

Where the flow was divided between parallel modules, the division was assumed to be even. The step ΔL was taken to be one tube in the module (2,3 m). The pressure drop was calculated using the Blasius formula for smooth pipes given based on Eqn (57) (Perry, 1963) :

$$\frac{\Delta P}{\Delta L} = -0.079\left(\frac{\rho v^2}{d}\right)Re^{-0.25} \tag{129}$$

An extra pressure drop corresponding to the extra and equivalent length of the hydraulic fitting and return bends was added for each tube.

After the transport equations had been solved for each step of the integration, the flows and concentrations on either side of the membrane were updated according to the quantities of water and solute transferred.

Thus considering the i th incremental section of RO tube, with membrane area, ΔA;

$$Q^i = Q^{i-1} - (N_A^i + N_B^i)\Delta A \tag{130}$$

$$c_b^i = \frac{c_b^{i-1} Q^{i-1} - c_p^i (N_A^i + N_B^i)}{Q^i} \tag{131}$$

Since a single permeate stream was produced by the plant, it was a mixture of the permeates produced by each RO tube in the plant. Its flow and composition were calculated as :

$$Q_p = \sum (N_{A_i}^i + N_B^i) \tag{132}$$

$$c_p = \frac{\sum\limits_i N_B^i}{Q_p} \tag{133}$$

2.8.5 Regression procedures

The free parameters, available for fitting the model to experimental data are k_1 in Eqn (127), k_2 and β in Eqn (102). For the purpose of the regression, an objective function is constructed of the form :

$$G = \sum_{i=1}^{n} w_1 (f_i^m - f_i^c)^2 + \sum_{i=1}^{n} w_2 (x_i^m - x_i^c)^2 \tag{134}$$

Here f_i^m and f_i^c are measured and calculated permeate flows corresponding to the i th data set, x_i^m and x_i^c are the measured and calculated solute concentrations. n is the number of data sets, and w_1 and w_2 are weighting constants which can be adjusted to give appropriate importance to the contributions of flux and concentration.

G is minimised by an appropriate choice of the regression parameters, by means of a modified Fletcher-Powell conjugate gradient algorithm, drawn from the *Numerical Recipes* collection of Press et al. (1986).

This is an iterative procedure. It was noticed while observing the progress of the minimisation that the estimates of k_1 and k_2 tended to follow each other, something which might have been expected from Eqn (11), which shows that the ratio $\frac{D}{A}$ is important for the model. It was found that the rate of convergence was greatly increased by transforming the regression parameter set to k_1 , $\frac{k_2}{k_1}$ and β .

3 TECHNOLOGY TRANSFER

Two forms of technology transfer occurred during this project. Firstly, a number of case studies involving industrial applications of membrane separations were undertaken. These were primarily meant to provide means to validate modelling procedures, however practical contributions to the processes and projects involved also resulted. Secondly, there was the more direct form of instructional technology transfer, in the form of courses, journal publications and conference publications.

3.1 The Lethabo Pilot Plant

In 1987 Eskom built a TRO plant to separate salts from the cooling water blowdown stream at the Lethabo Power Station near Sasolburg. The motivation was to reduce the volume of saline effluent to that required for the conditioning of the station's ash dumps, thus achieving a zero discharge of aqueous effluent to the environment. As a preliminary to the design of the plant, a pilot investigation was carried out using a plant which consisted of 30 Membratek modules, each containing 1,72 m² of cellulose-acetate membranes in 12,5 mm diameter tubes. (Schutte et al., 1987). The investigation covered more than 3 000 h of operation over a period of 10 months.

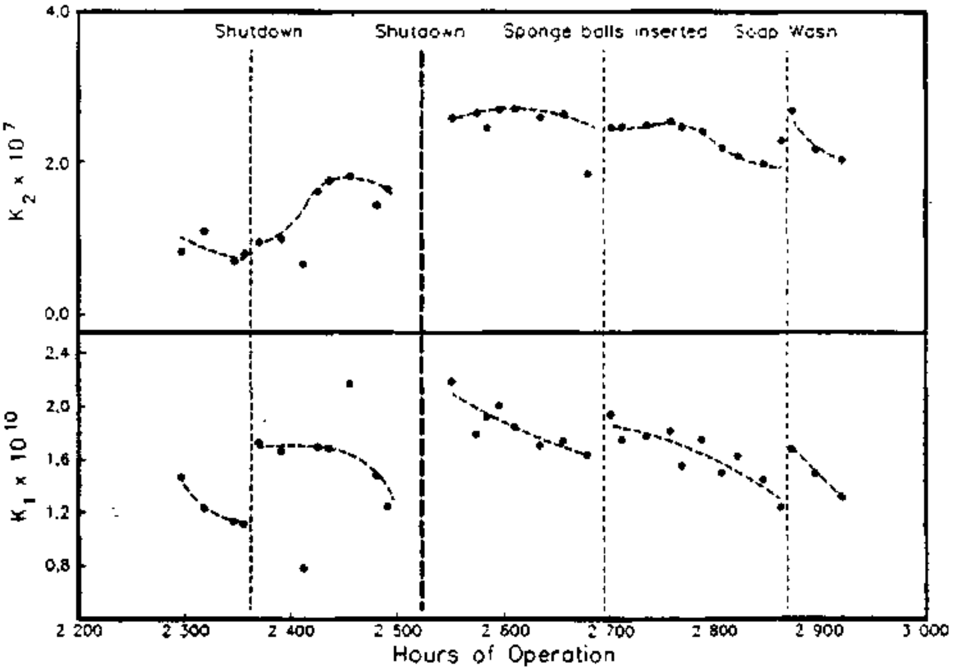

Figure 8 : Part of the history of the Lethabo pilot plant, in terms of values of the model parameters and various operational incidents.

Eskom made the data from the pilot-plant investigation available to provide a realistic test of modelling procedures. This data was used as the first major exercise for the single solute version of the model. The model was used to determine membrane transport parameters for the pilot plant and to track their values over its operating history.

It was possible to correlate changes in these parameters with incidents reported in the plant's operating log. Figure 8 illustrates a period of operation interpreted in terms of model parameters and operational incidents

The modelling study was presented in two publications, which are included as **Appendix 1** and **Appendix 2** of this report.

3.1.1 Conclusions

The model can be used to monitor a TRO plant by providing an indicator of the *state of the membranes, expressed in terms of values of the model parameters.*
Had this modelling been available at the time of the pilot investigation, it is certain that it would have provided valuable insights about what was occurring, and its implications for the design of the full-scale plant.

3.2 Lethabo Power Station

A visit to the Lethabo power station was undertaken during July 1992. The main purpose of the visit was to set up the tubular reverse osmosis (TRO) modelling program for the purpose of monitoring the TRO plant, and to instruct the Lethabo personnel in its use. Other objectives were to begin evaluating the requirements for implementing the algorithm in an on-line monitoring role as proposed in the provisional patent, and to gather a set of measurements, including full chemical analyses of the various streams, to provide data for the multi-solute version of the TRO model.

While applying the model to the plant operating data, it became evident that the software was not sufficiently convenient for the plant personnel to use on a routine basis, and that its user interface still needed attention before it would be useful. Problems included the use of different engineering units to those used for plant logging, and the need to transfer data manually from the data logging system to the TRO simulation program.

During the course of setting up the model to match the plant data, a number of problems with the plant operation came to light. These included the dilution of the feed stream with potable water to reduce the level of total dissolved solids (TDS), a concern about barium sulphate scaling, and a module failure rate of about twelve per month. When it became clear that the software would need to be modified, the objective of training the Eskom personnel in its operation was postponed, and the remaining time on site was devoted to an investigation of the plant's technical problems.

A detailed report which was originally submitted to Eskom is included as **Appendix 3**.

3.2.1 Conclusions

Although the original objectives of setting up the TRO model for routine use by Eskom personnel at Lethabo was not achieved, a number of other useful tasks were accomplished. As can be seen from the following table, the TRO model was found to simulate the plant operation accurately, and the process of applying it to the plant led to important insights into the plant operation. Areas of weakness in the program's user interface were identified, and ideas for improvements were obtained.

Time	11:00		13:24	
	Measured	Simulated	Measured	Simulated
Flow rates (m^3/h)				
Feed	96,5	-	96,2	-
Permeate	52,5	52,8	57,5	57,9
Reject	44,0	43,7	38,7	38,3
Conductivities (mS/cm)				
Feed	1 940	-	2 570	-
Permeate	186	184	240	242
Reject	4 060	4 059	5 990	6 086
Pressures (MPa)				
Feed	3,6	-	3,65	-
Reject	2,8	2,8	2,9	2,9

The three problems of feed dilution, barium sulphate scaling and module failures constituted significant threats to the viability of the plant's operation, and it was recommended that these should be addressed as soon as possible.

3.3 The Secunda Pilot Plant

Data from a TRO plant at Secunda was provided by Sastech. The feed to the plant was mine water. Although the data were essentially in the same form as that from the Lethabo Pilot Plant, significantly less detail was available. The measurements were at intervals of between 20 and 50 hours operation. No operational incidents were reported. When analysed in terms of the membrane parameters, the history of the plant seems to have been largely uneventful (see Figure 9), possibly indicating that there were no events to report.

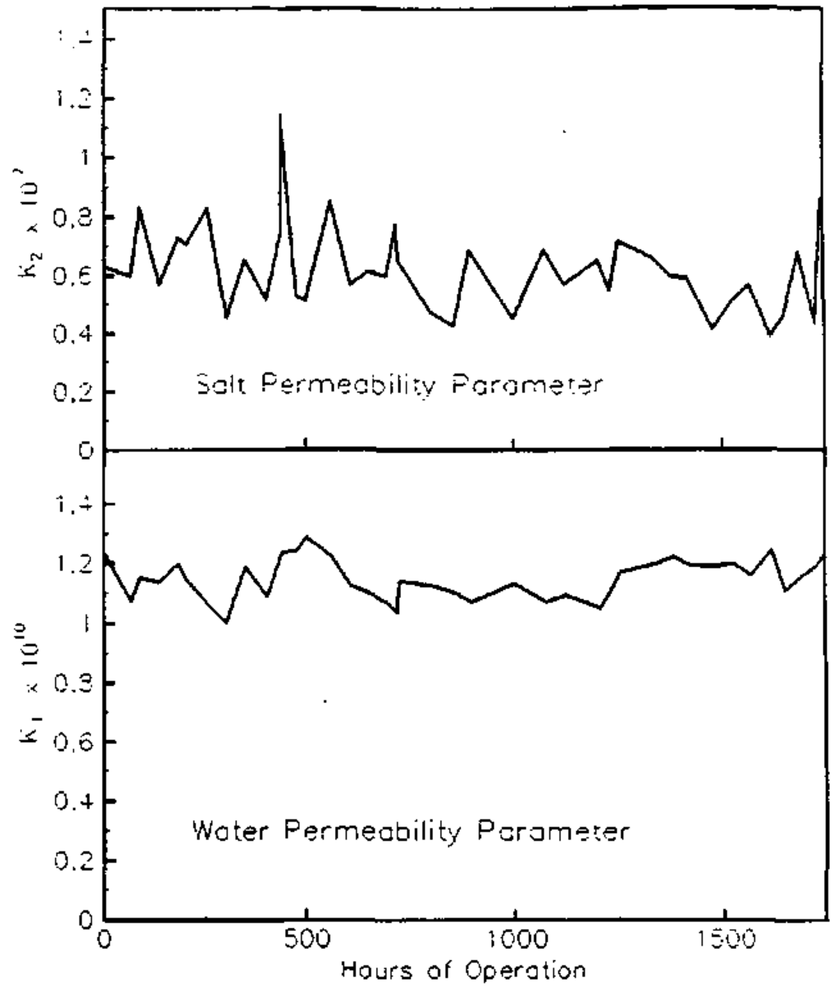

Figure 9 : History of the Secunda Pilot Plant operating on mine water, expressed in terms of the membrane parameters

3.3.1 Conclusions

Given such featureless data, the conclusions that could be drawn from this exercise have been limited. However, the following points are significant :

(a) The parameter values are similar to those obtained from the Lethabo data. This is significant, in that the water compositions were generally similar at the two plants, even though the arrangements and numbers of modules differed.

(b) The plant was operated at a water recovery of 60 % up to 1 380 h operation, after which the water recovery was increased to 70 %. The change in operating conditions was not reflected by a change in parameter values required for the model to fit the data.

It appears that the model is successfully accounting for changes in module configuration and operating conditions.

It was unfortunate that Sastech's involvement in the project could not be maintained and the modelling was discontinued. Recent approaches from Sastech indicate that they are anxious to co-operate on membrane research projects and are excited by prospects of the completed RO modelling program. The Pollution Research Group has been approached to act as an adviser to review design and operational aspects of a proposed new plant to treat clear ash effluent.

3.4 Tubular Ultrafiltration at Cato Ridge Abattoir

3.4.1 Experimental Investigation

Tests have been carried out at the effluent plant at the Cato Ridge Abattoir to investigate the use of 9 mm diameter tubular membranes supplied by the Institute for Polymer Science, University of Stellenbosch These tubes are unsupported and are housed in sets of three in 32 mm diameter PVC tubes. Two membrane types were tested : the 719 membrane (which has been used previously on the same effluent in the 12,5 mm diameter tubular format) and the 442 membrane, which has a lower molecular mass cut-off than the 719 membrane.

The tests were carried out on the combined effluent from the abattoir as it enters the effluent plant. The effluent had undergone fat-skimming and rough screening. Further screening was carried out manually to remove solids that might block the modules. The effect of flow rate and pressure on the flux was investigated. An air purge device was tested to determine whether it could have the same effect on the flux as high linear flow rates would, that is, to limit the extent of gel layer formation.

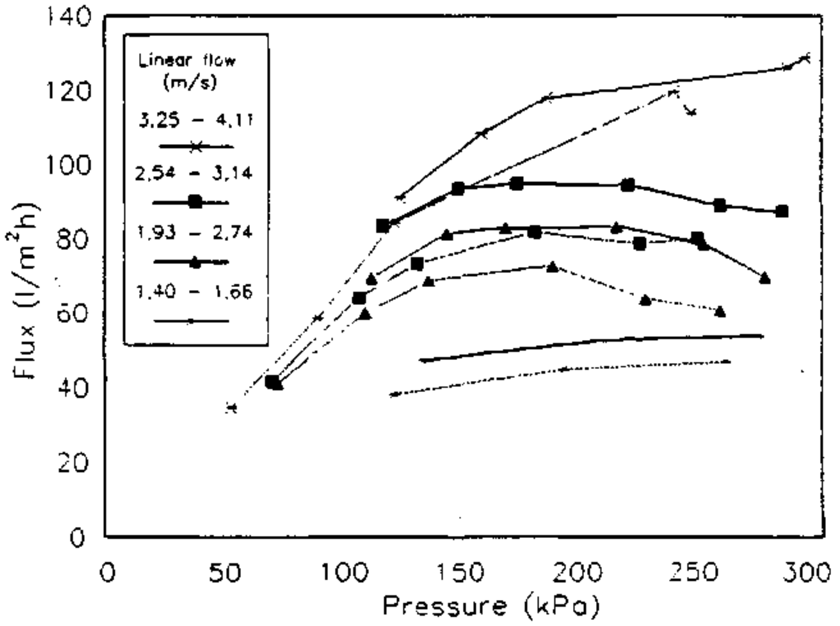

Figure 10 : Fluxes obtained during ultrafiltration of Cato Ridge Abattoir effluent at low water recoveries using tubular 719 polysulphone membranes.

It was found that the dependence of the flux on the linear flow rate was strong. It was observed that for each linear flow rate, there was a limiting pressure above which increases in pressure no longer lead to increases in flux. This critical pressure increased with increasing flow rate. The results for the 719 membranes at low water recovery are shown in Fig. 10, which illustrate the typical trends. The tests were carried out at pressures between 100 kPa and 400 kPa. The construction of the modules limited the maximum operating pressure to 400 kPa. The results of the use of the air purge unit were inconclusive, but it appeared to benefit the 719 membranes more than the 442 membranes.

A maximum water recovery of 91 % was attained. At this water recovery the fluxes were still reasonably high (above 15 $\ell.m^{-2}.h^{-1}$ at a linear flow rate of 1,5 $m.s^{-1}$). Hence higher water recoveries (at least 95 %) should be attainable.

The COD (Chemical Oxygen Demand) of the permeate was below 700 $mg.\ell^{-1}$ for the tests at high water recoveries. This corresponds to a COD retention of 96 % to 98 %. The point retention of phosphate varied from 50 to 66 % at zero water recovery, and was 93 % at 91 % water recovery. When effluent taken close to source was used, the phosphate retention was 89 %. In all the tests, the concentration of phosphate in the permeate ranged from 2,7 to 5,3 $mg.\ell^{-1}$.

A detailed report on the experimental investigation is included with this report as **Appendix 4**.

3.4.2 Modelling

The construction of the experimental rig was such that it proved difficult to set operating pressures and flow rates to precise pre-determined values, although, once set, these could be measured accurately. A further difficulty in obtaining reproducible operating conditions was due to the rapid fouling of the membranes which caused their characteristics to change continuously while the measurements were taking place. The fact that almost all the process variables changed between different data sets made the interpretation of the results in terms of trends difficult. As far as the design of the equipment was concerned, sophisticated controls were not provided because it was anticipated that a model would be developed, and would be able to compensate for variations in conditions; however nothing could have been done to avoid membrane fouling in any case.

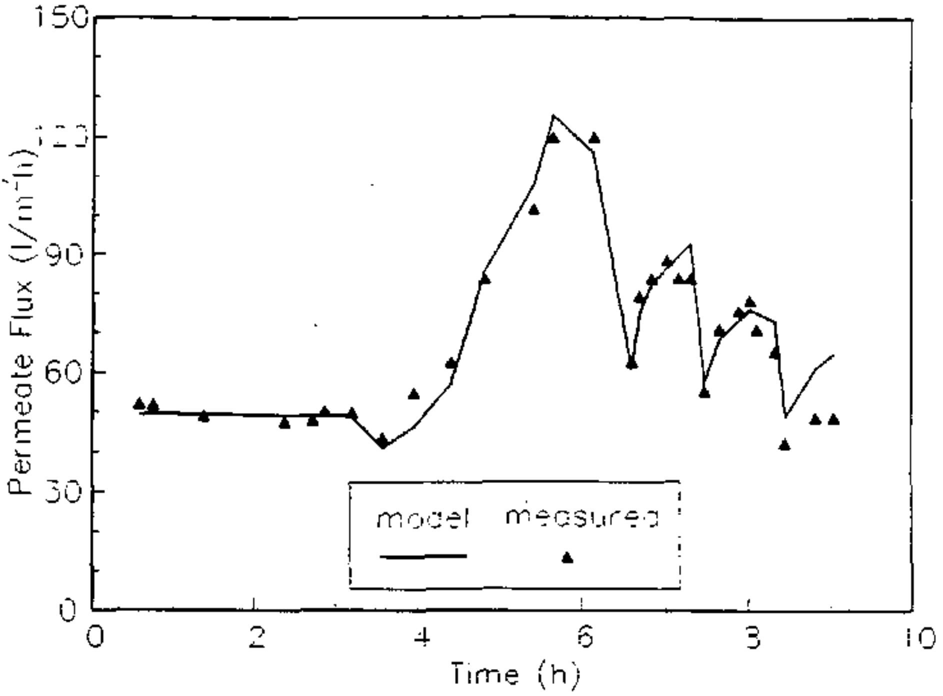

Figure 11 : Comparison of measured and modelled fluxes during an experiment treating abattoir effluent with 719 tubular ultrafiltration membranes. The measured data are the same as shown previously in Fig. 10.

The most significant new characteristics of the process when compared to those that had been modelled previously were the gel polarisation and membrane fouling. Although fouling was a factor in the Lethabo pilot-plant study, it occurred so gradually that it could be accounted for as a slow drift in the membrane transport parameters over a period of days. In the case of the abattoir effluent, its effect was noticeable in the time that it took to make a single measurement (about 10 minutes).

A model was constructed using the Spiegler-Kedem (1966) model for the transport through the membrane, and a model proposed by Sourirajan and Matsuura (1985) for the fouling. This was very successful in correlating the data, as illustrated in Fig. 11. This work formed the basis of a paper presented at the *Engineering of Membrane Processes, Environmental Applications* Conference, held in Il Ciocco, Italy, 26-28 April, 1994. That paper is included with this report as **Appendix 5**.

3.4.3 Conclusions

In summary, the major results of this experimental and modelling study were:

(i) The ultrafiltration of abattoir effluent is a technically viable process.

(ii) With some reservations concerning membrane cleaning noted above, the low pressure PVC module design seems to be a suitable candidate for the application.

(iii) The low molecular mass cutoff 442 membranes have an advantage over the medium molecular mass cutoff 719 membranes under gel-polarised conditions.

(iv) The model is able to represent the performance of membranes over a range of conditions, and should be useful in producing an efficient plant design.

3.5 Nanofiltration Tests at Huletts Refineries Ltd.

Tests using tubular nanofiltration membranes have been carried out on waste brine from the resin plant used for purifying sugar solutions at Huletts Refineries Ltd. The waste brine is the regeneration effluent from the anion exchange resin used to decolourise cane sugar liquor at the Huletts Refinery in Durban. The effluent is produced at 83 °C and contains, on average, 50 $g.\ell^{-1}$ of sodium chloride and 5 $g.\ell^{-1}$ (as total carbon) of organic matter. The organic matter includes natural sugar cane colourants and alkaline degradation products of reducing sugars. The compounds range in molar mass from less than 500 $g.mol^{-1}$ to more than 20 000 $g.mol^{-1}$ and most are negatively charged. Sodium chloride passes through the nanofiltration membrane, while the membrane retains most of the organic matter. The aim of the investigation was to determine whether the permeate was sufficiently pure to recycle as regenerant make-up.

Laboratory-scale tests were first carried out using small flat sheet samples of FilmTec NF40 membrane and later using 12,7 mm diameter tubular elements of SelRO^{TM} MPT-30, MPT-10 and MPT-31 membranes (Membrane Products Kiryat Weizmann). The initial laboratory-scale tests showed that the process was feasible, hence a pilot-scale study was initiated by Huletts Sugar Refineries using MPT-30 membranes and later MPT-31 membranes. The results are given in an MScEng dissertation by Wadley (1993).

Since the water balance limits the amount of brine that can be recycled to the regenerant make-up system, the fraction of the effluent containing the highest concentration of salt was selected for treatment by nanofiltration. This fraction contains 60 to 110 $g.\ell^{-1}$ of sodium chloride and 2 to 6 $g.\ell^{-1}$ of total carbon. Batch concentration tests on this fraction using the pilot plant fitted with the MPT-30 membrane gave point retention values ranging from 0 to 15 % for sodium chloride and from 71 to 93 % for total carbon, where the final water recoveries were between 69 and 83 %. Mass balance calculations showed that at least 30 % reduction in effluent volume and 40 % reduction in salt consumption could be achieved by recycling of the permeate from the membrane process to the regenerant make-up system.

Consideration of NF required the use of a multi-solute model, and a departure from the Sourirajan theory to account for a solute (in this case the sodium chloride) which is only slightly retained by the membrane. The data provided by the pilot plant was therefore ideal for testing and verifying the model. Figure 12 shows the correspondence between the model and data for the batch-concentration tests on the pilot plant.

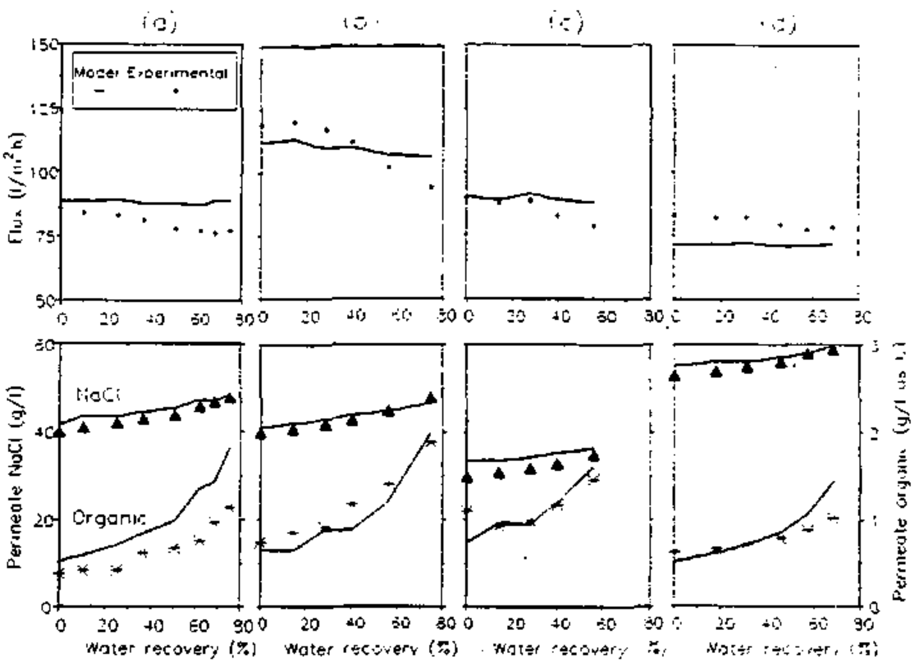

Figure 12 : Comparison of measured and modelled fluxes and permeate concentrations during four batch-concentration experiments treating ion-exchange regenerant brine effluent at the Huletts Sugar Refinery.

3.5.1 Conclusions

The model was able to correlate the experimental data successfully, and used in a conceptual design study for a plant to treat the entire regeneration effluent stream. A preliminary costing of the plant by Tongaat-Huletts has indicated that the process would have a payback period of about two years, based on the reduced sodium chloride consumption and effluent disposal cost. This work was presented at the *Engineering of Membrane Processes, Environmental Applications* Conference, held in Il Ciocco, Italy, 26-28 April, 1994. A copy of that paper is included with this report as **Appendix 6**.

3.6 Mass Transfer Enhancement for Tubular Reverse Osmosis Systems

3.6.1 Introduction

An investigation was carried out as an MScEng project by Mr. Q.E. Hurt into methods for enhancing mass transfer in TRO systems, and so to reduce concentration polarisation.

The investigation set out to compare the effectiveness of strategies for mass transfer enhancement. Three strategies were proposed to alter the hydrodynamic nature of the feed flow: (i) pulsed flow; (ii) baffled flow; and (iii) pulsed-baffled flow. The intention was to propose or compare mechanisms by which RO systems might be modified without altering the nature of the membrane. By these means it was hoped that the economics of RO might be improved.

In keeping with these aims, all the experiments were conducted with low linear feed flows in an attempt to obtain superior RO performance in the laminar and transition regimes that would be associated with consequently low pumping costs.

The experimental equipment used a recirculating feed solution in an small-scale TRO test unit. The configuration of the equipment is shown in Fig. 13.

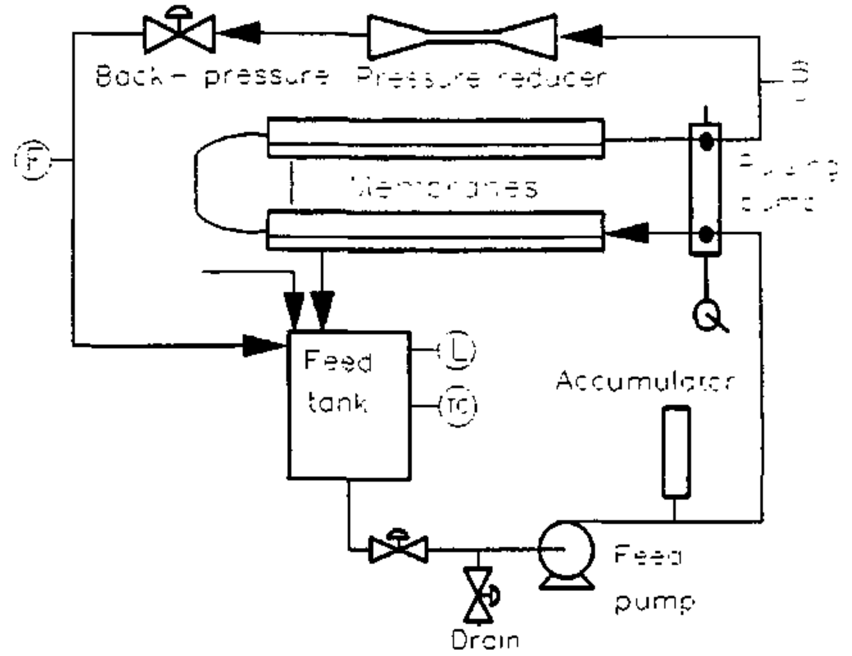

Figure 13 : Diagram of the experimental equipment used in the examination of mass transfer enhancement for tubular RO systems, depicting RO tubes bridged by the pulsing pump

Central to the design of the experimental apparatus was the pulsing pump that bridged the set of membrane tubes. The tubes were connected in series. The pump was driven by an independent, low-power source. The power requirements of the pump were only sufficient to act against the pressure drop through the membrane tubes, which in turn was kept low by restricting the mean flow rate to the laminar and transition regimes.

A more detailed account of this work is included as **Appendix** 7 of this report.

3.6.2 Conclusions

On the basis of the gains in mass transfer coefficient over open tube, steady flow TRO, the effectiveness of the enhancement techniques were rated as follows : pulsed, baffled TRO was most effective, followed by pulsed flow, open TRO and then steady flow baffled TRO. All techniques were effective but the gains for both pulsed flow techniques were markedly higher than for the steady baffled flow experiments.

Although significant gains were realised in terms of improving the mass transfer coefficient, it was found that the effect on the overall flux and salt retention was relativly small. This is because the principal transport resistance in RO occurs in the membrane rather than in the liquid boundary layer. Greater process benefits should be obtained in ultrafiltration and microfiltration, where concentration polarisation plays a greater role.

3.7 Roughing Demineralisation for Power Stations

3.7.1 Introduction

The Eskom Technology, Research and Investigations division (TRI) has been considering means for reducing the chemical addition requirement in the production of ultrapure water for power station boilers. Their motivation is two-fold : to reduce the degree of salination of the environment by effluents, and to protect their operation against the rising cost of chemicals, particularly sodium hydroxide. The use of RO as a pre-treatment for ion-exchange has been used successfully in a number of cases (for example see McAfee et al., (1990)) ; the purpose of this investigation has been to adapt the process to local conditions.

Mr C. Chibi of TRI has been the principal investigator : support for him from this project has taken the form of the loan of an RO test apparatus from the University of Natal, and the interpretation of the experimental results in terms of the RO model, which is the subject of this report. A further minor service has been determination of the Silt Density Index (SDI) determinations for the feed water used in the tests.

The details of this investigation are included with this report as **Appendix 8**.

3.8 Miscellaneous

The following miscellaneous activities stemmed from the WRC Project 325. While none of the activities were specifically sponsored by the Project, these activities stemmed from or contributed to the Project as a whole.

3.8.1 Columbus Stainless Steel

The Pollution Research Group was approached by Debex Desalination to advise Columbus Stainless Steel on the incorporation of RO treatment into the design of the proposed effluent treatment plant. It was established that their proposed configuration was unworkable as it would have been subject to scaling by heavy metal salts. A pre-treatment scheme was worked out to allow the use of RO; however the design consultants decided that it would add too much to the cost, and opted to use another treatment route.

3.8.2 Informal research visits

Informal visits to Bath and Cambridge Universities in the United Kingdom were undertaken by Mr Quentin Hurt. He met with researchers involved in the study of mass transfer enhancement in membrane systems. During the meetings he described the objectives of his research in the field of tubular reverse osmosis systems, discussed recent developments in the field and examined laboratory equipment.

The visits were useful as a comparison of equipment used in the UK experiments, as a means of sharing academic research findings and in networking with foreign researchers in similar fields of study. Valuable primary data was obtained which has been included in Mr Hurt's thesis.

During 1994, CJ Brouckaert and S Wadley visited a number of British organisations in connection with membrane research. These were: Patterson Candy International (PCI), Dow Separation Systems (FilmTec), Thames Water, Yorkshire Water, Professor John Howell and the University of Bath, Dr Simon Judd at the School of Water Sciences, Cranfield University, Professor ET Woodburn at the University of Manchester Institute of Science and Technology (UMIST), and Dr LM Evison at the School of Water and Enviromental Engineering, University of Newcastle.

3.9 Membrane Processes Book

Prof Buckley and Dr OO Hart acted as editors of the Water Science and Technology Volume 25 Number 10 that dealt with *Membrane Technology in Wastewater Management*. The issue was published in 1992 and reflected the proceedings of the IAWPRC International Specialised Seminar held in Cape Town between 2 and 5 March 1992.

A Chapter was written in the book, *Reverse Osmosis: Membrane Technology. Water Chemistry and Industrial Applications*. The book was edited by Zahid Amjad and published by van Nostrand Reinhold in 1993 (ISBN 0-442-23964-5). The chapter was entitled *RO Application in Brackish Water Desalination and in the Treatment of Industrial Effluents*. The chapter was written by CA Buckley, CJ Brouckaert and CA Kerr.

3.10 Reverse Osmosis Modelling Courses

An Introduction to RO Technology was given by Ms S Wadley and Mr CJ Brouckaert at the 1993 WISA Conference held in Durban. The course introduced basic RO theory and discussed some applications of RO processes.

A questionnaire, issued after the completion of the first course, was used to modify the course content to make it less theoretical and more practical. The revised course was presented as part of the Afriwater Conference held in Johannesburg between 8 and 10 June 1994. An introduction to membrane processes, theoretical background to the mathematical model, practical problems, an introduction to the RO modelling program and a demonstration of EMILY formed the basis of the course. Twelve people attended the course.

The courses form part of the PRG strategy to publicise RO theory in an effort to make the technology more widely accepted. Once the theory is understood by a sufficiently large section of the water treatment community, it is likely to gain widespread acceptance as a feasible water processing route.

3.11 Papers Presented at Conferences

HURT, Q.E., 'Improving the Performance of Membrane Systems by Mass Transfer Enhancement' 2nd Biennial Conference/Exhibition, World Trade Centre, Kempton Park, Johannesburg, 13-16 May 1991 (Poster Presentation).

BROUCKAERT, C.J., 'Simulation of Tubular Reverse Osmosis' 6th National Meeting of the South African Institution of Chemical Engineers, Elangeni Hotel, Durban, 7-9 August 1991.

BROUCKAERT, C.J. 'The Use of Computer Simulation of Tubular Reverse Osmosis in Conjunction with Pilot-plant Studies', IAWPRC Specialised Conference on Membrane Technology in Wastewater Management, The Cape Sun Hotel, Cape Town, 2-5 March 1992.

BROUCKAERT, C.J., JACOBS, E.P., MACTAVISH, F., COWAN, J.A.C. and HART, O.O., 'Cleaning Strategies for Membranes Operating on Red-meat Abattoir Waste Streams', International Membrane Science and Technology Conference, Sydney, Australia, 10-12 November 1992.

JACOBS, E.P., BROUCKAERT, C.J., MACTAVISH, F., HART, O.O. and COWAN, J.A.C., 'Cleaning Strategies for Membranes Operating on Red-Meat Abattoir Waste Streams', 3rd Biennial Conference, Water Institute of Southern Africa, Elangeni Hotel, Durban, 24-27 May 1993.

BROUCKAERT, C.J., BROUCKAERT, B.M. and BUCKLEY, C.A.,'Prediction of Osmotic Pressure of Inorganic Ionic Solutions from Equilibrium Speciation', 3rd Biennial Conference, Water Institute of Southern Africa, Elangeni Hotel, Durban, 24-27 May 1993 (Poster).

BROUCKAERT, C.J., WADLEY, S. and BUCKLEY, C.A., 'Reverse Osmosis Fundamentals', A One-day Speciality Topic Workshop, 3rd Biennial Conference, Water Institute of Southern Africa, Durban, 23 May 1993.

BUCKLEY, C.A. and BROUCKAERT, C.J., 'Situation Assessment - Membrane Research in South Africa', Workshop on the Development of a Strategic Plan for Membrane Research in South Africa, Water Research Commission, Pretoria, 14-16 June 1993.

WADLEY, S., BROUCKAERT, C.J., BADDOCK, L.A.D. and BUCKLEY, C.A., 'Modelling of nanofiltration applied to the recovery of salt from waste brine at a sugar decolourisation plant', Engineering of Membrane Processes II : Environmental Applications, Il Ciocco, Italy, 26 to 28 April, 1994

BROUCKAERT, C.J., WADLEY, S. and JACOBS, E.P., 'Ultrafiltration of Red Meat Abattoir Effluent : A Pilot-Plant and Modelling Investigation', Engineering of Membrane Processes II : Environmental Applications, Il Ciocco, Italy, 26 to 28 April, 1994.

BROUCKAERT, C.J., BADDOCK, L.A.D. and BUCKLEY, C.A., 'Modelling of nanofiltration applied to the recovery of salt from waste brine at a sugar decolourisation plant', Engineering of Membrane Processes II : Environmental Applications, Il Ciocco, Italy, 26 to 28 April, 1994

HURT, Q.E, BROUCKAERT C.J. and BUCKLEY C.A., 'Mass-Transfer Enhancement for Tubular Reverse Osmosis Systems', Engineering of Membrane Processes II : Environmental Applications, Il Ciocco, Italy, 26 to 28 April, 1994 (Poster).

BROUCKAERT, C.J., BADDOCK, L.A.D., WADLEY, S., SAAYMAN, H. and BUCKLEY, C.A., 'A Computer Model for the Interpretation and Archiving of Membrane Separation Data', Engineering of Membrane Processes II : Environmental Applications, Il Ciocco, Italy, 26 to 28 April, 1994 (Poster).

CHIBI, M.C., VINNIECOMBE, D.A. and BROUCKAERT, C.J., 'Roughing Demineralisation and Enhanced UV Irradiation for Ultrapure Water Production in the Power Industry', Engineering of Membrane Processes II : Environmental Applications, Il Ciocco, Italy, 26 to 28 April, 1994 (Poster)

3.12 Publications

BROUCKAERT, C.J. and BUCKLEY, C.A., 'Simulation of Tubular Reverse-Osmosis' Water SA, 18(3), pp. 215-223, July 1992.

COWAN, J.A.C, MACTAVISH, F., BROUCKAERT C.J. and JACOBS, E.P., 'Membrane Treatment Strategies for Red Meat Abattoir Effluent', Water Science and Technology, 25(10), pp. 137-148, 1992, ISSN 0273-1223.

BROUCKAERT C.J. and BUCKLEY, C.A., 'The Use of Computer Simulation of Tubular Reverse Osmosis in Conjunction with Pilot-plant Studies', Water Science and Technology, 25(10), pp. 291-298, 1992, ISSN 0273-1223.

BROUCKAERT, C.J., 'The Use of Computer Simulation of Tubular Reverse Osmosis in Conjunction with Pilot-plant Studies, Filtration & Separation, 30(1), pp. 59-62, January/February 1993, ISSN 0015-1882.

JACOBS, E.P., SWART, P., BROUCKAERT, C.J. and HART, O.O., 'Membrane Performance Restoration. I. Abattoir Process Streams, Cleaning Regimes for UF Membranes', Water SA, 19(2), pp. 127-132, April 1993, ISSN 0378-4738.

JACOBS, E.P., BROUCKAERT, C.J., MACTAVISH, F., HART, O.O. and COWAN, J.A.C., 'Cleaning Strategies for Membranes Operating on Red-Meat Abattoir Waste Streams', Proceedings of the 3rd Biennial Conference of the Water Institute of Southern Africa, pp. 124-125, May 1993 (Abridged Paper).

BROUCKAERT, C.J., BROUCKAERT, B.M. and BUCKLEY, C.A.,'Prediction of Osmotic Pressure of Inorganic Ionic Solutions from Equilibrium Speciation', Proceedings of the 3rd Biennial Conference of the Water Institute of Southern Africa, pp. 156-157, May 1993 (Extended Abstract of Poster).

3.13 Books

BUCKLEY, C.A., BROUCKAERT, C.J. and KERR, C.A., Chapter on 'RO Application in Brackish Water Desalination and in the Treatment of Industrial Effluents' in *Reverse Osmosis : Membrane Technology, Water Chemistry and Industrial Applications*, Z. Amjad (ed), Van Norstrand Reinhold Publishing Company, New York, pp. 275-299, 1993, ISBN 0 442 23964 5.

3.14 Patents

A patent has resulted from this project. The patent is entitled :

Pressure Driven Semi-Permeable Membrane State : Method and Apparatus. (Provisional Patent Application No. 92/4962 in the name of the Water Research Commission).

The claims of the patent are described below.

3.14.1 Claims

1. A method of monitoring the condition of a semi-permeable membrane including the steps of :

   monitoring the selected parameters of the feed fluid, reject fluid and/or permeate fluid, and

   automatically calculating, either continuously or at selected intervals, the condition of the membrane from values of the monitored parameters.

2. A method according to claim 1 wherein the parameters being monitored are one or more of :

   (i) feed pressure, temperature, flow rate and concentration

   (ii) reject pressure, temperature, flow rate and concentration

   (iii) permeate flow rate, temperature and concentration.

3. A method according to either preceding claim wherein, from time to time, correction factors are applied to the monitored parameters to remove second and third order effects from the calculations.

4. A method according to any preceding claim wherein there are a plurality of membranes, and selected parameters for each of the membranes are monitored, either continuously or at selected intervals, to determine the condition of the respective membranes.

5. A method according to any preceding claim wherein said calculations are performed by a processor device the method including the further steps of controlling a plant using the output from the processor such that the plant will not operate under scaling conditions, and/or activating alarms or interrupting the operation of the plant when an undesirable operating state is detected.

6. Apparatus for monitoring the condition of a semi-permeable membrane comprising, a series of probes for monitoring selected parameters of the feed fluid, reject fluid and/or permeate fluid associated with the membrane, and a processor device adapted to receive information in accordance with a pre-programmed algorithm, and produce an output indicative of the condition of the said membrane.

7. Apparatus according to claim 6 wherein it is adapted for use in monitoring a plurality of membranes in a plant or system, probes being associated with at least a significant member of the membranes in a plant or system.

8. Apparatus according to claim 6 or 7 wherein the probes are adapted to monitor one or more of :

   (i) feed pressure, temperature, flow rate and concentration

   (ii) reject pressure, temperature, flow rate and concentration

   (iii) permeate flow rate, temperature and concentration.

9. Apparatus according to any one of claims 6 to 8 wherein at least some of the probes are adapted to measure the conductivity of the liquid in which the probes are in use located.

10. Apparatus according to any one of the claims 6 to 9 wherein the processor device is adapted to produce a numerical simulation of the membrane-separation process as it occurs at a particular membrane.

11. A method of monitoring a semi-permeable membrane substantially as hereinbefore described with reference to the drawings.

12. Apparatus for monitoring the condition of semi-permeable membrane substantially as hereinbefore described and illustrated.

4 CONCLUSIONS

Conclusions specific to each of the case studies undertaken during the project have been set out previously in the relevant sections of the report; this section presents general conclusions related to the project as a whole.

Membrane separation is a mature technology in terms of materials and equipment, but still needs development in terms of processes, particularly in the field of industrial waste water treatment. Computer modelling has a role to play in process development through interpreting, correlating and extrapolating experimental data. The modelling techniques applied during this project have not been developed to the point where they can replace experimental data, but they can be used to reduce experimental effort.

To do this most effectively, modelling and experimentation should be carried out together, so that the implications of results can be assessed immediately, and that areas where data are required can be identified.

Modelling can also be used to help find the optimal design for a new plant, in optimising the operation of an existing plant, or in monitoring its performance and investigating operational problems. The Lethabo experience has shown that even when the modelling does not help directly to identify a problem, the discipline of gathering the data required to describe the process in a fundamental way will probably lead to identifying the problem.

With regard to the generalised multi-solute computer program developed in this project: as it now exists, it does not yet incorporate all the techniques which were found useful in the application case studies, although its framework has been designed to incorporate them. Thus there is still a need to improve its capability and ease of use.

The technology transfer aspect of this project can be divided into two components: the promotion of the use of RO modelling as an engineering technique, and the technical spinoffs which have resulted from involvment in the various case-studies.

During the course of the project, the first of these components was only partially successful, in that although a variety of people were introduced to the modelling programs, no one outside the project made use of it independently. Subsequently the model has been made available to the Internet community through the EMILY (Electronic Membrane Information LibrarY), the FTP site established at the Computing Centre for Water Research (CCWR). This has resulted in the model being taken up by a number of researchers, and several improvements have been implemented.

The project has undoubtedly made significant contributions to the processes with which it became involved. The Lethabo plant is now fully operational, and Eskom has expressed appreciation for the contributions made by this project. Both the abattoir effluent treatment process and the sugar refinery brine recovery process have been shown to be technically feasible, and commercial implementations are being seriously considered. A demonstration TRO plant is in operation at Secunda, and it is confidently expected that a full-scale plant will be installed during 1995.

5 RECOMMENDATIONS

(i) Membrane researchers, consultants and users should be encouraged to use modelling in data interpretation, plant design and process monitoring. The Electronic Membrane Information Library (EMILY) on the CCWR computer is the natural way to support this. Data obtained from experimental investigations could be reduced to model parameters and stored on EMILY where it would easily available to others. Courses on membrane separation modelling should continue to be given occasionally.

(ii) The computer programs which constitute the model need further improvement to make them accessible to a wider range of users. These improvements involve the coding of well-defined procedures, and could be effected by short, targetted exercises: for instance involving post-graduate students.

(iii) The programming framework which has been developed has potential as the basis for modelling other water related unit operations. For instance, the *IMPULSE* computer program for residence time distribution modelling, which was developed as part of WRC project number 363, *The Development of Small Scale Water Treatment Equipment*, used a very similar basis. The concerns of modelling are usually similar for most fields of application, and in a family of related models, each would benefit from developments to others. Thus consideration should be given to applying the same approach to other unit operations.

6 REFERENCES

ALLISON,J.D.,BROWN,D.S. And NOVO-GRADAC,K.J.(1990). **MINTEQA2/PRODEFA2, A Geochemical Assessment Model for Environmental Systems: Version 3.0.** Athens: U.S Environmental Protection Agency, Georgia.

Belfort, G. (1984). **Synthetic Membrane Processes.** Academic Press, Orlando.

BROUCKAERT, B.M. (1991). **Laboratory Investigation of the Relationship Between TDS, Conductivity and Osmotic Pressure for the Lethabo TRO Pilot Plant.** Pollution Research Group Internal Report.

Brouckaert, B.M. (1992). **Prediction of Osmotic Pressure from Equilibrium Speciation of Inorganic Ionic Solutions.** Water Research Commission Document No. 4.3/92.

Brouckaert, C.J. and Buckley C.A. (1992). **The Use of Computer Simulation of Tubular Reverse Osmosis in Conjunction with Pilot Plant Studies.** Presented at the IAWPRC Specialized Conference on Membrane Technology in Wastewater Management, Cape Town, 2-5 March 1992, (Water Research Commission document No. 4.6/92).

Cheryan M. (1986). **Ultrafiltration Handbook.** Technomic Publishing Company, Inc. Pennsylvania, USA. pp. 73-116.

Chibi, C. and Kruger, S. (1993). **Roughing Demineralization as Pretreatment.** Eskom Technology, Research and Investigations Internal Report, Johannesburg.

Davies, C.W.(1962). **Ion Association.** Washington D.C.: Butterworths Publications

Erdey-Gruz, T. (1974). **Transport Phenomena in Aqueous Solutions.** London: Adam Hilger Ltd. 255-260

Finnigan, S.M. and Howell, J.A. (1989). **Chem Eng Res Des**, 67 pp 278-282

Finnigan, S.M. and Howell, J.A. (1990). **Desalination**, 79 pp 181-202

Flemmer R.L.C., Buckley C.A. and Groves G.R. (1982). An Analysis of the Performance of a Spiral-Wound Ultrafiltration Membrane, with a Turbulence-Promoting Net. *Desalination*, 41, pp. 25-32.

Flemmer R.L.C. (1983). Performance of a Spiral-Wound Ultrafiltration Membrane with Turbulence-Promoting Net under Conditions of Strong Pressure Gradient and Fouling. *Desalination*, 48, pp. 321-329.

Helgeson, H.C. (1969). **Thermodynamics of Hydrothermal Systems at Elevated Temperatures and Pressures.** American Journal of Science 267:729-804.

Mackley, M.R., Tweedle, G.M. and Wyatt, I.D. (1990). **Chem Engng Sci**, 45(5), pp 1237-1242

Matz R. and Meitlis Y. (1978). Design and Operating Parameters for Tubular Ultrafiltration Membrane Modules. *Desalination*, 24, pp. 281-294.

McAfee, A.L., Nowlin, W., and Beardsley, S. (1990). **Pretreatment of an ion exchange demineralizer with reverse osmosis.** Ultrapure Water Vol 7 No 7, pp 54-62.

Mickley, M.C. (1985). A Charged Ultrafiltration Membrane Process for Water Softening, *International Desalination Association Journal*, 1(1), pp. 1-13.

Perry, M. and Linder, C. (1989). **Intermediate Reverse Osmosis Ultrafiltration (RO UF) Membranes for Concentration and Desalting of Low Molecular Weight Organic Solutes,** *Desalination*, 71, pp. 233-245.

Perry, R.H., Green, D., and Maloney J.O., (1984). **Perry's Chemical Engineers' Handbooks**, McGraw-Hill, Singapore.

Press, W.H., Flannery, B.P., Teukolsky, S.A., Vetterling, W.T., **Numerical Recipes**, Cambridge University Press, Cambridge, 1986.

Pitera, E.W. and Middleman, S. (1973). **Convection Promotion in Tubular Desalination Membranes,** *Ind Eng Chem Process Des Dev*, **12**(1), p 52.

Rautenbach, R. and Albrecht, R. (1989). *Membrane Processes*, John Wiley & Sons, p. 136.

Reid, R.C, Prausnitz, J.M. and Poling, B.E. (1987). **The properties of Gases and Liquids.** 4th Ed. McGraw-Hill, New York.

Robinson, R.A. And Stokes ,R.H. (1959). **Electrolyte Solutions**, 2nd Edition. London: Butterworths Scientific Publications.

Schirg, P. and Widmer, F. (1992). **Characterisation of Nanofiltration Membranes for the Separation of Aqueous Dye-salt Solutions,** *Desalination*, **89**, pp. 89-107.

Schutte, C.F., Spencer, T., Aspden, J.D. and Hanekom, D. (1987). **Desalination and Re-use of Power Plant Effluents: From Pilot-Plant to Full-Scale Application,** Desalination, **67**, pp 225-269

Sourirajan, S., and Matsuura, T. (1985). **Reverse Osmosis/Ultrafiltration Process Principles**, National Research Council, Canada Publications, Ottawa.

Sourirajan, S. (1970). **Reverse Osmosis**. New York: Academic Press.

Spiegler, K.S. and Kedem, O., (1966). Thermodynamics of Hyperfiltration (Reverse Osmosis) : Criteria for Efficient Membranes, *Desalination*, 1, pp. 311-326.

Talbot J.D.R, House W.A. and Pethybridge A.D. (1990). **Prediction of the temperature dependence of electrical conductance for river waters.** Water Research 24, 10, 1295-1304.

WEAST, R.C. (1983). **CRC Handbook of Chemistry and Physics**, 64th Edition. Boca Raton: CRC Press, Florida.

WATER RESEARCH COMMISSION PROJECT NO. 325

RESEARCH ON THE MODELLING OF TUBULAR REVERSE OSMOSIS SYSTEMS

Appendix 1

Modelling of the Lethabo Power Station TRO Pilot Plant

Simulation of Tubular Reverse Osmosis

Published in WaterSA Vol 18 No 3, July 1992

CJ Brouckaert and CA Buckley

Pollution Research Group
Department of Chemical Engineering
University of Natal
Durban

February 1995

Simulation of Tubular Reverse Osmosis*

C J Brouckaert and C A Buckley**

Pollution Research Group, Department of Chemical Engineering, University of Natal, King George V Avenue, Durban 4001, Republic of South Africa

Abstract

The rational design of reverse osmosis systems is made difficult because the engineering variables of pressure, flow rate, solute rejection and permeate flux are inter-related in a complex way, even before such effects as membrane fouling and degradation are taken into account. Where pilot-plant data may be available, unless they cover a very comprehensive range of operating conditions, it will still be difficult to estimate the consequences of varying the parameters in the process of seeking the most economic design. A similar situation applies to an existing plant which has to be adapted to changing circumstances.

Although complex, the underlying mechanisms of reverse osmosis are quite well understood, and are readily amenable to computer simulation. A computer package is being developed to serve as a tool for the analysis or design of reverse osmosis plants. Its use is demonstrated by means of a hypothetical case study based on pilot-plant data gathered at the Lethabo Power Station near Sasolburg.

Introduction

Reverse osmosis (RO) first became a commercially viable desalination process in the late 1960s, and rapidly established itself in the field of potable water production from brackish water, and later also from sea water. Today it is the preferred technology for these applications.

Almost from the beginning, the potential of RO for the treatment of industrial effluents and pollution control was recognized, since it provides a means for effecting a pure separation of solutes from water, with minimal or no addition of treatment chemicals, and with no phase change. Progress in this field has, however, not matched the spectacular achievements of the natural water desalination applications. Part of the reason for this is the sensitivity of RO membranes to fouling and chemical damage, together with the variability of industrial effluents, both from location to location, and with respect to time at a single location, so that the accumulation of relevant expertise is a relatively arduous process.

---

* Revised Paper. Originally Presented at the 6th National Meeting of the South African Institution of Chemical Engineers, Elangeni Hotel, Durban, Republic of South Africa, 7-9 August 1991.

** To whom all correspondence should be addressed.

Commercial RO membranes are generally packaged in one of three major configurations : tubular, spiral-wrapped and hollow-fine-fibre modules. The latter two are very efficient in terms of providing a large surface area per unit volume, but are very sensitive to fouling, since mechanical cleaning of any sort is impossible. Tubular membranes typically have a 12,5 mm tube diameter, and are relatively tolerant of particulates in the feed, and can be cleaned by passing sponge-balls through them in addition to chemical cleaning methods. Thus, they may be the only practical choice for some effluents, in spite of their low capacity.

A computer model of tubular reverse osmosis (TRO) is being developed by the Pollution Research Group of the University of Natal, under the sponsorship of the Water Research Commission, as a tool to be used in the investigation, design and evaluation of aqueous effluent treatment plants, with special reference to the TRO modules manufactured by Membratek of Paarl..

In 1987 Eskom built a TRO plant to separate salts from the cooling tower blow-down at the Lethabo Power Station near Sasolburg. The motivation was to reduce the volume of saline effluent to that required for the conditioning of the station's ash dumps, thus achieving a zero aqueous effluent discharge to the environment. In the previous year, a pilot investigation was carried out using a plant consisting of 30 Membratek TRO modules, each containing 1,72 m^2 of cellulose-acetate membrane in 12,5 mm diameter tubes (Schutte et al., 1987). Eskom have made some of the data gathered from the pilot-plant available to provide a realistic test of the modelling procedures.

This paper explores, through simulation, some aspects of the relationship between the pilot-plant and the full-scale plant that was designed from it, to illustrate the use of computer modelling in conjunction with pilot-plant investigations.

The basis of the computer model

There are two major theories of transport through RO membranes in the literature, the so-called solution-diffusion model, and the finely-porous-capillary model (Rautenbach and Albrecht, 1989). The latter model is largely due to the work of Sourirajan and co-workers over the last 30 years (Sourirajan and Matsuura, 1985). It has been shown (Muldowney and Punzi, 1988) that the predictions of the two models are virtually identical in practice. The formulation used in this work is based on the one due to Sourirajan.

The conceptual basis of the model is illustrated in Fig. 1.

Water is driven through the membrane by the pressure gradient. As the solute is rejected by the membrane, it is concentrated in a layer adjacent to the membrane surface. This raises the osmotic pressure, Π_m, of the solution at this point. The concentrating tendency is limited by turbulent diffusion of the solute back into the bulk flow. The flux of water N_w through the membrane is taken as proportional to the difference in the effective pressure ($P - \Pi$) across the membrane :

$$N_w = \frac{A}{\mu} [(P_m - \Pi_m) - (P_p - \Pi_p)] \qquad (1)$$

where A is a constant, characteristic of the membrane,
μ is the viscosity of water,
P is the piezometric pressure,
Π is the osmotic pressure of the solution,
subscripts m and p refer to positions at the inner and outer membrane surfaces respectively.

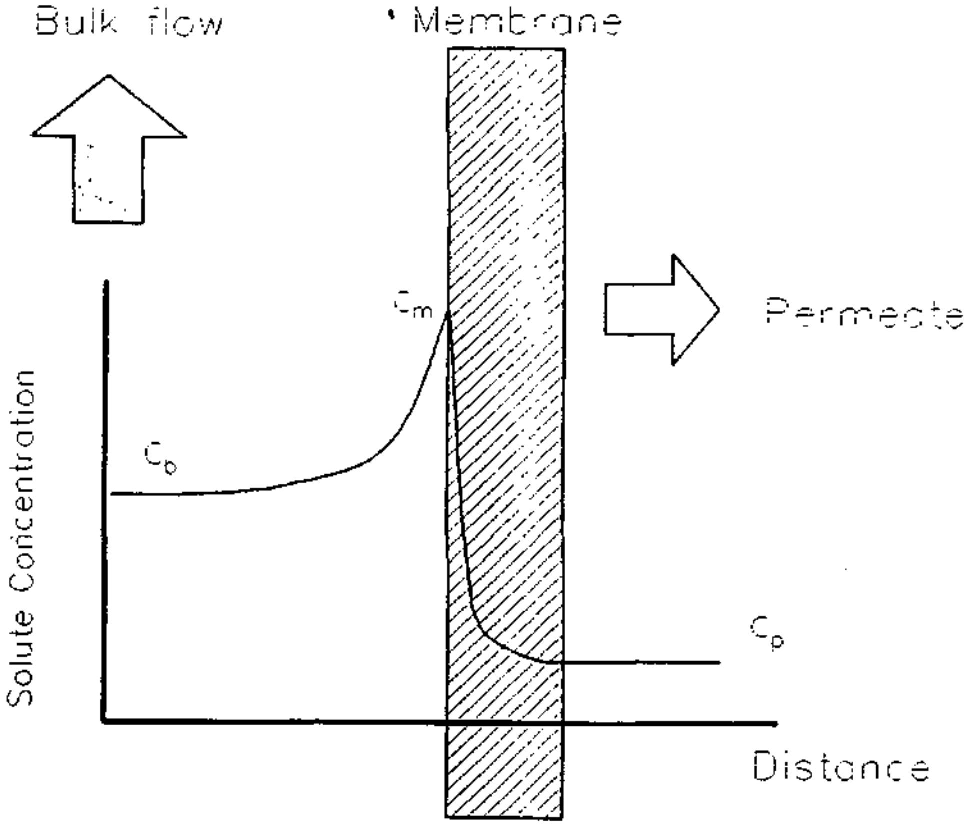

Figure 1
A schematic diagram of the reverse osmosis model. The solute concentration increases from c_b in the bulk solution to c_m adjacent to the membrane, and then decreases through the membrane to c_p in the permeate.

Although the solute is rejected by the membrane, some does diffuse through. The solute flux N_s is given by

$$N_s = D(c_m - c_p) \tag{2}$$

Here D is a transport coefficient which is dependent on the membrane material, its effective thickness, and nature of the solute. c_m and c_p are the solute concentrations at the inner and outer membrane surfaces respectively.

Finally, the concentration at the inner membrane surface, c_m, is determined by a balance between the convective transport of solute towards the membrane by the water flux, and the opposing turbulent diffusion of solute away from the surface. Standard film-diffusion theory yields the relationship :

$$N_w = k(1 - c_p) \ln \left[\frac{c_m - c_p}{c_b - c_p} \right] \tag{3}$$

where N_w is the flux of water through the boundary layer film, and k is a turbulent mass transfer coefficient, the magnitude of which is related to the Reynolds number of the flow in the tube. At steady state the flux through the boundary layer is the same as the flux through the membrane.

Simultaneous solution of these three equations yields the water and solute fluxes at any point in the TRO train. To calculate the performance of the whole system, these point predictions must be integrated down the length of the tubes, taking into account the changing pressure, flow rate and concentrations as the RO process takes place. Further details of the numerical procedures appear in the Appendix.

The adjustable parameters in this scheme are the constants A and D, which depend on the membrane and the solute involved. The turbulent mass transfer coefficient, k, can be determined from literature correlations. The correlation used in this study was (Belfort, 1984) :

$$Sh = 0.0096 \; . \; Re^{0.913} \; Sc^{0.346} \tag{4}$$

where Sh is the Sherwood number, Re is the Reynolds number, and Sc is the Schmidt number.

The Lethabo TRO pilot-scale and full-scale plants

The Lethabo pilot-scale and full-scale plants have been described by Schutte et al. (1987). The pilot plant consisted of three banks of TRO modules. The first bank contained three parallel rows of four modules in series, the second bank 2 x 4, and the third 1 x 10 (see Fig. 6b). This *tapered* configuration was aimed at maintaining the flow velocities in the tubes as the overall volumetric flow rate progressively decreased down the tubes. The full-scale plant does not make use of a tapered configuration; it consists of 5 184 modules in essentially a 432 x 12 array, although they are physically organized in smaller blocks.

The pilot-plant data, which Eskom made available for this study, consisted mainly of pressures, flow rates and conductivities measured on the feed, permeate and concentrate streams. In addition a limited number of detailed chemical analyses were performed on samples of these streams. A representative set of analyses appears in Table 1.

TABLE 1

Typical analyses of pilot-plant streams

Determinand		Feed	Permeate	Concentrate
Cl^-	mg/ℓ	270	45,8	650
SO_4^{2-}	mg/ℓ	1 140	54,5	2 491
Ca^{2+}	mg/ℓ as $CaCO_3$	425	2,8	1 078
Mg^{2+}	mg/ℓ as $CaCO_3$	90	1,2	214
Na^+	mg/ℓ	406	47	956
K^+	mg/ℓ	76	3,3	250
PO_4^{3-}	mg/ℓ	0,48	0,02	0,73
SiO_2	mg/ℓ	39,3	14,8	82,7
Conductivity	mS/m	313	27	722
pH		5,5	5,5	5,9

In its present stage of development, the model only allows for a single solute. Furthermore it requires, as data, a relationship between solute concentration and osmotic pressure, a quantity which had not been measured by Eskom. It was decided to use total dissolved solids (TDS) as a single *pseudo-solute*, and to determine relationships between TDS, conductivity and osmotic pressure from synthetic solutions, made up in the laboratory to match the Eskom analyses. Since the different ionic species are rejected to different extents by the RO membranes (for instance, divalent ions tend to be more strongly rejected than monovalent) the relative proportions of the ions differ in the feed, permeate and concentrate streams. Thus there were potentially three sets of these relationships for the three streams. Three stock solutions were made up to match the relative salt concentrations shown in Table 1, and then three solutions were made from each of these by dilution.

Figures 2 and 3 show the results of these measurements. The data are satisfactorily represented by a single set of relationships. In the case of the conductivities, the values reported in the Eskom analyses could be compared with those determined for the synthetic solutions : the correspondence shown in Fig. 2 is quite satisfactory.

The relationships used for the model were obtained from the data by simple linear regression :

$$Conductivity\ (mS/m) = 1.391 \times 10^2 \times TDS\ (g/l) \quad (5)$$

$$Osmotic\ pressure\ (kPa) = 43.55 \times TDS\ (g/l) \quad (6)$$

The simple relationships that were found seem to justify to some extent the approximations involved in representing the mixed solute as a single entity.

Equations (5) and (6) represent the physical chemistry of the solutions for modelling purposes. The remaining modelling parameters needed to be obtained from the pilot-plant performance data. These were the membrane parameters, A and D in Eqs. (1) and (2), and an additional parameter representing the hydraulic pressure drops across the module array.

The pressure drop in the RO tubes is calculated according to the standard friction factor correlation for turbulent flow in pipes; however, additional pressure drop is incurred by the u-bend connectors between tubes within the modules, and the inter-connectors and manifolds between the modules. These were modelled simply as an extra length L of (impermeable) tube for each RO tube in each module. Simulations of the pilot-plant configuration were run for a specific feed pressure, flow rate and conductivity, and the values of A, D and L adjusted to fit the permeate flow rate and conductivity, and the concentrate exit pressure.

The available pilot-plant data covered nine months of operation, during which time the membranes went through a number of cycles of progressive fouling, followed by cleaning, possibly with longer term irreversible deterioration also taking place. One would expect to find the modelling parameters to be correlated with the varying condition of the modules, and it would be very interesting to subject the data to such an analysis. For the purpose of this paper, however, a single set of parameters was chosen corresponding to conditions just after the membranes had been cleaned, as summarized in Table 2.

TABLE 2

Pilot-plant operating conditions selected for model parameter determination.

Model Parameters		*Measured*	*Simulation*
A	kg/m^2	-	2,21x10^{-6}
D	m/s	-	2,01x10^{-6}
L	m	-	0,11
Input Variables			
Temperature	°C	27	27
Feed Pressure	MPa	2,9	2,9
Feed Flow rate	m^3/h	1,46	1,46
Feed Conductivity	mS/m	370	370
Output Variables			
Exit Pressure	MPa	1,9	1,82
Permeate Flow rate	m^3/s	1,05	1,06
Permeate Conductivity	mS/m	27	25

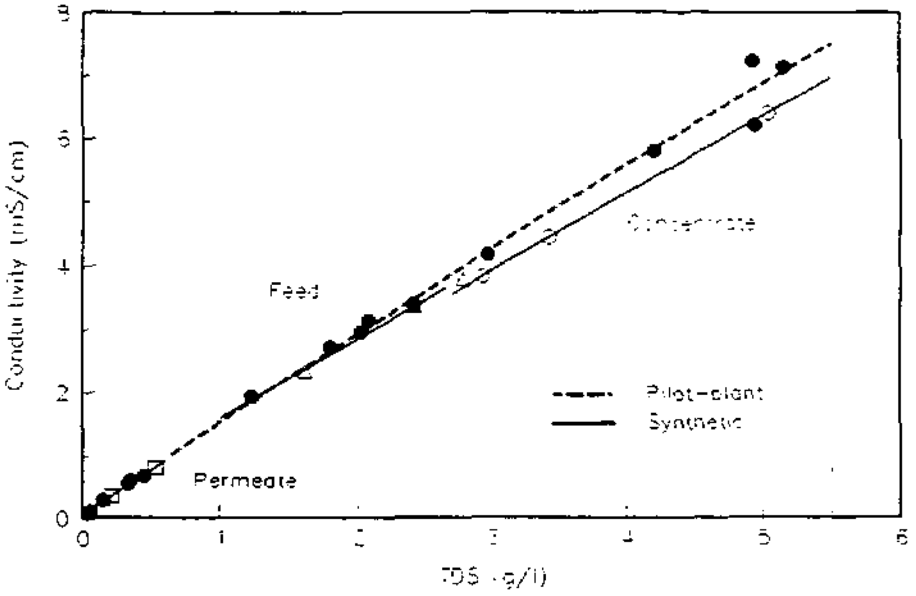

Figure 2
The relationship between TDS and conductivity for the Lethabo pilot-plant streams. Representative data from the pilot-plant feed, permeate and concentrate streams are compared with synthetic solutions based on the analyses shown in Table 1.

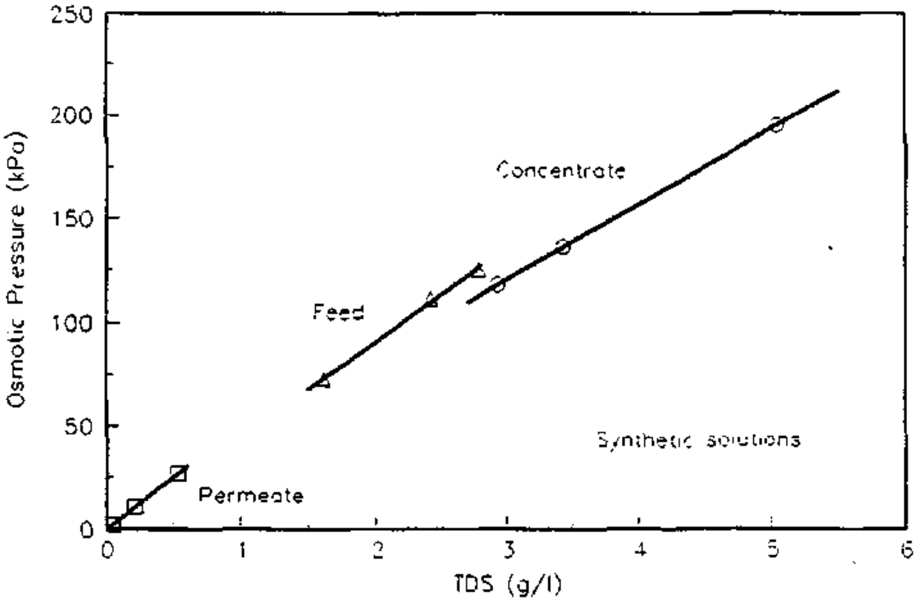

Figure 3
The relationship between TDS and osmotic pressure for the Lethabo pilot-plant streams. Measurements on synthetic solutions are based on the analyses shown in Table 1.

Simulations of the full-scale plant configuration

As mentioned above, the full-scale plant consists of 432 parallel rows of 12 modules in series. Schutte et al. (1987) presented a set of operating conditions, from which the following figures (Table 3) have been extracted :

TABLE 3

Operating conditions for full-scale plant

		Feed	Permeate	Concentrate
Flow	m^3/h	375	263	112
TDS	mg/ℓ	1 300	81	4 276
Temperature	°C	25 - 30		

Unfortunately no operating pressure was reported, so a complete comparison between plant data and the simulation was not possible. For feed conditions as in Table 2, and a feed pressure of 4 MPa, the model gave the following results (Table 4) :

TABLE 4 : Simulated performance of the Lethabo plant at 4 MPa

		Permeate	Concentrate
Flow	m^3/h	268	107
TDS	mg/ℓ	60	4 400

The agreement is sufficiently good to show that the simulation is reasonably realistic, which is all that is required for the purpose of this paper.

Comparison between the pilot-plant and full-scale plant configurations

A pilot study is undertaken in order to obtain data on which to base the eventual design of the plant. This data includes the relationships between equipment performance measures, such as flux and rejection, and operating parameters, such as pressure, flow rate and water recovery, as well as safe operating limits, and some assessment of the requirements for maintenance procedures such as membrane cleaning and membrane replacement.

Given the complex interdependence of variables in RO equipment, there is an interesting question as to what the relationship is between measurements made in the pilot-plant and the equivalent variables for the full-scale configuration. This question is, of course, a crucial one for the engineer who bases his design on the pilot-plant data. Simulation provides a convenient method for investigating such questions, given that the model is reasonably realistic.

Figures 4 to 6 show the results of a set of comparative simulations for the Lethabo pilot-plant and full-scale plant configurations. For all simulations feed conditions of 1 300 g/ℓ TDS and 27 °C were used. Two feed pressures were investigated, 2 MPa and 4 MPa and appropriate feed flow rate ranges for each configuration. In order to allow direct comparison of the two configurations, the results are presented in terms of water recovery and pressure. Since the permeate flow rate is largely determined by the pressure, for a given pressure there is an inverse relationship between water recovery and feed flow rate.

The first point of difference between the two configurations is that the full-scale configuration can be operated over a considerably wider range of water recoveries than the pilot plant. This is because the latter has a greater number of modules in series, as well as a tapered configuration, which leads to a higher hydraulic pressure drop. The lower limit for water recovery corresponds to the situation where the outlet pressure drops to atmospheric pressure. Naturally this would not be a practical operating condition as the flux through the later modules in the train would be much reduced. The driving force for permeation is the hydraulic pressure difference minus the osmotic pressure difference across the membrane; its value at the plant exit for the two configurations is shown in Fig. 4a.

The behaviour of the permeate quality, shown in Fig. 4b is very interesting. For the full-scale configuration it passes through a minimum at 40 to 50 % water recovery. The water is driven through the membrane by pressure, whereas the solute passes through by a concentration gradient driven diffusion. At higher water recoveries, the permeate concentration increases due to the higher concentration in the tubes, whereas at lower water recoveries, the increase is due to the lower water flux as a result of the reduced average pressure caused by the high flow rate. In the case of the pilot plant, the pressure drop limit is reached before the minimum occurs.

As can be seen from Fig. 5, the reject concentration is almost entirely determined by water recovery, and is very little dependent on pressure or configuration. One of the reasons that the reject concentration is of interest is that salts in the solution may be concentrated above their saturation limit, and cause scaling of the equipment. The critical component of the Lethabo effluent in this regard is gypsum ($CaSO_4{\cdot}2H_2O$). For the feed composition shown in Table 1, it was calculated from solubility data quoted in Rautenbach and Albrecht (1989) that gypsum exceeds its solubility limit at a TDS of 5,2 g/ℓ. The concentration is expressed as a per cent scaling potential in Fig. 5 by taking 5,2 g/ℓ as 100 %. This occurs at a water recovery of about 75 %, which may be compared with the Lethabo plant operating figure of 70 % quoted by Schutte et al. (1987). It is interesting that the pilot plant was initially operated at 76 % water recovery, but this was later dropped to 70 % after scaling problems were encountered, and the latter value was chosen for the full-scale plant design.

Figure 4
Simulated results for the Lethabo pilot plant and full-scale plant at feed pressures of 2 MPa and 4 MPa

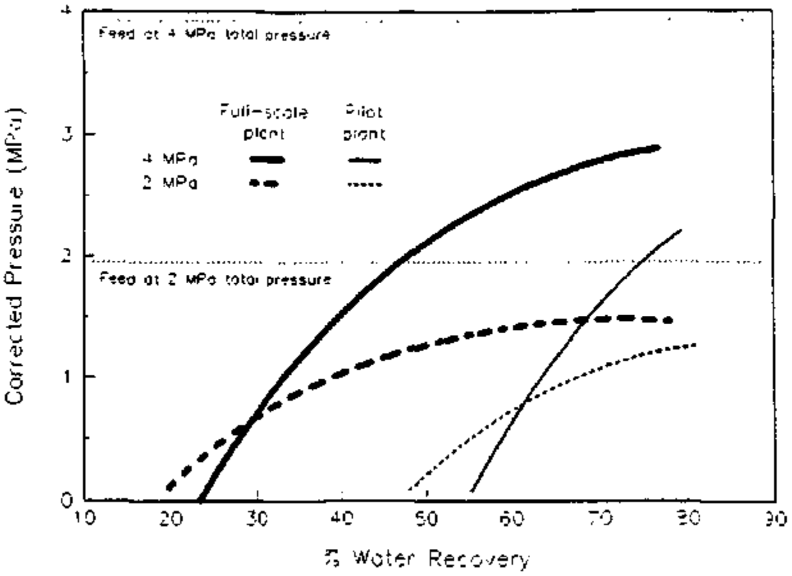

Figure 4a
Effective pressure driving force for water permeation (total pressure - osmotic pressure) across the membrane at the plant exits. Hydraulic pressure drop prevents the pilot plant from being operated at water recoveries below about 50%

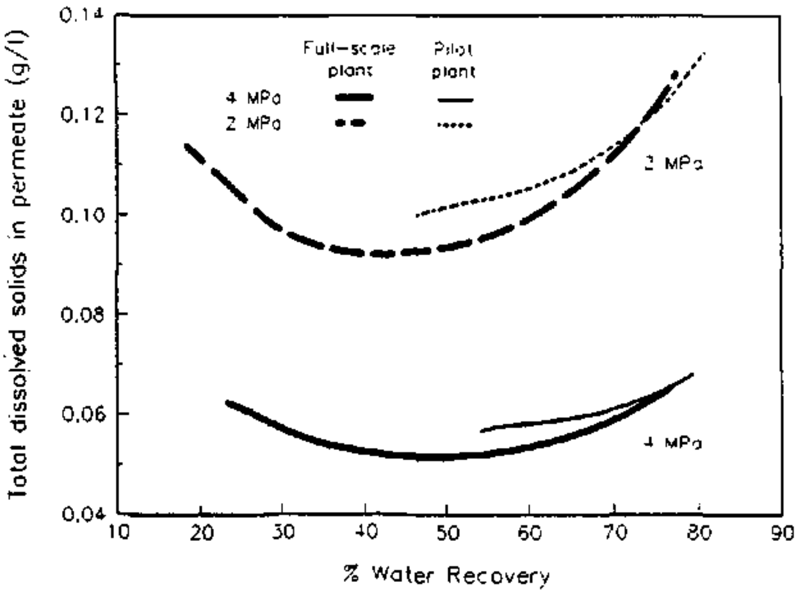

Figure 4b
Total dissolved solids in the permeate stream

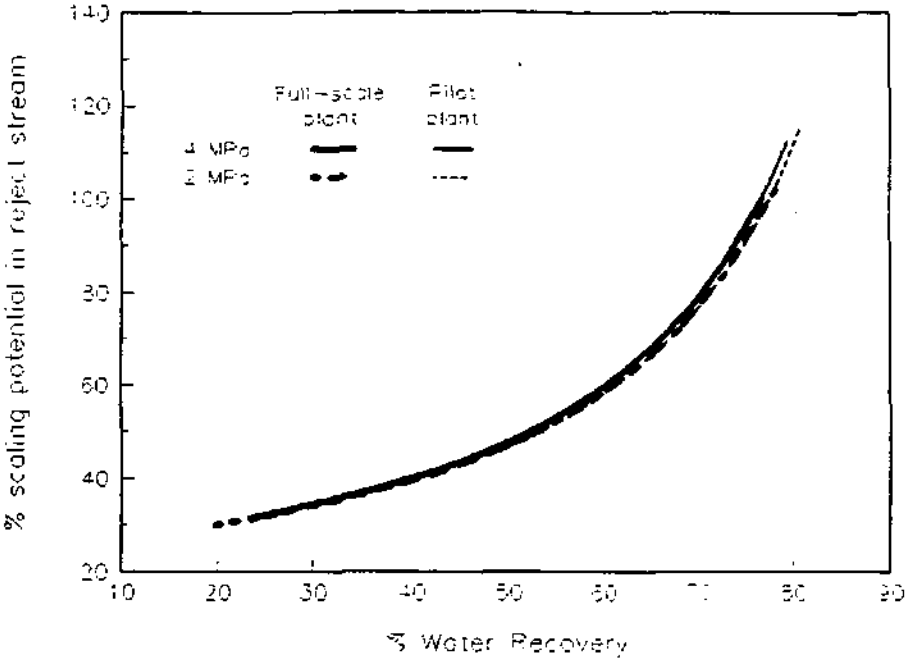

Figure 5

Solute concentrations in the concentrated brine streams of the Lethabo pilot plant and full-scale plants, expressed in terms of $CaSO_4{\cdot}2H_2O$ scaling potential

If one considers the diagram in Fig. 1, the reject concentration corresponds to the bulk concentration at the plant exit, c_b. It is clear that this is not the highest concentration that the membranes encounter; instead the highest concentration is in the boundary layer immediately adjacent to the membrane surface, c_m. This concentration is not easily observable in an experimental sense; however, it is a key variable in the model. From Fig. 6a it can be seen that the pilot-plant configuration generates higher flow velocities at the exit, which lead to high turbulent mass transfer, and a lower concentration rise in the boundary layer.

Figure 6b shows the variation of c_m at the plant exits, once again expressed as per cent scaling potential. It can be seen that, for the feed conditions chosen, the full-scale plant is appreciably more prone to scaling that the pilot-plant. In particular, at 70 % water recovery the pilot-plant is in a non-scaling region, wheres the full-scale plant is in a scaling region. The steepness of the curves at this point indicates that the situation would be very sensitive to changes in conditions, such as an increase in feed concentration.

Figure 6
Simulated results for the Lethabo pilot plant and full-scale plant at feed pressures of 2 MPa and 4 MPa

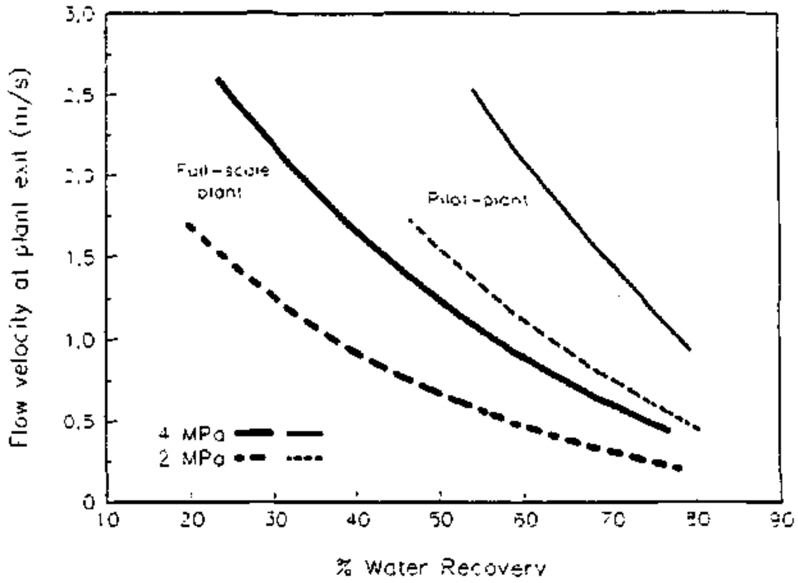

Figure 6a
Flow velocities in the concentrated brine streams at the plant exits

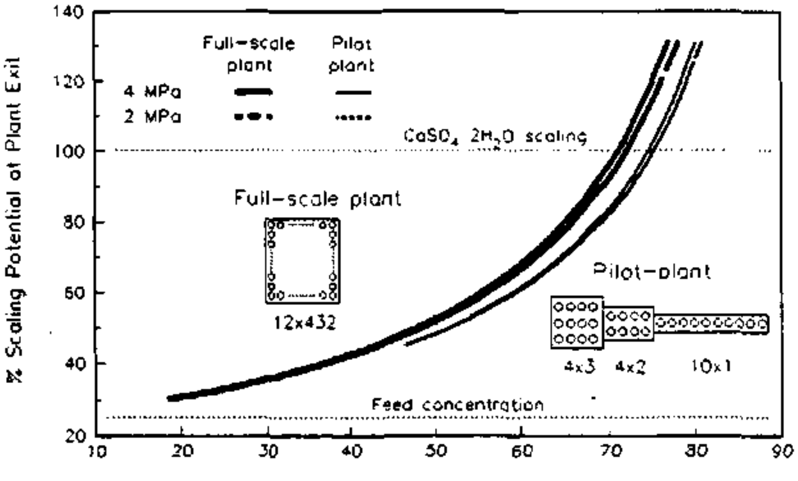

Figure 6b
Solute concentrations in the boundary layer adjacent to the membrane surface at the plant exits. expressed in terms of CaSO4.2H2O scaling potential

The effect of operating variables on the performance of the Lethabo full-scale plant

A set of simulations was run for the following feed conditions :

Pressure : 2,5 to 4,5 MPa
Flow : 250 to 450 m^3/h
TDS : 1 300 mg/ℓ
Temperature : 27 °C

It turned out that not all these combinations of pressure and flow gave feasible solutions : at high pressures and low flows the tubes *ran dry* before the exit was reached. In practice, a limit would be reached even sooner than the model indicated, because of precipitation of scale on the membranes. As previously discussed, the TDS value at which $CaSO_4 \cdot 2H_2O$ would start to precipitate was taken as 5,2 g/ℓ.

Figure 7 shows the response surface for the membrane concentration, with the scaling limit contour plotted. Since this contour represents an important limitation on the plant's operation, it has been transferred to some of the other response surface plots for reference.

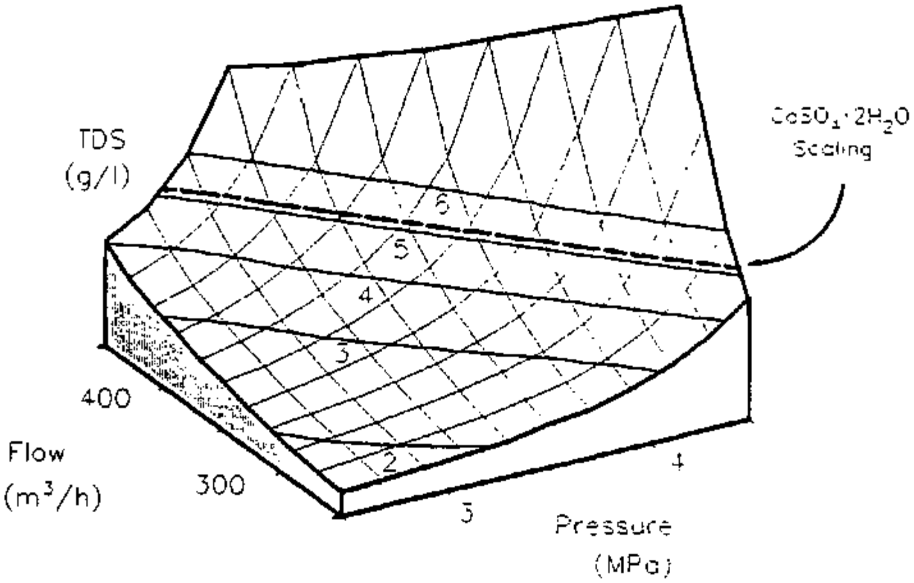

Figure 7
Simulated response surface for membrane concentration for the full-scale Lethabo TRO plant. The broken line indicates the limiting locus of conditions which will result in gypsum starting to precipitate on the membrane surfaces at the plant exit.

Figure 8 shows the corresponding plot for the solute concentration in the concentrate stream. It can be seen that the scaling limit on the membranes occurs before the solubility product is exceeded in the concentrate.

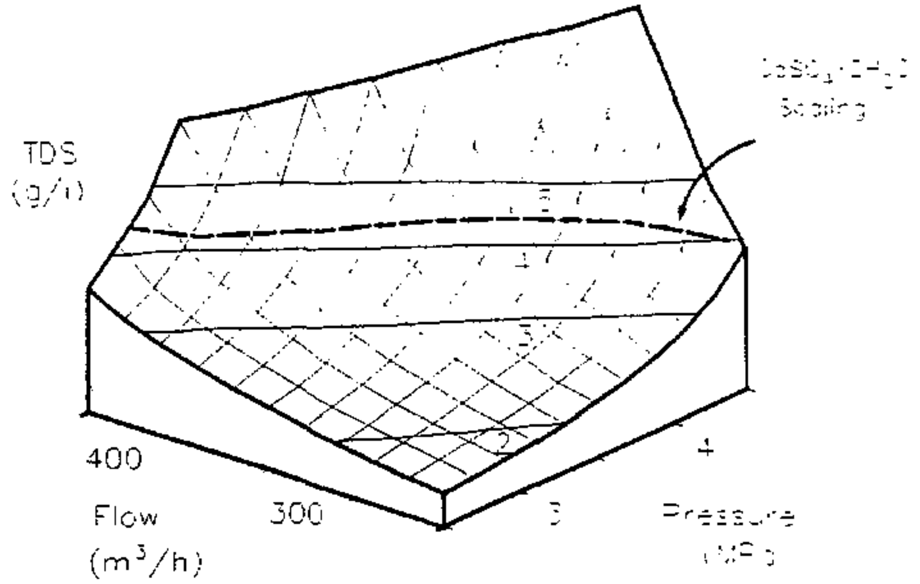

Figure 8

Simulated response surface for exit concentration for the full-scale Lethabo TRO plant to feed pressure and flow rate. The broken line indicates the limiting locus of conditions which will result in gypsum starting to precipitate on the membrane surfaces at the plant exit.

Figures 9 and 10 are the corresponding response surfaces for the permeate flux and concentration. Note that the viewing orientations have been changed from the other plots in order to get a better impression of the surface shapes.

Optimizing a design according to some economic objective is a standard design technique. Ideally this objective function should include contributions for capital costs, running costs, maintenance etc. Since the purpose of this paper is only to illustrate a methodology, a simplified objective function is presented in Fig. 11.

The purpose of the plant is to remove salt from the cooling tower circuit, while replacing the water. The benefit, therefore, can be expressed as the mass of salt removed from the permeate, calculated as :

$$Permeate\ flow \times (Feed\ TDS - Permeate\ TDS)$$

The power cost incurred is simply $pressure \times flow\ rate$ for the feed.

The ratio of these quantities can be termed the plant *productivity* expressed as kg salt removed per kJ of energy expended.

Figure 11 shows the plot for productivity, thus defined. It can be seen how the productivity is favoured by high pressures and low flow rates, and how it is limited by membrane scaling.

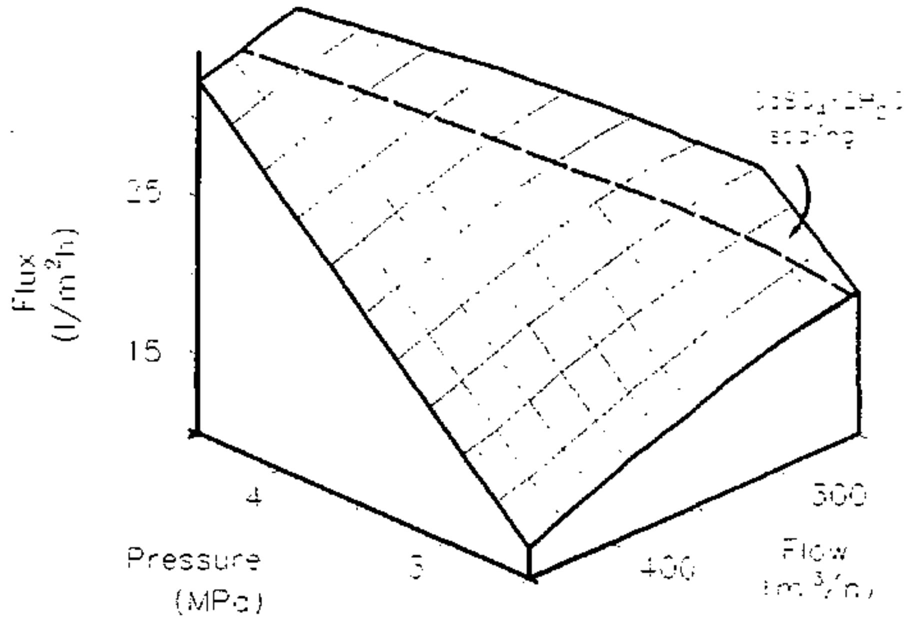

Figure 9
Simulated response surface for permeate flux of the full-scale Lethabo TRO plant to feed pressure and flow rate.

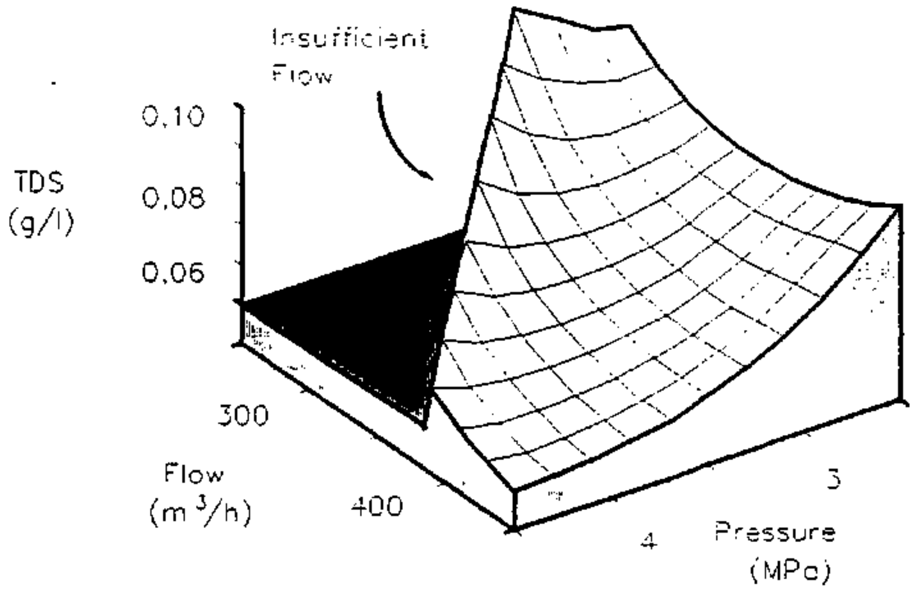

Figure 10
Simulated response surface of permeate concentration of the full-scale Lethabo TRO plant to feed pressure and flow rate. At the higher pressures the lower feed flow rates are insufficient to maintain a reject stream flow at the plant outlet.

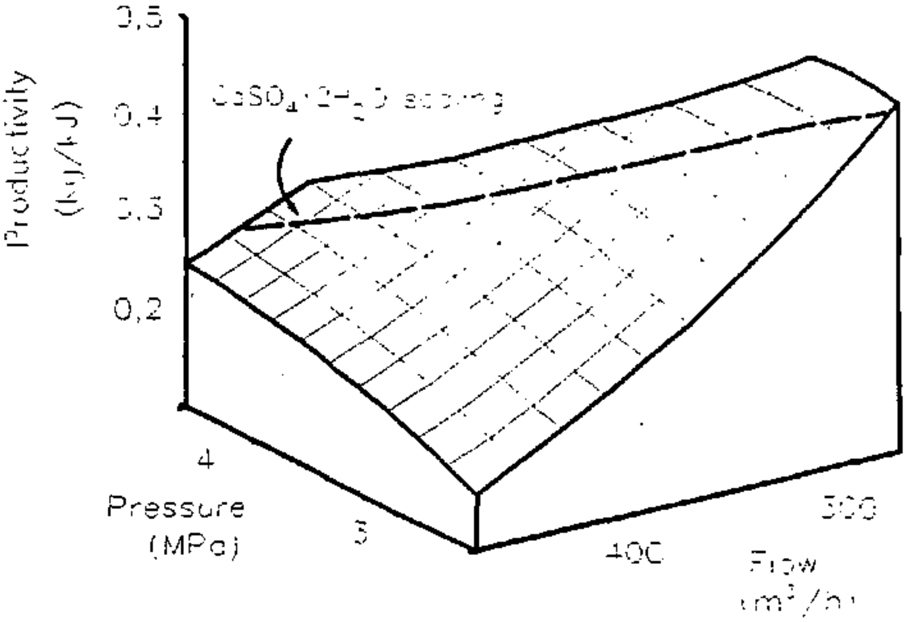

Figure 11
Simulated response surface of the productivity of the full-scale Lethabo TRO plant to feed pressure and flow rate.

It is worth noting that the benefits of such an optimization could not be realized by adjusting the pressure and flow after the plant was built, because reducing the feed pressure to the plant by throttling the pumps would not reduce their power consumption.

Finally, Fig. 12 shows the productivity surface for a different configuration of 5 184 modules, consisting of 8 rows of 432 modules, followed by 8 rows of 216 modules - a tapered configuration. It can be seen that the productivities of this latter configuration are much the same as for the former, but that a new constraint appears, in that the lower pressures are not able to achieve some of the higher flow rates through the plant. As might be expected, the $CaSO_4 \cdot 2H_2O$ scaling is slightly less restricting, because of the higher flow velocities at the back-end of the plant. This alternative configuration is not proposed here as being superior to the original, but is included to illustrate the point that having a model available would allow a designer to explore the characteristics of alternative configurations in order to choose the optimum one.

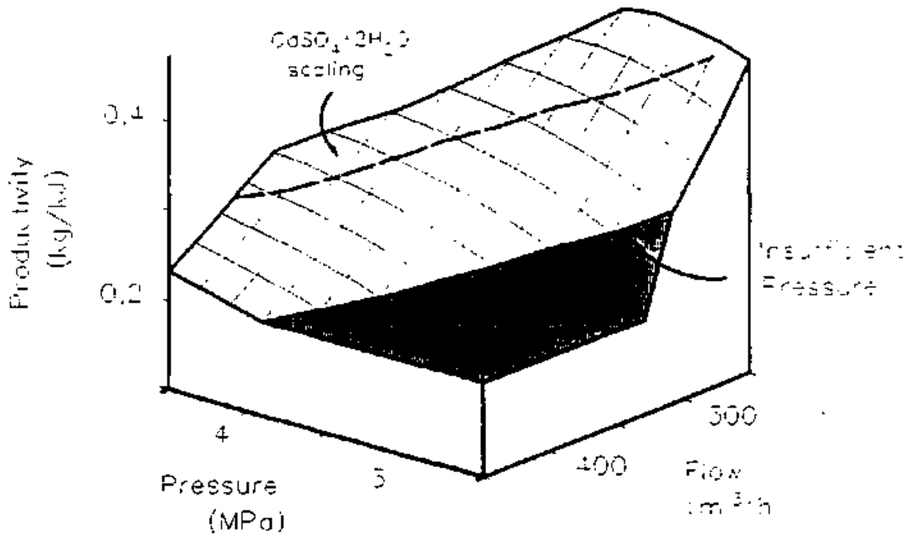

Figure 12
Simulated response surface for the productivity of a tapered-configuration TRO plant, equivalent in size to the full-scale Lethabo TRO plant, to feed pressure and flow rate. At the higher flow rates the lower pressures are insufficient to overcome the hydraulic resistance of the plant.

Conclusions

This study has shown that the model, even in its present relatively simple form, is able to represent the performance of a real plant to a useful degree of accuracy, and should be able to enhance the quality of information obtained from pilot-plant work, by allowing investigators to explore the implications that their findings hold for the eventual design.

Since only a limited amount of the pilot-plant data was used in determining the simulation parameters, important considerations such as membrane fouling, cleaning and degradation, as well as variations in feed quality, are not reflected in the simulations that have been presented. Consequently the results should not be seen as constituting a commentary on the actual design of the Lethabo plant.

Acknowledgements

The authors wish to acknowledge the contributions of :

> Eskom and Miss. B.M. Brouckaert for the laboratory work and the preparation of the diagrams.

This investigation was undertaken in terms of a Water Research Commission project.

References

BELFORT, G. (1984). *Synthetic Membrane Processes.* Orlando : Academic Press.

MULDOWNEY, G.P. and PUNZI, V.L. (1988). **A Comparison of the Solute Rejection Models in Reverse Osmosis Membranes. System : Water-sodium Chloride-Cellulose Acetate.** *Ind. Eng. Chem. Process Res. Dev.*, **27**, 2341.

PERRY, J.H. (1963). *Chemical Engineers' Handbook*, McGraw-Hill, Tokyo.

RAUTENBACH, R. and ALBRECHT, R. (1989). *Membrane Processes.* Chichester : John Wiley & Sons.

SCHUTTE, C.F., SPENCER, T., ASPDEN, J.D. and HANEKOM, D. (1987). **Desalination and Re-use of Power Plant Effluents from pilot-plant to full-scale application.** *Desalination*, **67**, 255-269.

SOURIRAJAN, S. and MATSUURA, T. (1985). *Reverse Osmosis/Ultrafiltration Process Principles.* Ottawa : National Research Council, Canada.

Nomenclature

A = RO membrane pure water permeability coefficient, kg/m^2

c = Solute concentration, kg/m^3

d = Tube diameter, m

D = RO membrane solute transport coefficient, m/s

$\mathcal{D}$ = Molecular diffusivity of solute in water, m^2/s

k = Turbulent diffusion mass transfer coefficient, m/s

L = Equivalent length of RO tube per module to account for pressure drops through fittings, m

N = Flux, kg/m^2.s

P = Pressure, Pa

Q = Flow rate through RO tubes, m^3/s

v = Flow velocity, m/s

ΔA = incremental membrane area in numerical integration, m^2

ΔL = incremental tube length in numerical integration, m

ΔP = incremental pressure drop in numerical integration, Pa

μ = Viscosity of water, Pa.s

Π = Osmotic pressure, Pa

ρ = Density of fluid, kg/m^3

Sh = Sherwood Number $\frac{kd}{\mathcal{D}}$

Re = Reynolds Number $\frac{\rho v d}{\mu}$

Sc = Schmidt Number $\frac{\mu}{\rho \mathcal{D}}$

Subscripts

b = in the bulk solution within an RO tube

m = in the solution at the membrane surface

p = in the RO permeate

s = solute

w = water

APPENDIX 1

DESCRIPTION OF THE TUBULAR REVERSE OSMOSIS MODEL ALGORITHM

The transport of water and solute through the TRO membrane at any point is governed by Eqs. (1), (2) and (3), the membrane parameters A and D, and the local values of the variables P, c_b and k. A standard modelling situation is considered, in which A and D are known, as are P, c_b and Q, the flow rate for the feed stream. Thus the transport equations can be solved at the entrance to the plant, to yield permeate flux and concentration.

From a material balance and hydraulic pressure drop calculation, the change in the conditions of the solution flowing in the tubes may be calculated as it passes through a length of the tubes, ΔL. Repeated application of this procedure constitutes an Euler method numerical integration of the whole process along the length of the tubes.

Solution of the transport equations at a point

The numerical solution of the transport equations is considered in some detail by Sourirajan and Matsuura (1985), and their method was followed in this work, with some modifications. In the standard modelling situation, the three equations contain 4 unknowns, N_s, N_w, c_b and c_p.

The material balance on the solute :

$$c_p = \frac{N_s}{N_w + N_s}$$

completes the description of the process. Since the equations are non-linear and require numerical solution, it is advantageous to reduce as much as possible the number of equations that must be solved simultaneously. By combining the four equations, it is possible to reduce them to two equations involving c_m and c_p. Various combinations are possible, and the one chosen here was :

$$A[P - \pi_m + \pi_p]c_p - D(1 - c_p)(c_m - c_p) = 0$$

$$c_m - c_p - (c_b - c_p)\exp\left[\frac{D(c_m - c_p)}{kc_p}\right] = 0$$

This choice was different to the one adopted by Sourirajan and Matsuura, and was selected because it led to an algorithm that was less likely to cause computer arithmetic errors (numerical overflow or division by zero) when the numerical solution procedure tried unrealistic values for c_m and c_p. The above two equations were solved using a standard Newton-Raphson method.

Hydraulic modelling

Where the flow was divided between parallel rows of modules, it was assumed that the division was even. For the Euler integration, the step ΔL was taken as the length of one tube in the module (2,3 m). The pressure drop down the tube was calculated using the Blasius formula (Perry, 1963) for smooth pipes :

$$\frac{\Delta P}{\Delta L} = -0.079 \cdot \left(\frac{\rho v^2}{d}\right) \cdot Re^{-0.25}$$

An extra pressure drop corresponding to the extra and equivalent length of the hydraulic fitting and returned bends was added for each tube.

Material balance

After the transport equations had been solved in each step of the integration, the flows and concentrations on either side of the membrane were updated according to the quantities of water and solute transferred.

Thus, considering the *i*th incremental section of RO tube, with membrane area, ΔA:

$$Q^i = Q^{i-1} - (N_w^i + N_s^i)\ \Delta A$$

$$c_b^i = \frac{c_b^{i-1}\ Q^{i-1} - c_p^i\ (N_w^i + N_s^i)}{Q^i}$$

Since a single permeate stream was produced by the plant, it was a mixture of the permeates produced by each RO tube in the plant. Its flow and composition was calculated as :

$$Q_{permeate} = \sum_i (N_w^i + N_s^i)$$

$$c_{permeate} = \frac{\sum_i N_s^i}{Q_{permeate}}$$

WATER RESEARCH COMMISSION PROJECT NO. 325

RESEARCH ON THE MODELLING OF TUBULAR REVERSE OSMOSIS SYSTEMS

Appendix 2

Modelling of the Lethabo Power Station TRO Pilot Plant

The use of Computer Simulation of Tubular Reverse Osmosis in conjunction with Pilot-Plant Studies

Published in Water Science and Technology, Vol 25 No 10, July 1992

CJ Brouckaert and C A Buckley

Pollution Research Group
Department of Chemical Engineering
University of Natal
Durban

February 1995

THE USE OF COMPUTER SIMULATION OF TUBULAR REVERSE OSMOSIS IN CONJUNCTION WITH PILOT-PLANT STUDIES

C.J. Brouckaert and C.A. Buckley

Pollution Research Group, Department of Chemical Engineering
University of Natal, Durban 4001, Republic of South Africa

ABSTRACT

A computer model, based on the equations formulated by Sourirajan and Matsuura (1985), has been used to analyse data generated by a tubular reverse osmosis (TRO) pilot-plant treating a cooling-tower blow-down stream at Lethabo power station near Sasolburg, South Africa. These data, covering more than 3 000 hours of operation over a period of 10 months, were examined in terms of the variation of modelling parameters, as determined by regression, with time. This transformation of the data has yielded valuable insight into the effect of the plant's operating history on the condition of the membranes. Furthermore, using the model to simulate the operation of a full-scale plant has made it possible to explore some of the implications that the pilot-plant measurements hold for an eventual design.

Simulation is not yet able to substitute for pilot-plant investigation, particularly in cases of complex and/or fouling streams such as are often encountered in industrial effluent treatment applications, but may be used very effectively to enhance the quality of information gained from such studies.

INTRODUCTION

In 1987 the Electricity Supply Commission (ESKOM) built a TRO plant to separate salts from the cooling tower blow-down at the Lethabo power station near Sasolburg. The aim was to reduce the volume of saline effluent to that required for the conditioning of the station's ash dumps, thus achieving a zero aqueous effluent discharge to the environment. In the previous year, a pilot investigation was carried out using a plant consisting of 30 Membratek TRO modules, each containing 1,72 m^2 of cellulose-acetate membrane in 12,5 mm diameter tubes (Schutte et al., 1987). ESKOM have made some of the pilot-plant data available to provide a realistic test of the modelling procedures.

THE LETHABO TRO PILOT- AND FULL-SCALE PLANTS

The Lethabo pilot- and full-scale plants have been described by Schutte et al. (1987). The pilot-plant consisted of three banks of TRO modules. The first bank contained 4 rows in series of 3 modules in parallel, the second bank 4 x 2, and the third 10 x 1. This *tapered* configuration maintained the flow velocities in the tubes as the overall volumetric flow rate progressively decreased down the tubes. The full-scale plant does not make use of a tapered configuration; it consists of 5 184 modules in what is essentially a 432 x 12 array, although they are physically organized in smaller blocks.

Both pilot-plant and full-scale plant were equipped with automatic flow-reversal/sponge-ball cleaning systems. On the pilot-plant, this system was not in operation for the whole of the test period. The sponge-ball cleaning was supplemented, as the need arose, with soap washes, using a 2 % "Biotex" detergent solution. These occurred at approximately weekly intervals.

The blow-down stream from the cooling towers, which formed the feed to the pilot-plant, contained 2 000 to 3 000 mg/ℓ total dissolved solids (TDS), consisting largely of Na^+, K^+, Ca^{++}, Mg^{++}, Cl^-, SO_4^{--} ions, and SiO_2. On the pilot-plant pressures, flow rates and conductivities of the feed, permeate and concentrate streams were measured, together with a few sets of relatively complete chemical analyses of the three streams.

Figure 1 attempts to summarize the entire data set by plotting flux and rejection (based on conductivity) as a function of hours of operation. The gaps in the record are periods for which the data from the logsheets was not transferred to the computer.

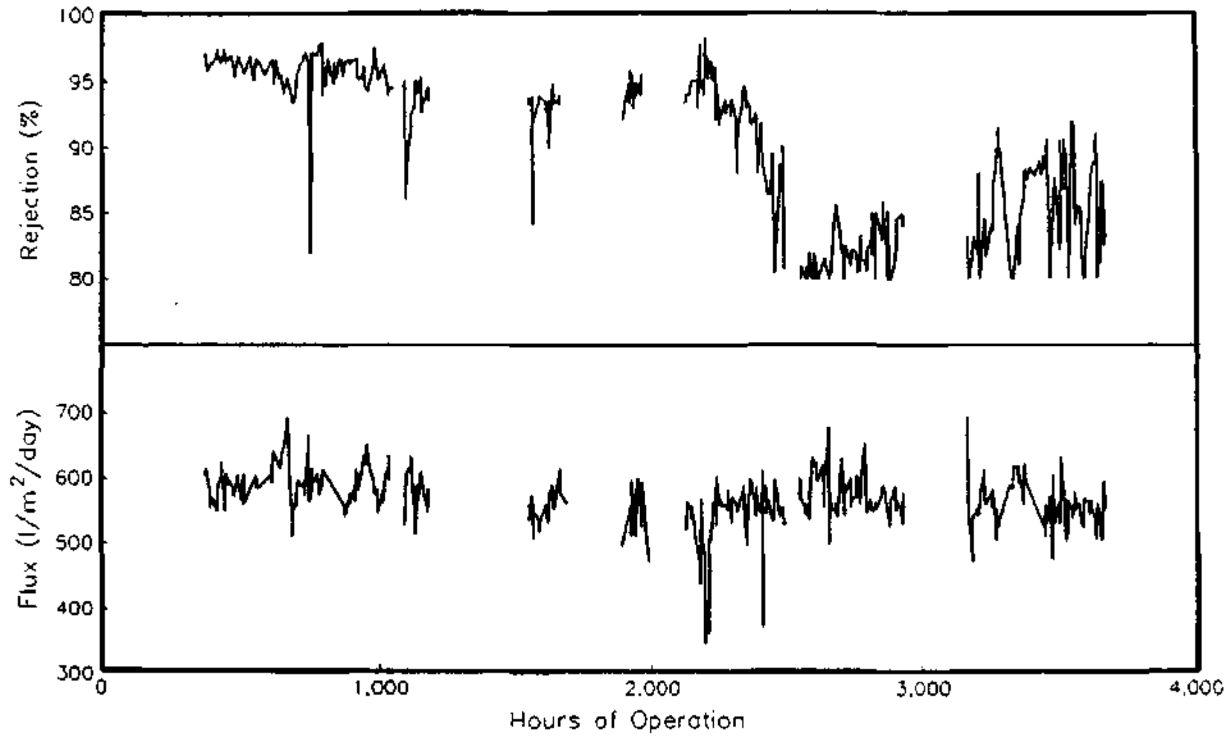

Fig. 1. Flux and rejection (based on feed and permeate conductivities) for the Lethabo TRO pilot-plant

What cannot be determined easily from such a representation is how much the observed variations in flux and rejection are due to changes in feed concentration, operating pressure or water recovery, and how much are attributable to changes in the state of the membranes.

OUTLINE OF MODELLING PROCEDURES

A detailed description of the modelling procedures has been reported previously (Brouckaert and Buckley, 1992). A brief summary is given below.

Synthetic solutions were made up according to the detailed chemical analyses provided by ESKOM. Relationships between TDS, conductivity and osmotic pressure were determined. The mixed solute was modelled as a single entity, with the total dissolved solids (TDS) measurement taken to represent its concentration.

A potential limitation on the operation of plant was the possibility of salts in the feed being concentrated above their saturation limits and precipitating to form a scale on the membrane surface. The critical component of the Lethabo effluent in this regard was gypsum ($CaSO_4{\cdot}2H_2O$). From the chemical analysis of the concentrate stream and solubility data (Rautenbach and Albrecht, 1989) it was calculated that gypsum should exceed its solubility limit at a TDS concentration of 5,2 g/ℓ.

Sourirajan's model (Sourirajan and Matsuura, 1985) considers three coupled mass-transfer processes occurring at the reverse osmosis (RO) membrane interface. These involve :

a) the flux of solvent (water) through the membrane under the influence of the pressure gradient across it. This is represented in the model by a *pure water permeability* parameter A. Sourirajan has noted from experimental observation that A is not constant for a particular membrane-solvent-solute system, but varies with system temperature and pressure. The sub-model for A used for this work, following Sourirajan's suggestion, was :

$$A = \frac{k_1}{\mu}\exp(-\alpha P) \tag{1}$$

where P = the piezometric pressure on the high pressure side of the membrane

α = an empirical constant, representing the tendency of the membrane to become reversibly compressed.

μ = the viscosity of water at the system temperature.

k_1 = an empirical regression coefficient.

b) the flux of solute through the membrane by a diffusional mechanism, driven by the concentration difference across the membrane. This is represented in the model by the *solute transport parameter* $\mathcal{D}$. $\mathcal{D}$ is also the subject of an empirical sub-model, which is (following Sourirajan) :

$$\mathcal{D} = k_2\exp(0{,}005T)\,P^{-\beta} \tag{2}$$

where β = another empirical constant, similar to α above

T = the absolute system temperature in K

k_2 = an empirical regression coefficient

c) the flux of solute, rejected by the membrane surface, back through the concentration boundary-layer adjacent to the surface into the bulk flow on the high-pressure side of the membrane, by a turbulent diffusion mechanism. This is represented by the film diffusion mass-transfer coefficient $\mathcal{K}$, which was calculated from the correlation (Belfort, 1984) :

$$Sh = 0,0096 \ . \ Re^{0.913} \ Sc^{0.346} \tag{3}$$

where Sh = the Sherwood number
Re = the Reynolds number
Sc = the Schmidt number

DETERMINATION OF MODEL PARAMETERS

In the above equations, the empirical parameters k_1 and k_2 were fitted to the pilot-plant measurements by regression. These measurements were available at hourly intervals, and four consecutive sets were used to determine a pair of parameters representative of the state of the membranes at a particular time. The measurements were combined in this way to reduce the scatter of results due to the influence of random errors in the recorded measurements.

The remaining empirical parameters α and β were inferred from measurements which had been made in the laboratory on Membratek cellulose-acetate membranes of the same type as used in the modules. Their values were $\alpha = 4.25 \times 10^{-5}$ (kPa^{-1}) and $\beta = 0.0435$.

The reason for the different methods used to establish the various parameters was that the pilot-plant data were not sufficiently precise to determine meaningful values for all four parameters by regression. The model is not very sensitive to the values chosen for α and β.

INTERPRETATION OF THE PILOT-PLANT DATA IN TERMS OF MEMBRANE MODELLING PARAMETERS

Figure 2 represents a transformation of the data presented in figure 1 into terms of the regressed membrane coefficients k_1 and k_2. If the modelling is a reasonably accurate representation of the process, then these parameters should be properties of the membranes, and independent of pressure, temperature, feed concentration and water recovery. Unfortunately k_2 is not independent of the ionic composition of the feed, since the membrane permeabilities of different ions are known to differ, and the regressed value is therefore necessarily an average value for the ions present. However only a few detailed analyses were available, so it was not possible to make any allowance for variations in feed composition. Had the relevant measurements been available, it should have been straightforward to do so.

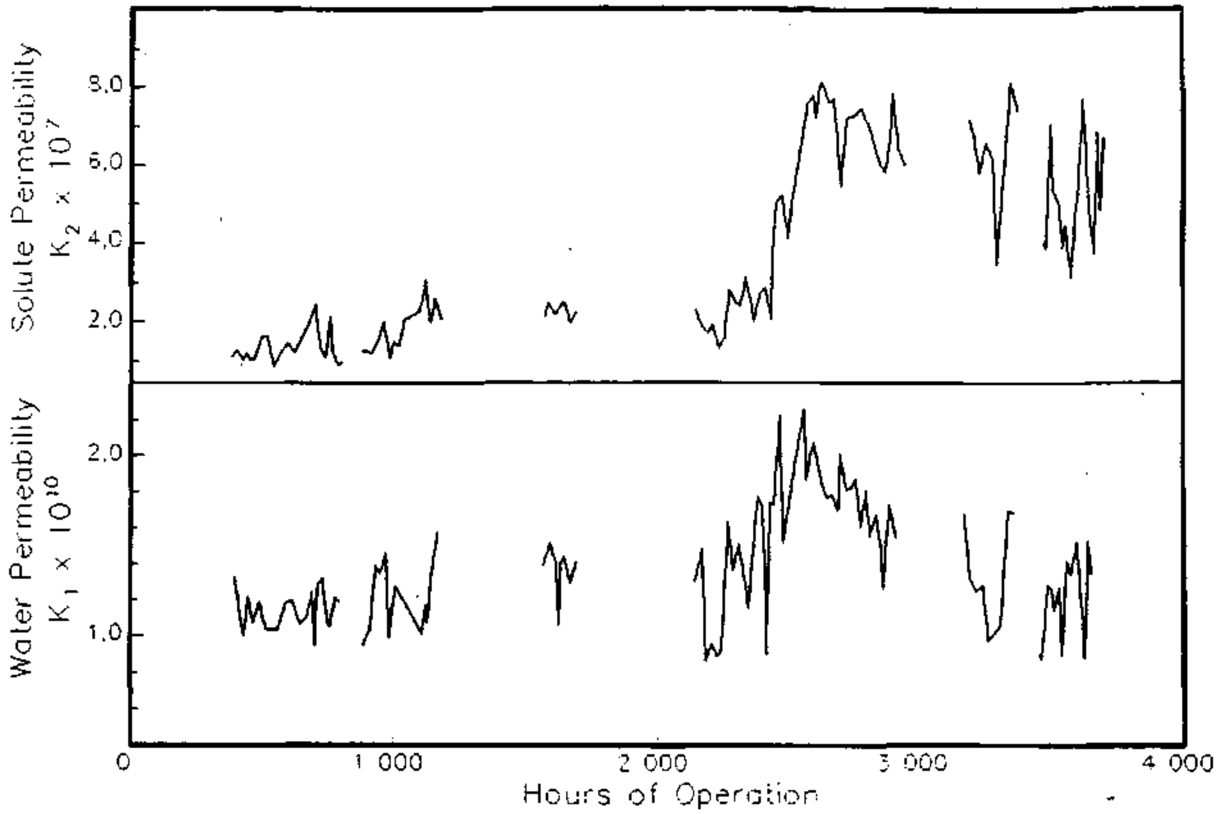

Fig. 2. Regressed values of the model parameters k_1 and k_2, which are related to the permeability of the membrane for water and solute respectively. Each point on the graph is regressed from four sets of measurements which were taken at hourly intervals on the pilot-plant

Considering the trace as a whole, the values are subject to short term variation, with a major change occurring at about 2 500 hours. While some of the short term scatter is undoubtedly due to noise in the experimental data, (either measurement error or incorrect recording), closer examination reveals that much of it can be related to the fouling-cleaning-fouling cycle. Figure 3 is an expanded view covering one of the soap wash incidents. Interestingly, the permeabilities of the membrane for both water and solute appear to decline with fouling, indicating that the foulant layer has some slight salt-rejecting character.

Equally interesting is the major shift in parameter values at about 2 500 hours. Figure 4 takes a closer look at this period. The shift in parameters follows immediately after two plant shut-downs which were required to make mechanical repairs. The first shut-down occurred at 2 365 hours and lasted 18 days. The second at 2 500 lasted 34 days. During at least part of the latter period a preservative formalin solution was introduced to prevent bacterial attack on the cellulose-acetate membranes. It is not clear from the operating log whether this was also done during the first shut-down. It is evident from the increase solute permeability that the membranes suffered some form of damage. The very high peak in both water and solute permeability immediately after the second shut-down may have been due to several modules being particularly badly damaged, since 6 modules were replaced between 2 500 and 2 750 hours. This is reflected in the partial return of the regressed parameters to lower values.

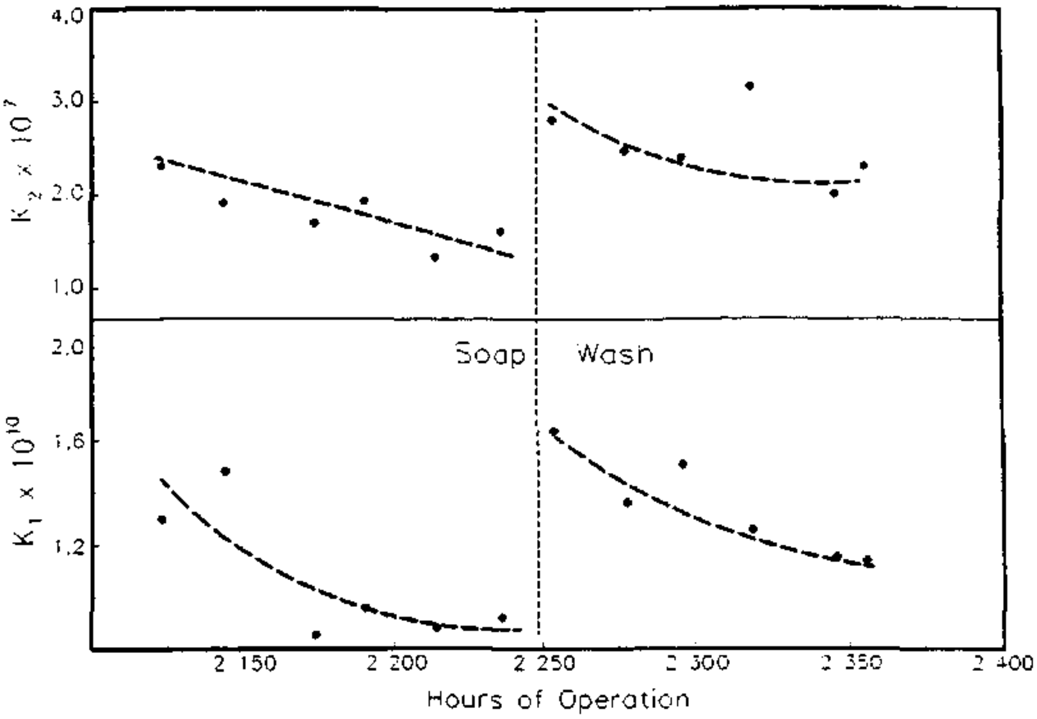

Fig. 3. Regressed values of the model parameters k_1 and k_2 for the period spanning a soap wash on the Lethabo TRO pilot-plant.

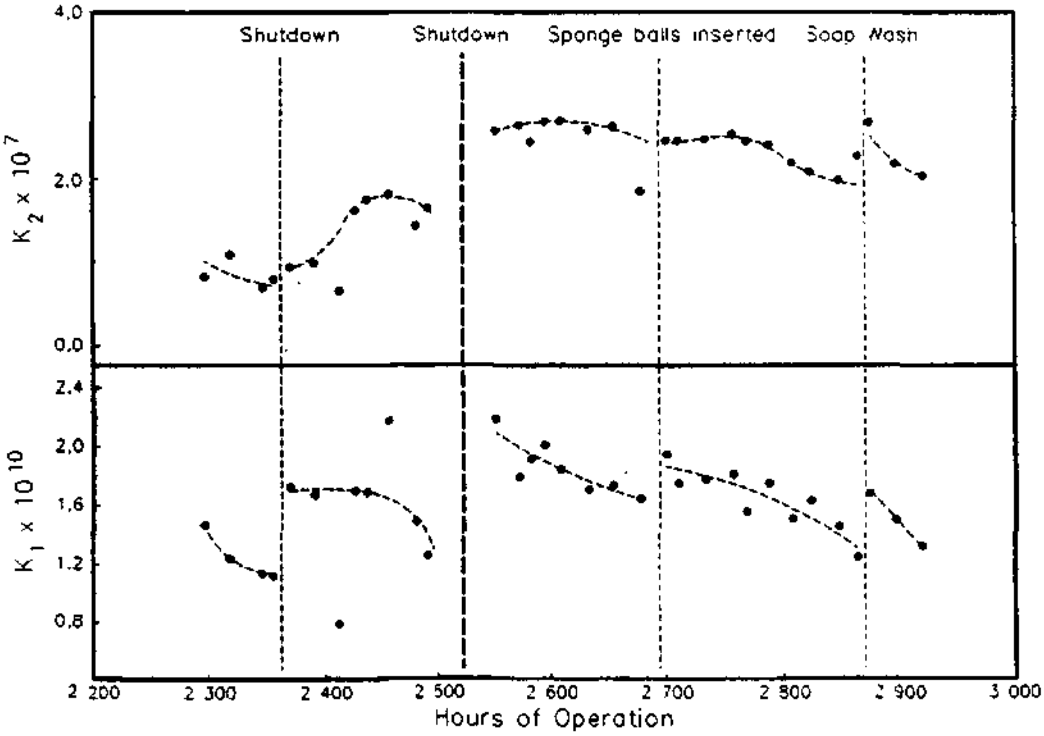

Fig. 4. Regressed values of the model parameters k_1 and k_2 for the period spanning two shut-downs on the Lethabo TRO pilot-plant.

THE EFFECT OF MEMBRANE CONDITION ON THE PERFORMANCE OF THE LETHABO FULL-SCALE PLANT

The most striking feature of the membrane parameter record was the almost three-fold increase in the solute permeability following the plant shut-downs. In the design of the full-scale plant it would be of interest to know what difference this would make to its economic performance. To illustrate how the computer model could be used to address such a question, two sets of simulations were run for a 432 x 12 module array, corresponding to the configuration of the full-scale plant. The first simulation used parameter values taken from the period before 1 000 hours of operation, and the second used values taken from the period after 3 500 hours of operation, after the grossly damaged modules had been replaced. The simulations used the following feed conditions :

Pressure	:	2,5 to 4,5 MPa
Flow	:	250 to 450 m^3/h
TDS	:	1 300 mg/ℓ
Temperature	:	27 °C

Not all these combinations of pressure and flow gave feasible solutions for the 'damaged' membrane parameters : at high pressures and low flows the tubes *ran dry* before the exit was reached. In practice, a limit would be reached even sooner than the model indicated, because $CaSO_4 \cdot 2H_2O$ would start to precipitate on the membranes at a TDS concentration of 5,2 g/ℓ.

Some economic objective function is required to make an assessment of the membrane performance. Ideally this objective function should include contributions for capital costs, running costs, maintenance etc. A simplified objective function, which accounts for only the energy cost, is presented in Figure 5.

The purpose of the plant is to remove salt from the cooling tower circuit, and return the desalinated water. The benefit, therefore, can be expressed as the mass of salt transferred from the permeate to the reject stream, and is calculated as :

$$Permeate\ flow \times (Feed\ TDS - Permeate\ TDS)$$

The power cost incurred is simply $feed\ \ pressure \times feed\ \ flow\text{-}rate$

The ratio of these quantities can be termed the plant *productivity* expressed as kg salt transferred per MJ of energy expended.

Figure 5 shows the plot for productivity, thus defined. Productivity is favoured by high pressures and low flow rates. In the shaded region, the TDS in the concentrated boundary layer immediately adjacent to the membrane surface exceeds 5,2 g/ℓ, the concentration at which $CaSO_4 \cdot 2H_2O$ becomes saturated. Since the plant was designed to run without precipitation inhibitor dosing, this region constitutes a limitation on its operation. For best energy efficiency, the plant should be operated at as high a pressure and as low a feed flow as is possible to remain safely within the non-scaling regime.

Comparison of the simulations using the "before" and "after" parameter values shows that the three-fold increase of salt permeability would result in a decrease in energy efficiency of about 25 %. The model can be used to evaluate the sensitivity of the design to other factors which are subject to uncertainty in a similar way: a facility which will be of value in the design stage.

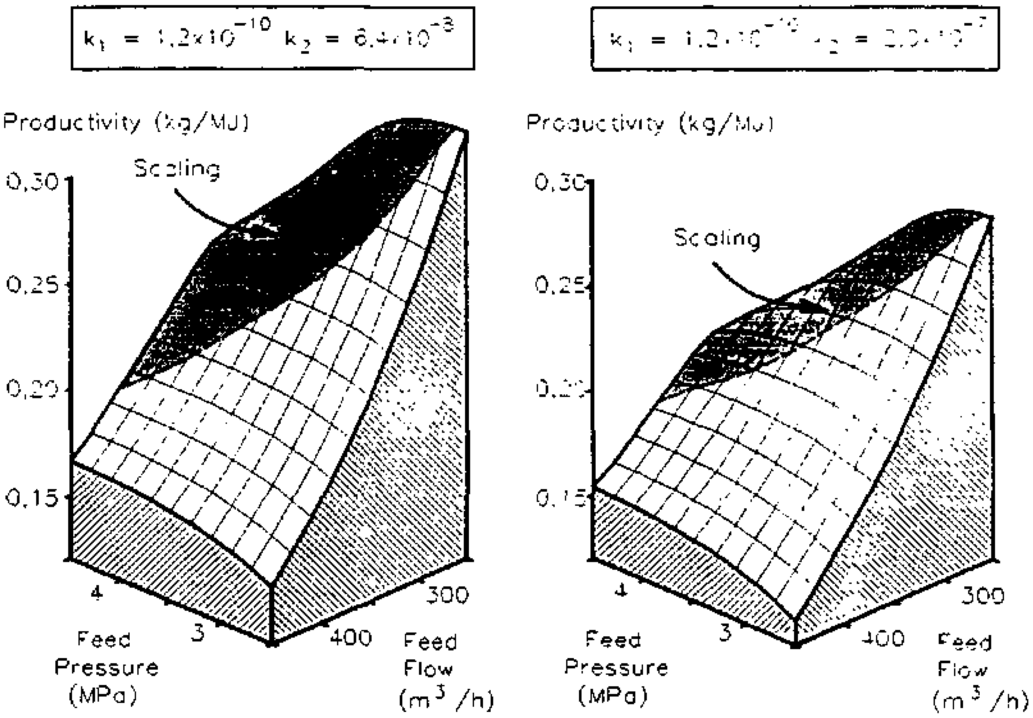

Fig. 5. Simulated productivity of the Lethabo full-scale TRO plant using water and solute permeability parameters determined from pilot-plant measurements before and after the shut-downs which occurred at 2 365 and 2 500 hours operation

CONCLUSIONS

This study has shown that the modelling of TRO is able to enhance the quality of information obtained from pilot-plant work, both as an aid to interpreting the significance of operating experiences, and by allowing investigators to explore the implications that their findings hold for an eventual full-scale design. As the modelling was carried out after the experimental work, there was no opportunity for a feedback of information between the two activities, but there seems little doubt that both would have been improved had this been possible.

ACKNOWLEDGEMENTS

The author wishes to acknowledge the contributions of :

ESKOM and

Miss. B.M. Brouckaert for the laboratory work and the preparation of the diagrams.

This investigation was undertaken in terms of a Water Research Commission project.

REFERENCES

Belfort, G. (1984). *Synthetic Membrane Processes.* Orlando : Academic Press.

Brouckaert, C.J. and Buckley, C.A. (1992). Simulation of Tubular Reverse Osmosis. *Water SA*, submitted for publication.

Rautenbach, R. and Albrecht, R. (1989). *Membrane Processes.* Chichester : John Wiley & Sons.

Schutte, C.F., Spencer, T., Aspden, J.D. and Hannekom, D. (1987). Desalination and Re-use of Power Plant Effluents from pilot-plant to full-scale application. *Desalination*, 67, 255-269.

Sourirajan, S. and Matsuura, T. (1985). *Reverse Osmosis/Ultrafiltration Process Principles.* Ottawa : National Research Council, Canada.

NOMENCLATURE

A = RO membrane pure water permeability coefficient, kg/m^2

c = Solute concentration, kg/m^3

d = Tube diameter, m

D = RO membrane solute transport coefficient, m/s

$\mathcal{D}$ = Molecular diffusivity of solute in water, m^2/s

$\mathcal{K}$ = Turbulent diffusion mass transfer coefficient, m/s

k_1 = Pure water permeability regression coefficient

k_2 = Solute permeability regression coefficient

P = Pressure, Pa

v = Flow velocity, m/s

μ = Viscosity of water, Pa.s

ρ = Density of fluid, kg/m^3

Sh = Sherwood Number $\frac{\mathcal{K}d}{\mathcal{D}}$

Re = Reynolds Number $\frac{\rho v d}{\mu}$

Sc = Schmidt Number $\frac{\mu}{\rho \mathcal{D}}$

WATER RESEARCH COMMISSION PROJECT NO. 325

RESEARCH ON THE MODELLING OF TUBULAR REVERSE OSMOSIS SYSTEMS

Appendix 3

Report on a visit to the Lethabo Power Station TRO Plant

CJ Brouckaert

Pollution Research Group
Department of Chemical Engineering
University of Natal
Durban

February 1995

1 SUMMARY

A visit to the Lethabo power station was undertaken during July 1992. The main purpose of the visit was to set up the tubular reverse osmosis (TRO) modelling program for the purpose of monitoring the TRO plant, and to instruct the Lethabo personnel (Dirk Hanekom and Johan Roux) in its use. Other objectives were to begin evaluating the requirements for implementing the algorithm in an on-line monitoring role as proposed in the provisional patent, and to gather a set of measurements, including full chemical analyses of the various streams, to provide data for the multi-solute version of the TRO model.

While applying the model to the plant operating data, it became evident that the software was not sufficiently convenient for the plant personnel to use on a routine basis, and that its user interface still needed attention before it would be useful. Problems included the use of different engineering units to those used for plant logging, and the need to transfer data manually from the data logging system to the TRO simulation program.

During the course of setting up the model to match the plant data, a number of problems with the plant operation came to light. These included the dilution of the feed stream with potable water to reduce the level of total dissolved solids (TDS), a concern about barium sulphate scaling, and a module failure rate of about twelve per month. When it became clear that the software would need to be modified, the objective of training the Eskom personnel in its operation was postponed, and the remaining time on site was devoted to an investigation of the plant's technical problems.

The following main conclusions were reached :

(a) The use of dilution water to reduce the TDS of the TRO plant feed is probably unnecessary. The main reason why a limitation was placed on the TDS of the plant feed was the fear of scaling of the membranes by gypsum ($CaSO_4.H_2O$). A figure of 1 800 mg/ℓ had been established during the pilot-plant study on which the reverse osmosis (TRO) plant design was based. However the composition of the cooling water had changed since the pilot-plant study, and although the TDS had increased (to about 2 200 mg/ℓ) the calcium and sulphate levels had actually decreased, and the danger of $CaSO_4.H_2O$ scaling had become less **(Refer to section 1.1)**.

(b) A thermodynamic analysis of the potential for $BaSO_4$ scaling showed that this was indeed probable, with or without the use of dilution water. The use of a precipitation inhibitor is strongly advisable **(Refer to section 1.2)**.

(c) It seems most likely that the cause of module failure is too rapid a changes in pressure during flow reversals. Flow reversals were set to occur every hour during the time of the visit. The modules at the ends of the banks experience a pressure change of 1 MPa within 0,5 to 0,75 s when the flow reverses. It is suggested that flow reversal be engineered to produce a less abrupt transition, and that the frequency of flow reversals be reduced **(Refer to section 1.3)**.

(d) The salt concentration of the brine concentrate stream undergoes a considerable change immediately after a flow reversal, and takes approximately 15 minutes to return to a steady value. Any sample taken during this time would be completely unrepresentative of the plant's operation, and, if presented to the computer model, would yield quite incorrect values of parameters representing the state of the membranes. It is therefore important to be aware of the time of flow reversals when taking plant measurements, and to avoid sampling within about 30 minutes of the previous flow reversal **(Refer to section 1.3)**.

(e) The computer simulation of the plant corresponded very satisfactorily with measurements that were made during the visit, confirming the basic technical accuracy of the TRO model **(Refer to section 2.3)**.

(f) The membrane state parameters determined by the model corresponded well with values expected for Membratek modules in good condition. It can be concluded that neither fouling nor degradation of the membranes had occurred to any significant extent **(Refer to section 2.3)**.

(g) The pressure drop across the plant was found to be higher than expected from the experience of the pilot-plant modelling. This may be a consequence of the design of the new sponge-ball traps which were installed as part of the re-commissioning of the plant **(Refer to section 2.3)**.

2 INVESTIGATION OF THE TRO PLANT OPERATION

1.1 Gypsum Precipitation

The cooling-water system includes continuous lime-softening to which introduces calcium ions into the system, and causes the pH to be relatively high (9,5 - 10). The cooling-water is not suitable for direct introduction into the TRO because it is saturated with $CaCO_3$, and the pH is too high for the cellulose-acetate membranes. Both problems are reduced by acidification with sulfuric acid. This drives most of the carbonate off as carbon dioxide, although it is questionable whether the decarbonation process is given sufficient time to complete before the water enters the TRO plant.

The solubility of gypsum ($CaSO_4.2H_2O_3$), although low, is considerably higher than that of calcite ($CaCO_3$), so considerable concentration by the TRO plant is possible before the gypsum precipitation becomes a limiting factor. It should be noted that the sulfate introduced by reducing the pH from 9,7 to 5,5 constitutes only about 10 % of the total sulfate in the resulting solution.

During the week of the visit, the cooling water was being diluted with potable water before being fed to the TRO plant. The reason for this apparently illogical procedure was that the TDS of the cooling water was 2 200 mg/ℓ, which is higher than the figure of 1 800 mg/ℓ which prevailed during the pilot-plant trials which formed the basis of the TRO plant design. One of the conditions of Membratek's guarantee on new modules is that the plant should be operated within the limits of the conditions established during the pilot-plant investigation; hence the dilution of the feed to 1 800 mg/ℓ TDS.

The effect of this dilution on the purpose and viability of the plant is serious. The TDS of the potable water was 216 mg/ℓ, which implies that 1 part of potable water was required for every 4 parts of cooling water treated to reduce the TDS from 2 200 to 1 800 mg/ℓ.

Consideration of the cooling water analyses at the time of the pilot-plant trial and at the present (Table 1) shows that the dilution is probably unnecessary. Table 1 compares the analysis of the feed-water to the pilot-plant in September 1988 to that of the feed-water to the TRO plant in July 1992. The comparison is somewhat complicated by the dilution of the cooling-water with potable water, so an analysis of the overflow from one of the clarifiers is also given. The clarifier overflow can also be directly compared with the pilot-plant feed, as it would have to be acidified with sulphuric acid as discussed above. The effect of acid addition was simulated using the MINTEQA2 speciation program, and the results of this calculation form the last entry in the table (acidified cooling water). This represents the water that would have been fed to the TRO plant had there been no dilution.

Table 1 : Chemical Analyses of Various Lethabo Water Streams

Stream	Ca mg/ℓ $CaCO_3$	SO_4 mg/ℓ	Mg mg/ℓ $CaCO_3$	Na mg/ℓ	Cl mg/ℓ	K mg/ℓ	M-alk mg/ℓ $CaCO_3$	pH	TDS mg/ℓ	$CaSO_4.2H_2O$ saturation index
Pilot-plant feed										
14 Sept 1988	323	928	69	414	187	67	24,5	6,4	1 916	-0,458
9 May 1988	425	1 140	90	406	270	76	11,4	5,5	2 221	-0,306
TRO-feed										
24 July 92	120	653	120	369	390	65	17,2	6,3	1 795	-0,964
Cooling water										
21 July 1992	105	871	165	460	405	102	58,8	9,7	2 207	-0,984
Acidified cooling water	105	911	165	460	405	102	17,2	6,3	2 247	-0,953

It is clear from these figures that, although the TDS of the cooling water has increased since the pilot-plant experiments were undertaken, the concentrations of calcium and sulphate have decreased. This is probably due to more efficient operation of the lime-softeners. In particular, the $CaSO_4.2H_2O$ saturation index of the simulated TRO feed water of 21 July 1992 *without dilution* is substantially lower than the feed presented to the pilot-plant in 1988. Consequently the dilution of the TRO plant feed is not *justified in terms of* $CaSO_4.2H_2O$ *precipitation.*

1.2 Barium Sulphate Precipitation

The solubility of barium sulphate is very much lower than that of $CaSO_4.2H_2O$, and hence the presence of barium in the TRO plant feed would present a more acute problem than that caused by calcium. Barium concentrations are not routinely determined at Lethabo, which presented a problem in assessing the situation. The only figure that was available was an estimate of 0,1 mg/ℓ in raw water from the Sterkfontein dam. Since the solubility product is $1{,}08 \times 10^{-10}$, this translates to a maximum sulphate concentration of 14,2 mg/ℓ, which may be compared with the sulphate figure of 11,8 mg/ℓ reported for the raw water at Lethabo on 8 July 1992. Hence the intake water is probably close to saturation with $BaSO_4$. In the cooling circuit the evaporative concentration and the addition of sulphate ions from various sources must inevitable lead to the cooling water being saturated or super-saturated in $BaSO_4$ by the time it gets to the TRO plant. The figure of 653 mg/ℓ SO_4 for the TRO feed on 21 July 1992 (Table 1) implies a barium saturation level of 0,0022 mg/ℓ, which is fifty times smaller than the estimated figure for the un-concentrated incoming water. Hence operation of the plant must be based on the assumption that $BaSO_4$ scaling is likely to occur, although rather slowly due to the very low concentrations involved. This calls for dosing with a precipitation inhibitor such as Flocon 100.

1.3 Adverse Effects of Flow-reversal

At the time of the visit to Lethabo, the flow direction through the RO module was being reversed every hour in order to clean the membrane surfaces with sponge-balls. Two possible adverse effects that might result from this practice are :

(a) the membranes are subjected to a sudden change in pressure as the flow-reversal occurs, which may be a cause of the module failures being experienced at the time, at a rate of about 12 modules per month.

(b) The concentrated brine which has just reached the plant outlet at the point of flow reversal is sent back through the modules, becoming even more concentrated in the process, and possibly leading to the formation of a precipitated scale.

To obtain some data related to these potential problems, the following observations were made on 24 July 1992.

(a) A pressure gauge was attached, in turn, to the manifolds at each side of the module bank, and the pressure increase and decrease during a flow reversal was monitored. The transitions were too fast for any more than a visual impression to be recorded. The transitions occurred between pressures of 2,6 and 3,6 MPa, and were completed within approximately ½ sec. In the case of a pressure rise, a small overshoot of ±0,1 MPa was observed. It should be noted that the measurement set-up was not suited to measuring very rapid pressure changes, as the pressure gauge dial contained vibration damping fluid, and the instrument was connected to the manifold with a flexible rubber hose, which would also have absorbed to some extent very rapid pressure shocks. Thus the observed rate of pressure increase is probably an underestimate. It therefore seems quite probable that these pressure transitions are contributing to the module failure rate.

(b) Reject brine conductivities were measured at one minute intervals after a flow reversal, in order to get some idea of the concentration rise.

These measurements are depicted in Figure 1. The transient in reject concentration lasts for about 15 minutes and is distributed more-or-less evenly above and below the mean level. The peak conductivity was about 7 000 (µS/cm), however this was a mixed sample in the manifold, and differences in individual flow rates through the modules would cause the peak in the manifold to be less sharp than in the individual modules.

While it is not possible to give a definite interpretation of how the brief exposure of very high concentrations would effect the membranes, it seems unlikely that any build-up of scale would result, since the period of high concentration is matched by a corresponding period of low concentration, which would tend to dissolve any precipitated material.

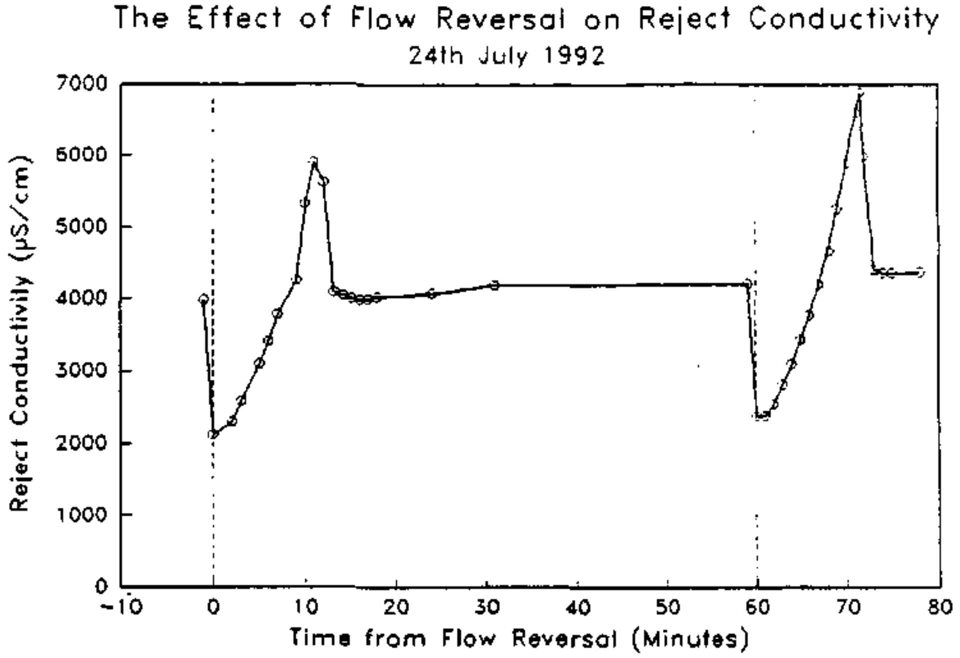

Figure 1 : The Effect of Flow Reversal on Reject Conductivity. Data Measured on 24 July 1992

The wide variation in concentrations associated with a flow reversal shows the importance of sampling the streams at the correct time for monitoring purposes. Any samples taken within 15 minutes of the previous flow-reversal will give a completely unrepresentative picture of the plant's operation.

3

4 MODELLING OF THE TRO PLANT

2.1 Physical Chemistry of the Brine

For modelling purposes the physical chemistry of the brine is characterised by two relationships : osmotic pressure as a function of total dissolved solids (TDS), and conductivity as a function of TDS.

Conductivity and TDS are routinely measured as part of the water analyses conducted on the TRO plant streams, and ample data were available from the plant records.

A method for calculating osmotic pressure from the chemical analysis of a brine was detained in a previous report (Brouckaert, 1992). This involved the use of the MINTEQA2 chemical speciation software (Allison et al., 1990) to calculate the distribution of ionic species, from which the osmotic pressure can be estimated using a correlation. Osmotic pressures were calculated for three streams, one each of TRO feed, concentrate and permeate, and the results correlated with the corresponding TDS values.

The equations fitted to these data were :-

Conductivity (μS/cm) = 1,409 x TDS (mg/ℓ)
Osmotic pressure (kPa) = 0,0451 x TDS (mg/ℓ)

The data and equations are plotted in Figures (2) and (3).

2.2 Plant Measurements

The plant measurements that are routinely recorded which are relevant to the RO model are :-

Feed	:	Temperature, flow rate, conductivity, pressure.
Permeate	:	Flow rate, conductivity
Concentrate	:	Flow rate, conductivity, pressure

Since process instrumentation is often inaccurate, checks measurements were made where possible. Conductivities were checked using a portable conductivity meter which had been standardized in the laboratory, and pressures were checked with a pressure gauge connected in turn to the inlet and outlet manifolds.

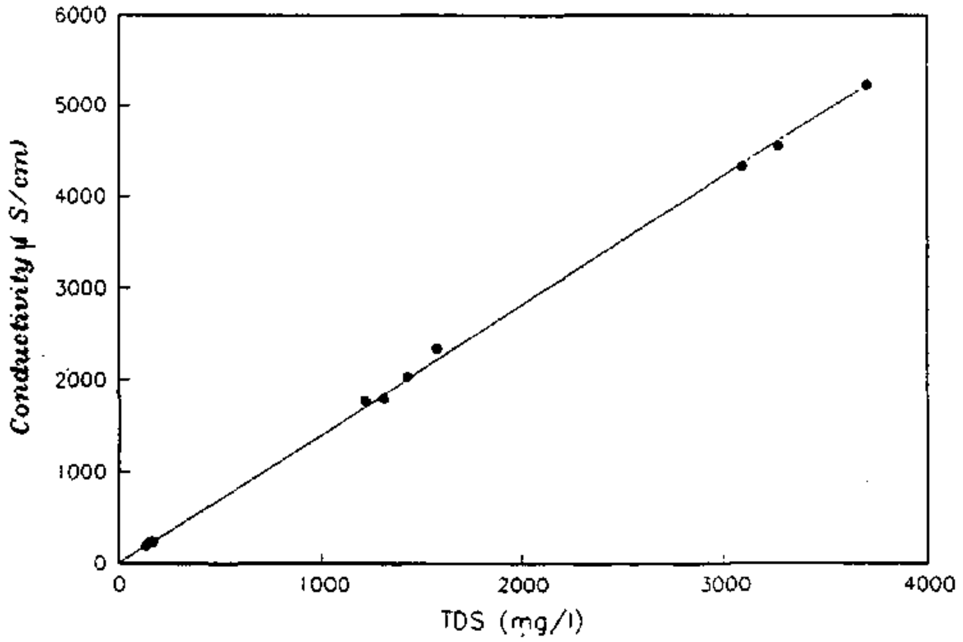

Figure 2 : The Relationship Between Total Dissolved Solids and Conductivity for the Lethabo TRO Plant Feed, July 1992

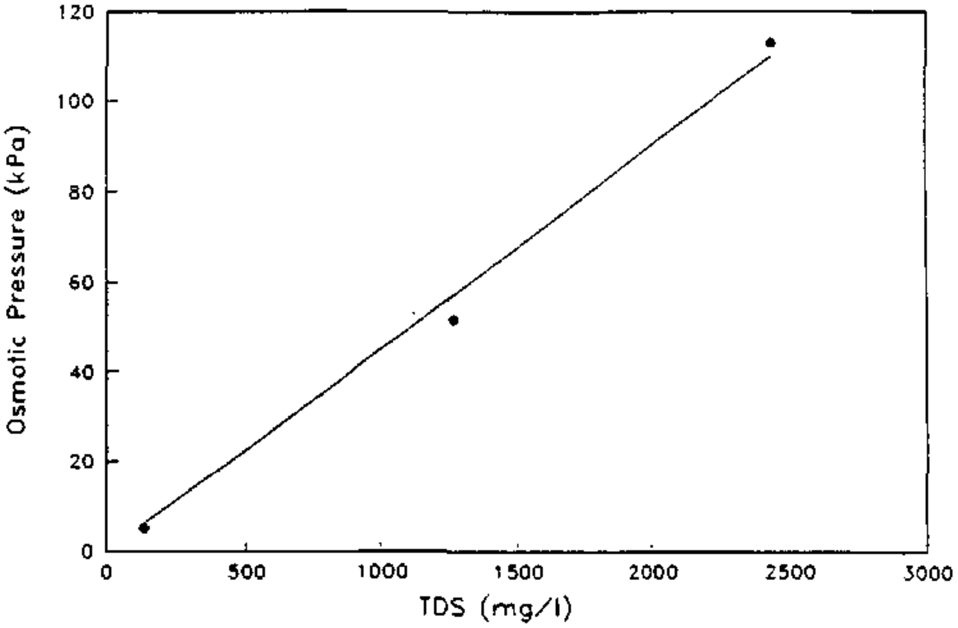

Figure 3 : The Relationship Between Total Dissolved Solids and Osmotic Pressure for the Lethabo TRO Feed Plant, July 1992

Measurements	Process Instrument	Check Measurement
Feed pressure	3,25 MPa	3,45 MPa
Reject pressure	2,65 MPa	2,5 MPa
Feed conductivity	2 800 mS/cm	2 240 mS/cm
Reject conductivity	5 500 mS/cm	4 060 mS/cm
Permeate conductivity	185 mS/cm	185 mS/cm

It was not possible to check the flow meters directly. However since all three inlet and outlet flows were measured, the consistency of the three measurements could be checked. Furthermore, a balance on the conductivity measurements allowed a further consistency check.

The following measurements were recorded :-

	Feed	Permeate	Reject
Flow (m^3/h)	90	57,5	38,7
Conductivity (mS/cm)	2 570	240	5 990

The permeate and reject flows add up to 96,2 m^3/h, which is 6,2 m^3/h higher than the feed measurement.

The conductivities indicated a water recovery of 59,5 % (permeate flow/feed flow).

Comparing this with the flow-meters :

$$\frac{Permeate}{Feed} = \frac{57.5}{90} = 0.638$$

whereas :

$$\frac{Permeate}{Permeate + Concentrate} = \frac{57.5}{96.2} = 0.597$$

Hence it would appear that the most probable situation is that the permeate and reject flow meters are correct, while the feed flow meter is reading a little low.

2.3 Comparison of TRO Simulations Plant Measurements

Two data sets measured on the 24 July 1992 were selected for comparison with the model.

Time	**11:00**		**13:24**	
Measured	**Simulated**	**Measured**	**Simulated**	
Flow rates (m^3/h)				
Feed	96,5	-	96,2	-
Permeate	52,5	52,8	57,5	57,9
Reject	44,0	43,7	38,7	38,3
Conductivities (mS/cm)				
Feed	1 940	-	2 570	-
Permeate	186	184	240	242
Reject	4 060	4 059	5 990	6
086				
Pressures (MPa)				
Feed	3,6	-	3,65	-
Reject	2,8	2,8	2,9	2,9

The model was clearly able to simulate the measured results very satisfactorily. The modelling parameters which gave these results were :

Pure water permeability parameter	$K_1 = 1{,}07 \times 10^{-10}$
Solute permeability parameter	$K_2 = 1{,}05 \times 10^{-7}$

These values fall into the ranges of values determined for the Lethabo pilot plant during the initial part of the test (Brouckaert and Buckley, 1992). This is a very encouraging result as it shows that the model has successfully accounted for the difference in configuration between the pilot-plant and the full-scale plant. It also indicates that, on average, the plant membranes are currently in a very good state.

The pressure drop across the plant was substantially greater than would have been expected from the pilot-plant. The reason for this is not known at present, but may be connected to the new sponge-ball traps which were installed when the plant was refurbished.

5 CONCLUSIONS

Although the original objectives of setting up the TRO model for routine use by Eskom personnel at Lethabo was not achieved, a number of other useful tasks were accomplished. The TRO model was found to simulate the plant operation accurately, and the process of applying it to the plant led to important insights into the plant operation. Areas of weakness in the program's user interface were identified, and ideas for improvements were obtained.

The three problems of feed dilution, $BaSO_4$ scaling and module failures constitute significant threats to the viability of the plant's operation, and should be addressed as soon as possible.

6 REFERENCES

Allison, J.D., Brown, D.S. and Novo-Gradac, K.J. (1990) MINTEQA2/PRODEFA2, A Geochemical Assessment Model for Environmental Systems. Environmental Research Laboratory, Office for Research and Development, U.S. Environmental Protection Agency, Athens, Georgia 30613.

Brouckaert, B.M. Prediction of Osmotic Pressure from Equilibrium Speciation of Inorganic Ionic Solutions. Water Research Commission Document No. 4.3/92.

Brouckaert, C.J. and Buckley C.A. (1992) The Use of Computer Simulation of Tubular Reverse Osmosis in Conjunction with Pilot Plant Studies. Presented at the IAWPRC Specialized Conference on Membrane Technology in Wastewater Management, Cape Town, 2-5 March 1992, (Water Research Commission document No. 4.6/92).

WATER RESEARCH COMMISSION PROJECT NO. 325

RESEARCH ON THE MODELLING OF TUBULAR REVERSE OSMOSIS SYSTEMS

Appendix 4

Experimental Data from Cato Ridge Abattoir Effluent Investigation

S Wadley and CJ Brouckaert

Pollution Research Group
Department of Chemical Engineering
University of Natal
Durban

February 1995

SUMMARY

Tests have been carried out at the effluent plant at the Cato Ridge Abattoir to investigate the use of 9 mm diameter tubular membranes supplied by the Institute for Polymer Science, University of Stellenbosch. These tubes are unsupported and are housed in PVC tubes. Two membrane types were tested : the 719 membrane (which has been used previously on the same effluent in the 12,5 mm diameter tubular format) and the 442 membrane, which has a lower molecular mass cut-off than the 719 membrane.

The tests were carried out on the combined effluent from the abattoir as it enters the effluent plant. The effluent had undergone fat-skimming and rough screening. Further screening was carried out manually to remove solids that might block the modules. The effect of flow rate and pressure on the flux was investigated. An air purge device was tested to determine whether it could have the same effect on the flux as high linear flow rates would, that is, to limit the extent of gel layer formation.

It was found that the dependence of the flux on the linear flow rate was strong. It was observed that for each linear flow rate, there was a pressure above which increases in pressure no longer lead to increases in flux. This critical pressure increased with increasing flow rate. The tests were carried out at pressures between 100 kPa and 400 kPa. The construction of the modules limits the maximum operating pressure to 400 kPa. The results of the use of the air purge unit were inconclusive, but it appeared to benefit the 719 membranes more than the 442 membranes.

A maximum water recovery of 91 % was attained. At this water recovery the fluxes were still reasonably high (above 15 ℓ/m^{2}h at a linear flow rate of 1,5 m/s). Hence higher water recoveries (at least 95 %) should be attainable.

The COD (Chemical Oxygen Demand) of the permeate was below 700 mg/ℓ for the tests at high water recoveries. This corresponds to a COD retention of 96 % to 98 %. The point retention of phosphate varied from 50 to 66 % at zero water recovery, and was 93 % at 91 % water recovery. When effluent taken close to source was used, the phosphate retention was 89 %. In all the tests, the concentration of phosphate in the permeate ranged from 2,7 to 5,3 mg/ℓ.

Table of Contents

1 INTRODUCTION

The effluent under consideration in this investigation is the combined effluent from the Cato Ridge Abattoir. The use of ultrafiltration to treat this effluent is aimed at :

(i) reducing the organic load (COD) in the effluent,

(ii) removing phosphates from the effluent, and

(iii) recovering an organic concentrate, which is of suitable composition to be processed further in a by-products recovery system.

The aim of the present investigation is to test two types of 9 mm diameter tubular membranes when operated under the following conditions :

(i) linear flow rates of 1 to 3 m/s

(ii) applied pressures of 100 to 400 kPa

(iii) ambient temperature (20 to 35 °C)

(iv) maximum water recovery (more than 90 %)

(v) minimum feed pretreatment (fat-skimming and wedge-wire screening)

(vi) minimum cleaning (air-purge cycle during operation, daily flushing with fresh water, intermittent enzymatic cleaning and sanitation)

Enzymatic cleaning was carried out using a 1 % solution of a 1:1 mixture of *Alkazyme* and *Zymex* for 30 min, followed by rinsing and then cleaning using a 1 mℓ/ℓ solution of *Sanochlor* for 10 min.

The following conditions are to be optimised :

(i) flow rate

(ii) pressure

(iii) air purge frequency

(iv) water recovery

The modules and the air purge unit were provided by the Institute for Polymer Science, University of Stellenbosch.

2 DESCRIPTION OF EQUIPMENT

The plant was constructed to enable testing of the two types of membranes under the same operating conditions. This was done by connecting two modules of each type in series (via a U-bend) and connecting the two pairs in parallel. Ball valves were fitted to the inlet of each pair of modules so that the modules can be shut off when not used. The pressure and flow rate were regulated using the diaphragm valves on the outlet of each pair of modules and the ball valve on the by-pass. The permeate from each module could be collected separately. The specifications for the ultrafiltration modules are given in Table 1. The 442 membrane has a lower molecular mass cut-off than the 719 membrane.

Table 1 : Ultrafiltration membrane specifications

Membrane types	442 and 719
Membrane configuration	tubular
Tube inner diameter	9 mm
Tube length	2,3 m
Number per module	3 (in parallel)
Membrane area per module.	0,195 m^2
Module housing	32 mm PVC pipe
Maximum pressure	*500 kPa*

The inlet pressure (in), outlet pressure (out) and pressure at the U-bend (mid) can be measured for both sets of modules using a single pressure gauge. The pressure gauge is connected to a manifold with 6 small brass ball valves. The valves are connected to the pressure points via 1 to 2 m lengths of ¼" clear polyflow tubing. The manifold also has a ball valve on one end so that it can be flushed with tap water to keep the line clean and prevent corrosion of the brass fittings. A stainless steel feed tank of 200 ℓ capacity, fitted with cooling coils, was used. Circulation was provided by a MONO CD40 single stage progressive cavity pump with a 5 kW motor. The feed and permeate flow rates were calculated by determining the time taken to fill containers of known volumes.

The air purge unit was placed in the line between the pump and the modules. Its operation involved a phase in which it filled with air (supplied by an air compressor) to a predetermined level at the operating pressure of the ultrafiltration system. After a fixed time interval, a solenoid valve in the feed line closed and this air was carried through the system with the feed. At the end of a second fixed time interval, the valve opened again and filling with air resumed.

3 RESULTS AND DISCUSSION

Each of the following sections contains the results of the experiments carried out on one day. The system was flushed with water at the end of each day and the modules were left filled with water.

3.1 Pure water fluxes on new membranes

Date : 9/3/93
Feed : Fresh water from mains

Pressure (kPa)						Ave. Pressure (kPa)				Flux (ℓ/m^2h)			
719			442			719		442		719		442	
in	mid	out	in	mid	out	(1)	(2)	(1)	(2)	(1)	(2)	(1)	(2)
98	95	91	99	92	87	97	93	96	90	107	112	64	61
202	200	195	200	200	195	201	198	200	198	431	224	136	133
302	300	295	305	305	300	301	298	305	303	596	318	195	192

Pure water flux determination at three pressures was the only characterisation carried out on these modules. The test was carried out using fresh water directly from the mains tap. In the water flux tests carried out after this the inlet and outlet pressures were made equal by using very low flow rates. The pure water flux should be independent of flow rate.

3.2 Tests using air purge during total recycle on effluent

Date : 10/3/93
Feed : Screened effluent (coarse screen)
Started on effluent at 9:50 (no air purge)

Time	Elap Time	Pressure (kPa)						Average Pressure (kPa)				Permeate flux (ℓ/m^2h)				Feed flow (m/s)		WR	T
	(h)	719 in	719 mid	719 out	442 in	442 mid	442 out	719 (1)	719 (2)	442 (1)	442 (2)	719 (1)	719 (2)	442 (1)	442 (2)	719	442	(%)	(°C)
10:00	0,17	250	200	145	240	205	162	225	173	223	164							0	
10:10	0,33	275	235	180	280	245	200	255	208	263	223	164,0	79,2	109,3	97,7			0	
10:30	0,67	310	270	220	330	300	280	290	245	315	290	106,8	71,8	95,7	85,0	3,39	2,65	0	
11:10	1,33	265	200	145	260	200	145	233	173	230	173	102,1	70,7	96,7	79,9			0	
11:30	1,67	265	200	145	260	200	145	233	173	230	173	102,1	81,6	91,8	73,5			0	
11:50	2,00	270	205	145	260	200	140	238	175	230	170	112,7	73,2	102,6	79,9	3,81	2,90	0	
12:10	2,33	265	205	145	265	205	155	235	175	235	180	117,0	76,2	108,1	89,6			0	29,5
12:40	2,83	270	205	145	260	200	140	238	175	230	170	108,7	71,8	105,0	82,7			0	28,5
12:52	3,03	265	200	155	260	200	145	233	178	230	173	112,7	72,6	105,0	84,3	3,81	2,90	0	
13:00	3,17	220	205	190	220	200	185	213	198	210	193	52,5	32,2	72,9	70,1	1,51	1,60	0	
13:01	3,18	220	205	190	220	205	190	213	198	213	198	45,7	28,4	64,6	62,4			0	
13:04	3,23	240	230	220	240	230	220	235	225	235	225	43,3	28,0	57,7	58,8			0	
13:11	3,35	215	200	190	215	195	180	208	195	205	188	39,1	25,5	56,7	55,0			0	
13:22	3,53	215	200	185	215	200	185	208	193	208	193	38,6	25,8	53,4	50,7			0	28
13:26	3,60	215	200	185	215	200	185	208	193	208	193	40,3	25,9	50,2	48,6			0	
13:52	4,03	215	200	185	210	195	180	208	193	203	188	38,6	25,0	46,8	46,8			0	
14:13	4,38	215	200	185	215	200	185	208	193	208	193	33,6	24,7	45,7	44,6			0	

Time	Elap Time	Pressure (kPa)						Average Pressure (kPa)				Permeate flux (ℓ/m^2h)				Feed flow (m/s)		WR	T
	(h)	719 in	719 mid	719 out	442 in	442 mid	442 out	719 (1)	719 (2)	442 (1)	442 (2)	719 (1)	719 (2)	442 (1)	442 (2)	719	442	(%)	(°C)
14:20	4,50	Air purge unit switched on																	
14:24	4,57	200	180	160	200	190	165	180	160	190	173	38,4	25,6	49,9	45,9			0	
14:35	4,75	235	210	195	220	210	200	223	203	215	205	43,7	30,1	48,6	49,6			0	
14:40	4,83	220	205	190	220	205	190	213	198	213	198	43,5	27,7	46,1	45,9			0	
14:51	5,02	225	205	195	220	210	195	215	200	215	203	38,4	26,5	44,8	44,3			0	
15:00	5,17	230	220	210	230	220	210	225	215	225	215	41,4	26,2	43,9	43,7			0	
15:19	5,48	220	200	185	215	200	190	210	192	208	195	41,4	25,2	39,9	39,6			0	
15:30	5,67	Switched off pump and flushed system with water																	

For the first 3 h the test was carried out at very high flow rates (around 3 m/s). Comparison of the fluxes obtained during the first hour is difficult because the operating conditions were varying. The flux remained relatively constant until the flow rate was decreased after 3 h of operation. The high flow rate was limiting the build up of the gel layer on the membrane surface. This high flow rate is not feasible since the pressure drop over each pair of modules was more than 100 kPa.

At a flow rate of about 1,5 m/s, a decrease in flux with time was observed (3 to 4,5 h elapsed time). When the air purge was switched on, there was an initial increase in flux for all modules. The air purge unit was used for 1 h, at a cycle time of 4,75 min. During this time, the flux did not appear to decline further for the 719 modules, although for the 442 modules further flux decline was observed (see Figure 1).

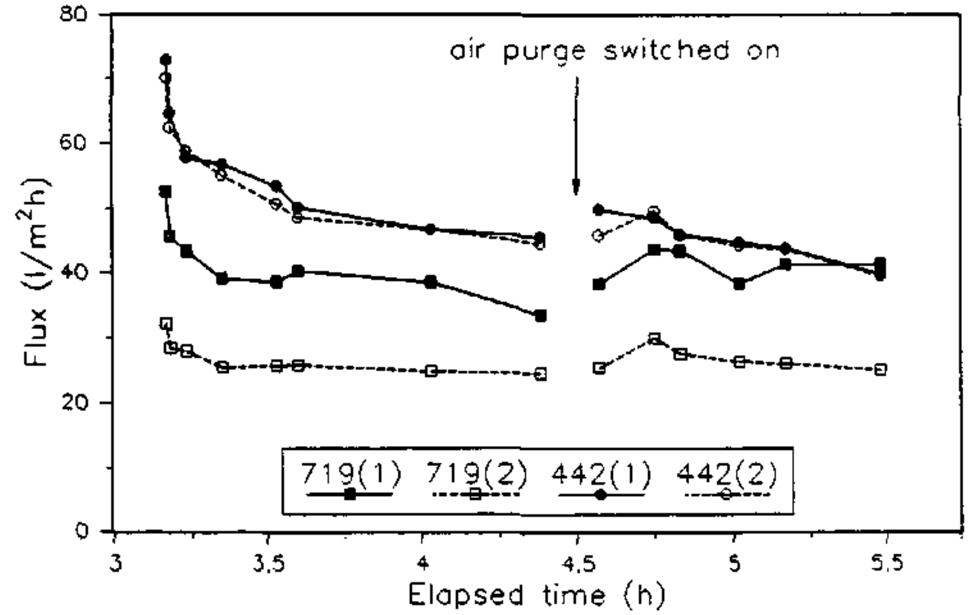

Figure 1 : (10/3/93) Effect of the use of air purging on flux (linear flow rate : 1,5 m/s for 719 modules and 1,6 m/s for 442 modules; average pressure : 188 to 235 kPa; temperature : 28 °C)

3.3 Pure water fluxes and tests using air purge at 50 % water recovery

Date : 11/3/93
Feed : Fresh water from mains
Temperature : 26,5 °C

Pressure (kPa)						Ave. Pressure (kPa)				Flux (ℓ/m^2h)			
719			442			719		442		719		442	
in	mid	out	in	mid	out	(1)	(2)	(1)	(2)	(1)	(2)	(1)	(2)
100	95	90	100	90	85	98	93	95	88	91,5	70,8	53,0	47,1
200	200	200	200	190	180	200	200	195	185	146,0	138,3	101,7	96,3
305	305	300	295	295	300	305	303	295	298	191,7	217,0	164,3	163,1

The pure water fluxes after contact with the effluent are much lower than for the new modules, especially for the 719 modules.

Feed : Screened effluent (coarse screen)
13:25 Started on effluent
13:30 Commenced batch concentration (using air purge, cycle time 4,75 min)

Time	Elap Time	Pressure (kPa)						Average Pressure (kPa)				Permeate flux (ℓ/m^2h)				Feed flow (m/s)		WR	T
	(h)	719 in	719 mid	719 out	442 in	442 mid	442 out	719 (1)	719 (2)	442 (1)	442 (2)	719 (1)	719 (2)	442 (1)	442 (2)	719	442	(%)	(°C)
13:50	6,08	260	195	135	255	185	135	228	165	220	160					3,54	3,89		30
14:50	7,08	295	250	190	290	240	190	273	220	265	215								
14:55	7,17	Changed to total recycle, approx. 50% water recovery														3,54	3,23	50	
15:14	7,48	225	222	220	225	220	215	224	221	223	218	14,2	7,5	14,3				50	
15:54	8,15	220	200	180	220	200	185	210	190	210	193	26,5						50	
16:05	8,33											31,7			27,8			50	
16:30	8,75	Switched off pump and flushed system with water																	

3.4 Membrane cleaning

Date : 18/3/93
Feed : Recycled water
Temperature : 24,5 °C

Pressure (kPa)	Permeate flux (ℓ/m²h)			
	719(1)	719(2)	442(1)	442(2)
100	84,6	45,0	37,3	28,0
200	174,9	84,9	55,4	38,9
300	235,9	129,2	109,5	89,0

Cleaned with a 1 % solution of a 1:1 mixture of *Alkazyme* and *Zymex* for 30 min; rinsed; cleaned with a 1 mℓ/ℓ solution of *Sanochlor* for 10 min; rinsed thoroughly; carried out water flux determination.

Feed : Recycled water
Temperature : 25 °C

Pressure (kPa)	Permeate flux (ℓ/m²h)			
	719(1)	719(2)	442(1)	442(2)
100	178,3	101,1	39,0	31,5
200	362,2	231,2	80,0	41,9
300	528,7	351,1	128,5	109,8
100	176,2	113,3	43,2	33,6

For the 719 membranes, the water fluxes increased by more than two fold after cleaning and were almost the same as the original values for the membranes when new. For the 442 membranes, only a slight improvement in flux was obtained.

3.5 Tests on effluent at constant flow rate

Date : 19/3/93

Feed : Screened effluent (coarse, then fine screen)

Started on effluent at 11:53.

Time	Elap Time	Pressure (kPa)						Average Pressure (kPa)				Permeate flux (ℓ/m^2h)				Feed flow (m/s)		WR	T
	(h)	719 in	719 mid	719 out	442 in	442 mid	442 out	719 (1)	719 (2)	442 (1)	442 (2)	719 (1)	719 (2)	442 (1)	442 (2)	719	442	(%)	(°C)
12:28	9,33	225	215	200	225	215	190	220	208	220	203	55,9	48,0	59,4	53,8	1,59	1,68	0	29
12:38	9,50	235	220	205	230	230	205	228	213	225	213	55,4	48,2	57,0	53,0			0	
13:16	10,13	235	220	205	230	220	205	228	213	225	213	52,7	45,4	57,9	52,7			0	
14:16	11,13	235	220	205	230	215	200	228	213	223	208	51,0	44,2	54,4	51,7			0	
14:37	11,48	335	320	310	335	320	310	328	315	328	315	49,3	46,7	63,2	60,3	1,53	1,64	0	29
14:45	11,62	335	320	310	335	320	310	328	315	328	315	53,2	47,4	61,7	57,3			0	
15:05	11,95	340	325	310	335	320	310	333	318	328	315	53,2	46,6	61,1	58,6			0	
15:27	12,32	130	115	100	125	110	100	123	108	118	105	47,8	39,1	38,2	28,9	1,49	1,58	0	28,5
15:50	12,70	230	210	195	225	215	200	220	203	220	208	57,3	52,3	62,2	56,6	1,52	1,62	0	28,5

16:02 12,90 Switched off pump and flushed system with recycled water

Table 2 : Results of the analysis of feed sample taken on 19/3/93

(0 % water recovery)	Concentration (mg/ℓ)				
Sample	**PO_4**	**COD**	**TS**	**TSS**	**TDS**
Initial feed	13,2	3 520	2176	1 236	940

PO_4 = phosphate, COD = chemical oxygen demand, TS = total solids,
TSS = total suspended solids, TDS = total dissolved solids

The fine screen was used because sufficient fibrous material had previously passed through the coarse screen, causing partial blocking of the diaphragm valves, which lead to increasing pressure drops with time.

The experiment was carried out at around 1,5 to 1,6 m/s. From a plot of flux verses pressure (Figure 2), it is seen that the flux was not higher at 300 kPa than it was at 200 kPa, but it was lower at 100 kPa than it was at 200 kPa. Hence the point at which the flux is no longer pressure controlled (i.e. where gel-polarisation commences) occurs at around 200 kPa for these particular operating conditions. This point is expected to vary with feed concentration, flow rate and temperature.

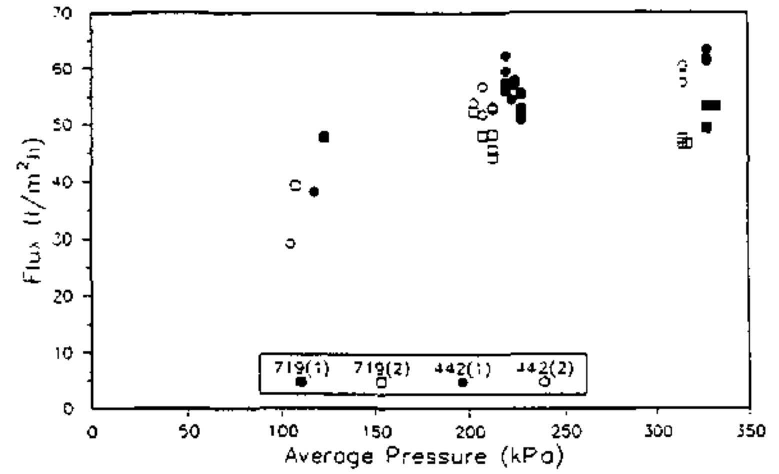

Figure 2 : (19/3/93) Effect of pressure on flux
(linear flow rate : 1,5 to 1,6 m/s, temperature : 29 °C)

3.6 Tests on effluent at various pressures and flow rates

Date : 24/3/93
Feed : Screened effluent (fine screen)
Started on effluent at 12:00

Time	Elap Time	Pressure (kPa)						Average Pressure (kPa)				Permeate flux (ℓ/m^2h)				Feed flow (m/s)		WR	T
	(h)	719 in	719 mid	719 out	442 in	442 mid	442 out	719 (1)	719 (2)	442 (1)	442 (2)	719 (1)	719 (2)	442 (1)	442 (2)	719	442	(%)	(°C)
12:15	13,15	165	90	20	165	85	15	128	55	120	50	91,1	34,4	36,7		4,11	3,94	0	28
12:40	13,57	200	125	60	195	135	85	163	93	165	110	108,2	58,6	56,4		3,99	3,45	0	30
13:16	14,17	225	155	95	220	155	100	190	125	188	128	117,9	84,4	65,9	28,7	3,68	3,49	0	33
13:30	14,40	320	270	220	315	265	215	295	245	290	240	126,0	119,5	104,5	61,7	3,25	3,14	0	33
14:00	14,90	325	280	225	325	275	225	303	253	300	250	128,7	113,6	101,1	57,9	3,25	3,14	0	30
14:21	15,25	145	95	50	140	95	50	120	73	118	73	83,3	41,6	34,8	10,9	3,14	3,07	0	28
14:33	15,45	175	130	90	175	130	90	153	110	153	110	93,4	64,1	45,8	18,6	2,91	2,82	0	28
14:42	15,60	200	155	115	200	155	115	178	135	178	135	94,8	73,3	53,3	24,7	2,88	2,71	0	28
14:52	15,77	245	205	165	240	200	165	225	185	220	183	94,4	81,8	66,9	35,9	2,59	2,69	0	28
15:00	15,90	285	245	215	280	245	215	265	230	263	230	88,9	78,6	77,3	45,3	2,54	2,47	0	28
15:09	16,05	310	275	235	305	270	235	293	255	288	253	87,2	80,0	84,4	52,7	2,61	2,56	0	28
15:19	16,22	135	95	55	130	95	55	115	75	113	75	69,4	41,0	33,1	11,4	2,74	2,61	0	28
15:30	16,40	165	130	95	165	130	95	148	113	148	113	81,4	59,9	42,2	18,3	2,50	2,47	0	28
15:44	16,63	190	155	125	190	155	125	173	140	173	140	82,9	68,7	51,7	25,0	2,41	2,33	0	28
15:52	16,77	235	205	180	235	205	180	220	193	220	193	83,3	72,7	63,4	35,9	2,20	2,12	0	28
15:57	16,85	270	245	230	270	245	220	258	233	258	233	78,6	63,7	67,9	43,5	2,04	2,00	0	28
16:10	17,07	295	275	265	295	275	255	285	265	285	265	69,7	60,7	66,7	48,4	1,93	1,86	0	28
16:18	17,20	145	130	120	145	130	120	138	125	138	125	47,3	38,1	34,4	20,0	1,40	1,31	0	28
16:40	17,57	225	205	190	225	205	190	215	198	215	198	52,6	44,8	45,0	34,3	1,64	1,61	0	28
16:53	17,78	290	275	260	290	275	255	283	268	283	265	53,8	46,8	59,7	45,0	1,66	1,64	0	28
17:00	17,90	Switched off pump and flushed system with recycled water																	

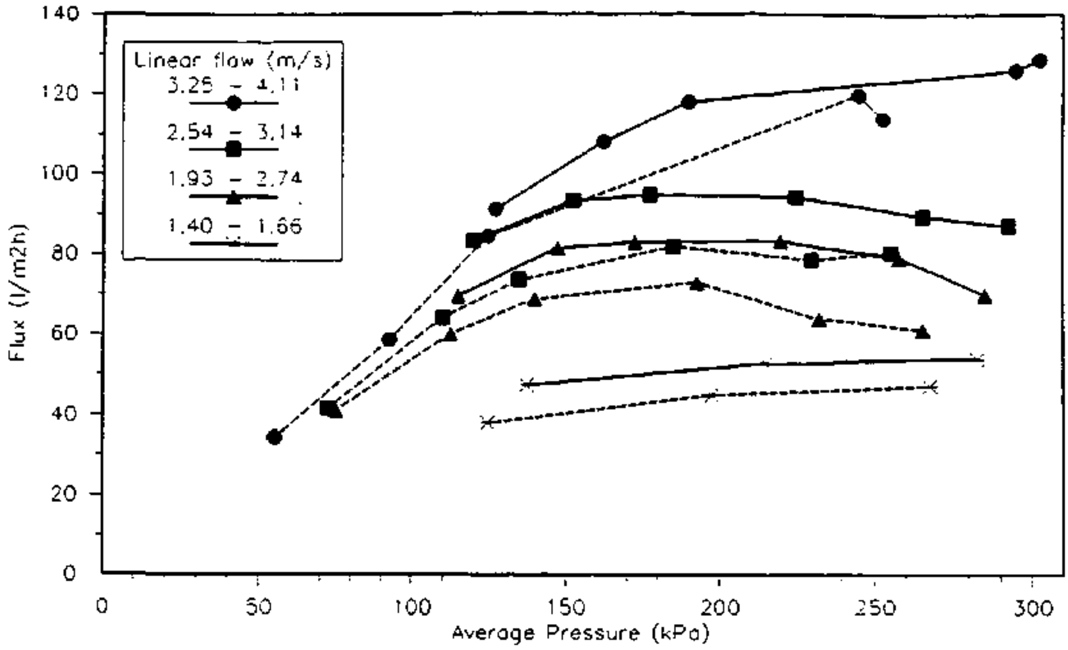

Figure 3 : (24/3/93) Dependence of flux on pressure at various flow rates for 719 modules (28 °C)

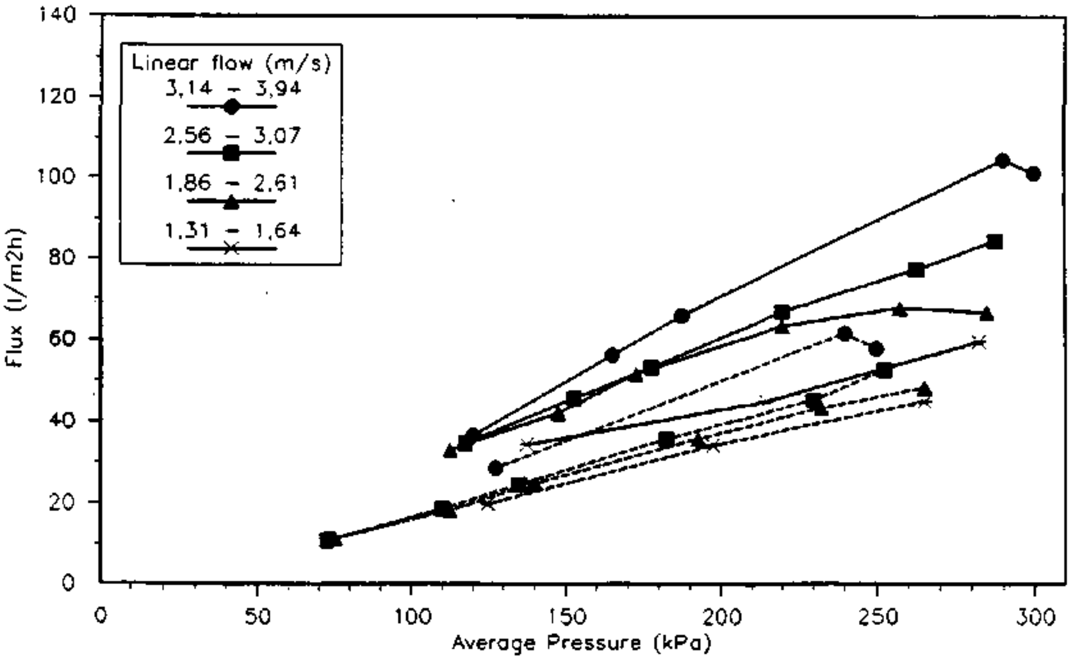

Figure 4 : (24/3/93) Dependence of flux on pressure at various flow rates for 442 modules (28 °C)

The plot of flux verses average pressure (Figures 3 and 4) indicate that, for constant linear flow rate, there is a linear pressure-dependant region at low pressures followed by a pressure-independent region at higher pressures. The region in which the change in slope takes place occurs at higher pressures as the linear flow rate increases. This is consistent with similar curves found in the literature (ref. 1). This trend was more evident in the results from the 719 membranes than for the 442 membranes because the pressure at which the change in slope occurs for the 442 membranes would be at a slightly higher pressure than was reached in these measurements.

Samples of feed and permeate were retained after 4,7 h of operation, at 200 kPa and 1,6 m/s. The results are given in Table 3.

Table 3 : Results of the analysis of samples taken on 24/3/93

(0 % WR)	**Concentration (mg/ℓ)**					**Retention (%)**				
Sample	**PO_4**	**COD**	**TS**	**TSS**	**TDS**	**PO_4**	**COD**	**TS**	**TSS**	**TDS**
Initial feed	3,6	2 080	1 446	734	712					
Permeate from 719	2,8	200	388	10,8	377,2	22	90	73	99	47
Permeate from 442	2,9	184	392	6,4	385,6	19	91	73	99	46

There appears to be an error in the phosphate determination for the feed sample, the phosphate concentration should be at least 13 mg/ℓ.

3.7 Membrane cleaning

Date : 26/3/93
Feed : Fresh water from mains
Temperature : 24,5 °C

Pressure (kPa)	**Permeate flux (ℓ/m²h)**			
	719(1)	**719(2)**	**442(1)**	**442(2)**
100	66,7	41,4	25,1	14,3
200	108,9	80,3	55,4	34,7
300	146,0	117,2	84,0	59,7

Cleaned with a 1% solution of a 1:1 mixture of *Alkazyme* and *Zymex* for 30 min at 40 kPa

Feed : Fresh water from mains
Temperature : 27 °C

Pressure (kPa)	Permeate flux (ℓ/m^2h)			
	719(1)	719(2)	442(1)	442(2)
100	115,0	72,2	33,2	18,0
200	230,0	152,1	71,0	44,9
300	358,0	253,4	106,0	71,4

Cleaned with a 1 $m\ell/\ell$ solution of *Sanochlor* for 10 min.

Feed : Fresh water from mains
Temperature : 25 °C

Pressure (kPa)	Permeate flux (ℓ/m^2h)			
	719(1)	719(2)	442(1)	442(2)
100	144,9	83,3	31,3	16,7
200	278,8	176,9	75,1	44,3
300	425,9	271,4	114,0	72,5

The water flux doubled for the 719 membranes after the *Alkazyme/Zymex* clean and increased by a factor of 1,2 after the *Sanochlor* clean. For the 442 membranes, the increase in flux was by a factor of 1,3 after the *Alkazyme/Zymex* wash and there was no flux increase after the *Sanochlor* wash.

3.8 Tests on effluent at various pressures, flow rates and water recoveries

Date : 30/3/93
Feed : Screened effluent (fine screen)
Started on effluent at 11:48

Time	Elap Time (h)	Pressure (kPa)						Average Pressure (kPa)				Permeate flux (ℓ/m^2h)				Feed flow (m/s)		WR (%)	T (°C)
		719 in	719 mid	719 out	442 in	442 mid	442 out	719 (1)	719 (2)	442 (1)	442 (2)	719 (1)	719 (2)	442 (1)	442 (2)	719	442		
12:13	18,32	230	205	180	225	200	180	218	193	213	190	71,6	56,3	62,2	39,0	2,1	2,0	0	28,5
12:50	18,93	225	202	180	222	200	180	214	191	211	190	59,4	48,9	55,1	35,4	2,1	2,0	12,6	
13:30	19,60	225	200	180	220	200	175	213	190	210	188	54,8	45,8	51,3	34,8	2,0	2,0	25,8	27,5
13:42	19,80	265	240	215	265	240	215	253	228	253	228	62,8	57,0	72,2	45,7	2,4	2,3	25,8	28,5
14:18	20,40	265	240	215	265	240	215	253	228	253	228	60,1	51,3	65,0	44,6	2,4	2,3	37,7	30
14:34	20,67	235	210	185	230	205	185	223	198	218	195	55,3	46,0	53,2	33,2	2,0	2,0	37,7	
15:05	21,18	275	243	212	270	240	212	259	228	255	226	59,2	49,5	56,8	35,7	2,4	2,4	50,3	
16:05	22,18	215	195	170	215	190	170	205	183	203	180	50,1	40,9	45,5	26,3	2,0	2,0	50,3	29
16:18	22,40	180	160	140	175	155	140	170	150	165	148	45,4	36,4	38,3	21,2	1,8	1,8	50,3	
16:30	22,60	285	265	245	280	260	245	275	255	270	253	43,0	41,8	51,3	38,3	1,8	1,8	50,3	32
16:48	22,90	320	302	282	320	300	282	311	292	310	291	46,8	42,5	52,3	43,8	1,9	2,0	50,3	32
16:56	23,02	350	338	318	348	335	315	344	328	342	325	46,7	41,6	50,7	46,3	2,0	2,0	50,3	

The decline in flux with increasing water recovery (at almost constant linear flow rate, temperature and pressure) is due to increasing thickness of the gel layer with time as well as increasing solids concentration. When the pressure is below 300 kPa, increases in pressure (at constant linear flow rate) lead to increases in flux. When the pressure is above 300 kPa, increases in pressure generally lead to similar or lower fluxes. The increase in flux with increasing pressure (for pressures above 200 kPa) is more marked for membrane 442 than it is for membrane 719. Hence the pressure at which the flux is no longer pressure controlled is higher for membrane 442 than it is for membrane 719.

Table 4 : Results of the analysis of samples taken on 30/3/93

(50 % water recovery) **Sample**	**Concentration (mg/ℓ)**			**Retention (%)**	
	PO_4	**COD**	**TSS**	**PO_4**	**COD**
Initial feed (0 % WR)	20,4	2 960	912		
Composite permeate (up to 38 % WR)	4,8	480	13		
Permeate from 719(1)	5,3	212	7,6	62	98
Permeate from 442(1)	5,3	192	7,2	62	98
Final retentate	13,8	10 080	1744		

Unfortunately the Total Solids determination was not carried out. The phosphate concentration in the final retentate should be higher than in the initial feed. The COD of the composite permeate up to 38 % water recovery was more than twice as high as that of the permeate at 50 % water recovery. This is attributed to the build up of a dynamic layer on the membrane which resists the passage of the organic matter.

Feed : **Fresh water from tank**
Temperature : 25 °C

Pressure (kPa)	**Permeate flux (ℓ/m²h)**			
	719(1)	**719(2)**	**442(1)**	**442(2)**
100	50,4	49,1	24,4	10,9
200	114,3	89,8	55,8	31,3

3.9 Tests on effluent at 83 % water recovery

Date : 15/4/93
Feed : Screened effluent (fine screen)

Replaced 719 modules by two Membratek modules (MM) in series (each 2,3 m x 19 tubes x 12,5 mm diameter; area = 1,72 m^2).

Started at 11:42.

Time	Elap Time (h)	Pressure (kPa)			Ave. Pres (kPa)		Permeate flux (ℓ/m^{2}h)				Feed flow (m/s)		WR (%)	T (°C)
		442 in	442 mid	442 out	442 (1)	442 (2)	M1	M2	442 (1)	442 (2)	MM	442		
12:15	23,75	365	360	350	363	355			18,1	17,2		1,24	15,0	27
12:24	23,90						24,5	19,1					20,0	
12:39	24,15											2,45	30,0	
12:59	24,48												40,0	
13:05	24,58												45,0	
13:06	24,60	365	340	310	353	325			35,2	34,6		2,35		
13:12	24,70												50,0	

Screened more effluent. Started again at 13:50.

Time	Elap Time (h)	Pressure (kPa)			Ave. Pres (kPa)		Permeate flux (ℓ/m^{2}h)				Feed flow (m/s)		WR (%)	T (°C)
		442 in	442 mid	442 out	442 (1)	442 (2)	M1	M2	442 (1)	442 (2)	MM	442		
13:57	25,45	365	340	310	353	325	21,9	18,7	40,6	39,7			37,1	
14:03	25,55												40,0	
14:10	25,07	400	355	360	378	358	21,9	19,5	61,5	52,0	1,70	3,21	42,9	
14:16	25,77										1,70	3,21	45,7	
14:22	25,87	400	350	300	375	325					1,70	3,21	48,6	
14:29	25,98										1,70	3,21	51,4	
14:32	26,03	395	345	295	370	320			65,5	54,4	1,70	3,21		
14:41	26,18										1,70	3,21	57,1	
14:48	26,30	400	350	300	375	325	22,1	18,4	61,5	54,1	1,70	3,21	60,0	
14:54	26,40	400	350	300	375	325			61,3	53,0	1,70	3,21	62,9	
15:01	26,52	400	350	300	375	325			60,7	52,0	1,70	3,21	65,7	
15:07	26,62	400	350	300	375	325			58,8	51,5	1,70	3,21	68,6	
15:26	26,93										1,70	3,21	77,1	28,5
15:42	27,20	400	350	300	375	325	18,2	15,7	49,9	47,2	1,70	3,21	82,9	

Reconnected 719 modules.

Time	Elap Time	Pressure (kPa)						Average Pressure (kPa)				Permeate flux (ℓ/m^{2}h)				Feed flow (m/s)		WR	T
	(h)	719 in	719 mid	719 out	442 in	442 mid	442 out	719 (1)	719 (2)	442 (1)	442 (2)	719 (1)	719 (2)	442 (1)	442 (2)	719	442	(%)	(°C)
16:20	27,83	400	385	375	400	385	370	393	380	390	375	19,8	20,5	18,8	18,8	1,86	1,83	82,9	28,5
16:31	28,02	400	380	355	400	380	355	390	368	390	368	23,4	24,0	23,1	23,5	2,15	2,13	82,9	
16:50	28,33	400	375	345	400	375	345	388	360	388	360	31,6	33,2	30,4	29,7	2,35	2,37	82,9	
16:55	28,42	335	310	285	335	310	285	323	298	323	298	29,2	28,1	26,3	24,9	2,09	2,15	82,9	
17:23	28,88	325	300	275	325	300	275	313	288	313	288	29,0	27,7	26,3	25,6	2,01	2,12	82,9	
17:30	29,00	325	295	270	325	295	270	310	283	310	283	32,1	31,6	29,2	28,9	2,25	2,22	82,9	

Left final retentate in system overnight.

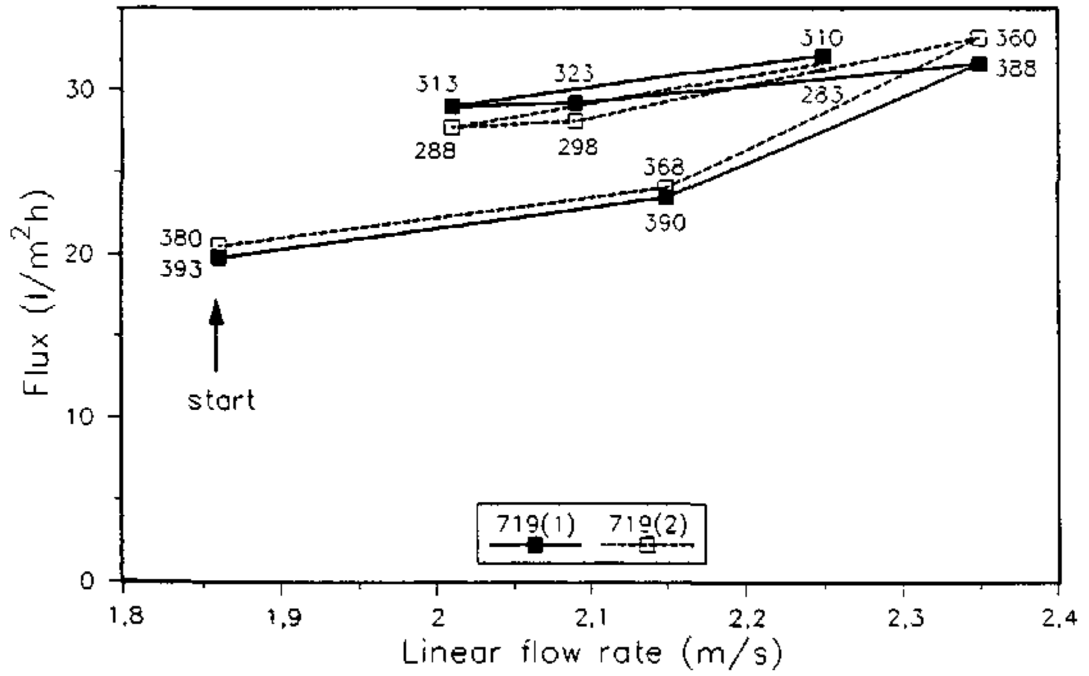

Figure 5 : (15/4/93) Effect of linear flow rate on flux for 719 modules (average pressures in kPa as shown, 83 % water recovery, 28,5 °C)

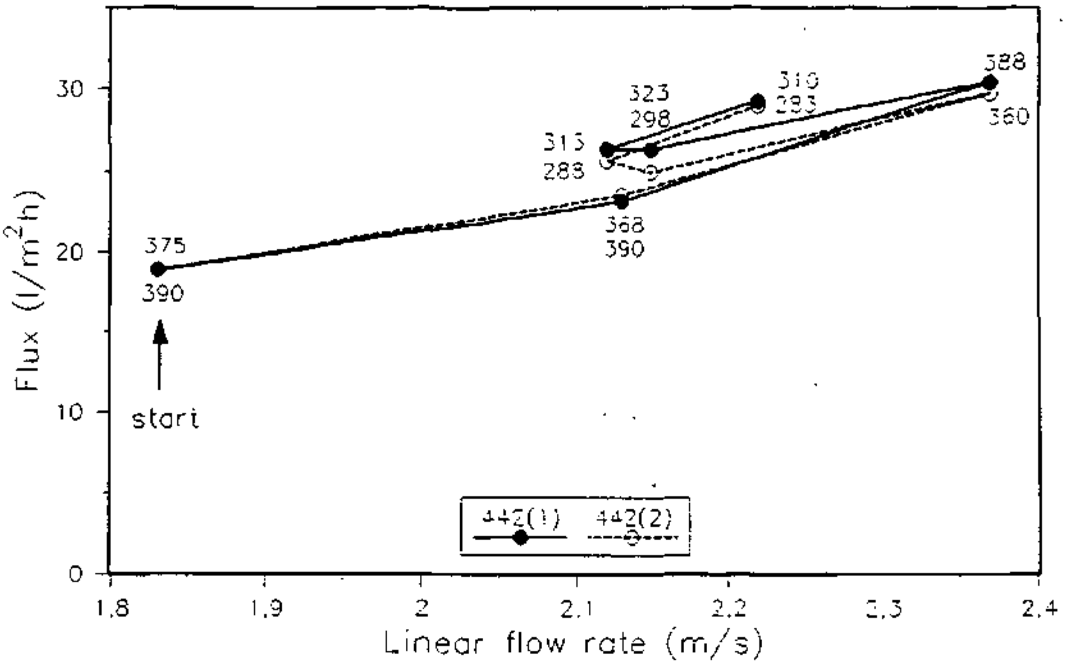

Figure 6 : (15/4/93) Effect of linear flow rate on flux for 442 modules (average pressures in kPa as shown, 83 % water recovery, 28,5 °C)

It is seen from Figures 5 and 6 that increases in the flow rate always lead to increases in the flux, whereas increases in pressure (at constant flow rate) often lead to decreases in flux.

Table 5 : Results of the analysis of samples taken on 15/4/93

(83 % water recovery)	**Concentration (mg/ℓ)**			**Retention (%)**		
Sample	**PO_4**	**COD**	**TS**	**PO_4**	**COD**	**TS**
Final retentate	15,6	17 760	9 062			
Permeate from 719(1)	4,1	648	672	74	96	93
Permeate from 442(1)	5,3	664	664	66	96	93

3.10 Tests on effluent at 91 % water recovery

Date : 16/4/93
Feed : Final retentate from previous day
Started on effluent at 8:55.

Time	Elap Time	Pressure (kPa)						Average Pressure (kPa)				Permeate flux (ℓ/m^2h)				Feed flow (m/s)		WR	T
	(h)	719 in	719 mid	719 out	442 in	442 mid	442 out	719 (1)	719 (2)	442 (1)	442 (2)	719 (1)	719 (2)	442 (1)	442 (2)	719	442	(%)	(°C)
09:32	46,03	325	300	275	325	300	275	313	288	313	288	57,9	54,9	52,9	50,1	2,09	2,04	82,9	28

Screened more effluent. Replaced 719 modules with Membratek modules.

Time	Elap Time	Pressure (kPa)			Ave. Pres (kPa)		Permeate flux (ℓ/m^2h)				Feed flow (m/s)		WR	T
	(h)	442 in	442 mid	442 out	442 (1)	442 (2)	M1	M2	442 (1)	442 (2)	MM	442	(%)	(°C)
10:57	46,45	400	320	250	360	285	20,1	17,2				1,24	68,0	27
11:12	46,70						20,2	17,0						
11:26	46,93						20,2	17,2					76,0	28,5
11:35	47,08						20,0	17,4						
11:47	47,28						20,0	17,4					84,0	29
12:06	47,60						19,2	16,6					90,6	30,5

Reconnected 719 modules.

Time	Elap Time	Pressure (kPa)						Average Pressure (kPa)				Permeate flux (ℓ/m^2h)				Feed flow (m/s)		WR	T
	(h)	719 in	719 mid	719 out	442 in	442 mid	442 out	719 (1)	719 (2)	442 (1)	442 (2)	719 (1)	719 (2)	442 (1)	442 (2)	719	442	(%)	(°C)
13:28	48,97	255	230	210	255	230	310	243	220	243	220	21,7	19,7	21,9	19,8	1,86	1,84	90,6	30,5
13:42	49,20	315	295	275	315	285	275	306	285	300	280	22,7	20,0	22,3	21,5	1,79	1,72	90,6	
13:59	49,48	370	350	332	370	350	335	360	341	360	343	22,1	21,2	22,8	22,6	2,00	1,74	90,6	
14:10	49,67	230	220	210	230	220	210	225	215	225	215	16,8	15,8	13,5	13,0	1,38	1,31	90,6	
14:25	49,92	352	342	332	352	340	330	347	337	346	335	14,2	13,6	16,5	15,5	1,29	1,38	90,6	
14:45	50,25	385	375	365	385	375	365	380	370	380	370	16,8	16,3	16,1	15,1	1,40	1,36	90,6	31
14:55	50,42	270	245	230	270	245	220	258	233	258	233	19,8	19,8	19,9	19,1	2,25	2,18	90,6	
15:10	50,57	370	342	315	370	345	320	356	329	358	333	22,3	23,8	27,5	27,1	2,29	2,20	90,6	

Rinsed system with dilute solution of *Zymex* and *Alkazyme*.

Table 6 : Results of the analysis of samples taken on 16/4/93

(91 % water recovery) Sample	Concentration (mg/ℓ)			Retention (%)		
	PO_4	COD	TS	PO_4	COD	TS
Final retentate	50,4	17 920	13 364			
Permeate from 719	4,1	376	746	92	98	94
Permeate from 442	3,4	388	816	93	98	94
Permeate from Membratek modules	5,3	668	822	89	96	94

A water recovery of about 91 % was attained by the end of these experiments. The water recovery was limited only by time and volume constraints, so a higher water recovery, should be attainable.

For both membrane types, fluxes of 20 to 23 ℓ/m²h were obtained at 91 % water recovery for linear flow rates of 1,7 to 2,0 m/s (pressures between 220 and 360 kPa). There was only a slight pressure dependence on these fluxes.

The feed flow rate has the greatest effect on the flux for pressures between 200 and 400 kPa. For a flow rate of 1,8 m/s, there does not appear to be any advantage in operating above 300 kPa.

The flux decline which accompanies a decrease in feed flow rate was observed to be not fully reversed when the flow rate is increased again, although given sufficient time (longer than 10 to 20 min) this may have occurred. Also there is a slow flux decline with time. These factors make the interpretation of the results difficult.

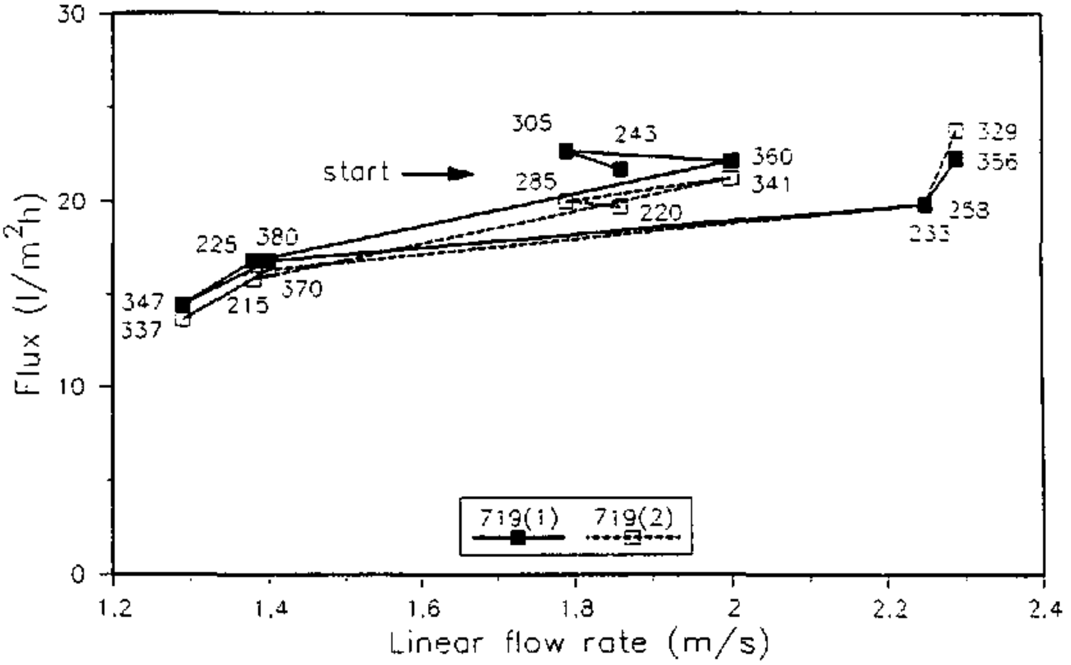

Figure 7 : (16/4/93) Effect of linear flow rate on flux for 719 modules (average pressures in kPa as shown, 91 % water recovery, 30,5 °C)

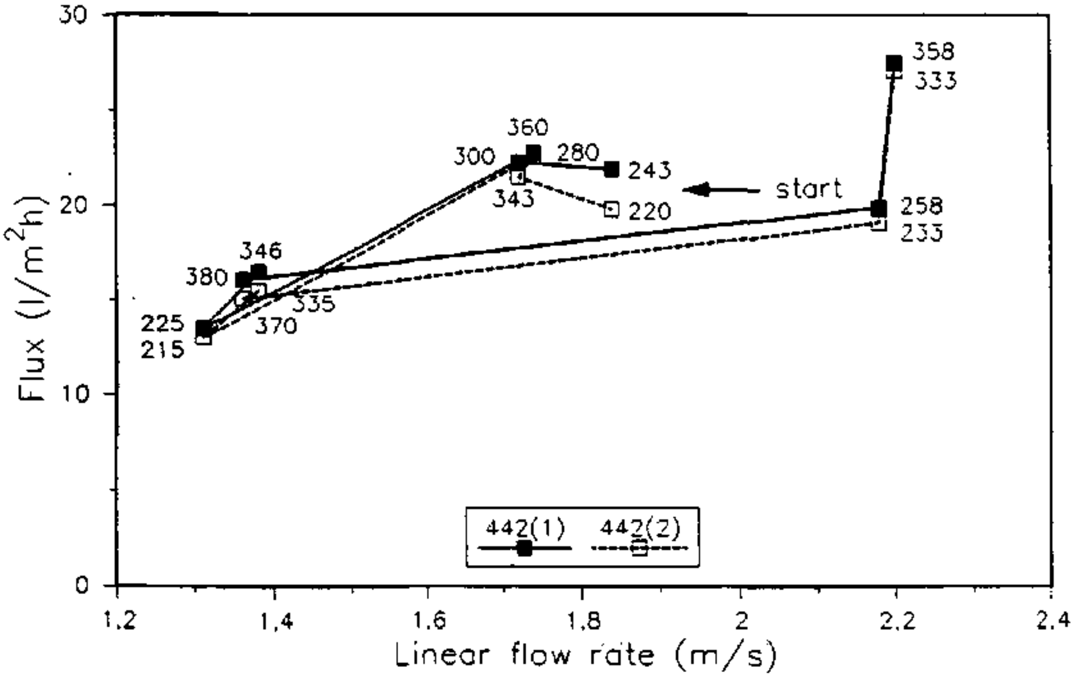

Figure 8 : (16/4/93) Effect of linear flow rate on flux for 442 modules (average pressures in kPa as shown, 91 % water recovery, 30,5 °C)

The two Membratek modules were fitted with type 719 membranes with 12,5 mm tube diameters. These modules were used in previous work on the same effluent, however all the tests were carried out at low water recoveries. Figure 9 shows the effect water recovery on the flux for these modules during the batch concentrations, first 82,9 % water recovery and then to 90,6 % water recovery. As can be seen, there was very little flux decline. The flux increased when the second batch of feed was added to the final retentate from the previous day (the effective water recovery was decreased from 82,9 % to 68 %).

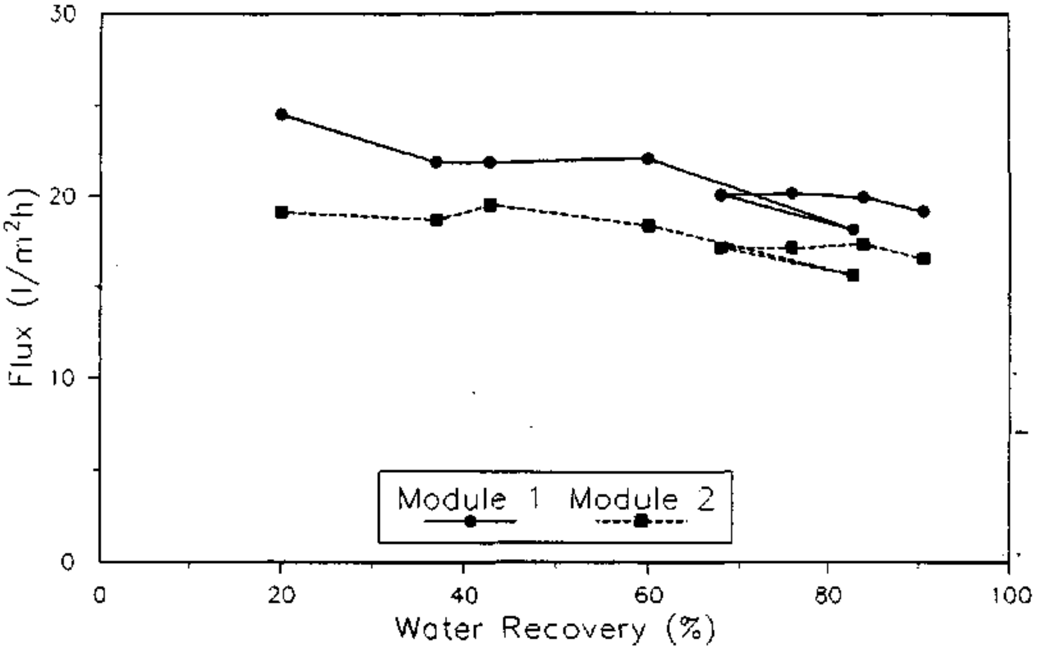

Figure 9 : (15 - 16/4/93) Effect of water recovery on flux for the Membratek modules (linear flow rate : 1,7 m/s)

3.11 Membrane cleaning

Date : 6/5/93

Feed : Fresh water from mains

Temperature : 26 °C

Pressure (kPa)	Permeate flux (ℓ/m^2h)			
	719(1)	719(2)	442(1)	442(2)
100	92,5	66,7	25,5	15,2
200	180,4	136,3	57,7	36,2
300	240,5	196,8	91,1	62,1

Pulsed for 10 min at 100 kPa

Feed : Fresh water from mains
Temperature : 23,5 °C

Pressure (kPa)	**Permeate flux (ℓ/m²h)**			
	719(1)	**719(2)**	**442(1)**	**442(2)**
200	158,0	123,5	62,0	39,7

Pulsed for 20 min.

Feed : Fresh water from mains
Temperature : 26 °C

Pressure (kPa)	**Permeate flux (ℓ/m²h)**			
	719(1)	**719(2)**	**442(1)**	**442(2)**
200	157,3	121,1	57,9	35,7

Cleaned with a 1% solution of a 1:1 mixture of *Alkazyme* and *Zymex* for 30 min at 40 kPa.

Cleaned with a 1 mℓ/ℓ solution of *Sanochlor* for 10 min.

Feed : Fresh water from mains
Temperature : 25 °C

Pressure (kPa)	**Permeate flux (ℓ/m²h)**			
	719(1)	**719(2)**	**442(1)**	**442(2)**
200	185,9	126,9	57,9	33,7

The cleaning procedure no longer seems effective.

3.12 Tests on fresh effluent at two flow rates

This experiment was carried out to determine whether the age of the effluent affected the phosphate retention. A sample of the effluent taken close to source was used.

Date : 28/7/93
Feed : Fresh water from mains
Temperature : 19 °C

Pressure (kPa)	Permeate flux (ℓ/m²h)			
	719(1)	719(2)	442(1)	442(2)
100	64,6	45,5	14,4	7,6
200	143,8	98,4	35,2	19,1
300	221,1	147,2	56,1	31,5

Feed : Screened sample of fresh effluent (fine screen)
Started on effluent at 12:08
(Note : The pressure was the same at corresponding points in the two sets of modules)

Time	Elap Time	Pressure (kPa)			Ave Press (kPa)		Permeate flux (ℓ/m²h)				Feed flow (m/s)		T
	(h)	in	mid	out	1	2	719 (1)	719 (2)	442 (1)	442 (2)	719	442	(°C)
12:18	51,0	220	210	200	215	205	40,2	41,8	34,2	19,7	1,36	1,27	23
12:30	51,2	220	210	200	215	205	37,7	40,4	36,8	20,3	1,36	1,27	
12:57	51,7	280	270	260	275	265	32,9	36,9	36,7	24,5	1,38	1,32	
13:10	51,9	280	270	260	275	265	32,3	36,2	33,3	25,1	1,38	1,32	
13:25	52,1	400	390	385	395	388	34,2	40,4	43,4	33,6	1,39	1,31	
13:40	52,4	400	393	390	397	392	33,5	40,2	37,7	31,0	1,39	1,31	
13:53	52,6	400	395	390	398	393	31,5	39,0	36,5	30,9	1,37	1,26	24,5
14:04	52,8	215	187	168	201	178	31,6	44,2	31,5	16,5	2,07	1,97	
14:16	53,0	215	190	170	203	180	34,8	46,0	28,5	16,2	2,04	1,98	
14:26	53,1	305	280	260	293	270	38,2	57,1	40,5	26,0	2,07	1,97	
14:45	53,5	305	280	260	293	270	31,5	52,0	39,7	25,0	2,07	1,97	
15:00	53,7	395	375	355	385	365	36,9	53,5	50,0	34,2	2,07	2,00	
15:12	53,9	395	375	356	385	365	34,7	44,0	46,5	33,9	2,09	2,00	24

Table 7 : Results of the analysis of samples taken on 28/7/93

Sample	Concentration (mg/ℓ)					Retention (%)			
	PO_4	COD	TSS	TS	TDS	PO_4	COD	TSS	TDS
Feed	24	4 720	1 280	3 418	2 138				
Perm from 719 at 12:30	12	960	58,4	1 016	597,6	50	80	95	72
Perm from 719(1) at 14:40	2,7	316	15,2	622	606,8	89	93	99	72
Perm from 719(2) at 14:40	12	960	45,8	902	856,2	50	80	96	60
Perm from 442 at 14:40	2,8	328	6,0	598	522	88	93	99,5	76

The initial permeate from all modules was darker (more red) than usual. This leakage of colour probably occurred because the feed was fresh and because the modules had been cleaned prior to this experiment. As the experiment proceeded the areas in the membrane that were allowing passage to the colour were closed up by the fouling and gel-polarised layers, hence the colour of the permeate decreased. The problem was more pronounced for the 719 modules than for the 442 modules. It was found that when the pressure was reduced, and the flow rate was returned to its initial value, the permeate from the 719(2) module became darker. This is attributed to a decrease in the thickness of the gel-polarised layer. The flux for the 719(2) module was also considerably higher than for the 719(1) module, especially at the higher flow rate. In previous experiments, the flux for the 719(2) module had been less than or equal to the flux for the 719(1) module. It is concluded that membrane degradation had occurred in the 719(2) module.

The flux was plotted against pressure for each flow rate (see Figures 10 and 11). Only the final flux at each operating pressure was plotted. For the 719 modules, the flux is under mass-transfer control for both linear flow rates (i.e. a gel polarised layer has formed). For the 442 modules, the flux is dependent on pressure at a linear flow rate of 2,0 m/s. For the 442(2) module, the flux was still under pressure control at a linear flow rate of 1,3 m/s.

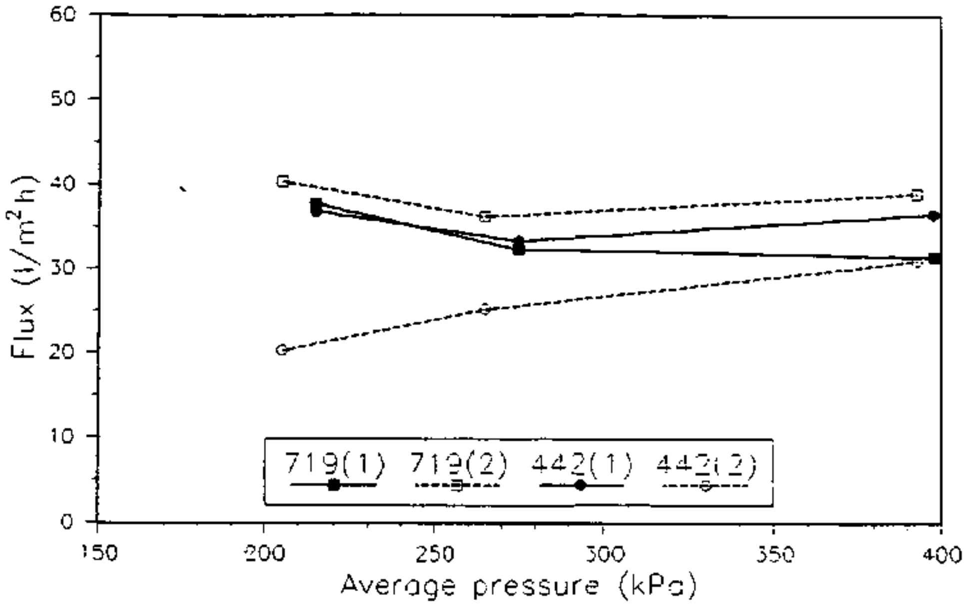

Figure 10 :(28/7/93) Dependence of flux on pressure for 719 and 442 modules at a linear flow rate of 1,3 m/s (24 °C)

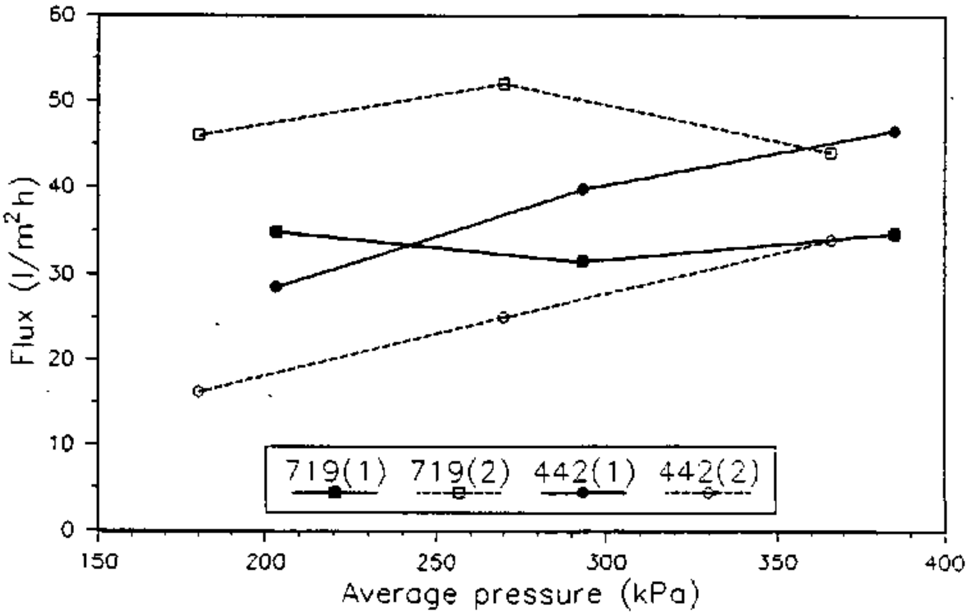

Figure 11 :(28/7/93) Dependence of flux on pressure for 719 and 442 modules at a linear flow rate of 2,0 m/s (24 °C)

4 CONCLUSIONS

4.1 Flux and Membrane Fouling

The water flux was used as a measure of the degree of membrane fouling. Table 8 shows the history of the water fluxes. It appears that the cleaning procedures are not adequate. This may be because the enzymatic and/or the chloralkali cleaners that were used were old.

Table 8 : Effect of contact time with effluent and cleaning procedures on the water flux

Date	**Membrane condition**	**Water flux (ℓ/m^2h) at 200 kPa**				**Temp**
		719(1)	**719(2)**	**442(1)**	**442(2)**	**(°C)**
9/3	New	430,8	223,5	135,7	132,9	
11/3	After 6 h contact	146,0	138,3	101,7	96,3	26,5
18/3	After 9 h contact (recycled, water)	174,9	84,9	55,4	38,9	24,5
	After clean (recycled water)	362,2	231,2	80,0	41,9	25
26/3	After 18 h contact	108,9	80,3	55,4	34,7	24,5
	After *Alkazyme/Zymex* clean	230,0	152,1	71,0	44,9	27
	After *Sanochlor* clean	278,8	176,9	75,1	44,3	25
30/3	After 23 h contact	114,3	89,8	55,8	31,3	25
6/5	After 51 h contact (enzyme soak)	180,4	136,3	57,7	36,2	26
	After clean	185,9	126,9	59,9	33,7	25
28/7	After flushing	143,8	98,4	35,2	19,1	19

The water fluxes for the 719 modules were always higher than for the 442 modules. Also, the cleaning procedure improved the flux more for the 719 membranes than it did for the 442 modules. However, the flux during treatment of the effluent itself was often higher for the 442 modules.

4.2 Operating Pressure and Flow Rate

The optimum operating pressure depends on the linear flow rate, feed concentration and temperature. The flux increases with increasing linear flow rate, increasing temperature and decreasing feed concentration.

In one of the tests (see Section 3.6), for the 719 modules, the pressure at which the flux no longer increased with increasing pressure was between 150 kPa and 300 kPa for flow rates between 1 m/s and 4 m/s (see Figure 3). For the 442 modules, the transition seemed to occur at higher pressures (see Figure 4), although the test was not carried out at pressures beyond 300 kPa. In the last test (see Section 3.12), two linear flow rates (1,3 m/s and 2,0 m/s) were used and the pressure was increased in the range 150 kPa to 400 kPa. It was found that except for the 442 modules at a linear flow rate of 2,0 m/s the pressure, the flux did not increase with increasing pressure (see Figures 10 and 11). Hence, the 442 modules can be operated at pressures of at least 400 kPa, while still exhibiting some flux improvement with increasing pressure.

The choice of operating pressure in a full-scale system would be restricted due to the relatively large pressure drops across the system. The relationship between linear flow rate and pressure drop over one pair of modules in series (tube length 2 x 2,3 m) was found to be :

$$\text{Pressure drop (kPa)} = 16 + 8.2 \times [\text{linear flow rate (m/s)}]^2$$

Hence, for a linear flow rate of 2 m/s, the total pressure drop was 49 kPa. Hence, if 12 modules were connected in series and the inlet pressure was 400 kPa, then (neglecting the decrease in flow rate due to permeation) the outlet pressure would be 106 kPa.

4.3 Air Purging

Due to increased pumping costs and pressure drops associated with high flow rates, the effect of using an air purge system was investigated. A cycle time of 4,75 min was used. For a test (at a linear flow rate of 1,5 m/s) in which the air purge was switched on after 1,5 h of operation (see Section 3.2, Figure 1), an initial increase in flux was observed. For the 719 modules, the flux remained above the value before the air purge was switched on. For the 442 modules, further flux decline occurred. The pressures decreased after the first air purge, hence the initial increase in flux may be due to the removal of material which had been partially blocking the modules. This led to a temporary increase in flow rate and a resultant increase in pressure drop. The pressures were adjusted to compensate for this.

Since flux depends strongly on flow rate, it is not possible to attribute the improved fluxes solely to the scouring effect of the air purge. The air purge unit was used in subsequent tests, but the results were not conclusive. The use of air purging will, however, prevent the accumulation of suspended matter in the modules.

4.4 Water Recovery

A maximum water recovery of 91 % was attained in one of these experiments (see Section 3.10). This was limited by the equipment, since a certain minimum level was required in the feed tank to allow effective cooling via the cooling coils. It is expected that a water recovery of at least 95 % should be attainable. This represents a 20 fold volume reduction. The maximum water recovery will be limited by flux considerations. The final fluxes obtained at 91 % water recovery were still acceptable (above 15 ℓ/m²h at a linear flow rate of around 1,5 m/s).

4.5 Permeate Quality

The composition of the permeate and the retention obtained during some of the tests is given in Tables 3 to 7 (in Sections 3.6, 3.8, 3.9, 3.10 and 3.12, respectively). The COD of the permeate was around 200 mg/ℓ for a test at zero water recovery (90 % retention) and was less than 700 mg/ℓ at high water recoveries (96 % to 98 % retention). The total solids retention was lower than the COD retention due to the passage of inorganic salts through the membrane.

The concentration of phosphate in the permeate ranged from 2,7 to 5,3 mg/ℓ. For the tests on effluent that was not fresh, the point phosphate retention was between 50 % and 66 % at zero water recovery, and increased to 93 % retention at 91 % water recovery. The retention of total phosphate depends on its form i.e. insoluble or soluble. Hence, the degree of degradation of the effluent would determine the ratio of soluble to insoluble phosphate. It was expected that the closer to source the sample is taken, the more phosphate would be insoluble (or bound) and the higher the retention. An experiment using an effluent sample taken close to source was carried out (see Section 3.12). The phosphate retention was around 89 % (except for the 719(2) module, which appeared to be leaking and had a phosphate retention of 50 %).

The quality of the permeate from the two membrane types is almost the same (except in the last experiment, where leakage from the 719(2) module occurred), hence the difference in pore size does not affect the overall retention performance in this application.

5 RECOMMENDATIONS FOR FUTURE WORK

Cleaning trials using fresh enzymatic and chloralkali cleaners are required to determine whether the membrane fouling is reversible. Further tests using the air purge unit at different purge frequencies are required. Analysis of the results using a computer simulation program is required to enable full interpretation of the results.

ACKNOWLEDGEMENTS

The following are thanked for their assistance :
The staff at the workshop at the Department of Chemical Engineering, University of Natal, for building the pilot plant.
The staff at the effluent plant at the Cato Ridge Abattoir, for helping to set up the equipment and for analysing the samples.

WATER RESEARCH COMMISSION PROJECT NO. 325

RESEARCH ON THE MODELLING OF TUBULAR REVERSE OSMOSIS SYSTEMS

Appendix 5

Modelling of Ultrafiltration of Effluent at the Cato Ridge Abattoir

Ultrafiltration of Red Meat Abattoir Effluent :
A Pilot-Plant and Modelling Investigation

Conference paper presented at
Engineering of Membrane Processes II : Environmental Applications
Il Ciocco, Italy, 26-28 April 1994

CJ Brouckaert

Pollution Research Group

Department of Chemical Engineering

University of Natal

Durban

February 1995

Ultrafiltration of Red Meat Abattoir Effluent :

A Pilot Plant and Modelling Investigation

C.J. Brouckaert, S. Wadley* and E.P. Jacobs***
* Pollution Research Group, Department of Chemical Engineering, University of Natal,
King George V Ave., Durban, 4001, Republic of South Africa.
** Institute for Polymer Science, University of Stellenbosch, Stellenbosch, 7600,
Republic of South Africa.

Paper presented at the *Engineering of Membrane Processes II - Environmental Applications* Conference, Il Ciocco, Italy, 26-28 April 1994.

INTRODUCTION

Abattoirs in water-scarce regions such as South Africa need to balance the three aspects of hygienic operation, water consumption and effluent quality. Measures which reduce water consumption tend to affect cleanliness and effluent quality adversely. Hence, in spite of continual pressure to reduce water consumption, the South African abattoir industry remains a major water user. The effluent that this industry produces has a particularly high pollution potential, with chemical oxygen demand (COD) values as high as 12 000 mg/*ℓ*, and soluble phosphate levels of up to 80 mg/*ℓ*. This effluent is far too concentrated for discharge to the environment or most municipal sewerage treatment works, but is too dilute for economic recovery of organic material.

Ultrafiltration (UF) offers a possible solution to this problem since it can be used to separate the effluent into a permeate which is reusable in limited areas of the abattoir, and a much reduced volume of retentate which is more amenable to processing than the original waste water. The South African Water Research Commission and the South African Abattoir Corporation have been investigating the use of ultrafiltration for treating the abattoir effluent with minimum pretreatment.

PILOT-PLANT STUDIES

A pilot-plant study using 12,5 mm diameter tubular polysulphone ultrafiltration membranes of medium molecular weight cut-off (type 719, supplied by Membratek, South Africa) was carried out at the Cato Ridge Abattoir. Effluent from the abattoir was used and was first screened to remove large suspended material. A 90 % reduction in COD was achieved, however the viability of the process was threatened by severe membrane fouling. A cost-effective cleaning programme was developed, which involved water flushing, sponge ball swabbing and enzymatic cleaning. The enzyme detergent formulation which was used is employed by the abattoirs for general cleaning. This work is described by Jacobs et al. (1992) and Cowan et al. (1992).

Further tests have been carried out using unsupported 9 mm diameter tubular membranes, instead of the supported 12,5 mm type. These tubes were housed in sets of three in 32 mm diameter PVC tubes. The idea was to test a low pressure (< 400 kPa), low cost design of module, as the previous investigation had shown that the membranes became *gel-polarised* at pressures above about 300 kPa, and no improvement in flux could be obtained by operating at higher pressures. Two membrane types were compared : the medium molecular weight cut-off 719 membrane and the 442 membrane (also available from Membratek), which has a lower molecular weight cut-off.

The tests were carried out on the combined effluent from the abattoir as it enters the effluent plant. At this stage the effluent had undergone fat-skimming and rough screening. Further screening was carried out manually to remove solids that might block the modules or lodge in the back-pressure valves. The effect of flow rate and pressure on the flux was investigated. An air purge device was tested to determine whether it could have the same effect on the flux as high linear flow rates would, that is, to limit the extent of gel layer polarisation.

RESULTS OF TESTS ON 9 mm TUBES

It was found that the dependence of the flux on the linear flow rate was strong. It was observed that for each linear flow rate, there was a pressure above which increases in pressure no longer lead to increases in flux. This critical pressure increased with increasing flow rate. The tests were carried out at pressures between 100 kPa and 400 kPa. The construction of the modules limits the maximum operating pressure to 400 kPa. The results of the use of the air purge unit were inconclusive, but it appeared to benefit the 719 membranes more than the 442 membranes.

A maximum water recovery of 91 % was attained. At this water recovery the fluxes were still reasonably high (above 15 ℓ/m^{2}h at a linear flow rate of 1,5 m/s). Hence higher water recoveries (at least 95 %) should be attainable.

The COD of the permeate was below 700 mg/ℓ for the tests at high water recoveries. This corresponds to a COD retention of 96 to 98 %. The point retention of phosphate varied from 50 to 66 % at zero water recovery. The point retention was 93 % at 91 % water recovery. When effluent taken close to source was used, the phosphate retention was 89 %. In all the tests, the concentration of phosphate in the permeate ranged from 2,7 to 5,3 mg/ℓ.

This paper presents the results of modelling of the data measured at low water recoveries. Figures 1 and 2 summarise the experimental results which were considered in the study.

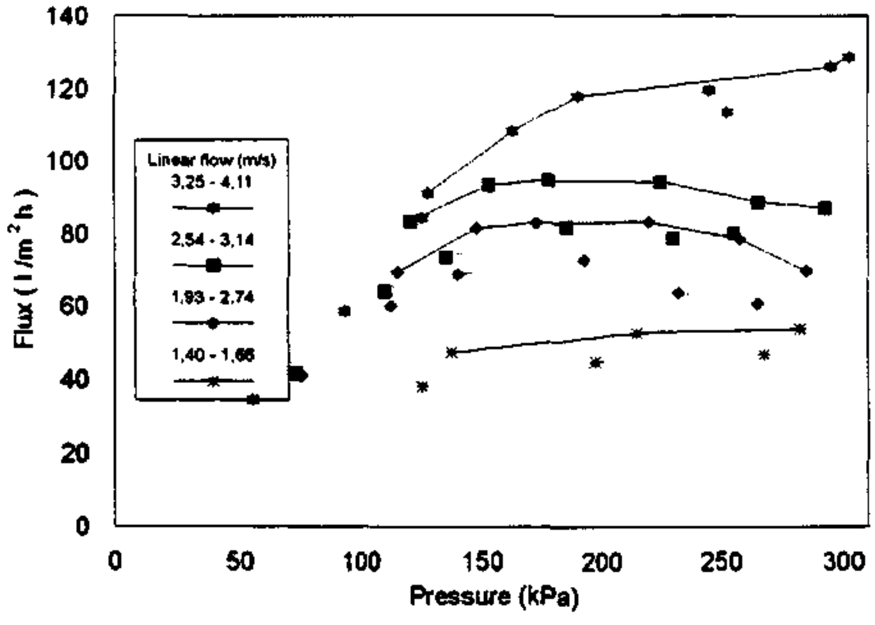

Figure 1: Experimental flux measurements using 719 membranes

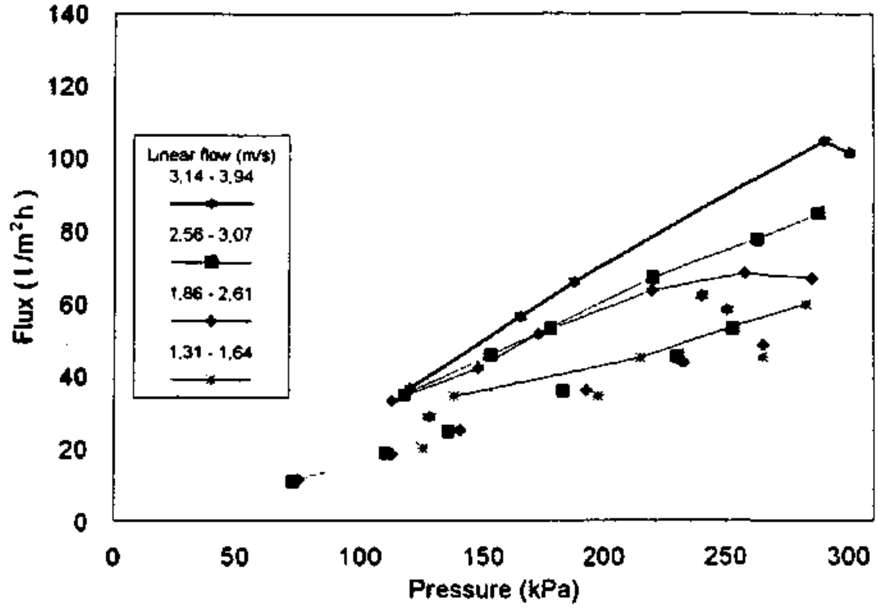

Figure 2 : Experimental flux measurements using 442 membranes.

A feature of the data which is evident from the graphs was the apparent scatter of the flux measurements. This was ascribed to two factors. Firstly, it was very difficult to control the experimental apparatus to operate at precise values of the operating parameters (pressure, flow rate and temperature), although these could be measured accurately enough. Thus part of the apparent scatter is due to the necessity of grouping results measured under conditions which were similar, rather than identical. Secondly, there was significant degradation of membrane performance due to fouling in the time that it took to make the measurements. It seemed that the only way to obtain a more satisfactory interpretation of the data would be to use a model which allowed for the uncontrolled variations in a way which represented adequately the fundamental processes which governed transport through the membrane.

MODELLING APPROACH

The model may be described as consisting of two major components : transport through the membrane and fouling. The equations used to describe the transport through the membrane have been reported elsewhere (Wadley, Brouckaert and Buckley, 1994). The fouling model considered two aspects : *reversible* and *irreversible* fouling, where the terms reversible and irreversible are used with reference to the hydrodynamic conditions prevailing at the membrane surface during operation; the fouling was not irreversible when subjected to enzymatic cleaning.

Reversible Fouling

Reversible fouling of ultrafiltration membranes is frequently referred to as *gel-polarisation*, although there is controversy over the physical reality of a gel layer at the membrane surface. The approach of Sourirajan and Matsuura (1985) was followed, which does not explicitly use the concept of a gel-layer. It simply postulates that concentration polarisation causes high solute concentrations at the membrane surface, which affect both the water and solute transport resistances of the membrane, through an unspecified mechanism such as pore-blocking. Empirical equations are used to describe the variations of the water and solute transport parameters for the membrane as functions of the solute concentration at the membrane surface.

The hydraulic permeability parameter P_l is described by

$$1 - \frac{P_l}{P_{lo}} = a \cdot c^{*b} \tag{1}$$

where

c^* is the solute concentration at the membrane surface.

P_{lo} is the value of P_l when c^* is zero.

a and b are empirical parameters.

The solute permeability parameter P_s is modelled by a similar relationship

$$\frac{P_s}{P_{so}} = d \cdot c^{*e} \tag{2}$$

Values of the permeability parameters and the empirical constants were determined by regression from the experimental data, except the exponent e. The experimental data consisted mostly of flux measurements, with only two measurements of COD in the permeate, and so did not contain sufficient information to provide a good determination of e. A value of -0,22 quoted by Sourirajan and Matsuura (1985) for ultrafiltration of polyethylene glycol solutions was used in the absence of more specific information.

Irreversible Fouling

In a previous study it had been found that the pure water fluxes declined more or less linearly with time of contact (t) of the membrane with the effluent stream. This correlated with measurements of lipids adsorbed onto the membrane surface. Accordingly, the irreversible component of the fouling was modelled as a simple linear decline of P_{lo} with time.

$$P_{lo} = k\,(1 - f\,t) \tag{3}$$

where k and f were empirical parameters, once again determined from the data by regression.

Due to the few measurements of permeate COD values, modelling the effect of fouling on P_s did not seem justified (this would have added further empirical parameters), and it assumed to be unaffected by the irreversible component of fouling.

RESULTS

Figures 3 and 4 show the correspondence obtained between the model and the measured data for the two membranes. Because of the complex sequence of pressures and flow rates, as well as the influence of progressive membrane fouling, all of which makes it very difficult to organise the diagrams on any informative basis, the diagrams have been simply plotted as flux against time of operation. The correspondence between model and data is remarkably good, and indicates that the main mechanistic processes are adequately represented.

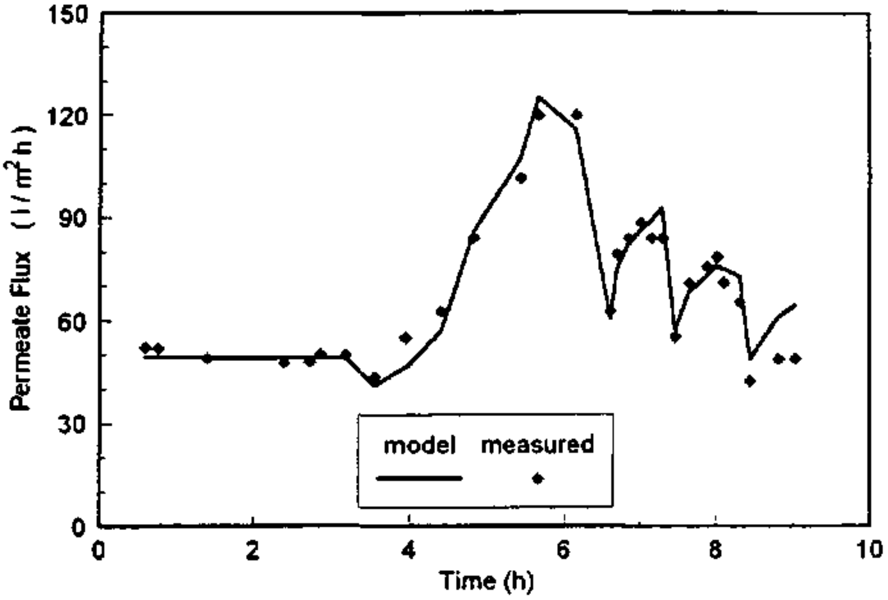

Figure 3: Comparison between model and measured fluxes for 719 membranes.

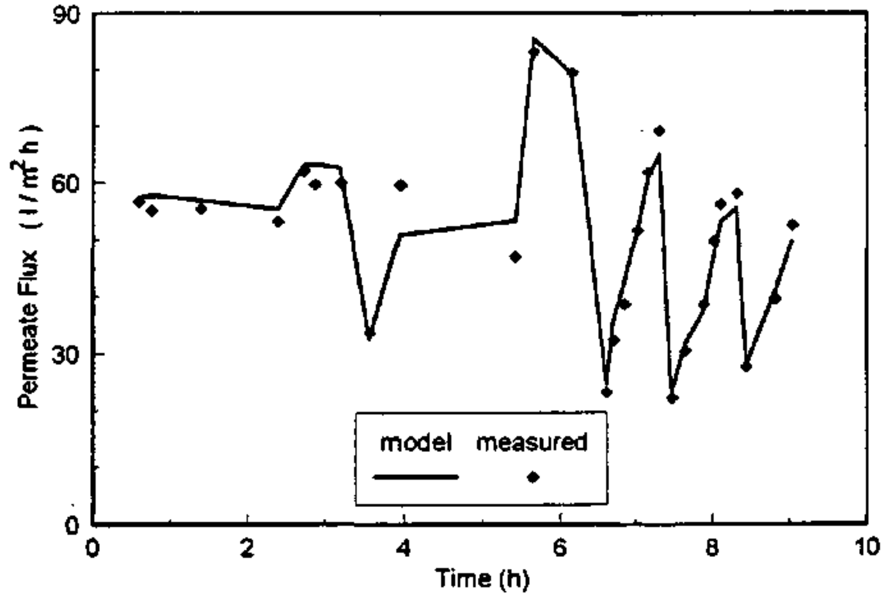

Figure 4: Comparison between model and measured fluxes for 442 membranes

An interesting feature of the results is the comparison of the response of the 719 and 442 membranes to the reversible component of fouling (or gel-polarisation, as it might be called).

The low molecular weight cut-off 442 membranes understandable have a lower permeability than the medium molecular weight 719 membranes, but the are much less affected by the gel-polarisation, to the extent that at higher membrane surface concentrations they produce the higher fluxes. This phenomenon was observed experimentally as the fluxes for the 442 membranes overtaking those for the 719 membranes as the pressure increased.

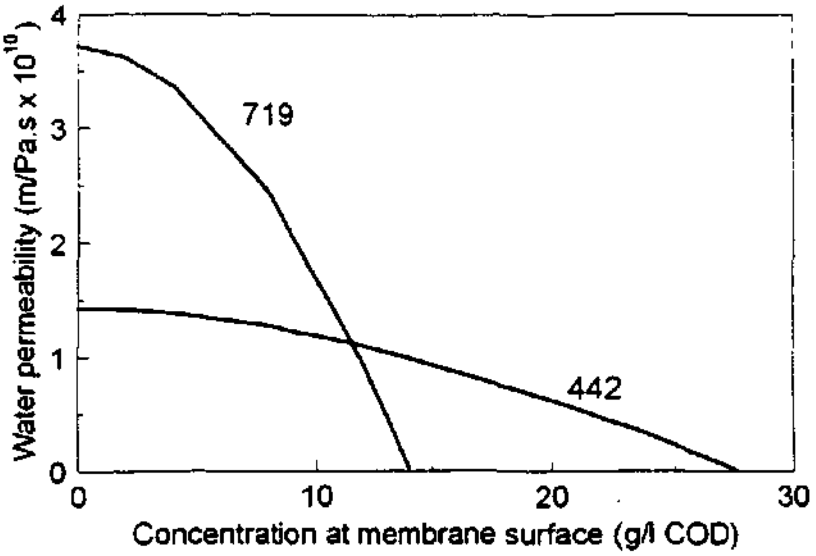

Figure 5: Comparison between response of 719 and 442 membranes to reversible fouling according to the model

The comparison between the two membranes is shown in Fig. 5 by plotting the relationship of equation (1) using the parameter values determined by regression for the two membranes.

DISCUSSION AND CONCLUSIONS

The response of the two membranes to the reversible fouling is most interesting, as it contradicts the simple intuitive notion of a concentrated layer of organic material at the membrane surface which adds a transport resistance in series to that of the membrane itself. If this were the case, the fluxes of the two membranes should have approached the same value as the fouling resistance became limiting. The only difference between these two membranes is in their porous structures; they have the same chemical makeup. This suggests that the critical resistance-producing mechanism occurs within the membrane pores, rather than in a layer outside the membrane surface. It may be that the organic material finds it more difficult to concentrate to the same extent within the smaller pores of the 442 membrane.

The achievement of an economic design of the process will require a combination of module design, optimisation of hydrodynamic conditions and plant configuration, taking into account the membrane fouling-cleaning cycle. The pressure drop across a plant required to maintain flow velocities imply that most of the modules will be operating in the gel-polarised regime, in which case the 442 membranes would be advantageous in terms of flux. The 719 modules would tend to perform better at the low pressure end of the plant.

Figure 5 shows the water permeabilities dropping to zero at about 15 and 28 g/*l* COD at the surfaces for the 719 and 442 membranes respectively. These values represent extrapolations of the model beyond the range of conditions encountered in the data, and are probably not realistic. Unfortunately simulations of a full-scale plant achieving the required 90 % or greater water recovery will involve concentrations as high as or even higher than these, so the model needs to be extended to deal with such conditions.

The use of the model has made a major contribution to the interpretation of the pilot-plant results by making it possible to compensate for uncontrollable factors which tended to obscure the trends. The model will also be very useful for optimising the design of a full-scale plant once it has been adapted to account for the full range of water recoveries that would be involved. The Microsoft Windows based model is available from an FTP site, Internet address *aqua.ccwr.ac.za*.

A preliminary design study based on the data obtained by these investigations has been carried out for a plant to treat the effluent from the abattoir in Port Elizabeth, South Africa. The economic viability of the process was found to be very sensitive to the figure assumed for membrane life. As a result a proposal has been made for a further long term test to establish a reliable estimate of membrane life. The investigations to date have not been able to detect permanent membrane degradation during their relatively short operating history, so there is every reason to believe that the membrane life should be very good.

ACKNOWLEDGEMENTS

The authors would like to thank the following organisations :

The South African Abattoir Corporation (ABAKOR),

Cato Ridge Abattoir, and

Membratek (Pty) Ltd.

This work was carried out as part of a project funded by the Water Research Commission of South Africa.

REFERENCES

Cowan J.A.C., MacTavish F., Brouckaert C.J. and Jacobs E.P., 1992, Membrane Treatment Strategies for Red Meat Abattoir Effluents, *Water Science and Technology*, 25(10), 137-148.

Jacobs E.P., Swart P., Brouckaert C.J. and Hart O.O., 1992, Membrane Performance restoration. I : Abattoir Process Streams, Cleaning Regimes for UF Membranes, *Water SA*, 19(2), 127-132.

Sourirajan S., and and Matsuura T., 1985, Reverse Osmosis/Ultrafiltration Process Principles, National Research Council Canada, Ottawa. 702-705.

Wadley S., Brouckaert C.J., and Buckley C.A., 1994, Modelling of nanofiltration applied to the recovery of salt from waste brine at a sugar decolorisation plant. Paper presented at the *Engineering of Membrane Processes II - Environmental Applications* Conference, Il Ciocco, Italy, 26-28 April.

WATER RESEARCH COMMISSION PROJECT NO. 325

RESEARCH ON THE MODELLING OF TUBULAR REVERSE OSMOSIS SYSTEMS

Appendix 6

Modelling of Nanofiltration of Brine Effluent at Hulett Refineries Ltd

Modelling of Nanofiltration Applied to the Recovery of Salt
from Waste Brine at a Sugar Decolourisation Plant

Conference paper presented at
Engineering of Membrane Processes II : Environmental Applications
Il Ciocco, Italy, 26-28 April 1994

Accepted for publication : Journal of Membrane Science, 1995

S. Wadley and CJ Brouckaert

Pollution Research Group

Department of Chemical Engineering

University of Natal

Durban

February 1995

MODELLING OF NANOFILTRATION APPLIED TO THE RECOVERY OF SALT FROM WASTE BRINE AT A SUGAR DECOLOURISATION PLANT

S. WADLEY, C.J. BROUCKAERT, L.A.D. BADDOCK and C.A. BUCKLEY

Pollution Research Group, Department of Chemical Engineering, University of Natal, King George V Ave., Durban, 4001, South Africa.

ABSTRACT

The implementation of a computer model to simulate reverse osmosis in systems with several components is described. The model was based on the Spiegler-Kedem theory of reverse osmosis. The results of a pilot-scale investigation of the use of nanofiltration to recover sodium chloride from waste brine from the regeneration of anion exchange resin were used in this study. This effluent contains around 50 *g/ℓ* of sodium chloride and 5 *g/ℓ* (as total carbon) of organic colourants, many of which are negatively charged. When using the SelRO™ MPT-30 or MPT-31 membrane at an operating pressure of 3 MPa, temperatures between 45 °C and 60 °C, and linear feed flow rates around 1.6 m/s, the retention of sodium chloride was found to be between 0 % and 20 %, while the organic compounds had an overall retention of 80 % to 97 %. The experimental results were used to obtain a set of parameters relating to the system, which were then used to generate design data for a full-scale plant. Suitable module arrangements were proposed and the system performance for each case was predicted.

Keywords : Computer modelling, nanofiltration, ion exchange regeneration effluent, sodium chloride, organic anions

INTRODUCTION

At some sugar refineries removal of colour from sugar liquor using anion exchange resin is practised. The waste brine arising from the regeneration of the resin usually poses a disposal problem. At the Hulett Refinery in Durban this regeneration effluent contains around 50 *g/ℓ* of sodium chloride and 5 *g/ℓ* (as total carbon) of organic matter, and has a chemical oxygen demand (COD) of about 13 000 mg/ℓ. Hence, it is not suitable for discharge to sewer. An investigation has been carried out at the Hulett Sugar Refinery in Durban to determine whether nanofiltration is a suitable method for recovering sodium chloride from this waste brine stream [1,2,3,4]. The proposed process for recovering and recycling the sodium chloride solution is illustrated in Figure 1.

The organic matter in the regeneration effluent consists of natural sugarcane pigments (mostly phenolic compounds) and colourants that are formed during the cane juice processing. The molar mass of the compounds ranges from less than 500 g/mol to more than 20 000 g/mol, with most of the colour being due to the compounds in the 5 000 to 20 000 g/mol range. The compounds are mostly negatively charged, with up to six or more functional groups conveying the negative charge on each species.

Nanofiltration tests were carried out on laboratory and pilot scale using SelRO™ MPT-30, MPT-10 and MPT-31 membranes (manufactured by Membrane Products Kiryat Weizmann Ltd). The results indicated that, when nanofiltration is carried out on the portion of the regeneration effluent containing the highest concentration of salt, the permeate is of suitable composition for recycle to the regenerant make-up system. This decreases the amount of fresh salt required and reduces the volume of effluent for disposal. The volume of brine that can be recovered is limited by the water balance for the regeneration system. The two major types of solute have different retention characteristics. Sodium chloride has a retention between 0 % and 20 %, while the organic compounds have an overall retention of 80 % to 97 %, based on total organic carbon concentrations [4].

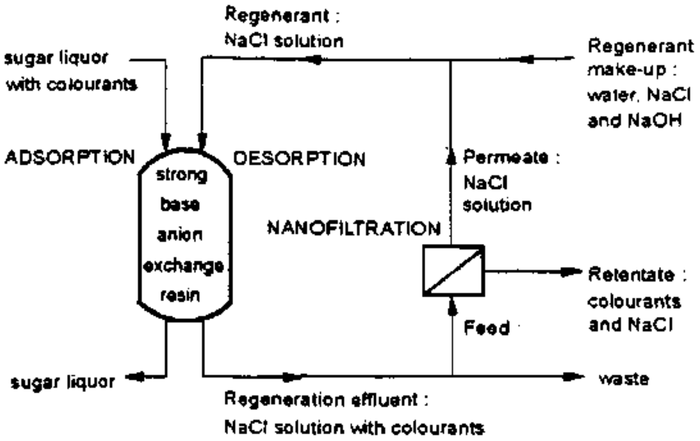

Figure 1 : Schematic diagram of the proposed process for recovering sodium chloride from waste brine at a sugar decolourisation plant

The laboratory investigations were carried out on single tubes (about 0,6 m in length), while the pilot plant had a single module containing 18 tubes (1,2 m in length) connected in series. The water recovery achieved in a single pass was less than 0,5 % for the pilot plant, hence batch concentration experiments were carried out (reaching water recoveries of around 70 %). At various times during the batch concentration, flux measurements were made and the retentate and permeate were sampled. The samples were analysed for chloride and total carbon. This information provides a picture of what is happening to the membrane during the experiment, however to interpret this information and to use it to design a full-scale plant, a computer model is required.

This paper describes a computer model for simulating reverse osmosis systems and its application to the data obtained during these nanofiltration experiments. This computer program can be used to investigate the effect of the operating conditions and the concentration of each solute type on the permeate flux and solute retention. Experimental data is used to obtain certain parameters which can then be used to predict the system's performance under other operating conditions or to study the effect of different arrangements of the modules on the performance of a full-scale plant. Hence, the computer model facilitates the generation of suitable design data for full-scale plants from laboratory-scale tests and pilot-plant tests on a single module.

The nanofiltration membrane and most of the organic solutes are negatively charged hence adsorption of organic material on the membrane surface is not expected to be a dominant feature of this system. The high concentration of sodium chloride present (50 to 100 g/ℓ) causes shielding of the charge on the membrane, thus reducing the membrane selectivity. Hence, the passage of organic species and multivalent inorganic ions is higher than it would be if the sodium chloride concentration was lower.

The main problem encountered in modelling this system is that the organic component involves a wide range of compounds with varying molar mass, charge and physical properties. The concentration of organic carbon is the only information available for the organic component in the feed and permeate. Hence, any model which is chosen needs to contain as few adjustable parameters as possible.

CHOICE OF MODEL

The model which was used is based on the Spiegler-Kedem theory of reverse osmosis, which uses non-equilibrium thermodynamics and the assumptions of the friction model of membrane transport processes. This theory describes a mechanism for retention of salts but does not take into account concentration polarisation [5]. A modification of this theory by Schirg and Widmer [6] which considers concentration polarisation was used.

This modelling approach was chosen rather than the Sourirajan model or the solution-diffusion model for various reasons. The Kimura simplification of the Sourirajan model (based on the preferential sorption-capillary flow mechanism) is only valid for the case where preferential sorption of the solvent occurs (for example, for dilute solutions of a simple inorganic salt) [7]. Hence, this model would not account for the high passage of sodium chloride observed in the present work. The surface force-pore flow model of Sourirajan would account for this effect, however it involves a large number of parameters including complex potential and friction functions. In the simple form of the solution-diffusion model, the pressure dependence of the solute flux is neglected. In the present work, the solute flux was observed to be dependent on the pressure.

It was anticipated that the extension of the Spiegler-Kedem theory by Perry and Linder [8] could be used. This model accounts for low and negative retention of sodium chloride in the presence of organic compounds with multiple negative charges. The mechanism for negative retention is based on the Donnan equilibrium which exists due to the negative charge density on the membrane. This theory was developed for the case where a single organic compound of known molar mass and charge is present, hence it is difficult to apply when a wide range of compounds is involved. In addition, the distributions of molar mass and charge on the compounds were unknown, and would vary from sample to sample. The large number of parameters used by Perry and Linder make this model more complex than was desired for the system under consideration. In the present work, the sodium chloride retention rarely approached negative values and this only occurred on the final measurements at high water recoveries. The objective of this modelling exercise was to produce an adequate representation of the system for the purpose of making engineering design decisions based on limited experimental data. Accordingly, one goal of this study has been to establish what degree of model complexity is necessary to reflect the most important features of the experimental data. The neglect of electrical effects in the membrane transport model represents an rough approximation which cannot be justified *a priori*. It is justified rather by the limitations in knowledge of the nature of the organic components in the effluent, and the achievement of an adequate representation of the experimental data, which had been obtained from relatively unsophisticated measurements made on the pilot plant, operating in an industrial environment.

THEORY

For a system involving a single solute in aqueous solution, the solute retention can be described by three transport coefficients [5] :

(i) specific (intrinsic) hydraulic permeability, $\bar{P}_l$,

(ii) local solute permeability, $\bar{P}$, and

(iii) the reflection coefficient, σ.

The permeability is the flux of a component (solvent or solute) through the membrane per unit driving force (in this case, the effective trans-membrane pressure). The reflection coefficient is a measure of the portion of the membrane through which the solute cannot be transferred [9].

The local flux equations in the Spiegler-Kedem theory are given by :

$$J_v \quad = \quad -\bar{P}_l\left(\frac{dp}{dx} - \sigma\frac{d\pi}{dx}\right) \qquad (1)$$

and

$$J_s \quad = \quad -\bar{P}\left(\frac{dc}{dx}\right) + (1-\sigma)cJ_v \qquad (2)$$

where J_s is the molar solute flux through the membrane,

J_v is the volume flux through the membrane,

p is the pressure,

π is the osmotic pressure,

x is the vertical distance from the membrane surface, and

c is the solute concentration.

Hence, the reflection coefficient is defined by

$$\sigma \equiv \left(\frac{\Delta p}{\Delta \pi}\right)_{J_v = 0} \tag{3}$$

where Δp is the trans-membrane pressure, and

$\Delta \pi$ is the trans-membrane osmotic pressure.

The observed retention coefficient (R_{obs}) is defined by the solute concentrations in the feed (c') and the permeate (c''), i.e.

$$R_{obs} = 1 - \frac{c''}{c'} \tag{4}$$

The retention of a membrane for a particular solute depends on its concentration at the membrane/feed interface rather than on its concentration in the bulk feed solution. The concentration at the interface cannot be easily determined by direct measurement, however it can be evaluated from experimental data by using Equation (12) below.

The real retention coefficient is given by

$$R_{real} = 1 - \frac{c''}{c^*} \tag{5}$$

where c^* is the solute concentration at the membrane/feed interface.

A balance over a differential element at the membrane/feed interface gives [6] :

$$J_v c - D\frac{dc}{dx} = J_v c'' \tag{6}$$

where D is the diffusion coefficient of the solute in water.

Integration of Equation (6) with the following boundary conditions :

$c = c^*$ at $x = 0$ and $c = c'$ at $x = l$ (where l is the thickness of the concentrated boundary layer solution), gives

$$\frac{c^* - c''}{c' - c''} = \exp\left(\frac{J_v l}{D}\right) \tag{7}$$

IMPLEMENTATION OF MODEL

The main features of the experimental data that needed to by accounted for in the model were :

(i) The solutes present had to be treated as at least two separate components, namely NaCl and organic compounds, with very different membrane transport characteristics. Regarding the organic components as a single entity was obviously an approximation, but as the concentration of organic matter was determined from total carbon analyses, a more discriminating representation could not be inferred directly from the experimental data.

(ii) Measurements were made under varying conditions of temperature, pressure, cross-flow rate and concentration, so that coefficients in the model equations needed to be able to vary with conditions according to appropriate correlations.

Volumetric flux

In Equation (1), it was assumed that the active membrane thickness was sufficiently small that the derivatives could be regarded as constant. It was further assumed that the osmotic pressure (π) could be expressed as a linear function of solute concentrations for each component i, i.e.

$$\pi = \sum_i \phi_i c_i \tag{8}$$

where ϕ_i is a constant for each component i and is termed the osmotic factor.

It was found necessary to use different values of the osmotic factor for the organic component on the high pressure and low pressure sides of the membrane, respectively. This was probably due to the fact that the organic material was not a single substance, therefore the molecular weight distribution of the fraction which penetrated the membrane was different from that of the retained fraction.

With these assumptions, Equation (1) becomes

$$J_v = P_l\left[\Delta p - \sum_i \sigma_i\left(\phi_i^* c_i^* - \phi_i'' c_i''\right)\right] \tag{9}$$

Solute fluxes

Integrating Equation (2) over the membrane, between concentrations c_i^* and c_i'' gives

$$c_i'' = c_i^*\left[\frac{1 - \sigma_i}{1 - \sigma_i F_i}\right] \qquad \text{where } F_i = \exp\left[\frac{(1 - \sigma_i)J_v}{P_i}\right] \tag{10}$$

Equation (7) becomes

$$\frac{c_i^* - c_i''}{c_i' - c_i''} = G_i = \exp\left(\frac{J_v l}{D_i}\right) \tag{11}$$

Equations (10) and (11) can be combined to give

$$c_i^* = c_i'\left[\frac{G_i(1 - \sigma_i F_i)}{1 - \sigma_i F_i - (1 - \sigma_i)(1 - G_i)}\right] \tag{12}$$

and
$$c_i'' = c_i'\left[\frac{G_i}{1 - G_i}\right]\left[\frac{(1 - \sigma_i F_i)}{1 - \sigma_i F_i - (1 - \sigma_i)(1 - G_i)}\right] \tag{13}$$

which may be substituted back into Equation (9).

When $\sigma_i = 1$, the above expressions cause numerical difficulties. For this case,

$$c_i^* = \frac{c_i' G_i (J_v + P_i)}{J_v + P_i G_i} \quad \text{and} \quad c_i'' = \frac{c_i' P_i}{J_v + P_i G_i} \tag{14}$$

Modelling procedure

In the standard modelling situation the flow rate, concentration and pressure on the high pressure side of the membrane are known, as are the various model parameters. The term l/D_i in Equation (11) is the film mass transfer coefficient, which may be obtained using established correlations for flow inside tubes (see Equation (15) below). Since the flow parameters, F_i and G_i, depend on the value of J_v, Equation (14) has to be solved by iteration. Once J_v has been found, all the remaining quantities may be found from the other equations (Equations (10) to (14)).

The mass transfer correlation for turbulent flow in tubes, found in the literature [10], is (see list of symbols for definitions of Sh, Re and Sc) :

$$Sh = 0,0096 Re^{0.913} Sc^{0.346} \tag{15}$$

Temperature correction

The hydraulic permeability, P_l, was taken to be inversely proportional to the viscosity of water (η_w).

i.e. $$P_l = k_l / \eta_w \tag{16}$$

where k_l is a permeability factor, which is taken to be constant for a particular membrane.

The diffusivities of the components in water were corrected for temperature according to the correlation recommended by Reid et al. [11] :

$$D_{i(T)} = \frac{D_{i\,(25)} \cdot (T+273)}{334\,000 \cdot \eta_w} \tag{17}$$

The solute permeability parameters for the membrane were assumed to be related to temperature by Equation (18), following data from Sourirajan and Matsuura [7] for cellulose acetate membranes. Values other than 0,005 for the temperature coefficient were tried, but gave no better representation of the experimental data.

$$P_{i\,(T)} = P_{i\,(25)} \exp[0,005(T-25)] \tag{18}$$

Parameter regression

To obtain the required parameters from the experimental data, the following input data was required :

(i) physical constants relating to each component (molecular mass, osmotic factor, diffusion coefficient);
(ii) transport parameters relating to the membrane (hydraulic permeability) and the membrane-solute interactions (reflection coefficients and overall solute permeabilities for each component);
(iii) membrane and module type and geometry;
(iv) the module bank arrangement;
(v) experimental data for each stream in each experimental data set (temperature, pressure, flow rate, concentration of each component).

After modifying some of these parameters by regression, the resulting parameter set was used to predict permeate composition and flow rate for other operating conditions.

Values of the transport parameters were obtained initially for sodium chloride alone using the results of a pilot-plant experiment on a sodium chloride solution. An initial guess for the specific hydraulic permeability was obtained from the pure water flux. These transport parameters were then used in runs on the data from experiments on the regeneration effluent. In these runs, regression was used to determine the transport parameters for the organic component and the hydraulic permeability. Since the osmotic coefficient and diffusivity of the organic matter were not known, these were also estimated by regression.

RESULTS

Experimental data obtained on laboratory scale using the MPT-31 membrane at 35 °C and for a range of pressures (2.0 to 3.5 MPa) were used to predict the flux and solute retention for a wider range of pressures (0.05 to 5.0 MPa). The parameters which were obtained are listed in Table 1 and the flux and retention coefficients are plotted against pressure in Figure 2 (the subscripts s and x denotes sodium chloride and the organic anion, respectively).

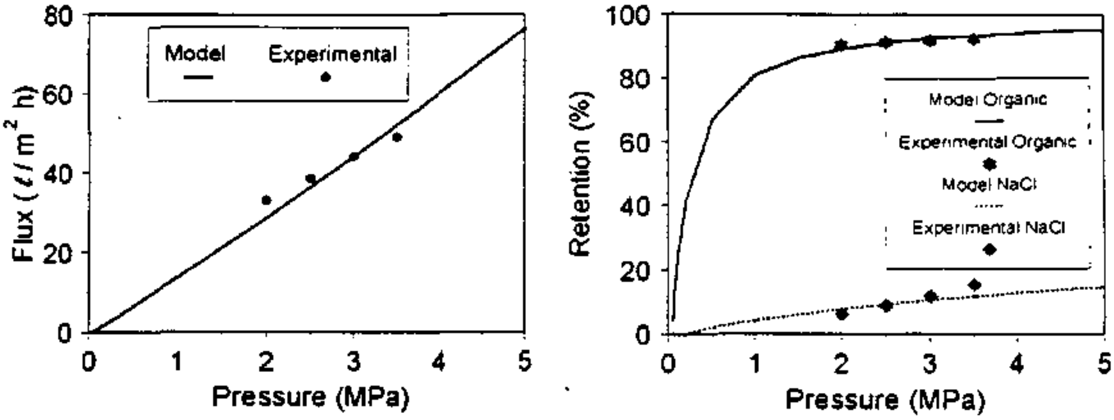

Figure 2 : Effect of pressure on flux and percentage retention from results of laboratory experiment on MPT-31 membranes.
Feed conditions : u = 1,62 m/s, T = 35 °C, c_s = 81,2 g/ℓ, c_x = 3,20 g/ℓ as C.

Table 1 : Parameters obtained from regression on results of laboratory-scale experiment on MPT-31 membranes at 35 °C (c_s = 81,2 g/ℓ, c_x = 3,2 g/ℓ as C)

Permeability factor	k_f = 4,089 x 10^{-15}		
Osmotic factor	ϕ_s = 4 639	ϕ_x^* = 12 499	ϕ_x'' = 18 340
Diffusion coefficient	D_s = 1,545 x 10^{-9}	D_x = 3,4 x 10^{-9}	
Reflection coefficient	σ_s = 0,445	σ_x = 1	
Overall solute permeability	P_s = 3,25 x 10^{-5} exp[0,005(T-25)]	P_x = 8,27 x 10^{-7} exp[0,005(T-25)]	

A similar regression was carried out on the results of four successive pilot-scale experiments using MPT-30 membranes. These were batch concentration experiments at various temperatures, pressures, flow rates and feed compositions. It was assumed that the condition of the membrane did not change during these experiments. The parameters obtained from regression on the whole data set are given in Table 2. The fluxes and permeate concentrations are plotted against water recovery for each batch concentration experiment in Figure 3.

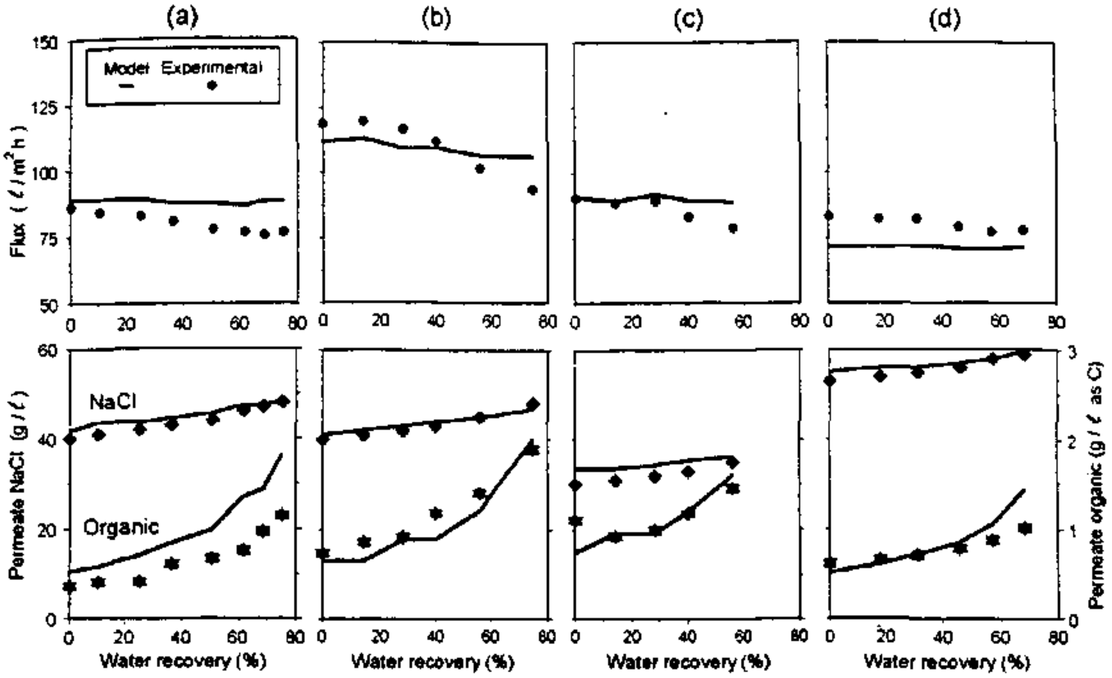

Figure 3 : Permeate flux and concentration of sodium chloride and organic matter in the permeate verses percentage water recovery for each batch concentration experiment on the pilot plant.

Feed conditions : **(a) p = 3,0 MPa, u = 1,62 m/s, T = 45 °C, c_s = 45,3 g/ℓ, c_x = 4,15 g/ℓ as C;**
(b) p = 3,0 MPa, u = 1,78 m/s, T = 45 °C, c_s = 45,2 g/ℓ, c_x = 6,10 g/ℓ as C;
(c) p = 3,0 MPa, u = 1,33 m/s, T = 60 °C, c_s = 35,6 g/ℓ, c_x = 5,60 g/ℓ as C;
(d) p = 2,5 MPa, u = 1,78 m/s, T = 45 °C, c_s = 58,8 g/ℓ, c_x = 3,64 g/ℓ as C;

Discussion

Figures 2 and 3 demonstrate that the model was successful in representing the experimental data over a fairly wide range of operating conditions, however there are several features which indicate possible improvements. In Figure 2, the model was unable to match the slope of the experimental flux verses pressure curve, although regression ensured that the average was correct. A similar discrepancy is evident in Figure 3, where the flux decline in each batch concentration experiment was not predicted by the model. A possible explanation of both of these discrepancies is the formation of a dynamic layer by the organic material at the membrane surface, which increases the hydraulic resistance to permeation.

As mentioned previously, the fact that the model seemed to require different osmotic factors on the retentate and permeate sides of the membrane indicates that the molecular weight distribution was different in the two streams, i.e. the permeate contained a lower molecular weight fraction. The model generally had greater difficulty in representing the behaviour of the organic matter. Hence, a more detailed representation of the organic material may be required, although the drawbacks associated with introducing further parameters to be determined by regression would have to be considered.

FULL-SCALE PLANT DESIGN

Once model parameters have been obtained by regression on plant data, the computer model can be used to simulate various plants by allowing for various module arrangements. This was carried out for the case under consideration here. The results of the following mass balance calculations for a full-scale nanofiltration plant to operate at the Hulett Refinery were used as a basis for these simulations.

Mass balances

Mass balances on water, sodium chloride and total organic carbon were carried out on the regeneration system for a single regeneration under the existing conditions at the resin plant (see Figure 4) and for the case where a full-scale nanofiltration plant is included to treat the salt-rich fraction of the regeneration effluent (see Figure 5). The mass balances were calculated using the amounts of water, sodium chloride and total organic carbon (TOC) in tonnes and expressing the concentrations as the ratio of solute mass to solution mass in percent [4].

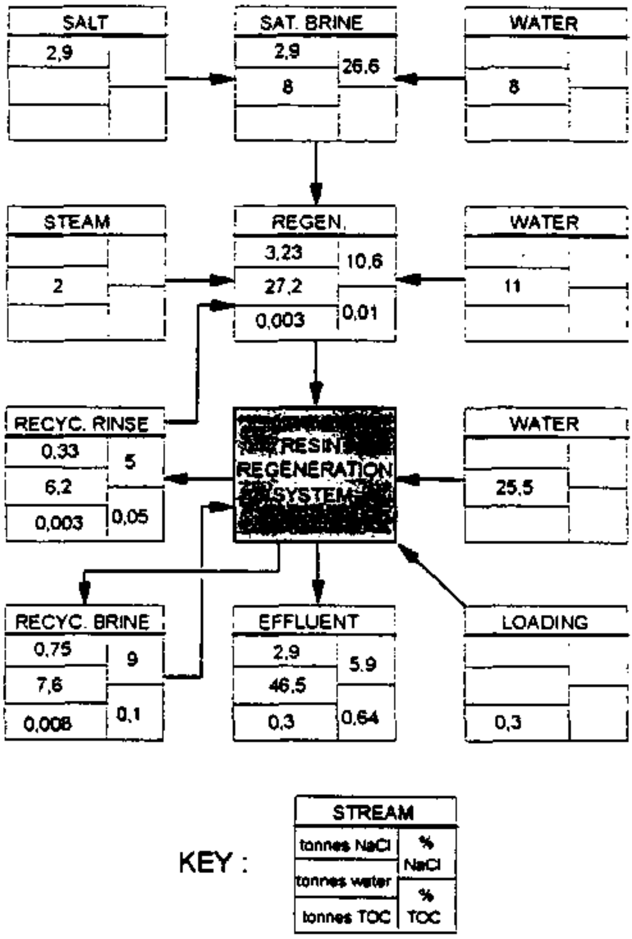

Figure 4 : Mass balance for one regeneration under existing conditions

The following plant data and assumptions were used to calculate the mass balance under existing conditions (see Figure 4) :

(i) 2,9 tonnes of fresh sodium chloride are used per regeneration;
(ii) 8 tonnes of water are used to make up the saturated brine (26,6 % NaCl);
(iii) 11 tonnes of water are used to make up the regenerant;
(iv) 2 tonnes of water are added as steam to the regenerant make-up for heating purposes;
(v) 6.2 tonnes of rinse water, containing 5 % NaCl and 0,05 % TOC, are recycled to regenerant make up;
(vi) 7,6 tonnes of brine, containing 9 % NaCl and 0.1 % TOC, are recycled as initial regenerant;
(vii) 25,5 tonnes of fresh water are used for brine displacement and rinsing; and
(viii) the pair of resin columns is loaded with 0,3 tonnes as carbon of total organic carbon during the service cycle.

For the case where a membrane plant is used for brine recovery, the following assumptions were made in addition to assumptions (iv) to (viii) above, while assumptions (i) to (iii) fall away :

(i) fresh water is used to make up the saturated brine;

(ii) the membrane plant operates on 20 tonnes of the salt rich fraction of the regeneration effluent, which contains 8 % NaCl and 0,4 % TOC; and

(iii) the plant operates at 71 % water recovery (calculated by water balance), where the overall retention is 5 % for NaCl and 85 % for TOC.

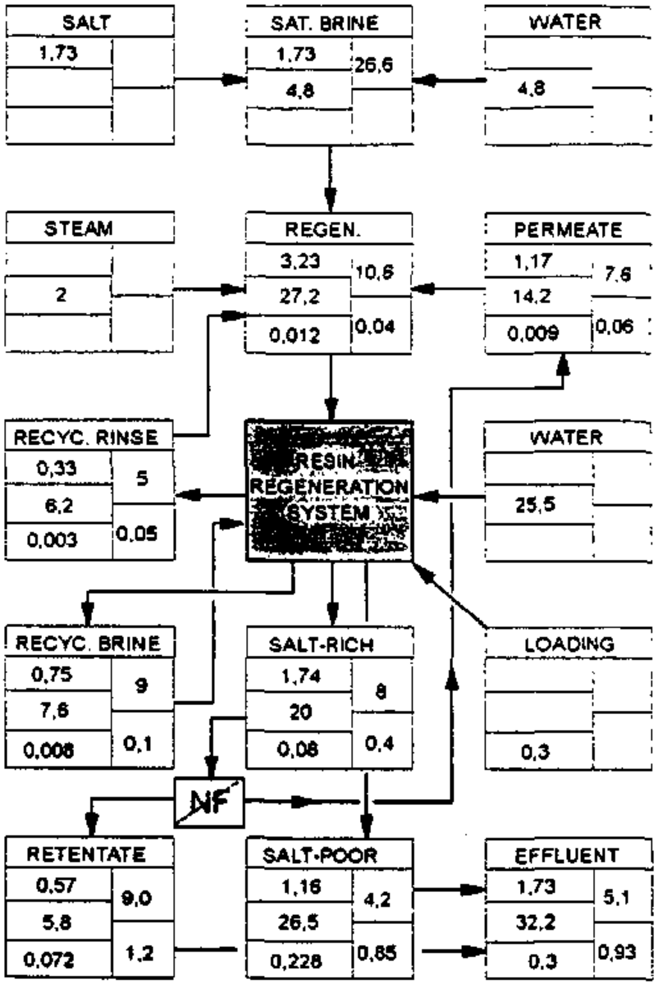

Figure 5 : Mass balance for one regeneration with nanofiltration plant operating at 71 % water recovery on salt-rich fraction (see Figure 4 for key)

This mass balance is shown in Figure 5. The amount of permeate that could be produced was limited by the water balance. It was found that only 4,8 tonnes of water would be required to make up the saturated brine, thus reducing the final effluent from 46,5 tonnes to 32,3 tonnes of water (31 % reduction). The fresh salt consumption would be decreased from 2,9 tonnes to 1,73 tonnes (40 % reduction). The average concentration of total organic carbon in the regenerant would be increased by a factor of four to 0,04 % or 0,4 g/ℓ.

Determination of required membrane area and module arrangement

The full-scale plant would be fitted with nanofiltration modules containing 18 tubes of length 3,6 m each, i.e. a total membrane area of 2,59 m^2 per module.

To determine the required number of modules the following assumptions were made :

(i) the plant must treat 20 m^3 of feed per regeneration with 4 regenerations per day, i.e. 80 m^3 of feed per day;

(ii) the plant availability is 75 %, i.e. the plant operates for 18 h per day;

(iii) the flow through each tube at the front of the first bank should be about $2,2 \times 10^{-4}$ m^3/s (or 1,7 m/s) as recommended by the membrane manufacturers;

(iv) an operating temperature of 70 °C and an inlet gauge pressure of 3 MPa is to be used;

(v) a final water recovery of 71 % is required; and

(vi) the concentrations of sodium chloride and total organic carbon in the feed is 80 g/ℓ and 4 g/ℓ respectively.

From assumptions (i) to (iii) it is clear that the first bank must contain 6 modules in parallel.

To estimate the total number of modules required the computer model was used, with the parameters obtained from regression on the pilot-plant results. It was found that using one bank containing 6 modules in parallel with 2 modules in series (i.e. 12 modules in total) lead to the required water recovery. However, with this arrangement the exit linear flow velocity was only 0,45 m/s. To increase the exit linear flow velocity, a *tapered* system was considered. The first bank was reduced to 6 modules in parallel and the remaining 6 modules were placed in a second bank containing 3 modules in parallel with 2 modules in series (see Figure 6). This arrangement gave an exit linear flow velocity of 0,93 m/s. The results of these simulations are given in Table 3.

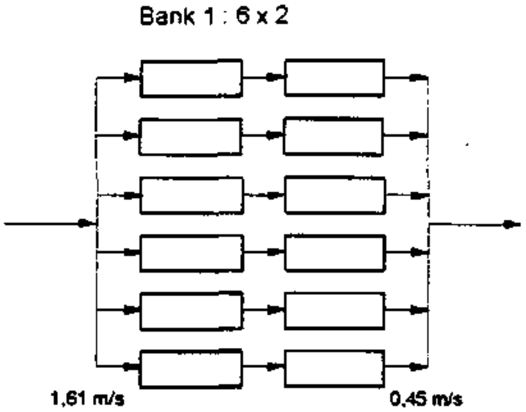

(a) Arrangement 1

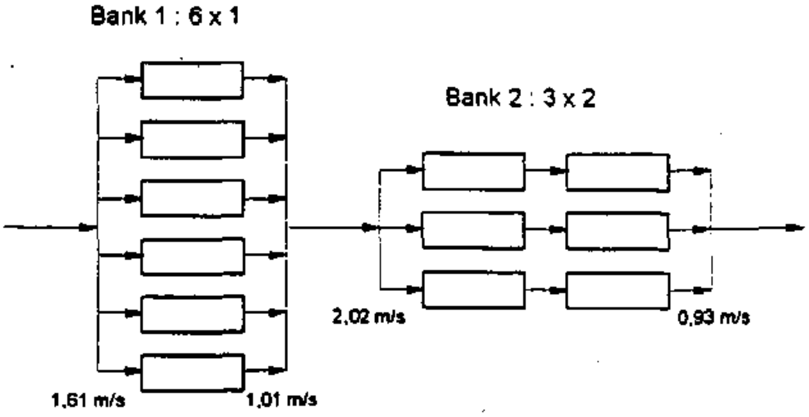

(b) Arrangement 2

Figure 6 : Alternative module arrangements for full-scale nanofiltration plant using 12 modules, each 3,6 m long (a) 6 x 2, (b) 6 x 1 and 3 x 2

Discussion

The results of the simulations given in Table 3 show that the performance of the system under the two module arrangements would be very similar. In terms of predicted performance alone Arrangement 1 appears to be preferable in all aspects except for retention of TOC. However the linear flow rate at the outlet for this arrangement is rather low, hence membrane fouling may be promoted due to the development of a gel-polarised layer. The present version of the computer model does not account for gel-polarisation, hence any loss of performance due to gel-polarisation would not have been observed in this simulation.

Table 3 : Comparison of two module arrangements for a full-scale plant design

Feed conditions : $p = 3$ MPa, $u = 1{,}61$ m/s, $T = 70$ °C, $c_s = 80$ g/ℓ, $c_x = 4$ g/ℓ as C

Plant arrangement	Arrangement 1	Arrangement 2	
Bank number	Bank 1	Bank 1	Bank 2
Module arrangement (parallel x series)	6 x 2	6 x 1	3 x 2
Outlet water recovery (%)	72.0	37.2	71.1
Outlet linear flow rate (m/s)	0.45	1.01	0.93
Outlet pressure (MPa)	2.87	2.91	2.70
Total permeate flow (m^3/s)	8.86×10^{-4}	8.74×10^{-4}	
Average permeate flux (m/s)	2.86×10^{-5}	2.82×10^{-5}	
Concentration of NaCl in permeate (g/ℓ)	76.2	75.7	
Concentration of TOC in permeate (g/ℓ)	0.673	0.618	
Concentration of NaCl in retentate (g/ℓ)	89.8	90.5	
Concentration of TOC in retentate (g/ℓ)	12.56	12.31	
NaCl retention (%)	4.77	5.34	
TOC retention (%)	83.2	84.5	

CONCLUSIONS

Arrangement 2 in Figure 6 appears to be a satisfactory configuration for the design of a full-scale plant to produce the required volume of permeate. The plant would have 12 full-scale modules (3.6 m in length), hence the total membrane area would be 31 m^2. These modules would be arranged in a tapered configuration, with 6 modules in parallel in the first bank and 3 modules in parallel with two in series in the second bank. The predicted average permeate flux is 2.82×10^{-5} m/s or 102 ℓ/m^2h at a temperature of 70 °C, a gauge pressure of 3 MPa and an inlet linear flow rate of 1,61 m/s.

The flow velocities of the streams leaving the module banks of arrangement 2 (1,01 and 0,93 m/s) are somewhat lower than those that were encountered during the pilot-plant investigation (1,3 to 1,8 m/s), which would imply an increased tendency to gel-polarization and fouling in those areas of the plant. This was not thought to be significant, since fouling did not present a serious problem on the pilot plant.

Whereas it is difficult to design a full-scale plant from raw experimental data such as that used here, representation of the data by a model enables a closer design. Further work will involve attempts to improve the model by refining the correlations used and allowing for conditions under which gel polarisation occurs. A preliminary costing of the full-scale plant carried out by Tongaat-Hulett Sugar Ltd. indicated that the process would have a pay-back time of around two years [3].

The computer model runs under Microsoft Windows and is available via the Internet from an FTP (file transfer protocol) site known as EMILY (Electronic Membrane Information Library). The access procedure is : **ftp aqua.ccwr.ac.za** then look in the **ftp/pub/emily** directory. Members of the membrane community are encouraged to use and modify the program. Contributions can be left in the **contrib** directory. Queries can be sent to Quentin Hurt at e-mail address : **hurtq@aqua.ccwr.ac.za**.

ACKNOWLEDGEMENTS

The authors would like to thank the staff at Tongaat-Hulett Sugar Ltd. and Hulett Refineries Ltd. for carrying out the pilot-plant work. The research was also carried out under funding from the South African Water Research Commission for Project No. 308 entitled : *Research into the Recovery of Water and Chemicals from Ion Exchange Regeneration Effluents* and Project No. 325 entitled : *Research on the Modelling of Tubular Reverse Osmosis Systems*.

List of Symbols

c : concentration of solute in solution, mol/m^3
D : diffusion coefficient of solute in water, m^2/s
d : membrane tube diameter, m
F : a dimensionless flow parameter, defined in Equation (10), -
G : a dimensionless flow parameter, defined in Equation (11), -
k : turbulent diffusion mass transfer coefficient on high pressure side of membrane, m/s
k_l : a permeability factor, defined in Equation (16), m
J_s : molar solute flux through membrane, mol/m^{2}s
J_v : volume flux through membrane, m/s
l : thickness of boundary layer solution adjacent to membrane surface, m
P : overall solute permeability, m/s
$\bar{P}$: local solute permeability, m^2/s
P_l : hydraulic permeability, m^2.s/kg
$\bar{P}_l$: specific hydraulic permeability, m^3 s/kg
p : operating (gauge) pressure, Pa (or kg/m s^2)
Δp : trans-membrane pressure difference, Pa
R_{real} : real retention coefficient, -
R_{obs} : observed retention coefficient, -
Re : Reynolds number, $Re = \dfrac{\rho d u}{\eta}$
T : operating temperature, °C
Sc : Schmidt number, $Sc = \dfrac{\eta}{\rho D}$
Sh : Sherwood number, $Sh = \dfrac{k d}{D}$
u : bulk linear flow velocity, m/s
x : distance into the boundary layer (normal to the membrane surface), m

Greek letters

η : viscosity. kg/m s
π : osmotic pressure. Pa
$\Delta\pi$: trans-membrane osmotic pressure difference. Pa
ϕ : osmotic factor. Pa m^3/mol
ρ : *density of solution. kg/m^3*
σ : reflection coefficient. -

Superscripts

$'$: feed phase
$''$: permeate phase
$*$: *membrane/feed interface*

Subscripts

i : component i
obs : observed (retention coefficient)
: salt (NaCl)
v : volume
x : organic anion
w : water

REFERENCES

1 S. Wadley, and C.A. Buckley. Recovery of sugar refinery ion exchange regeneration effluent by nanofiltration. Proceedings of the Water Institute of Southern Africa 2nd Biennial Conference. 13 to 16 May, World Trade Centre. Kempton Park. South Africa. 1991. pp. 623-634.

2 D.M. Meadows, S. Wadley, and C.A. Buckley.. Evaluation of nanofiltration for the recovery of brine from sugar liquor decolourising resin regeneration waste. *Water Science and Technology*, **25** (1992), *pp. 339-350.*

3 D.M. Meadows, and S. Wadley, The recovery of brine from resin regeneration effluent by nanofiltration. *Proceedings of The South African Sugar Technologists' Association*. 1992. pp. 159-165.

4 S. Wadley, Recovery of brine from sugar decolourising resin regeneration effluent by nanofiltration. MScEng Dissertation, Department of Chemical Engineering. University of Natal. Durban. South Africa. 1994.

5 K.S. Spiegler, and O. Kedem, Thermodynamics of hyperfiltration (reverse osmosis) : Criteria for efficient membranes, *Desalination*, **1** (1966), pp. 311-326.

6 P. Schirg, and F. Widmer, Characterisation of nanofiltration membranes for the separation of aqueous dye-salt solutions, *Desalination*, **89** (1992), pp. 89-107.

7 S. Sourirajan, and T. Matsuura, *Reverse osmosis/ultrafiltration process principles*. National Research Council Canada Publications, Ottawa, 1985, p. 104.

8 M. Perry, and C. Linder, Intermediate reverse osmosis ultrafiltration (RO UF) membranes for concentration and desalting of low molecular weight organic solutes. *Desalination*, 71(1989), pp. 233-245.

9 V. Gekas, Terminology for pressure-driven membrane operations, *Desalination*. 68 (1988), pp. 77-92.

10 G. Belfort, Synthetic membrane processes, Academic Press, Orlando. 1984.

11 R.C. Reid, J.M. Prausnitz, and B.E. Poling, The properties of gases and liquids, McGraw-Hill, Fourth edition, New York, 1988, p. 62.

WATER RESEARCH COMMISSION PROJECT NO. 325

RESEARCH ON THE MODELLING OF TUBULAR REVERSE OSMOSIS SYSTEMS

Appendix 7

Mass Transfer Enhancement in TRO Systems

Q E Hurt

Pollution Research Group
Department of Chemical Engineering
University of Natal
Durban

February 1995

1 Mass transfer enhancement for tubular reverse osmosis systems

1.1 Introduction

RO applications have been limited by the costs involved. To overcome the osmotic pressure differences and allow for a reasonable driving force, high feed pressures are required. The retained species tend to accumulate adjacent to the membrane, forming a second barrier to permeation through the membrane. Where the RO configuration has allowed, high feed flow rates are used to aid fluid mixing adjacent to the membrane to restrict the build-up of the retained species. Further, the ratio of feed to permeate collected is often low, requiring the recycle of the treated fluid or increased membrane area to increase recovery.

All these factors lead to high operating costs. Reluctance to introduce RO equipment has usually been associated with the high capital cost, the limited operating life of the RO membrane, the small operating window dictated by the membrane materials and the membranes' susceptibility to damage and degradation.

1.1.1 Performance enhancement

The key to improving RO economics lies in either decreasing the operating cost or the capital cost of the systems. One route to reducing the operating cost is to use a lower feed flow rate without sacrificing the membrane product flux. This route is evaluated for the purposes of this work as a possible alternative to traditional RO operating methodologies.

1.1.2 Aims of the investigation

The aim of the investigation was to compare the effectiveness of strategies for mass transfer enhancement for tubular reverse osmosis. Three strategies were proposed to alter the hydrodynamic nature of the feed flow: (i) pulsed flow; (ii) baffled flow; and (iii) pulsed-baffled flow. The intention was to propose or compare mechanisms by which RO systems might be modified without altering the nature of the membrane. By these means it was hoped that the economics of RO might be improved.

In keeping with these aims, all the experiments were conducted with low linear feed flows in an attempt to obtain superior RO performance in the laminar and transition regimes that would be associated with low running cost and consequently low pumping costs.

The work of a number of authors in the field of mass and heat transfer enhancement (most notably Finnigan et al. (1989/90); Mackley et al. (1990); Pitera et al. (1973) and Thomas et al. (1968)) was evaluated to assess the effectiveness of various equipment configurations. As a result, novel pulsing pump and baffle designs were proposed. The pump design is simple and does not significantly increase the energy requirements of the system. The effectiveness of a diagonal baffle design, conceived to exploit the hydrodynamic features that occur within the RO tube (both steady and pulsing flow) without increasing the energy requirements to the extent that conventional baffles do, was also evaluated.

All comparisons were made on the basis of mass transfer coefficients calculated for each of the flow conditions on the basis of the experimental results obtained. The mass transfer coefficient describes RO membrane performance by condensing the dependent variables into a single value, the value of which is an indication of the effectiveness of the convection promotion of each of the strategies employed. Although not initially central to the work, the effectiveness of this strategy itself will also be evaluated.

1.2 Experimental equipment

The experimental equipment used a recirculating feed solution in an existing reverse osmosis test unit. The configuration of the equipment is shown in Fig. 1.

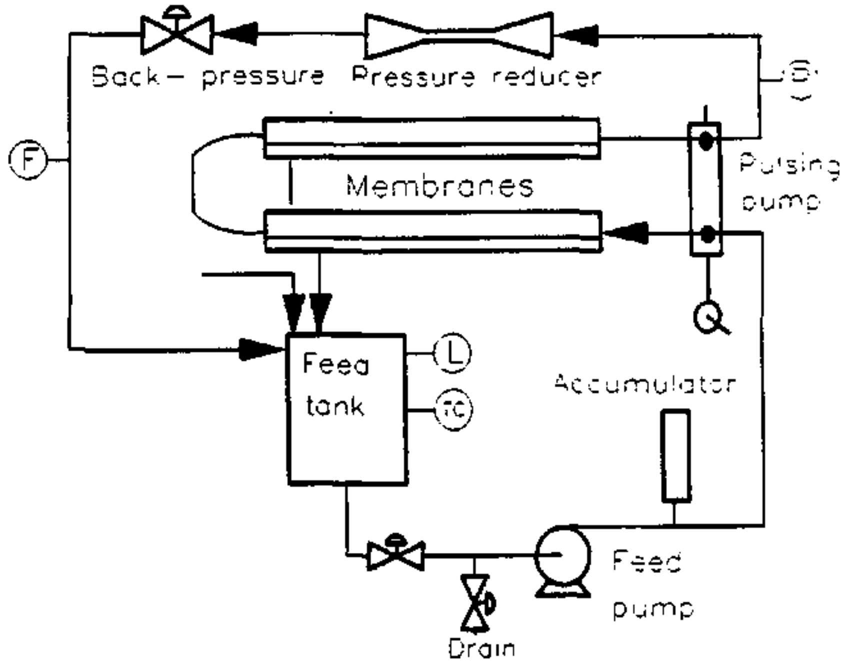

Figure 1 : Diagram of the experimental equipment used in the examination of mass transfer enhancement for tubular RO systems, depicting RO tubes bridged by the pulsing pump

Central to the design of the experimental apparatus was the novel pulsing pump that bridged the set of membranes. The membranes were connected in series. The pump was driven by an independent, low-power source. The power requirements of the pump were only sufficient to act against the pressure drop through the membranes which in turn was kept low by restricting the flow through the membranes to the laminar and transition regimes.

Two baffle designs were tested simultaneously in the tubular membranes. The feed solutions and other experimental conditions could be considered virtually identical for all comparative baffle experiments.

For ease of comparison, the tubes were referred to as tubes A and B. Minor differences in the performance of the tubes were investigated and factored into the results of the experiments.

1.3 Results

1.3.1 The significance of the membrane parameters

An error analysis was conducted to establish the validity of the results obtained in the study. The values of the pure water permeability parameters, A differed for the two tubes used in the experiments but remained practically constant (a maximum difference of 2 % was calculated) for the open and baffled tube experiments. Tube A was calculated to have a higher pure water permeability than tube B. This finding corresponded with the experimental results which showed higher permeate flows for tube A.

The values of the solute transport parameters, $\left(\frac{D_{AM}}{K\delta}\right)$, showed that tube A should have had a higher solute passage than tube B. This corresponded with the experimental findings. The values of this parameter increased (for both tubes) after the insertion of the baffles into the tubes, indicating that the insertion may have caused some damage to the membranes. Future work done in this field might well benefit from using the modelling technique alongside the experimental work to determine such potential damage immediately.

1.3.2 The significance of the mass transfer coefficient

The mass transfer coefficient $\mathfrak{k}$ was calculated for each feed flow condition. Since the value of this coefficient is dependant only on the hydrodynamic conditions in the tube, it facilitated comparison of the effectiveness of each of the techniques used to alter the flow patterns within the tubes. A higher $\mathfrak{k}$ value implied better fluid mixing within the tube and hence reduced concentration polarisation. This led to enhanced TRO performance in terms of decreased salt passages and increased permeate flows.

The degree to which the salt passages decreased and the permeate flows increased with increased mass transfer coefficients differed according to magnitude of A and $\left(\frac{D_{AM}}{K\delta}\right)$ for each of the tubes. The mass transfer coefficient was shown to be relatively insensitive to permeate flow. Thus, an error analysis conducted on the mass transfer coefficient (using its variation with salt passage as a basis) revealed that the magnitude of the error in $\mathfrak{k}$ varied according to the nature of the feed flow : the maximum error range (for a statistical 90 % significance) for the steady flow experiments (baffled and open tube) was 36 to 34 % while the error range for the pulsed flow experiments (baffled and open tube) was 55 to 125 %.

The error analysis implied that the magnitude of the mass transfer coefficient became less significant as its value increased, leading to progressively smaller decreases in salt passage for larger increases in $\mathcal{K}$ at its higher values. In other words, the improvement in the feed mixing for the water-sodium nitrate system caused by pulsing the feed flow became less significant as the intensity of the mixing increased. To minimise this error, the concentration polarisation at the tube wall would need to be greater than that experienced for this system. The feed solution should have a higher viscosity, the solute concentration should be higher, the feed flow Reynolds numbers should be lower and the system pressures should be greater than those investigated.

The results of the error analysis posed a problem for the explanation of the findings. Since the aim of the work was to compare the effectiveness of different techniques for enhancing mass transfer in TRO systems, it was necessary that the results associated with a particular technique indicate a categorical improvement compared to another (i.e. pulsing the feed flow in an open tube should improve the mass transfer in the tube, compared to that for open tube, steady flow, to the extent that the possible values of the mass transfer coefficients for the pulsed flow are consistently higher than the steady flow values for the same mean feed flow Reynolds numbers). The magnitude of the error in $\mathcal{K}$ dictates the magnitude of the range of the possible $\mathcal{K}$ values.

In most instances comparisons of relative performance for variations in the application of a technique (e.g. comparing the performance of one pulsing amplitude with another for the same feed flow in an open tube) became impossible if the implications of the error analysis had been strictly applied. In such instances the conclusions drawn were based on broad trends but should be considered in the light of the error analysis argument.

1.3.3 Open tube steady flow tubular reverse osmosis

The results of the open tube, steady flow TRO experiments were used as a set of mass transfer coefficients against which those for the other enhancement techniques could be compared. The values of $\mathcal{K}$ were used to predict salt passages and the permeate flows and good agreement with the experimental values was shown. The value of $\mathcal{K}$ increased exponentially with flow rate in the experimental range of feed flows. The values of $\mathcal{K}$ in the two tubes for the same feed flows showed little disagreement indicating similar hydrodynamic conditions in the tubes. The results indicated that $\mathcal{K}$ provided a convenient measurement of TRO performance since the difference in values of salt passage and permeate flow for each of the tubes for the same feed conditions (as a result of their different membrane parameters, A and $\left(\frac{D_{AM}}{K\delta}\right)$) became inconsequential.

1.3.4 Pulsed flow open tubular reverse osmosis

Pulsing the feed to a TRO membrane led to gains in the mass transfer coefficient of up to 800 %. Increasing both the frequency and amplitude of the pulse led to increases in the mass transfer coefficient.

A theory (based on an exponential relationship of mass transfer coefficient with the absolute value of the linear feed flow) under-predicted the gains in mass transfer coefficient for pulsed flow. This was attributed to the fact that the theory neglects the effects of natural convection and the mixing effects of eddies generated by the rapid acceleration at the beginning and ends of each of the pulse cycles.

Apparent differences in the hydrodynamic conditions in tubes A and B (on the basis of mass transfer coefficient) for the same feed conditions could be ascribed to experimental error. As stated previously, it would be useful during any future work of this nature to use the model concurrently with the experiments to update the fundamental membrane coefficients and parameters.

1.3.5 Steady flow in baffled tubular reverse osmosis

Orifice (doughnut) baffle performance was tested against the performance of angled elliptical baffles designed specifically for these experiments. The gains in mass transfer coefficient for the elliptical baffles are higher than those for the doughnut baffles (but this may be due to experimental error). The gains are highest at the lowest flow rates.

1.3.6 Pulsed flow in baffled tubular reverse osmosis

The elliptical baffles appear to perform better than the doughnut baffles for the same feed conditions but this may be a result of experimental error. Increasing the frequency of the pulse increased the mass transfer coefficients but his was not necessarily so for increasing amplitude. This might correspond with the findings of Mackley et al. (1990) who stated that there would be no improvement for amplitudes greater than half the baffle spacing. Further experiments for amplitudes in this region (with systems with lower error characteristics) would be required to confirm this finding.

1.4 Conclusions

On the basis of the gains in mass transfer coefficient over open tube, steady flow TRO, the effectiveness of the enhancement techniques may be rated as follows : pulsed, baffled TRO was most effective, followed by pulsed flow, open TRO and then steady flow baffled TRO. All techniques were effective but the gains for both pulsed flow techniques were markedly higher than for the steady baffled flow experiments.

Although significant gains were realised in terms of improving the mass transfer coefficient, it was found that the effect on the overall flux and salt retention was relativly small. This is because the principal transport resistance in RO occurs in the membrane rather than in the liquid boundary layer. Greater process benefits should be obtained in ultrafiltration and microfiltration, where concentration polarisation plays a greater role.

WATER RESEARCH COMMISSION PROJECT NO. 325

RESEARCH ON THE MODELLING OF TUBULAR REVERSE OSMOSIS SYSTEMS

Appendix 8

Roughing Demineralisation in Ultrapure Water Production at Power Stations

CJ Brouckaert

Pollution Research Group
Department of Chemical Engineering
University of Natal
Durban

February 1995

1 Introduction

The Eskom Technology, Research and Investigations division (TRI) has been considering means for reducing the chemical addition requirement in the production of ultrapure water for power station boilers. Their motivation is two-fold : to reduce the degree of salination of the environment by effluents, and to protect their operation against the rising cost of chemicals, particularly sodium hydroxide. The use of RO as a pre-treatment for ion-exchange has been used successfully in a number of cases (for example see McAfee et al., (1990)) ; the purpose of this investigation has been to adapt the process to local conditions.

Mr C. Chibi of TRI has been the principal investigator : support for him from this project has taken the form of the loan of an RO test apparatus from the University of Natal, and the interpretation of the experimental results in terms of the RO model, which is the subject of this report. A further minor service has been determination of the Silt Density Index (SDI) determinations for the feed water used in the tests.

2 Experimental Work

The tests were carried out at the Kendal Power Station by Chibi, and have been described in an internal TRI report (Chibi and Kruger, 1993). A single FilmTec SW30-2514 spiral-wound module was used, operating on water pre-treated by the existing flocculation/ clarification/ filtration process which precedes the ion-exchange at Kendal.

A single set of analyses of feed and permeate was available to characterise the chemical compositions of these streams, the remainder of the data consisted of feed temperatures, pressures, flow rates and conductivities together with permeate flow rates and conductivities covering 8 hours' operation of the test apparatus.

2.1 FilmTec SW30-2514 Module Dimensions

This module consists of 4 leaves of flat sheet membranes, separated by polypropylene mesh spacers and wound into the typical spiral configuration. Total membrane area is 0,56 m^2. The gap between the membranes and the mesh spacing were measured with a travelling microscope at 0,00038 m and 0,002 m respectively.
The width of the membrane is 0,234 m which implies a length of 1,15 m for the coiled membrane, and a flow cross-sectional area of $4{,}38 \times 10^{-4}$ m^2.

2.2 Chemical Analyses

Determinand		Feed	Permeate
Conductivity @ 25 °C	(mS/m)	105	0,74
pH @ 25 °C		8,6	8,3
Total alkalinity	(mg/ℓ as $CaCO_3$)	30,0	0,032
Sodium	(mg/ℓ)	3,0	0,045
Potassium	(mg/ℓ)	1,04	< 0,001
Calcium	(mg/ℓ)	12,22	< 0,001
Magnesium	(mg/ℓ)	4,67	< 0,001
Chloride	(mg/ℓ)	13,1	0,035
Sulphate	(mg/ℓ)	5,8	0,05
Fluoride	(mg/ℓ)	0.11	< 0,001

2.3 RO Performance Data

	FEED				PERMEATE	
Operating Time (h)	Pressure (bar)	Temperature (°C)	Flow rate (ℓ/min)	Conductivity (mS/m)	Flow rate (ℓ/min)	Conductivity (mS/m)
0,00	36,0	15,5	1200	110,8	0,317	0,604
0,26	36,0	21,3	1200	134,0	0,389	1,200
0,55	36,0	23,7	1200	159,0	0,428	0,982
1,03	35,6	26,5	1200	177,0	0,438	1,260
1,50	36,0	37,0	1200	327,0	0,570	1,730
2,12	36,0	14,5	1200	116,1	0,317	1,170
2,50	36,0	23,5	1200	151,0	0,211	1,260
2,75	36,0	27,5	1200	150,0	0,398	1,210
3,03	36,0	21,5	1200	139,0	0,364	1,100
4,05	36,0	20,0	1200	124,1	0,372	0,916
4,25	36,0	20,0	1200	123,8	0,356	0,917
5,00	36,0	20,5	1200	124,5	0,356	0,902
5,77	36,0	21,0	1200	127,0	0,364	0,911
6,70	36,0	20,0	1200	123,6	0,349	0,910
7,37	36,0	19,3	1200	120,1	0,342	0,937
7,87	36,0	19,2	1200	118,9	0,342	0,919
8,12	36,0	19,3	1200	119,5	0,342	0,949

3 Modelling Procedures

3.1 Data Preparation

The same standard approach was adopted as that used for other applications undertaking as part of this project. The MINTEQA2 chemical speciation program (Allison, Brown and Novo-Gradac, 1990) was used to calculate the distribution of ions in the feed from its chemical analysis. The osmotic pressure of this feed solution was then calculated using the correlation developed during this project (see Section 2.2 of the final report). For other solutions occurring in the RO apparatus, the osmotic pressure and conductivity were assumed to be proportional to the total dissolved solids (TDS) ; the proportionality factors were calculated from the values of TDS, osmotic pressure and conductivity determined for the feed. The resulting relationships were:

$$Conductivity(mS/m) = 1821.3 \times TDS(g/l)$$

$$Osmotic Pressure(kPa) = 53.3 \times TDS(g/l)$$

The diffusivity of the solute is the final physical parameter required by the model. As the solution contained a number of different ionic solutes which are treated as one, an average diffusivity was required. As shown in Section 2.5.3 of the final report, the appropriate averaging formula is

$$\mathcal{D}_{av} = \frac{RT}{F^2} \cdot \frac{\Sigma m_i}{\Sigma \frac{m_i |z_i|}{\lambda_i}}$$

where

m_i is the molar concentration of the ith ion,

z_i is its ionic charge,

λ_i is its ionic conductance (m^2/ohm.g-equiv)

R is the universal gas constant (8,314 J/mol.K),

T is the absolute temperature (K), and

F is Faraday's constant (96 500 Coulombs/g-equiv).

Ionic conductances were obtained from Reid, Prausnitz and Poling (1988). Using the ionic concentrations tabulated in appendix C, the average diffusivity was calculated to be $1,5 \times 10^{-9}$ m^2/s.

3.2 Parameter Regression

Since the set of operating data supplied by TRI was somewhat limited, the scope of the modelling that could be undertaken was correspondingly limited. The data covered 8 hours of operation at a feed pressure of 3 600 kPa and a feed flow rate of 0,33 ℓ/s. Only the temperature and the feed conductivity showed any significant variation. Under these circumstances it was only possible to infer a pure-water permeability and a salt permeability from the model by regression; the determination of the mass transfer coefficient requires a variation in feed flow rate. The flocculation/ clarification/ filtration pre-treatment process produced a very good quality of water (SDI below 3), and no significant membrane fouling could be expected to manifest itself over 8 hours of operation.

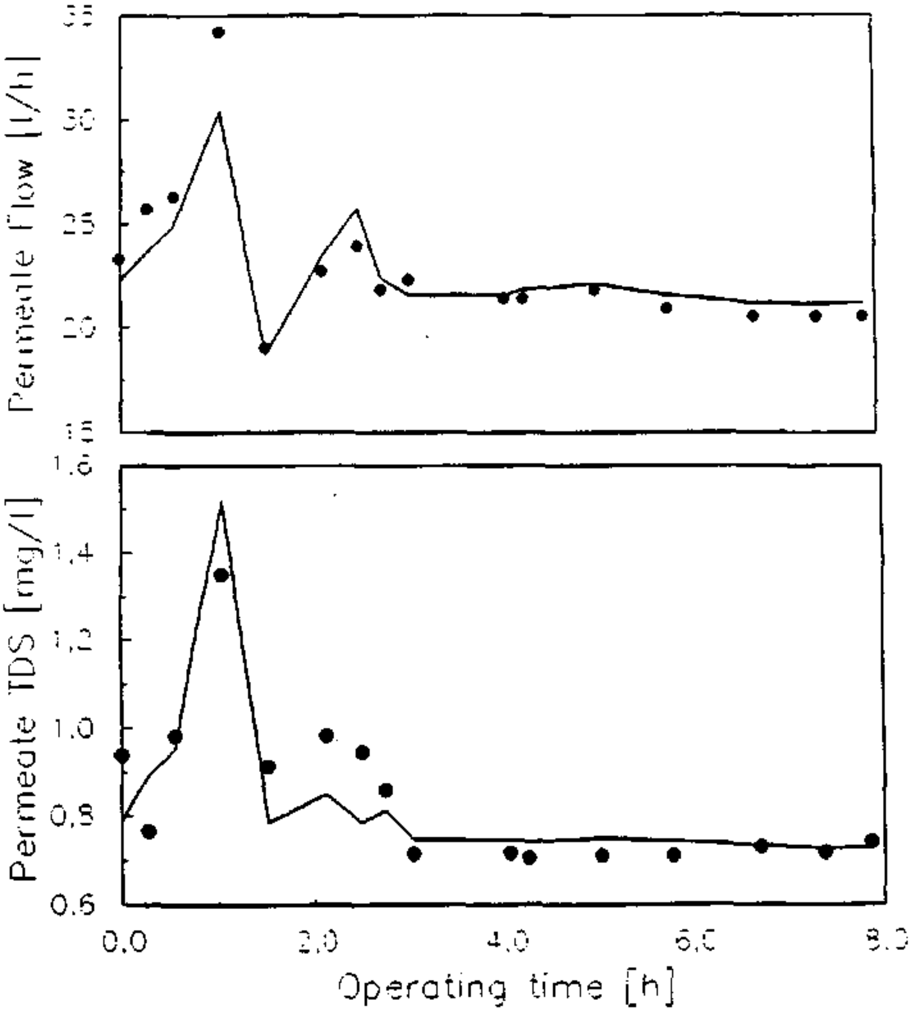

Figure 13 : Comparison of experimental data from the RO test apparatus at the Kendal Power Station with best-fit model results.

Fortunately the FilmTec SW30-2514 module used was geometrically identical to the NF40-2514 module investigated as part of this project (see Section 2.4.2 of this report). It was therefore reasonable to assume that the mass-transfer coefficient correlation which was found to be appropriate for the latter module would be applicable to the former.

In view of these considerations, it was decided to treat all the operating data as representing a single condition, and to determine a single set of water and salt permeability parameters for the membranes.

The mass transfer correlation determined previously was

$$Sh = 1.065\left(\frac{h}{l_{sp}} \cdot \frac{\eta_{sp}}{2-\eta_{sp}}\right)^{\frac{1}{2}} Re^{\frac{1}{2}} Sc^{\frac{1}{3}}$$

where

Sh	is the Sherwood number	$= 2hk/\mathcal{D}$,
h	is the flow channel width	($3{,}8 \times 10^{-4}$ m),
k	is the film mass-transfer coefficient	(m/s)
$\mathcal{D}$	is the solute diffusivity	($1{,}5 \times 10^{-9}$ m^2/s),
l_{sp}	is the mesh width of the spacer net	($2{,}8 \times 10^{-3}$ m)
η_{sp}	is the mixing efficiency of the spacer net	(taken as 0,5),
Re	is the Reynolds number	$= 2h\rho v/\mu$,
Sc	is the Schmidt number	$= \mu/\rho\mathcal{D}$,
ρ	is the solution density	(kg/m^3),
μ	is the solution viscosity	(Pa/s).
v	is the superficial flow velocity in the channel	(m/s)

The entire set of data was used to determine the water and salt permeability parameters in the reverse osmosis model. These best fit values were $1{,}9 \times 10^{-10}$ and $1{,}7 \times 10^{-8}$ respectively. Figure 1 shows the correspondence between experimental data and model results.

3.3 Full Scale Plant Simulation

The configuration of the full scale plant was based on that suggested by Eskom TRI. This consisted of six identical blocks of modules arranged in parallel. Within each block were two banks of pressure vessels arranged in series. The first bank consisted of 6 pressure vessels in parallel, each containing 6 FilmTec SW30-8040 modules, connected in series within the pressure vessel. The second bank contained identical pressure vessels to the first, but had only three in parallel. The plant was specified to provide 280 m^3/h of permeate at a water recovery of 60%.

The first problem that was encountered was that the MINTEQA2 speciation program indicated that the feed water was quite close to saturation with $CaCO_3$. Investigation using MINTEQA2 showed that the solution would become saturated with respect to $CaCO_3$ at a concentration factor of only 1,22 or approximately 18% water recovery. The use of anti-scalant polymer dosing does allow a certain degree of supersaturation to be incurred, however this would only extend the allowable water recovery to about 30%.

Further simulation with MINTEQA2 showed that adjusting the pH to 6,5 with sulphuric acid would move the solution away from the $CaCO_3$ saturation boundary by converting the carbonate to carbon dioxide. The acid dosage required to achieve this was calculated to be 12 mg/ℓ. Under these conditions 60 % water recovery proved possible without the use of anti-scalants. (Note that this conclusion is dependent on the feed water analysis. There might still be a problem associated with barium sulphate precipitation - barium was not reported in the analysis.)

The conditions assumed for the RO performance simulations were:

Feed temperature	25 °C
Feed TDS	100 mg/ℓ
Feed conductivity	128 mS/m
Feed flow rate	467 m^3/h
Permeate flow rate	280 m^3/h

The 60 % water recovery was achieved with 2,81 MPa feed pressure. The simulation results are summarized as:

Number of module banks	6
Number of pressure vessels	54
Total number of modules	324
Feed flow	467 m^3/h
Feed pressure	2,81 MPa
Permeate flow	280 m^3/h
Permeate TDS	1,4 mg/ℓ
Permeate conductivity	2,55 mS/m
Retentate TDS	248 mg/ℓ
Retentate conductivity	452 mS/m
Overall rejection	98,6% (based on TDS)

These conditions are very mild for sea water membranes, which are commonly employed at much higher feed salinities and pressures, and an investigation was carried out into whether a smaller plant could not be considered. It was noted that although the design production rate was 280 m^3/h, the average usage at the Kendal power station had been only 79 m^3/h in the 6 months prior to May 1993 (Chibi and Kruger, 1993). Thus the design rate is likely to required only infrequently when coping with process upsets.

According to information from the manufacturers of the modules (FilmTec, 1988) the feed rate and water recovery per module must be limited. The feed rate must be limited due to the tendency of hydraulic forces to *telescope* the spiral wound membranes. For the SW30-8040 modules, the maximum recommended flow rate is 12-14 m^3/h. The maximum recommended water recovery per module for the type of feed water being considered is 22-25 percent per module. The reason for this limit is the danger of scaling as a result of high exit concentrations and low exit velocities. For the given plant configuration the feed rate is 13 m^3/h and the recovery per module roughly 5%. As discussed previously, after pH adjustment the Kendal feed water is not likely to cause scaling. Consequently, any intensification of the process may involve greater water recovery, but must not increase the flow rate per module.

If the number of module banks is decreased from 6 to 5, the feed flow must be reduced to 389 m^3/h and the water recovery must be boosted to 72% to obtain 280 m^3/h of permeate. The simulation for this case gave the following results:

Number of module banks	5
Number of pressure vessels	45
Total number of modules	270
Feed flow	389 m^3/h
Feed pressure	3,34 MPa
Permeate flow	280 m^3/h
Permeate TDS	1,48 mg/ℓ
Permeate conductivity	2,69 mS/m
Retentate TDS	253 mg/ℓ
Retentate conductivity	460 mS/m
Overall Rejection	98,5 (based on TDS)

4 Conclusions

This modelling exercise has demonstrated that:

i) pH adjustment of the feed water is essential.

ii) The design performance can be achieved with a smaller plant than originally suggested.

iii) There is scope for economic optimisation of the design.

The average production rate of the plant appears to be about one quarter of the design rate, so it does not seem to make sense to install a plant which is operating below its capacity at the design rate. The higher flux and water recovery is achieved at the expense of a higher operating pressure, so there is a capital vs. running cost trade-off to be considered. In consequence these simulations must be seen in conjunction with an economic analysis of the design.

WATER RESEARCH COMMISSION PROJECT NO. 325

RESEARCH ON THE MODELLING OF TUBULAR REVERSE OSMOSIS SYSTEMS

Appendix 9

User Manual for the Single-Solute TRO Modelling Program

CJ Brouckaert

Pollution Research Group
Department of Chemical Engineering
University of Natal
Durban

February 1995

1 INTRODUCTION

This manual provides the information necessary to run the Reverse Osmosis Simulation Program (Version 1.00). The manual first provides an overview of what the program can do and then provides detailed instructions on performing each task.

2 OVERVIEW

two basic objectives

The Reverse Osmosis Simulation Program (Version 1.00), hereafter referred to as ROSP, has two basic functions:

regression

a) To calculate the parameters of Sourirajan's model for a particular reverse osmosis module from a set of experimental data by regression. These parameters are needed to predict the performance of an RO plant of a different configuration, or under different operating conditions, or may be useful as a diagnostic tool to infer aspects of the state of the equipment from operating data.

prediction

b) To make predictions about RO equipment performance under various operating conditions from the model parameters and equipment configuration.

equipment considerations

The program's operation is further subdivided according to the nature of the RO equipment being modelled.

point model: for small-scale RO apparatus

a) For small-scale equipment, such as might be used in preliminary screening tests, the water recovery and pressure drop during a single pass of the feed through the apparatus are often negligible, so that solute concentration, flow rate and pressure on the brine side of the membrane can be considered constant. Modelling such equipment only requires data representing the nature of the membrane. This type of model will be referred as a *point* model, as it is computationally equivalent to one point within a extended model of a larger RO apparatus.

extended model: for pilot- or full-scale RO plant.

b) In pilot-scale or full-scale equipment water recovery and pressure drop must be accounted for, and additional data on the equipment are required to model these effects. This comprises information on the mechanical design of the RO modules, and their configuration in the plant. This type of model will be called an *extended* model in this manual.

Input/output consideration

A third sub-division in the program's operation relates to the way it handles input and output of data and results:

Interactive mode

a) The program has a series of interactive input and output screen, which are chiefly useful for intensive investigation of a particular modelling case. These give the user easy access to and control over each individual data item or parameter. For convenience, each screen can be saved to a disk file for later recall. These screen-content files should not be confused with the batch input and output files described in the next section.

batch mode

b) When processing several similar cases, it becomes very tedious to handle each one interactively. This might occur when using the parameter regression procedure to interpret a large amount of plant operating data, or when simulating a given plant's performance over a range of operating conditions. For such cases the program accepts the variable part of the input data in the form of disk files, and puts out its results to a disk file. These batch files are separate from the screen-content files mentioned above. They are text files which may be viewed or altered by a text editor, or imported into or exported from a spreadsheet package program.

default mode is interactive

The default mode for the program is interactive, and it always starts up in interactive mode. Certain information can only be entered interactively, and this must be done before selecting batch mode. Such items of data will be identified as such when describing the relevant input screens. After completing a batch run, the program returns to interactive mode, and the data screen contain results and data corresponding to the last case modelled.

initial values

do not rely on preset values in a serious investigation

The program starts with a set of values in the data screens, which correspond to a particular pilot-plant, built with standard Membratek cellulose-acetate RO modules, that was studied during the development of the program. **These are not likely to apply to other situations**, but may be useful to guide the selection of initial estimates, and to help a new user to explore the various program options without having to assemble a set of consistent data.

parameter calculation

The model parameters are calculated from experimental data using a non-linear regression procedure. This requires that an estimate be supplied for each of the model parameters. The program allows several options for the regression, depending on which parameters are to be adjusted to fit the experimental data, and which are to be considered fixed.

performance prediction

To predict the performance of the reverse osmosis module the following data tables must be filled: the constant data table, the model parameters data table and the operating conditions data table. The results of the performance prediction are placed directly into the performance data table from where they can be viewed or stored onto a disk.

3 OPERATING INSTRUCTIONS

3.1 Running the Program

starting procedure

Step 1. If the program is on a floppy disk, place the disk in one of the disk drives. Change directory to the disk drive containing the floppy disk. *i.e.* if the floppy disk is in drive A, type:

A:↵

If the program is on the hard disk drive change the directory to the one containing the program.

Step 2. Type:

RO↵

3.2 Operating the program in interactive mode

3.2.1 On starting

Once you have run the program the following page will be displayed.

introductory page

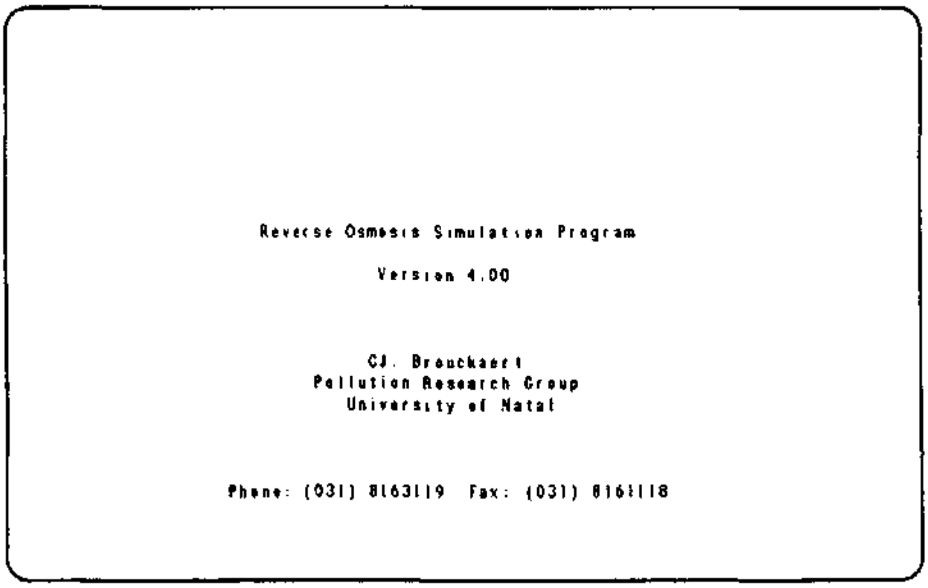

```
                 Reverse Osmosis Simulation Program

                            Version 4.00


                           CJ. Brouckaert
                      Pollution Research Group
                        University of Natal


              Phone: (031) 8163119  Fax: (031) 8161118
```

Screen 1. Introductory page.

This introductory page gives the program name, version number, and author. Pressing ↵ will move the program onto the next page.

3.2.2 The main menu

main menu

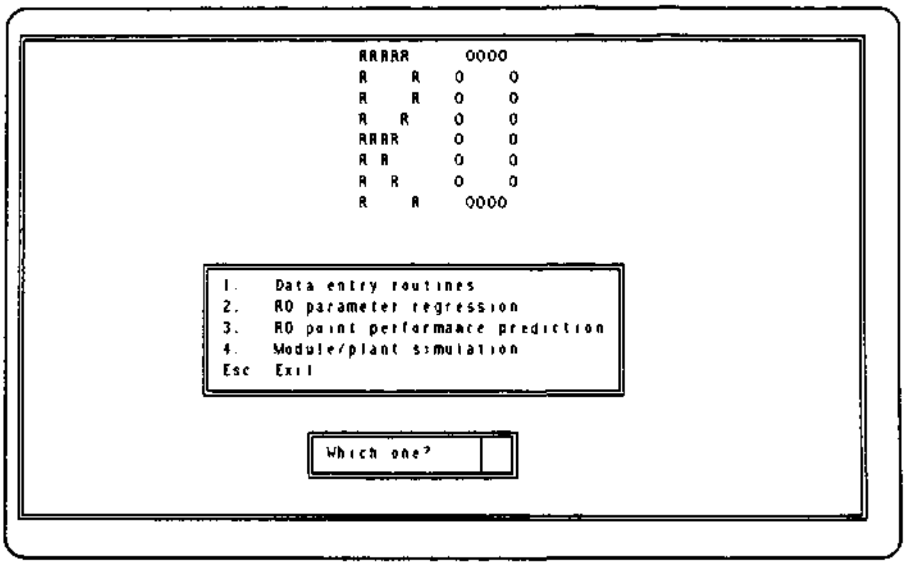

```
RRRRR      0000
R    R   0      0
R    R   0      0
R   R    0      0
RRRR     0      0
R R      0      0
R  R     0      0
R    R     0000

1.    Data entry routines
2.    RO parameter regression
3.    RO point performaace prediction
4.    Module/plant simulation
Esc   Exit

Which one?
```

Screen 2. Main menu.

This page presents the main program menu. The options presented are:

data entry routines

Pressing ① gives access to the interactive data entry screens, which are discussed in detail below. It is generally necessary to enter some data before selecting any of the other options on this menu, unless one is simply using the default values to try out the program's options.

RO parameter regression

Pressing ② starts the parameter regression procedure. This requires data to have been set up via option 1, the exact nature depends on the options which have been selected on the *Constant Data* screen. In all cases *osmotic pressure* data for the feed solution must have been entered. The equipment type and input/output mode determine what further information is required and how it must be supplied.

RO point performance prediction

Pressing ③ starts the point model prediction procedure for small-scale RO apparatus. Once again *constant data* and *osmotic pressure* must have been entered via the relevant screens, with *operating parameters* supplied either from a screen or from a batch file depending on the input/output mode.

Module/plant simulation

Pressing ④ starts the extended model prediction procedure for larger-scale RO equipment. In addition to the requirements of point predictions the *module design data* and *plant configuration* screen must have been filled in. These data cannot be supplied from a batch input file.

Exit

Pressing Esc ends the program. Before relinquishing control the user is asked "Are you sure?". Pressing Ⓨ confirms the exit, any other response causes the program to continue.

zeros or unrealistic values in tables

NOTE The program checks whether data has been entered or not by checking the table for zeros. If a zero is found where one is not allowed then the program assumes that the table has not been filled in. In general it is very difficult to detect unrealistic data values before attempting to use them. If such values are entered they could cause the program to hang up. It is wise to have saved input data before starting any of the calculation procedures.

3.2.3 Handling data tables

Choosing option 1, the data entry routines, gives the data entry menu shown in screen 3.

data entry and editing

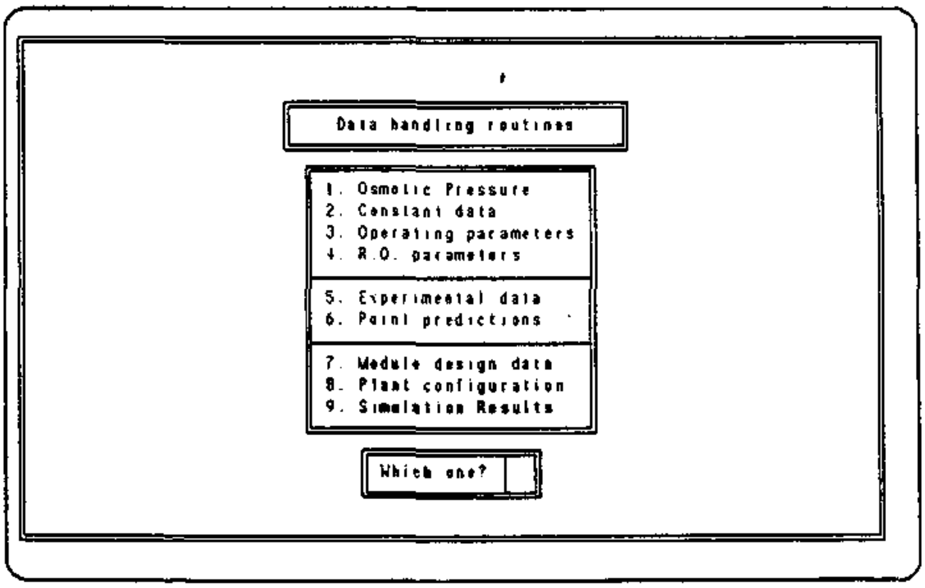

Screen 3. Data Entry and Editing Menu.

This menu presents nine options, one for each of the data tables. These are selected by pressing the associated number key. Each presents a template of the data required. Data tables containing sample data are shown in Screens 4 to 12.

Data can be entered using the following methods:

1. Data entry from the keyboard.

In order to enter data in a particular cell move the cursor to the cell required using any one of the direction keys shown below.

cursor movement commands

↑ Up arrow key - moves the cursor up.
↓ Down arrow key - moves the cursor down
← Left arrow key - moves the cursor left
→ Right arrow key - moves the cursor right

entering a number

Once the cursor is located on the required cell, type the appropriate number into that cell and press return (⏎). ROSP will then write the value specified into the cell using a pre-defined format. The format used by ROSP may result in fewer significant figures being displayed than were given. This does not mean that the figures not displayed have been lost or truncated. The number given is stored as it was entered. ROSP merely displays the number rounded to a convenient number of significant figures.

expansion of data arrays

When entering data into the experimental data table for the first time, only the cell specifying the number of data sets is displayed. In order to display the rest of the table, an integer number must be entered at this point. As soon as the number of cells is entered, the number of rows is displayed. The maximum number of rows that can be displayed at a time is 14. If the number of rows is greater than 14 only the first 14 rows are displayed. In order to enter data into rows 15 and onwards, move the cursor down to row 14. Pressing the down arrow key will cause the entire array to scroll up one row displaying row 15 and causing row 1 to disappear (temporarily). By using the down arrow key all the rows below 14 can be reached. If the down arrow key is pressed on the last row of the data, the cursor will move back to the first row.

2. Data entry from disk.

loading data from disk

In order to enter data from the disk, type L or l for load. ROSP will then give a prompt requesting the name of the file required. Type the name of the file required and press return. If the file requested does not exist or the name was incorrectly entered, then a warning message will be displayed and another prompt for the name given. Once the correct file name has been given ROSP will display the filled data table. The data can then be edited from the keyboard if required.

file names

NOTES

1. Only 14 spaces are allowed for the file name and the path to it. It is therefore advisable to keep the file names short and/or to run ROSP from the subdirectory or disk where the files are stored.

2. The program saves screen files with extensions which identify the type of screen, namely .OSM, .CON, .OPE, .PAR, .EXP, .PER, .TUB, .CFG, and .MOD. The file name must be typed without an extension, as this is added automatically. The files are text files which can be viewed or modified with a text editor, or imported to or exported from a spreadsheet program

3. These screen content files should not be confuse with batch-mode data files.

Once all the data has been entered into a data table you can either save the data onto a disk file or return to the data entry and editing menu, screen 3.

saving data onto disk

To save a data table onto a disk, type S or s for save. ROSP will then prompt for a file name. Enter the name of the file to which you wish to save the data. If the file already exists it will be overwritten. If it does not exist then a new file will be created.

returning to previous menu

To return to the data entry and editing page, screen 3, type Esc. The data remains stored in the computer and can be viewed and edited again by choosing that data table once more.

NOTE The Esc key always returns the program to the previous level. Thus from editing data in a data table Esc returns you to the data entry and editing menu. From the data entry and editing menu, Esc returns to the main menu.

3.2.4 Osmotic pressure data table

osmotic pressure data table

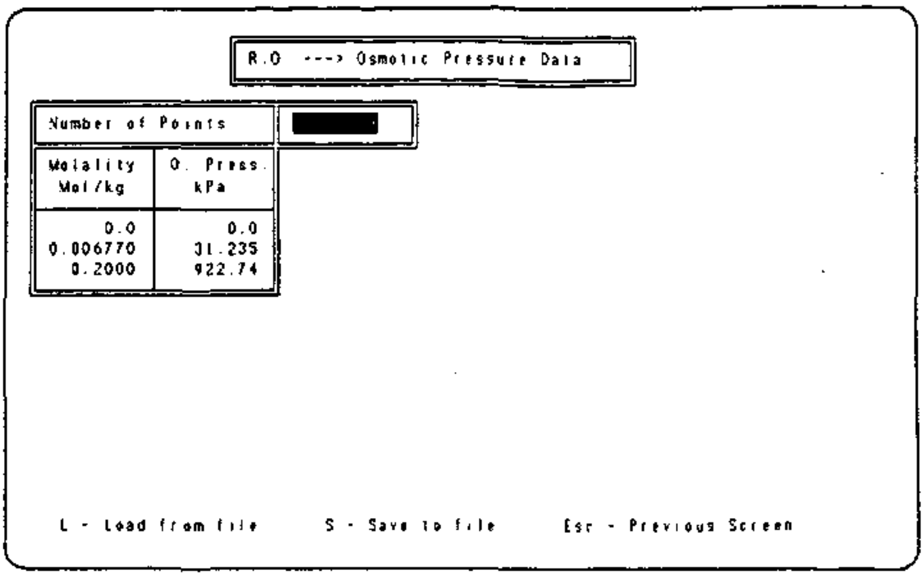

```
R.O ---> Osmotic Pressure Data

Number of Points

Molality    O. Press.
Mol/kg      kPa

     0.0        0.0
0.006770     31.235
  0.2000     922.74

L - Load from file     S - Save to file     Esc - Previous Screen
```

Screen 4.

When entering data from the keyboard the first number required is the number of pairs of values that you intend entering. Once this number is entered the table will expand to the required number of rows to fit in all the data sets. This number must be an integer (*i.e.* no decimal point) and the maximum value allowed is 15.

3.2.5 Constant data table

constant data table

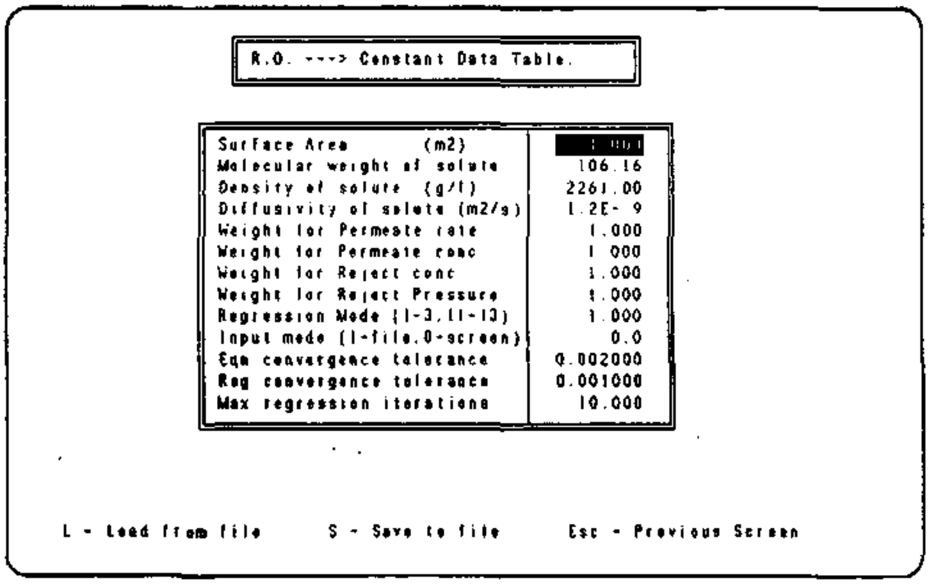

```
R.O. ---> Constant Data Table.

Surface Area         (m2)          1.001
Molecular weight of solute        106.16
Density of solute  (g/l)         2261.00
Diffusivity of solute (m2/s)     1.2E- 9
Weight for Permeate rate           1.000
Weight for Permeate conc           1 000
Weight for Reject conc             1.000
Weight for Reject Pressure         1.000
Regression Mode (1-3,11-13)        1.000
Input mode (1-file,0-screen)         0.0
Eqn convergence tolerance       0.002000
Reg convergence tolerance       0.001000
Max regression iterations         10.000

L - Load from file     S - Save to file     Esc - Previous Screen
```

Screen 5.

physical constants

Surface area [m^2]

The membrane surface area of a computational 'point' in the model. For a point type model, this corresponds to the entire membrane surface area of the RO apparatus, and must be entered here. For an extended model, this is the area of a computational cell in the numerical integration scheme, and is calculated by the program from the data entered into the *module design data* screen. The calculated value will overwrite any manually entered value.

Molecular weight of solute [g/mol]

The program only considers a single solute. In most practical cases the plant will be treating a mixed solute, and it will be necessary to use a representative average value. In such cases one must be careful to ensure that the molecular weight, diffusivity and osmotic pressure data are consistent with each other.

Density of solute [g/ℓ]

This is used to calculate the density of aqueous solutions, so should strictly be the density of the solute in a dilute solution standard state. However, in most cases the pure solute density should give sufficiently accurate results.

Diffusivity of solute [m^2/s]

The solute diffusivity in water at 20 °C is entered here. The program extrapolates this value to other temperatures using a correlation which is applicable to inorganic ionic solutes. For a mixed solute, use a molar average value.

Regression constants

Weighting factors

The regression procedure attempts to minimize the difference between predicted values and measured values by adjusting the model parameters. The measurements that it considers are the permeate stream flow rate and concentration for both the point and extended models, and additionally reject stream pressure and concentration for the extended model. As there may be different degrees of confidence in the accuracy of these measurements, they may be assigned different relative weightings. A measurement with a higher weighting factor will have a greater influence on the values of the parameters. The program automatically applies a weighting factor to each measurement which is the inverse of its magnitude, so that measurements which have large numerical values do not overshadow those with small ones. This effectively assumes that all measurements have the same accuracy relative to their sizes. These automatic weighting factors are multiplied by the weights entered on this screen which then represent the user's confidence in the relative accuracy of the measurements. Only the relative values of the weightings to each other are important, their absolute magnitudes have no significance. Weights should never be given negative values. Where no measurements are available for a particular variable, set the corresponding weight to 0.

Regression Mode

Possible values are 1, 2, 3 and 11, 12, 13. 1 to 3 are for a point model, and 11 to 13 for an extended model. The last digit in either case refer to the number of parameters which will be adjusted by the regression procedure (the remainder will remain at their entered values). The parameters adjusted in each case are:

Point model

1 - k_1
2 - k_1 , k_2
3 - k_1 , k_2 , k_3

Extended model

11 - k_1
12 - k_1 , k_2
13 - k_1 , k_2 , L

For the significance of k_1 , k_2 , k_3 see the *RO parameter* screen. L is explained on the *module design data* screen

input/output mode

1 entered here causes the program to enter batch mode when the regression or prediction procedure are started from the main menu. 0 causes it to use only the screen data.

program control constants

The **equation convergence tolerance** specified how closely the left and right hand sides of equations must agree in the non-linear solution procedure.

The **regression convergence tolerance** specifies when the error function between measured and predicted values has changed sufficiently little between subsequent iterations, at which point the program assumes that it has reached a sufficiently good set of model parameters.

If the regression procedure reaches the **maximum regression iterations** without reaching solution, it stops and asks the user how many more to continue for (0 may be entered at that point to terminate the regression).

3.2.6 Operating data table

The operating data table specifies the operating conditions for which the performance of the module must be predicted. The operating parameters that must be specified are the operating pressure, the feed solution concentration, the temperature and the feed solution flow rate. The units of these parameters are the same as specified for the *experimental data table.*

operating conditions data table

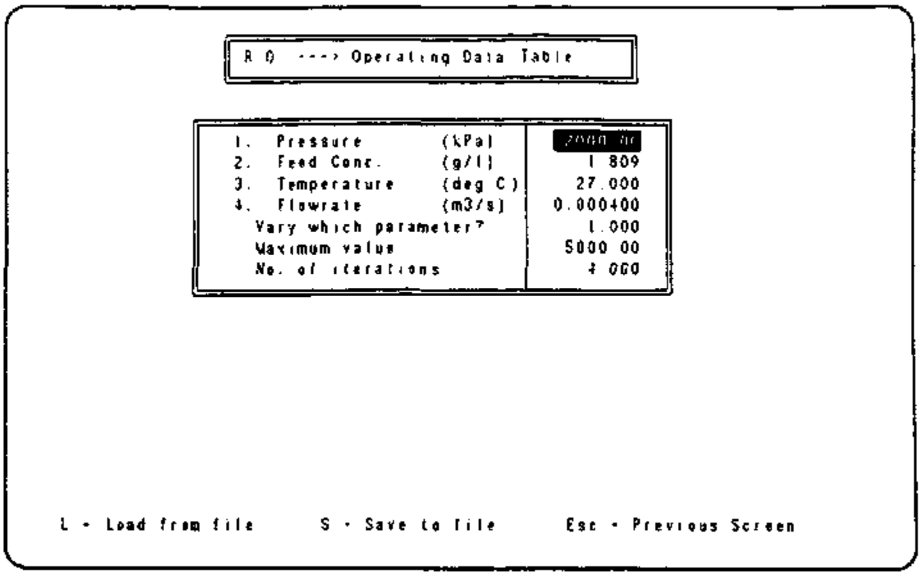

```
R O ---> Operating Data Table

1.  Pressure          (kPa)      2000.00
2.  Feed Conc.        (g/l)        1.809
3.  Temperature       (deg C)     27.000
4.  Flowrate          (m3/s)    0.000400
  Vary which parameter?            1.000
  Maximum value                  5000.00
  No. of iterations                4.000

L - Load from file     S - Save to file     Esc - Previous Screen
```

Screen 6. Operating conditions data table.

varying operating conditions

ROSP allow you to specify that one of the operating parameters vary over a range of values. For example, the temperature, feed flow rate and feed concentration can be set to fixed values and the performance of the module be obtained at 10 pressures from 4000 kPa to 5000 kPa. In order to do this, the parameter you wish to vary must be identified by its number in the "Vary which parameter?" cell. The numbers identifying each parameter are as follows.

parameter numbers

1	Pressure
2	Feed concentration
3	Temperature
4	Flow rate

The minimum value of the parameter is entered in the cell opposite the parameter name. The maximum value is then entered opposite "Maximum value". The number of points at which the module performance must be evaluated is entered opposite "No. of iterations". The example shown in screen 6 requires that the pressure be varied from 2000 kPa to 5000 kPa in 4 intervals

3.2.7 Parameter table

parameter sets

Each row of the parameter table represents a single set of the four parameters required to describe a RO membrane separation. The sum of squares also shown is entered by the regression procedure after calculating the parameter values, and is a measure of how well it was able to fit the model to the data (the smaller the value the better). k_1

is a measure of the membrane's permeability for water, k_2 represents it permeability for the solute. k_3 is a coefficient in an empirical equation for turbulent film mass transfer coefficient within the tube. In the current version of the program this is considered as a fixed parameter (the value of 0.0096 is taken from the literature). Beta is a coefficient which represents the compressibility of the membrane under operating pressure. This is also taken as fixed for cellulose-acetate membranes.

model parameter table

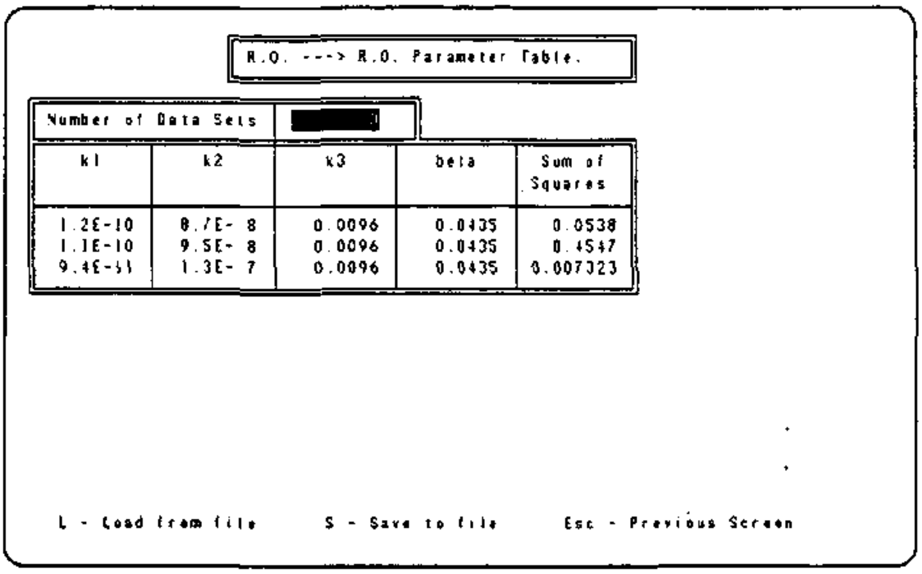

R.O. ---> R.O. Parameter Table.

Number of Data Sets

k1	k2	k3	beta	Sum of Squares
1.2E-10	8.7E- 8	0.0096	0.0435	0.0538
1.1E-10	9.5E- 8	0.0096	0.0435	0.4547
9.4E-11	1.3E- 7	0.0096	0.0435	0.007323

Screen 7. Reverse osmosis parameter table.

When data is entered manually or from disk, each row can be used for the model parameters of a different module. This enables the performance of different modules to be compared for the same operating conditions without having to enter a different set of parameters each time.

specifying the parameter set to use

In order to specify which model parameter set ROSP must use to predict module performance, the cursor must be moved to the row containing the required parameters before typing Esc to return to the data entry and editing menu. If the cursor is in the number of data sets cell then the last data set will be selected.

3.2.8 Experimental data table

experimental data table

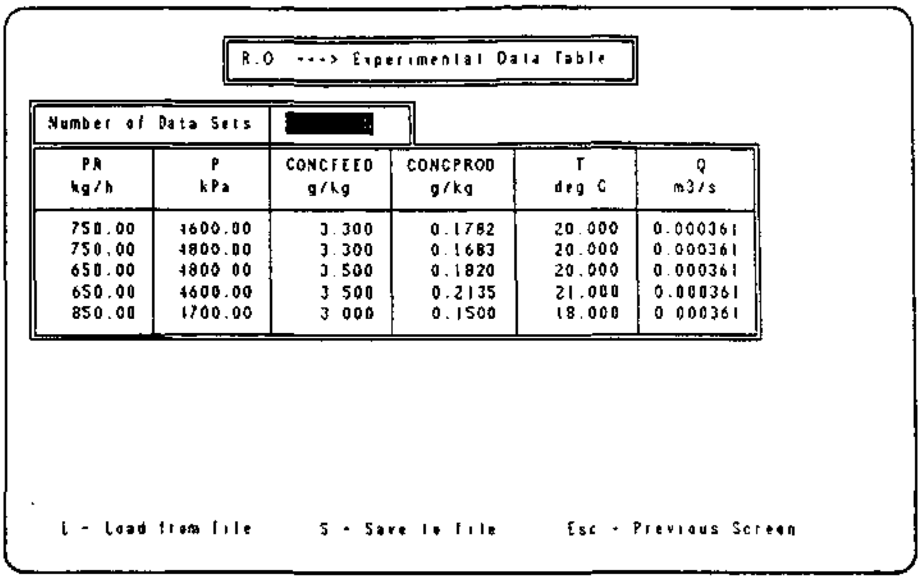

R.O ---> Experimental Data Table

Number of Data Sets	

PR kg/h	P kPa	CONCFEED g/kg	CONCPROD g/kg	T deg C	Q m3/s
750.00	4600.00	3.300	0.1782	20.000	0.000361
750.00	4800.00	3.300	0.1683	20.000	0.000361
650.00	4800.00	3.500	0.1820	20.000	0.000361
650.00	4600.00	3.500	0.2135	21.000	0.000361
850.00	1700.00	3.000	0.1500	18.000	0.000361

Screen 8. Experimental data table.

When entering data from the keyboard the first number required is the number of sets of data that you intend entering. Once this number is entered the table will expand to the required number of rows to fit in all the data sets. This number must be an integer (*i.e.* no decimal point) and the maximum value allowed is 100.

Below the cell where the number of data sets is entered, you will see a row of letters or acronyms representing the variable that must be entered into that column. The meanings of these acronyms are given below along with the units that must be used for each variable.

experimental data columns

PR	[kg/h] [l/h]	Product rate This is the permeate flow rate under the operating conditions described.
P	[kPa]	*Operating pressure* This is the gauge pressure at the feed side of the membrane.
CONCFEED	[g/ℓ]	Concentration of the feed solution
CONCPROD	[g/ℓ]	Concentration of the product or permeate solution.

T	[°C]	Operating temperature This is the temperature at which the experiment was conducted.
Q	[m³/s]	Feed solution flow rate This is the flow rate at which the feed solution is pumped through the module.

experimental data requirements

Experimental data must be entered in order to calculate the model parameters for a particular module. The minimum number of data sets required to calculate the parameters depends on the number of parameters being adjusted. Each experimental data set consists of several measurements, 2 for a point model, and up to four for an extended model. Theoretically one measurement is sufficient to determine one parameter, however one can seldom place much reliance on parameters derived from the minimum set of measurements. The program does not check whether the number of measurements are sufficient, so the user must do so.

3.2.9 Predicted performance data

This is the output screen for the *point predictions* procedure. Once ROSP has calculated the flux (permeate flow rate per unit area of membrane), product concentration and the salt rejection for all the conditions specified in the operating data table, it puts the results into the performance data table. The performance data table is shown in screen 9.

predicted performance data table

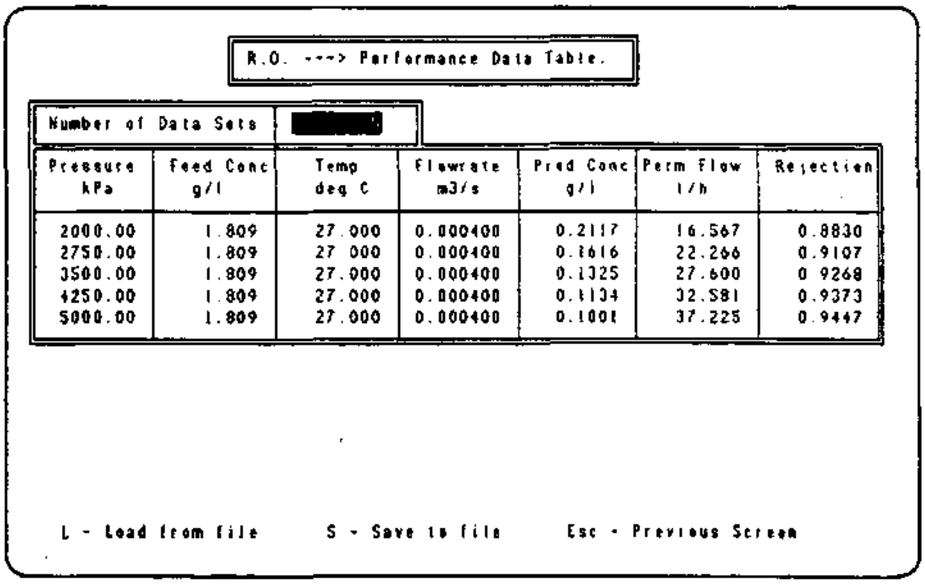

R.O. ---> Performance Data Table.

Number of Data Sets [redacted]

Pressure kPa	Feed Conc g/l	Temp deg C	Flowrate m3/s	Pred Conc g/l	Perm Flow l/h	Rejection
2000.00	1.809	27.000	0.000400	0.2117	16.567	0.8830
2750.00	1.809	27.000	0.000400	0.1616	22.266	0.9107
3500.00	1.809	27.000	0.000400	0.1325	27.600	0.9268
4250.00	1.809	27.000	0.000400	0.1134	32.581	0.9373
5000.00	1.809	27.000	0.000400	0.1001	37.225	0.9447

<u>Screen 9.</u> Performance data table.

view data only

The data on this table may only be viewed. No changes can be made to it. The data can be saved to a disk file from where it may be manipulated by another program such as Lotus 123 to produce graphs *etc.* The results of previous calculations can be loaded from disk and viewed if required.

The units of the results given in the performance data table are as shown previously except for the flux and rejection which are shown below.

units

Flux [ℓ/m^2h]
Rejection [dimensionless] (1 = total salt rejection by the membrane)

3.2.10 Module design data

module design data table

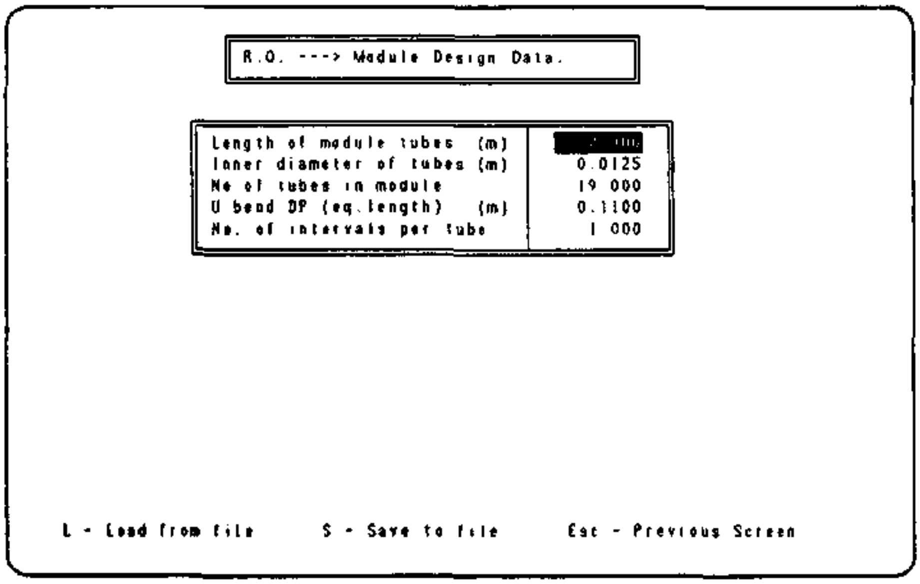

R.O. ---> Module Design Data.

Length of module tubes (m)	[illegible]
Inner diameter of tubes (m)	0.0125
No of tubes in module	19 000
U bend DP (eq. length) (m)	0.1100
No. of intervals per tube	1 000

Screen 10. Module design data.

The data in this screen is only required for extended models, that is models of relatively large scale RO plant. A TRO module consists of a number of membrane-lined tubes in series, connected by return bends. The data requirements on this screen are mostly self-explanatory, apart from the last two. The U-bend DP (L) is a discharge coefficient used to calculate the pressure drop across each return bend in the form

$$\Delta P = L\frac{(\rho v^2)}{2}$$

L is one of the parameters which can be adjusted by the regression procedure. This is only justified if the plant data includes measurements of both inlet and outlet pressures. The value that results will also include contributions from manifolds and fittings between modules in the plant.

The **number of intervals per tube** refers to the numerical integration procedure which divides the plant into a number of finite intervals in which conditions change sufficiently little to be considered approximately constant. The more intervals that are selected the more closely the numerical solutions approximate the true solutions of the governing equations, but the more computational time is required.

3.2.11 Plant configuration data

plant configuration data table

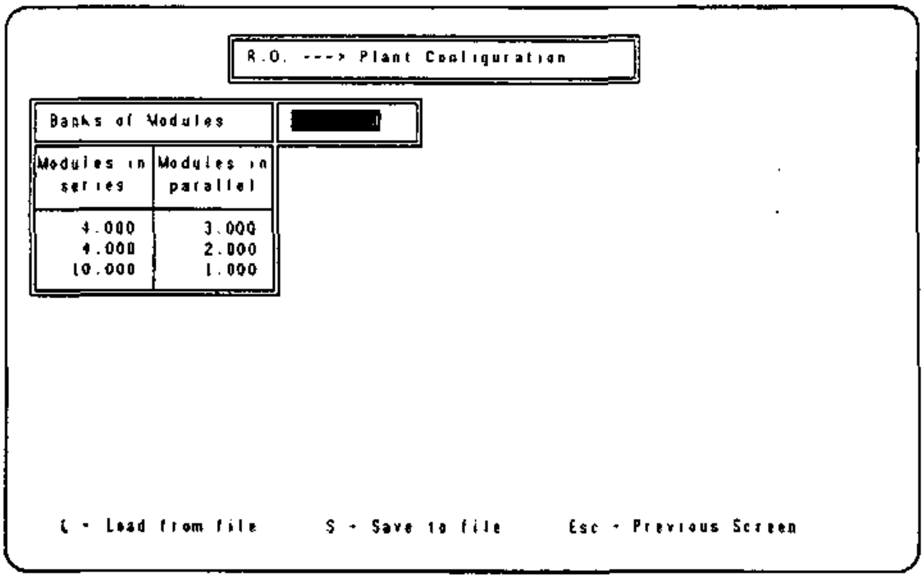

R.O. ---> Plant Configuration

Banks of Modules

Modules in series	Modules in parallel
4.000	3.000
4.000	2.000
10.000	1.000

Screen 11. Plant configuration data.

up to 3 banks of modules

The data in this screen is only required for extended models, that is models of relatively large scale RO plant. The arrangment of modules is expressed in terms of *banks* of modules which contain modules connected in parallel and in series. In a bank it is assumed that the flow is uniformly distributed between the parallel rows of modules. The solution leaving one bank is assumed to be completely mixed before being distributed to the next bank. Only a series connection between banks is allowed for. A maximum of three banks of modules is catered for, however the number of modules in a bank is not restricted.

3.2.12 Predicted performance data

This is the output screen for the *Module/plant simulation* procedure.

plant simulation results data table

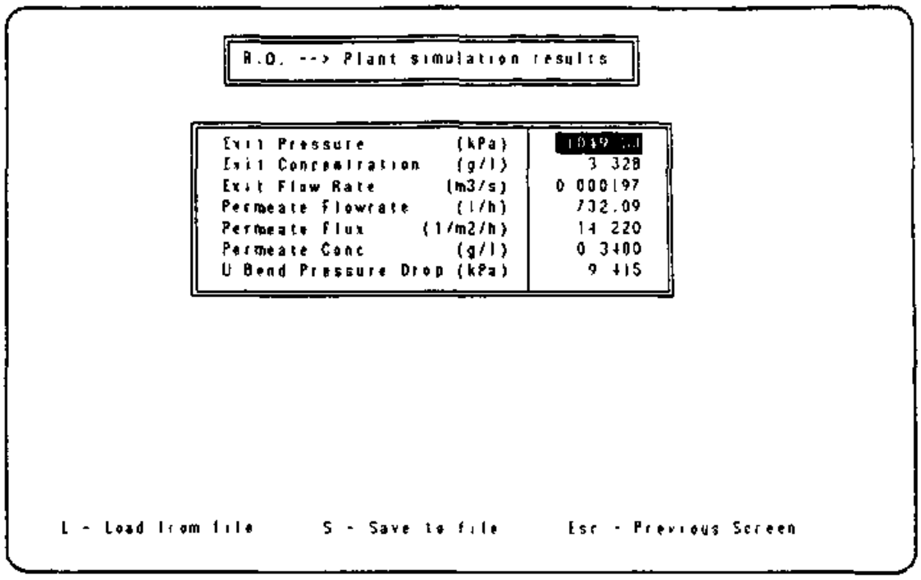

```
R.O. --> Plant simulation results

Exit Pressure             (kPa)    1049.[illegible]
Exit Concentration        (g/l)         3.328
Exit Flow Rate           (m3/s)      0.000197
Permeate Flowrate         (l/h)        732.09
Permeate Flux          (l/m2/h)        14.220
Permeate Conc             (g/l)        0.3400
U Bend Pressure Drop (kPa)              9.415

L - Load from file     S - Save to file     Esc - Previous Screen
```

Screen 12. Plant simulation results data table.

view data only

The data on this table may only be viewed. The space on the screen is somewhat limited to accommodate all the output that might be of interest in a plant simulation, however much more is available from a batch-mode output file.

3.3 Operating the program in batch mode

3.3.1 General considerations

The purpose of batch mode

The purpose of batch mode is to process a number of similar cases of either parameter regressions or performance simulations without having to enter required input data manually for each case. Those items which are likely to differ from case to case are read from a input disk file, and the computed results are written to a corresponding output disk file. The parameters which remain fixed from case to case are taken from the interactive input screens. The program operates by copying the relevant parameters from the input file to the input screens, and then carrying out the calculations in exactly the same way as in interactive mode. These values overwrite any that were entered interactively, so if there is any doubt whether a parameter should be entered interactively or not, it is safer to do so: it will then be available if it is needed, if not needed it will simply be replaced.

selecting batch mode

Batch mode is selected by setting the input mode parameter to 1 in the Constant Data Table (screen 5, see section 3.2.5) The program does not enter batch mode immediately, but remains in interactive mode until one of the calculation options (options 2, 3 or 4) is selected on the Main Menu (screen 2, see section 3.2.2).

specifying the input file

As soon as the parameter regression option is selected, the program will prompt for the name of an input file. This must be entered without any suffix: the program automatically adds the required suffixes : '.INP' for experimental data to be processed by the parameter regression routine, or '.CDN' for operating conditions for the performance simulation routine. The program automatically generates the name of output file by using the same prefix with suffixes '.RES' or '.SIM' respectively. If a file already exists of the same name it is overwritten with the new results. If no input file of the given name exists, the program displays an error message, and re-prompts. If no file name is eventually specified, the program returns to interactive mode without attempting any calculations.

3.3.2 Input and output file formats

Input and output files are ASCII text files, and can be prepared or modified by a text editor. They contain tables of input values, which are readily produced by exporting from a spreadsheet package. Values must be entered into the files on the correct line and in the correct order, however their column positions are immaterial. Values must be separated by spaces. Decimal points rather than decimal commas are used. There are two basic formats, one for input of RO measurements for fitting to the model by regression, and the other for input of operating conditions for a RO performance simulation.

3.3.2.1 Measured data input file format

File name

The filename must consist of up to 8 alphanumeric characters followed by the suffix '.INP'. When the program prompts for the filename, it automatically adds the suffix, which must therefore not be entered by the user. If the file resides on a disk drive other than the currently active one, the file name may be prefixed with the drive identification. For example, if the program is running from the C: drive, but the input file, called TESTDATA.INP is stored on the A: drive, the user must enter **A:TESTDATA** when asked for the file name. However if the file is on the same drive and directory as the program, only **TESTDATA** would be required.

line 1 The first line of the file is ignored by the program and can be used for column headings or identification purposes.

line 2 The second line contains control information for the regression procedure:

(i) The *number of data sets* in the group of experimental measurements which will be regressed together. The group should consist of data for which the model parameters are expected to be the same.

(ii) The *regression mode*, as before on screen 5. Values 1-3 are for point model data, while 10-13 are for extended model data. The last digit specifies the number of parameters to be adjusted in the regression (see section 3.2.5).

(iii) Starting estimates of the model parameters k_1, k_2, k_3 and Beta (see section 3.2.7). According to the regression mode, some of these parameter values will be altered by the regression procedure.

(iv) Starting estimate of the parameter L (see section 3.2.10). This value is only required for extended model data (regression modes 11-13). It is only adjusted if regression mode 13 is specified.

line 3 The third line contains the measured values which constitute the first data set. These are:

(i) Feed pressure (kPa)
(ii) Feed temperature (°C)
(iii) Feed flow (m^3/h)
(iv) Feed concentration (g/ℓ)
(v) Permeate flow (m^3/h)
(vi) Permeate concentration (g/ℓ)
(vii) Outlet pressure (kPa).
(viii) Reject concentration (g/ℓ)

Items (vii) and (viii) only apply to the extended model. Entering a negative value indicates that the measurement is not available.

Line 3 is repeated for each of the data sets in the group.

Further groups can be added to the file by repeating the usage of lines 2 and 3. The program continues accepting groups of data sets until it reaches the end of the file.

3.3.2.2 Parameter regression output file

File name

The output file has the same filename prefix as the input file, with suffix '.RES'. The output file will be written to the same disk drive as the one that the input file came from.

line 1

The first line of the file contains headings for the data columns. These are enclosed in double quotes so that they will be correctly imported into a spreadsheet program.

line 2

The second line contains the program output for the first data set of the first group. The first six values are echoes of the input data values (see *line 3* in the previous section 3.3.2.1). After these follow values calculated by the model for:

(i) Permeate flow (m^3/h)
(ii) Permeate concentration (g/ℓ)
(iii) Reject stream flow (m^3/h).
(iv) Outlet pressure (kPa).
(v) Reject concentration (g/ℓ)
(vi) solute concentration in the boundary layer adjacent to the membranes at the plant exit (g/ℓ).

In the case of a *point model* simulation, only (i) and (ii) from the above list appear, as the remainder are not relevant.

model parameters

Next there follow the model parameters k_1, k_2, k_3 and Beta (see section 3.2.7) that were determined for the data group. In the case of an *extended model* the value of the pressure drop parameter L is appended.

data heading

Finally the data heading from the input file is copied to the end of the line. If this starts with text characters, the whole heading is copied, enclosed in quotes so that it will be imported correctly into a spreadsheet program. If the first characters of the heading are numeric, then only the number is copied, without quotes. This is useful when one wishes to use the identifying numbers for subsequent plotting : for example the numbers might represent hours of operation of the plant.

subsequent lines

line 2 is repeated for each data set in the first group. Thereafter the subsequent groups are presented using the *line 2* format.

3.3.2.3 Plant simulation operating data input file

File name

The filename must consist of up to 8 alphanumeric characters followed by the suffix '.CDN'. When the program prompts for the filename, it automatically adds the suffix, which must therefore not be entered by the user. If the file resides on a disk drive other than the currently active one, the file name may be prefixed with the drive identification. For example, if the program is running from the C: drive, but the input file, called ROPLANT.CDN is stored on the A: drive, the user must enter **A:ROPLANT** when asked for the file name. However if the file is on the same drive and directory as the program, only **ROPLANT** would be required.

line 1

The first line of the file is ignored by the program and can be used for column headings or identification purposes.

line 2

The second line contains data for the first condition to be simulated. The quantities, in order, are:

(i) Feed pressure (kPa)
(ii) Feed temperature (°C)
(iii) Feed flow (m^3/h)
(iv) Feed concentration (g/ℓ)

Subsequent lines have the same format as line 2, and define further operating conditions to be simulated. The program continues to accept cases for simulation until the end of the file is reached.

target specifications

The above four variables constitute the most convenient specification of an operating condition for solution by the RO modelling algorithm, however it may be required to specify the operating condition in terms of some other combination of variables. To match such a specification the program has to find the correct combination of the four basic parameters. There is provision to vary any one of them to achieve a specified target for one other variable.

Four additional items must be added to the standard four values on the input line when a target specification is made.

target variable

(i) An integer value specifying which variable is to be fixed by the target specification, according to the following list:
1 - permeate flow rate (m^3/h).
2 - permeate concentration (g/ℓ).
3 - permeate flux (ℓ/m^2h).

4 - reject stream flow rate (m^3/h).
5 - Exit pressure (kPa).
6 - reject stream concentration (g/ℓ).
7 - solute concentration in the boundary layer adjacent to the membranes at the plant exit (g/ℓ).
8 - Flow velocity at plant exit (m/s).

target value (ii) The value set for the variable, expressed in the units listed above.

adjustment variable (iii) An integer in the range 1 to 4 specifying which if the four basic variables (feed pressure, feed flow, feed concentration, or temperature) will be adjusted to meet the target specification. Note that temperature will seldom be a suitable choice here, since its effect on the model is relatively small.

first step-size (iv) The value of the change in the adjustment variable that the program will make on the first step in the search for the value which meets the target. After the first step, the program determines the subsequent step-sizes.

3.3.2.4 Plant performance simulation output file

File Name The output file has the same filename prefix as the input file, with suffix '.SIM'. The output file will be written to the same disk drive as the one that the input file came from.

line 1 The first line of the file contains headings for the data columns. These are enclosed in double quotes so that they will be correctly imported into a spreadsheet program.

Each subsequent line contains the output of one simulation case.

line 2 The first five values are echoes of the operating conditions from the input file, namely :

(i) Feed pressure (kPa)
(ii) Feed temperature (°C)
(iii) Feed flow (m^3/h)
(iv) Feed concentration (g/ℓ)

Then follow the calculated results :

(v) Permeate flow rate (m^3/s)

(vi) Permeate concentration (g/ℓ)

(vii) Permeate flux (ℓ/m^2h)

The program then appends four results for *each* bank of modules in the plant configuration (see section 3.2.11). These relate to the stream *leaving* the bank : consequently the results for the last bank are also those for the reject stream.

(viii) Bank exit pressure (kPa).

(ix) Bank exit velocity (m/s).

(x) Bank exit concentration (g/ℓ).

(xi) Bank exit boundary-layer concentration (g/ℓ).

The last figure represents the highest concentration that is presented to the membranes in the bank, and is relevant for solutions which may precipitate a scale onto the membranes.

subsequent lines

line 2 is repeated for as many cases as were specified in the input file.

4 Operating problems

This first version of the program has been very little exposed to users other than the author up to now, and the problems mentioned here very probably will be far from complete. Please let me know of any that you come across so that they may be addressed in future version of the program.

failure to converge

Most problems present themselves as a failure of the numerical solution of the transport equations to converge. In almost all cases encountered so far this has been as a result of trying to solve a physically unrealistic problem, such as when the concentrate stream flow dries up because all the solution has been driven through the membrane. The difficulty is that often the conditions which give rise to this situation are not directly chosen, but occur as a consequence of choices which are less obviously incorrect. For example, a plausible set of conditions at the feed end of a simulated RO plant may lead to an unrealistic situation at the plant exit. This problem can be compounded when regressing for parameters, since the regression routine will try unpredictable combinations of parameters during the course of its search, some of which may well lead to such physically unrealistic situations.

point model calculations

The reason for failure to converge is usually relatively easy to track down with point model calculations, since conditions are directly specified. It is important to realize that a number of parameters which appear on different input screens must be consistent with each other.

Membrane area and permeate rate

Since the program deals with permeate flow rates rather than fluxes for input and output, it is important that the membrane area must be correctly specified in relation to flows. Where one is modelling data which has already been reduced to fluxes, it may be convenient to set the membrane area as 1 m^2 so that the permeate rate is numerically equal to the flux. Since the point model does not perform a material balance, the feed flow rates do not have to be made consistent with the membrane area, but must be consistent with the tube diameter to give the correct flow velocity for the calculation of the film mass transfer coefficient.

Solute physical constants

It is also necessary for the physical chemical characterisation of the solute to be constistent. This usually only an issue when modelling a mixed solute as a single solute using average properties. If the molecular mass, osmotic pressure table and diffusivity are not mutually consistent, or not consistent with the RO membrane parameters, it can cause failure to converge.

extended model calculations

In addition to the above considerations, an extended model may encounter problems due to the change in conditions through the plant due to the material balance. The membrane surface area for an extended model is defined by entries in the *module design data* and *plant configuration* screens, and it must be consistent with both the feed and permeate flow rates. When performing plant simulation calculations one can choose to print a trace of intermediate values either to screen, printer or disk file, and examination of these is normally sufficient to determine the cause of any problem. In most cases either the flow or the pressure in the tubes runs out.

parameter regression from plant data

Perhaps the most difficult situation to anticipate arises when regressing for model parameters from plant data, particularly if high water recoveries are involved. A good set of initial estimates of the parameters is usually the key to avoiding convergence failure. To estimatek_1 and k_2, simulate the performance of a plant with the appropriate module design and configuration, but using the preset parameters. By comparing these simulated results with the experimental values, and considering the permeate flux to be roughly proportional to k_1 and the solute flux (flux x concentration for the permeate) to be roughly proportional to k_2, sufficiently accurate starting estimates of the parameters should be obtained.

Index

WATER RESEARCH COMMISSION PROJECT NO. 325

RESEARCH ON THE MODELLING OF TUBULAR REVERSE OSMOSIS SYSTEMS

Appendix 10

User Manual for the Multi-Solute Membrane Separation Modelling Program

CJ Brouckaert

Pollution Research Group
Department of Chemical Engineering
University of Natal
Durban

February 1995

PREMSEP:
A PROGRAM FOR MODELLING PRESSURE-DRIVEN MEMBRANE SEPARATION PROCESSES

Version 1.021 (January 1995)

User Instructions

Developed during a Water Research Commission project

by

C.J. Brouckaert

L.A.D. Baddock

S. Wadley

Pollution Research Group,

Chemical Engineering Department, University of Natal

King George V Avenue,

Durban 4001, South Africa

e-mail brouckae@che.und.ac.za, fax (031) 260-1118

Updates to the manual and program are available on the Internet through *ftp* (file transfer protocol). The host computer is *aqua.ccwr.ac.za* and the directory is *ftp/pub/emily.*

TABLE OF CONTENTS

INTRODUCTION

The membrane-separation process modelling program is written in Borland C++ and runs under MS-Windows. In concept it tries to provide a framework in which a variety of membrane transport models could be set, and so was implemented as a set of *objects* which interact with each other in a similar way to their physical counterparts (at least in the context of a membrane separation plant). These objects are primarily chemical *components, membranes, modules, and streams*, although these may have sub-objects which handle various aspects of their behaviour. For instance, a stream has an *intensive thermodynamic state* object and one or more *experimental data set* objects associated with it. The idea is that when considering membrane transport modelling code, one should be able to focus on how the membrane interacts with a stream and its components, without being concerned with other aspects such as the module geometry or how to obtain model parameters from experimental data by regression. This ideal has by no means been completely realised in the current version of the program, as some short cuts were taken to get it up and running, however these will be gradually eliminated in further updates.

The basic calculation that the model performs is to produce a *permeate* stream and *reject* stream from a *feed* stream and a plant configuration, which comprises specifications of *components, membrane, modules* and *module banks*. The current version can only handle a steady-state continuous plant, without recycle, treating aqueous streams.

This version of the manual should be read in conjunction with the course notes (Appendix 1).

NEW FEATURES

New features which have been included with version 1.02 are:

Ionic components and charged membranes.

Previously PREMSEP could only handle neutral species, which meant that ions had to be grouped in pairs into neutral pseudo-components. The membrane transport model is now based on the extended Nernst-Planck diffusion equation, which calculated an electrical potential gradient that imposes electro-neutrality on the fluxes of the diffusing species. Charged membranes are modelled by including the concentration of fixed ionic groups in the electroneutrality condition. Neutral species are also accommodated in the same framework.

Indicators.

When dealing with a complex solution containing many species, chemical analyses are frequently expressed in terms of summary measurements instead of concentrations of the individual components. For instance, a solution containing sulphate will usually be analysed in terms of total sulphate, rather than the concentrations of the individual species which contain complexed sulphate. Another common example is the use of conductivity as an overall indicator of ionic concentration. In the program, an indicator is represented as a linear function of the model components. Experimental indicator values can be entered as data, to be compared with values calculated by the transport model.

"Module Scan" output option.

A new output option which records the conditions at the exit of each module in a series

Improved numerical error handling.

A large proportion of cases where the previous version failed to converge was due to either the flow or pressure going to zero in the numerical integration of the material and momentum balances. These cases are now trapped. Where this happens in a simulation run, an informative message is issued; during a parameter fitting run, the integration simply terminates and allows the regression routine to try different parameter values, in the hope that they will not cause the same problem.

Mathematical errors such as division by zero, floating-point overflow or underflow, square root of negative argument and the like are also trapped. These will cause whatever calculation routine is running to be aborted, and return to the menu after displaying an error message.

RUNNING THE PROGRAM

To run the program, you must have MS-Windows and a mouse. It is also necessary to have a spreadsheet program such as LOTUS-123, QUATTRO-PRO or the like, as the output of results is still somewhat primitive. An output file is produced which is best viewed and manipulated by importing it into a spreadsheet program. This should not be a great disadvantage as Windows allows one to have the modelling program and the spreadsheet open simultaneously, and to swap between the two using the Alt-TAB keystroke. It also has the advantage that the spreadsheet facilities can be used for graphing or manipulating the results.

The program can be invoked by any of the standard Windows methods (perhaps the easiest is to double-click on the PREMSEP.EXE file from the Windows File Manager utility.)

THE MENUS

When started the program displays a window with the following menu items:

File **Edit** **Run** **Options** **Help**.

The File Menu

The three options in this menu are **Load**, **Save as**, and **Exit**.

Load brings up a window to load a model from a file saved previously using the **Save as** option. The window has a standard Windows format for handling files. The model files have a default extension of .RO. They contain the entire state of the model as it was at the time that the file was saved, apart from the state of check boxes which are used to indicate parameters which can be varied by regression.

Save as saves all the parameters of the current model in a file specified by the user. The program is not yet secure from crashing due errors brought about by incompatible combinations of parameters, so it is a good idea to save the model before attempting to run any of the calculation options.

Exit closes the model program. It does not automatically save its current state to a file.

The Edit Menu

The options in the **Edit** menu are:

Components, Indicators, Membranes, Modules, Module banks, Streams and **Description.**

Apart from **Description**, each of the editing windows invoked from this menu have a number of features in common. Each has an editing box for the *name* of the particular item which is currently being edited (e.g.. Na+ or Cl- for a component) and a box containing a list of the items already in the model. An item can be selected from the list using the mouse, it then is made current, and its parameter values are loaded into the editing boxes. Each window has an **Add** and **Remove** button which adds the current item to the list, or removes it from the list (effectively deleting it from the model). Some windows also have an **Update** button which makes the currently displayed set of parameter values permanent for an existing list item. For those the do not have an **Update**, the **OK** button which closes the window performs the update function. Where it is necessary to **Update** explicitly, the **Ok** button is replaced by an **Exit** button. The **Cancel** button closes a window without updating any changed values. A number of parameter boxes have small square *check boxes* located immediately on their right. Clicking with the mouse in one of these causes the box to be marked with an x, which indicates that the corresponding parameter is *adjustable* when running the program's regression procedure (refer to the **Run** menu section). To cancel a parameter's adjustable status, click again in its check box, which is indicated by clearing the x from the box. The status of the check boxes are not saved in a model file.

The default units for parameters are according to the S.I. system : that is, based on meters, seconds, kilograms, Pascals, degrees Kelvin and gram moles. A number of parameters have associated unit boxes which allow other units to be used. Changing units causes the numerical value to be changed simultaneously. S.I. units are always used for output. For those parameters which have not been provided with unit boxes yet, S.I. units must be used.

Components

There are currently five items defining a chemical component: *name, molecular weight, osmotic coefficient, diffusivity* and *ionic charge.* The molecular weight is not used for anything in the current version. The osmotic coefficient is based on the assumption that the component contributes to the solution osmotic pressure linearly with its molar concentration, and is the effective slope of the osmotic pressure molality curve. The diffusivity is the diffusivity of the component in water at 25 °C: the program adjusts diffusivities for temperature.

Note that the **Update** button must be clicked for each component separately, otherwise edited changes will be lost.

Indicators

The indicator editor presents a list of indicators and a list of components. Each indicator has a coefficient for each component. Its value is displayed in the **Coefficient** box when both the indicator and the component are selected in their respective list boxes. The **Update** button mush be selected to make edited changes to the coefficient permanent. A new indicator is defined by entering its name into the **Indicator** box and selecting the **Add** button. **Remove** deletes the selected indicator from the model. An indicator is defined globally for all streams in the system.

Membranes

The membrane editor window has two halves. The top half deals with items which are dependent on the membrane only, while the bottom half deals with parameters which reflect how the membrane interacts with different components.

In the top half are the membrane type (name), its permeability towards pure water, and two correction coefficients which reflect the effect of pressure and the pure water permeability and the solute permeabilities. Ion diffusivities are less commonly quoted than ionic mobilities or limiting ion conductivities, but can be readily calculated using the formulae:

$$D = \lambda \cdot \frac{RT}{z^2 F^2} = \mu \cdot \frac{RT}{zF}$$

where

D is the diffusivity (m^2/s)
λ is the ionic molar conducutivity ($S.m^2/mol$)
μ is the ionic mobility ($m^2/s/V$)
R is the gas law constant (8,314 J/mol)
T is the absolute temperature (K)
z is the ionic charge
F is Faraday's constant (96485 C/mol)

The overall flux of permeate through the membrane is modelled by the equation:

$$J_v = K_p \cdot (\Delta P - \Delta\pi)/\eta_w \cdot (\Delta P/P_0)^{-a}$$

Here J_v is the volumetric flux through the membrane (m/s)
K_p is the pure water permeability parameter (m)
η_w is the viscosity of water at the system temperature (Pa.s)
ΔP is the trans-membrane pressure difference (Pa)
$\Delta\pi$ is the trans-membrane osmotic pressure difference/(Pa)
σ is the reflection coefficient (see below)
P_0 is a reference pressure, taken to be 10^6 Pa
a is the first correction coefficient

In the bottom half of the editing window are a list of components and editing boxes for the transport parameters which describe how each component passes through the membrane. Selecting a component from the list makes it current, and loads its parameters into the boxes for editing. The **Update** button must be used to make any edited changes permanent for each component individually.

There is place for 5 transport parameters per component, currently only the first 4 are in use.

The flux of solute through the membrane is modelled by the differential equation

$$J_s = (1-\sigma)J_v c - P_s \frac{dc}{dx} - P_s c z \phi$$

where c is the local concentration of the solute in the membrane, and x is the distance through the membrane. This is sometimes referred to as the *Extended Nernst-Planck equation.*

The first parameter σ is the *reflection coefficient* as used by Spiegler and Kedem (1966). It can take on values between 0 and 1. A value of 1 indicates that the solute passes through the membrane driven purely by its concentration gradient, and independent of the flux of water. This is usually valid for high rejection membranes such as reverse osmosis membranes. A value of zero indicates that the flux of solute and water are perfectly coupled, and would be appropriate for a component which passes unhindered through a membrane, such as NaCl with an ultrafiltration membrane.

The second parameter sets P_s, the effective diffusivity (m/s) of the component in the membrane phase. Note that P_s has units of diffusivity over length, because the thickness of the active layer of the membrane is almost always unknown, and this is incorporated in the diffusivity parameter. The value which appears is scaled by dividing the actual value of P_s by the pure water permeability parameter K_p and by the viscosity of water at 25°C. Linking the water and solute permeabilities in this way helps the process of finding paramter values by regression.

The third parameter is a partition constant K for the solute between the solution and the membrane phase. The equilibrium at the membrane interface is modelled by the equation

$$c_m = K\exp(-z\psi)\cdot c_s$$

where

c_m is the concentration of the solute in the membrane phase,

c_s is the concentration in the solute phase.

In the above two expressions, ϕ and ψ are dimensionless electrostatic potentials which prevent separation of the ionic charges. The model adjusts these potentials to impose electroneutrality on the concentration distributions.

The fourth parameter in the list is only used for pseudo-components which represent a range of different molecules (usually organic fractions). Because a certain amount of fractionation occurs in passing through the membrane, the molecular weight distribution in the permeate is not the same as in the feed, and the osmotic pressure coefficient is different on the permeate and feed sides of the membrane. This effect is clearly a function of both the component and the membrane, which is the reason for representing it here. The fourth parameter represents the effective osmotic coefficient of the component on the permeate side of the membrane. A value of zero (or less) is interpreted by the program as a signal to use the same osmotic coefficient on both sides of the membrane.

The fifth transport parameter is not used in this version of the program.

Modules

The module editor is very simple, it only deals with the module name, its geometric type and the membrane it uses. It has a button which invokes a separate editor for the geometric configuration. Note that the **Update** button on this screen updates changes made in the geometric configuration editor, if it is not selected such changes will be lost.

The program caters for three types of modules in the present version, *tubular, spiral-wound* and *test cell*. The geometric configuration editor adjusts its format for the different types. Most of the dimensional parameters are self-explanatory.

The tubular module configuration allows for tubes to by connected in series or parallel.

In the spiral module configuration, the feed and permeate channel gaps are the distances between the layers of membrane on the feed and permeate side as maintained by the spacer mesh wound between the membrane layers. The mesh spacing is required in the correlation for the film mass-transfer correlation. In the present version of the program, the mass-transfer resistance and pressure drop on the permeate side are assumed negligible, so only the entries for the feed channel side are used.

The test cell is meant to represent a bench scale laboratory cell, in which the water recovery and pressure drop are negligible. It has only two geometric parameters: the membrane area, and the effective hydraulic diameter of the flow channel on the high pressure side of the membrane. This is used to calculate the Reynolds number of the flow in order to determine the film mass transfer coefficient.

Each module configuration includes correlations for pressure drop and film mass-transfer coefficient, with constants which can be edited or adjusted by regression. (In the case of the test cell, pressure drop is neglected.) The correlation editor window has a heading which indicates the form of the equation and the meaning of the constants, and then three entries for each parameter, each with regression check boxes.

The first entry contains the current value of the parameter. If the corresponding check box is activated, it will be adjusted when the regression procedure is run.

The second entry contains an optional lower limit for the parameter which, if its check box is activated, will be observed during the regression procedure.

The third entry is similarly an upper limit for the parameter.

Tubular modules.

The pressure-drop correlation is the standard one for smooth tubes, and is dimensionless:

friction factor = 0,079 (Reynolds Number) $^{-0.25}$

A separate correlation is provided for the pressure drop due to return bends connecting the tubes in the module.

This has the simple form

(pressure drop) = a (flow velocity) ^{2}

In this case the pressure drop is expressed in Pa, and the velocity in m/s.

The mass transfer coefficient correlation is dimensionless of the form:

Sherwood number = a (Reynolds number) ^{b} (Schmidt number) ^{c}.

Spiral Modules

The pressure drop correlation is similar in form to that for tubes:

friction factor = a (Reynolds number) ^{b}

The Reynolds number and friction factor are expressed in terms of the hydraulic diameter which is taken as 2h, twice the channel gap.

The mass-transfer correlation is of the form:

Sherwood no = a (channel gap/mesh spacing) $^{0.5}$ (Reynolds number) ^{b} (Schmidt number) ^{c}

Module Banks

Module banks are very simple, a bank contains a rectangular array of modules, with a number of parallel trains of modules connected in series. All that needs to be specified is the name of the bank, the type of module making it up, the number in parallel and the number in series. The names of banks can take any format, but the current version of the program only uses banks with sequential numbers 1, 2, 3 etc. as names, and takes these as being incorporated in a plant in series, in numerical order. This allows a typical tapered plant configuration to be simulated.

Streams

Once again, although any number of streams with any names can be entered, the program currently only uses *Feed*, *Permeate* and *Reject*. Each of these can have a number of experimental data sets associated with it. The program uses the Feed data sets as input specifications to calculate simulated permeate and reject streams. The experimental data sets for the permeate and reject are copied to the stream output file for comparison with the simulated values, but their main purpose is in determining model parameters by regression. Thus it is not necessary to enter experimental data sets for permeate and reject where simulation without regression is required; the feed must always be specified. Furthermore, the regression procedure does not require all the entries in the permeate and feed streams to be completed: if any value is zero or less than zero it is ignored in calculating the sum of squared errors between the model and experimental results. Refer to the discussion in the *Parameter Regression* section below.

The top level stream editor window handles the stream names and selects an experimental data set. This is achieved by scrolling the number up or down using the arrow buttons next to the box - the box does not accept typed input. The other functions associated with streams are handled by the sub-editing screens selected using the buttons.

Experimental data

The stream information editor is split into two sections: the top half deals with properties of the stream as a whole, whereas the bottom half deals with the concentrations of components and indicators, which obviously depend on the lists of components and indicators in the model.

In the top half, the entries for conductivity and osmotic pressure are not used by the current version of the model. The entry for time is intended to be used for modelling time-dependent fouling of the membranes, and would typically be the time from the last membrane cleaning operation. Note that no fouling model has yet been incorporated.

In the bottom half, a component is selected by clicking on it in the list box, which causes its concentration to be copied into the editing box. The **Update** button must be used for each component individually otherwise edited changes will be lost. Indicators are handled in the same way as components. The indicator values are nominally regarded as concentrations. Where a value is entered as 0, it is taken by the regression procedure to signify 'no data' rather than an actual zero value - this applies to both components and indicators.

Extra Parameters

The **extra parameters** associated with a stream are not used in the present version of the model.

Importing data from a file, or from the clipboard.

Large sets of experimental data are often more conveniently entered from an separate file, rather than by entering each item individually using the editing boxes. Data can be imported from a ASCII file, which is usually generated by export from a spreadsheet program.

The file must contain the data for a single stream to be imported in a specific fixed order, which may be found by selecting the **Format?** button. Each data set must be arranged on a single line, in the following order:

Flowrate time temperature pressure conductivity osmotic pressure <component concentrations> <indicator concentrations>

The lists of component and indicator concentrations must appear in the reverse order to that in which they were created when setting up the model. (The correct order will be shown when the **Format?** button is selected). Values to be imported must be expressed in S.I. units, this is not necessary for interactive entry.

Instead of using an ASCII file as the import medium, it is also possible to use the Windows clipboard. The program treats the clipboard as though it were a file, so the format is identical.

THE RUN MENU

This has just three options: **Run Regression, Stream output** and **Module Scan.**

Run Regression.

Before the regression procedure can be run, experimental data sets for at least the feed and permeate must have been entered, and the required parameters must have been made adjustable in their own editing windows by filling in the regression check-boxes. **It is the user's responsibility to ensure that sufficient experimental information is available to provide a meaningful determination of the regressed parameters.** The current version of the program does not give any assistance in the problem of assessing the statistical significance of regressed values. As a general rule the number of items of data should be significantly greater than the number of adjustable parameters in the regression, but there are many subtleties which can affect the problem in different circumstances. For instance, a particular set of data may not contain any variations of conditions which reflect the effect of a particular parameter, and therefore contain no information which allows it to determined by regression, even though the number of measurements appears to be sufficient. On the other hand if a data set is very precise, and the model is known to be a very accurate representation of the data, the parameters might be well determined from a minimal set of measurements. Thus at this stage one can only recommend a cautious trial-and-error approach to regressing for model parameters, making use of literature values wherever possible.

The progress of the regression is monitored by displaying the current value of the sum-of-squares objective function. The regression tries to make this value as small as possible. The procedure terminates when it cannot make any further progress, or when it reaches a maximum number of iterations which can be set on the options menu.

The parameter values entered are taken as starting estimates by the iterative regression procedure. **A starting value for an adjustable parameter must not be zero.**

The success of the regression procedure is dependent on the starting values - a poor set can lead the program into regions where the model equations do not converge. When tackling a problem where one has little idea of the values that the parameters should take, it is sensible to first make a few trials manually (using the **Stream Output** option) to get them into the right order of magnitude, and then let the program adjust just a few parameters at a time allowing only one or two iterations. As the values of the parameters get closer to what they should be, one can allow more to be adjusted, and run for more iterations. It is also a good idea to save the status of the model whenever a significant improvement has been achieved in case the model crashes on the next trial.

Stream output.

The stream output option causes the program to perform a simulation corresponding to the feed specification of every data set. The results are output to a disk file specified by the user.

This file contains simulated values of flows, temperatures, pressures and composition for feed, permeate and reject streams, together with the experimental values for comparison.

The program queries the user whether the output should be formatted "vertically". This refers to placing the output for the permeate, feed an reject streams below each other in the file, as opposed to horizontally next to each other. The latter option is usually more convenient for examining and manipulating the data in a spreadsheet program, however it leads to lines which are too long to import into some spreadsheets, hence the vertical option.

The file has a default .PRN extension, and can be imported into spreadsheet using the *Input Numbers* option which most such programs have.

Module Scan

The module scan output option is simlar to the stream output, except that the conditions at the brine outlet of each module in series are output to the file.

THE OPTIONS MENU

This currently has only one option **Setup.**

In the setup window one can set the *number of experimental data sets*. Increasing it causes blank sets to be added. Reducing this number causes sets to be deleted, and any data they contain is lost. The number is also affected by deleting a data set in the stream editor window.

The *Maximum Solution Iterations* limits the number of iterations in solving the membrane transport model equations before the program decides it is unable to find a solution. Increasing this occasionally helps to overcome convergence problems, particularly when regressing, as the regression procedure may well try unfortunate combinations of parameters..

The *Maximum Regression Iterations* limits the number of trials the regression procedure will make in searching for the best set of parameter values. Refer to the discussion in the regression section.

REFERENCE

K.S. Spiegler and O. Kedem, **Thermodynamics of Hyperfiltration (Reverse Osmosis): Criteria for Efficient Membranes**, Desalination, 1 (1966), pp. 311-326.